Identification of pathogenicity genes in the crucifer anthracnose *Colletotrichum higginsianum*, using random insertional mutagenesis

Inaugural–Dissertation

zur

Erlangung des Doktorgrades

der Mathematisch-Naturwissenschaftlichen Fakultät

der Universität zu Köln

vorgelegt von

Aurélie Huser

aus Epernay, Frankreich

Köln, September 2008

Die vorliegende Arbeit wurde am Max-Planck-Institut für Züchtungsforschung in Köln in der Abteilung für Molekulare Phytopathologie (Direktor: Prof. Dr. P. Schulze-Lefert) angefertigt.

Berichterstatter:	Prof. Dr. Paul Schulze-Lefert Prof. Dr. Marcel Bucher
Prüfungsvorsitzender:	Prof. Dr. Ulf-Ingo Flügge
Tag der Disputation:	3. Dezember 2008

Publications

Tanaka S., Yamada K., Yabumoto K., Fujii S., **Huser A.**, Tsuji G., Koga H., Dohi K., Mori M., Shiraishi T., O'Connell R., Kubo Y. (2007) *Saccharomyces cerevisiae* SSD1 orthologues are essential for host infection by the ascomycete plant pathogens *Colletotrichum lagenarium* and *Magnaporthe grisea*. Molecular Microbiology. 64(5):1332-49.

Huser. A. C., Takahara, H., Schmalenbach, W., O'Connell, R. Identification of pathogenicity genes in the crucifer anthracnose *Colletotrichum higginsianum*, using random insertional mutagenesis. (submitted)

Table of Abbreviations

AS	Acetosyringone
ATMT	*Agrobacterium tumefaciens*-mediated transformation
ABC	ATP-binding cassette
Avr	Avirulence
bp	Base pair
BSA	Bovine Serum Albumin
cAMP	cyclic Adenosine monophosphate
CDA	Czapek Dox Agar
CoA	Coenzyme A
CWDE	Cell wall degrading enzymes
DNA	Deoxyribonucleic acid
DIC	Differential interference contrast
DHN	Dihydroxyraphaltene
ETI	Effector-triggered immunity
ETS	Effector-triggered susceptibility
EDTA	Ethylenediaminetetraacetic acid
e. g.	*exempli gratia*
EST	Expressed sequence tag
f. sp.	*Forma specialis*
GPI	Glycosylphosphatidylinisotol
gfp	Green fluorescent protein gene
GTPase	guanylyltransferase
HST	Host specific toxin
hph	hygromycin B phosphotransferase gene
HR	Hypersensitive response
i. e.	*id est*
IPTG	Isopropyl ß-D thiogalactoside
kb	kilobase
LIPK	Lipid-induced protein kinase
LB	Luria Benturia
MFS	Major facilitator superfamily
Km	Michaelis constant
µ	micro
MAPK	Mitogen activated protein kinase
MCS	Multiple cloning site
NADPH	Nicotinamide adenine dinucleotide phosphate (reduced form)
NTP	Nucleoside triphosphate
OD	Optical density

ODC	Ornithine decarboxylase
ORF	Open reading frame
PAMP	Pathogen-associated molecular pattern
PCR	Polymerase Chain Reaction
PDA	Potato dextrose agar
PH	Primary hyphae
PKA	Protein kinase A
PR	Pathogenicity related
PTI	PAMP-triggered immunity
R	Resistance
REMI	Restriction enzyme-mediated integration
RB	Right border
RE	Restriction endonuclease
RNA	Ribonucleic acid
SG	Synthetic medium with galactose
SD	Synthetic medium with glucose
TAE	Tris/EDTA/acetate buffer
TAIL	Thermal Asymmetrical Interlaced
T-DNA	Transferred DNA
Ti	Tumour-inducing
TM	transmembrane
Tris	Tris(hydroxymethyl)aminomethane
v/v	Volume per volume
w/v	Weight per volume
X-Gal	5-bromo-4-chloro-3-indolyl-ß-D-galactopyrynoside

Abstract

The crucifer anthracnose agent *Colletotrichum higginsianum* is an ascomycete fungus which can be genetically transformed. The pathogen uses a two-stage hemibiotrophic infection process, initially growing biotrophically inside a living host cell before switching to a destructive and invasive necrotrophic phase. In this study, the *Arabidopsis thaliana – C. higginsianum* pathosystem was used to identify fungal pathogenicity genes required for different steps of this infection process.

A library of 8,850 random insertional transformants of *C. higginsianum* was generated by *Agrobacterium tumefaciens*–mediated transformation and screened for mutants failing to cause disease on *A. thaliana* plants. Forty pathogenicity mutants were identified and subjected to cytological analysis to characterise their infection phenotypes. Six mutants failed to form melanised appressoria, fifteen had reduced ability of penetrating the host, fourteen induced more visible host defence responses such as the hypersensitive response or callose deposition and five were reduced in their ability to enter the necrotrophic stage.

The tagged genes were isolated from twelve mutants by obtaining the DNA sequence flanking the T-DNA insertions using thermal asymmetric interlaced PCR and inverse PCR and using these to screen a genomic DNA library. The putative pathogenicity genes identified showed homology to phosphate transporter, genes involved in arginine biosynthesis (carbamoyl phosphate synthetase and ARG-6 precursor), ornithine decarboxylase, importin ß, ATP-binding endoribonuclease, ß-1,3(4)-glucanase and five fungal hypothetical proteins. Two further predicted open reading frames had no significant homology to known proteins. To verify that the mutations in these genes are indeed responsible for the observed pathogenicity phenotypes, complementation with the wild-type gene and/or targeted gene disruption are required.

Selected mutants were characterised in more detail. This includes a putative Major Facilitator Superfamily transporter tagged in penetration mutant *path*-12. A role in phosphate uptake for this protein was confirmed using complementation of yeast phosphate transporters mutant and rescue of the pathogenicity phenotype by supplementation of phosphate in plant tissue. Expression analysis indicates the transporter is expressed during

germination, appressorium formation and during the biotrophic phase, when phosphate availability is suggested to be limited.

Apart for ornithine decarboxylase, none of these genes identified in this study were previously reported to play roles in fungal pathogenicity. Further functional characterisation of these genes should give new insights into the establishment and maintenance of biotrophy and the switch to necrotrophy in *C. higginsianum*.

.

Zusammenfassung

Das Kruziferen Anthracnose Pathogen *Colletotrichum higginsianum* ist ein Ascomycet welcher genetisch transformiert werden kann. Die Pathogenese erfolgt in zwei Phasen bei der das Pathogen zunächst innerhalb einer intakten Wirtszelle biotrophisch wächst und anschließend zu einem invasiven nekrotrophischen Wachstum wechselt, welches die befallenen Wirtszellen zerstört. In dieser Arbeit wurde das *Arabidopsis thaliana – C. higginsianum* Pathosystem zur Identifizierung von Pathogenitätsfaktoren von Pilzen, die für die verschiedenen Schritte des Infektionsprozesses essentiell sind, eingesetzt.

Eine Sammlung von 8,850 zufällig inserierten *C. higginsianum* Mutanten wurde durch *Agrobacterium tumefaciens*-vermittelter Transformation generiert und nach den Mutanten gemustert, die für *A. thaliana* nicht mehr pathogen sind. Insgesamt wurden 40 Pathogenitätsmutanten identifiziert und deren Infektionsphänotypen cytologisch untersucht. Sechs Mutanten generierten keine melanisierten Appressorien, 15 Mutanten wiesen reduzierte Penetration des Wirtes auf. Vierzehn Mutanten induzierten stärker sichtbare Wirtsabwehrmechanismen, wie z.B. eine hypersensitive Reaktion oder Kalloseeinlagerungen. Fünf zeigten eine reduzierte Fähigkeit von der biotrophen in die nekrotrophe Wachstumsphase zu wechseln.

Markierte Gene von 12 Mutanten wurden isoliert, indem deren DNA Sequenzen, die die T-DNA Insertionen flankieren, durch „thermal asymmetric interlaced PCR“ und inverse PCR identifiziert wurden und diese Sequenzen anschließend für die Musterung von genomischen DNA-Banken verwendet wurden. Die identifizierten putativen Pathogenitätsfaktoren wiesen Homologie zu Phosphattransporter, Gene involviert in der Arginin-Biosynthese (Carbomylphosphatsynthetase und eine ARG-6 Vorstufe), Ornithindecarboxylase, Importin β, ATP-bindende Endoribonuclease, β-1,3(4)-Glucanase und fünf hypothetischen Proteinen auf. Zwei weitere prognostizierte offene Leserahmen wiesen keine signifikante Homologie zu bekannten Proteinen auf. Um zu bestätigen, dass die Mutationen in diesen Genen den beobachteten Pathogenitätsphänotyp determinieren, wurden Komplementationen mit dem Wildtypgen und/oder dem gezielt disruptierten Gen benötigt.

Ausgewählte Mutanten wurden detaillierter charakterisiert. Das beinhaltete auch den putativen „Major Facilitator Superfamily“ Transporter der in der Penetrationsmutante *path*-12 markiert ist. Eine Rolle in der Phosphataufnahme wurde für dieses Protein durch die

Komplementierung des Phosphattransporters von Hefe und durch die Komplementierung des Pathogenitätsphänotyps durch die Zugabe von Phosphat zu pflanzlichem Gewebe bestätigt. Expressionsanalysen weisen darauf hin, dass der Transporter während der Keimung, der Appressoriumbildung und der biotrophen Phase expremiert wird, bei denen Phosphatverfügbarkeit vermutlich limitiert ist.

Abgesehen von Ornithindexarboxylase ist für keines der hier identifizierten Gene bisher eine Rolle in der Pathogenität von Pilzen beschrieben worden. Weitere funktionelle Charakterisierungen dieser Gene werden neue Einblicke in die Aufrechterhaltung von Biotrophie und dem Wechsel zu Nektrotophie von *C. higginsianum* geben.

Table of contents

Index of Figures and Tables

Figures:

Tables:

Supplementary Data:

1 Introduction

Plant diseases have had major effects on civilisation since humans began relying on crop cultivation for food. Fungal plant pathogens cause serious diseases on a variety of plants, including crop plants, resulting in important economical damage and a serious threat to food security. Plant pathogens have therefore been subject to a lot of attention in order to understand pathogenesis and develop ways to prevent or control diseases.

Fungi have evolved to adapt to many specialised environments. Plant tissue is an attractive ecological niche for fungi as it offers a constant supply of nutrients. Some fungi developed ways to exploit this environment as a pathogenic interaction, while others have established intimate symbiotic relationships. In an ongoing co-evolutionary battle, plants have developed several layers of defence to prevent infection by fungal pathogens, which in their turn have evolved multifaceted attack strategies to overcome these defences and successfully colonise a particular host. As a result, interactions between a pathogen and host plant can be extremely sophisticated.

The nutritional lifestyles of pathogenic fungi range from obligate biotrophy to necrotrophy, with hemibiotrophic species employing a combination of both modes of nutrition. Obligate biotrophs, such as powdery mildews and rust fungi, require living host tissue for their growth and reproduction. Necrotrophs, such as *Botrytis cinerea* and *Cochliobolus heterostrophus,* are unable to attack living tissue and produce host-specific toxins (HSTs) and cell wall degrading enzymes (CWDEs) to kill plant tissue in advance of fungal invasion and feed on the dead host tissue. Hemibiotrophs such as *Magnaporthe grisea* and *Colletotrichum* species initially establish a biotrophic infection but then switch to a necrotrophic mode of nutrition.

Plant pathogens have specialised to infect specific plant tissues *e. g.* leaves, roots, vascular tissues, fruits. Necrotrophic fungi tend to macerate host tissue and grow extensively intercellularly and intramurally (inside plant cell walls). Fungi which have adopted a biotrophic lifestyle may colonise the plant in a variety of ways. Some pathogens remain entirely in the apoplast, growing within intercellular spaces *e. g. Cladosporium fulvum* (Joosten and de Wit, 1999), while others are subcuticular *e. g. Venturia inaequalis*

(MacHardy *et al.*, 2001) and some species grow both inter- and intra-cellularly *e. g. Claviceps purpurea* (Tudzinsky and Sheffer, 2004). Yet other biotrophic pathogens remain extracellular, with only their feeding structures (haustoria) inserted into epidermal cells *e. g.* powdery mildews or in the parenchyma cells *e. g.* rust fungi (Mendgen and Hahn, 2002). Some hemibiotrophs such as *Magnaporthe grisea* and *Colletotrichum* species form intracellular hyphae during their biotrophic phase and grow intracellulary and intramurally during necrotrophy (Perfect and Green, 2001).

Most plant pathogenic fungi have a narrow host range while others, like *Botrytis cinerea* attack multiple hosts or like the rust fungi, require multiple hosts to complete their lifecycle. In addition, some pathogenic species for example, *Leptosphaeria maculans,* are facultative parasites and can survive many years as a saprophyte on crop debris (Howlett, *et al.* 2001).

1.1 Plant Resistance

Although many microorganisms are capable of causing disease, most plants species are resistant to any given pathogen. Resistance has been well-studied in crop plants and in the model plant *Arabidopsis thaliana,* where many molecular components of plant recognition and defence responses have been identified. Plants defend themselves against attack by microbial pathogens using multiple forms of defence responses. These include passive and active defence mechanisms.

Passive mechanisms include mechanical or chemical barriers such as the cuticle and the cell wall, tissue architecture or pre-formed antimicrobial metabolites (phytoanticipins). These defences are important to prevent entry and survival of unadapted fungal species.

Plants also have an inducible innate immunity which allows them to recognise and respond to molecules common to classes of microbes but absent in plants called pathogen-associated molecular patterns (PAMPs) *e. g.* chitin oligomers, bacterial flagellin or lipopolysaccharides, or in response to effector molecules which are virulence factors delivered into the host plant to enhance microbial fitness. The current model for innate immunity is best described as the “zigzag model” (Jones and Dangl, 2006). Upon detection

of PAMPs by plant transmembrane pattern recognition receptors, activation of mitogen-activated protein kinase (MAPK) cascades leads to the expression of defence responses that may include callose deposition and cell wall thickening, cross-linking of cell wall proteins, production or reactive oxygen species and focal accumulation of antimicrobial secondary metabolites. This is sufficient to stop invasion by unadapted pathogens, resulting in PAMP-triggered immunity (PTI) or basal resistance. However, some pathogens are successful in delivering one or more effectors that interfere with PTI rendering the plant susceptible. This is called effector-triggered susceptibility (ETS). Host plants in turn may have evolved to recognise the effector via cell surface or cytoplasmic nucleotide binding (NB)-leucine rich repeat (LRR) proteins, the products of plant resistance (R) gene. Recognition typically results in a hypersensitive response (HR), a form of plant programmed cell death, in an attempt to stop further pathogen growth. HR is typically associated with the production of reactive oxygen species, nitric oxide, and antimicrobial phytoalexins. Because this NB-LRR-mediated disease resistance results in death of the host cell, it is effective against pathogens such as obligate biotrophs and hemibiotrophs that require a living host cell but not against necrotrophs. Effectors which are recognised by resistance (R) proteins are referred to as avirulence (avr) gene products, a phenomenon first termed as resistance gene-mediated immunity, but now also known as effector-triggered immunity (ETI). In response, pathogens may have lost or modified the effector during evolution so that it is no longer recognised by NB-LRR receptors, again resulting in disease. Alternatively, the pathogen may have acquired new effectors which suppress the ETI and result in disease. In this evolutionary battle, selection favours both the evolution of new pathogen effectors and of new NB-LRR alleles that recognise these newly acquired effectors, resulting again in ETI.

1.2 Fungal Pathogenicity

Many fungal genes involved in pathogenicity have already been identified using both forward and reverse genetics approaches in a large variety of plant pathogenic fungi. They include genes that are specific to certain species or even one race, e.g. host specific toxins, detoxification enzymes or effectors (typically secreted proteins or metabolites) which can manipulate the host, but also more general factors which are widely conserved among

multiple fungal pathogens. These include genes involved in the sensing of environmental cues, morphogenesis and downstream signalling pathways, infection structure morphogenesis (*e. g.* formation of germ tubes, appressoria, penetration hyphae, sporing bodies), nutrition and adaptation to changing nutritional environment and survival inside the host and effectors.

1.2.1 Adhesion to the host

The first step in the establishment of infection is the adhesion of spore to the surface of the plant. Anchoring of the spore to the surface of the host is important to avoid it being dislodged but also for proper host recognition and penetration. Fungal adhesives vary among fungi and are typically water-insoluble glycoproteins, lipids and polysaccharides (Xiao, *et al.* 1994; Sugai, *et al.* 1998). Depending on the fungal species, adhesion may either be passive or require energy. Thus, pre-formed adhesives are released upon hydration from spore tips of the rice blast fungus *Magnaporthe grisea* (Hamer, *et al.* 1988) whereas *Colletotrichum graminicola* and *Nectria haematococca*, synthesise proteins and glycoproteins in their spores *de novo* and release these onto the substratum as adhesins (Jones and Epstein, 1989; Mercure *et al.* 1994; Mercure *et al.* 1995). In addition, some species *e. g.* some powdery mildew fungi and the rust *Uromyces viciae-fabae* release hydrolytic enzymes such as cutinases and esterases to make both the host and the spore surface more hydrophilic and promote attachment (Kunoh, *et al.* 1988; Deising, *et al.* 1992).

1.2.2 Germination on the host surface

The next step in pathogenesis is spore germination on the host surface, triggered by environmental cues. Nutrient availability may be an important stimulus for germination for necrotrophs, whereas starvation might be the cue for biotrophs and hemibiotrophs (Dean, 1997). Hydration is also important to trigger germination of conidia of *Magnaporthe grisea* (Hamer and Talbot, 1998), while conidia of *Blumeria graminis* f. sp. *hordei* rely on physical stimuli such as surface contact (Wright *et al.* 2000). Germ tubes of certain fungal pathogens are capable of directional growth and sense the surface topography and hardness,

plant chemical signals, nutrients and surface hydrophobicity to determine where to grow and when to stop. For example, germ tubes of the rusts *Puccinia graminis* f. sp. *triciti* and *Uromyces appendiculatus* rely on sensing host surface topography to grow perpendicular to anticlinal cell walls which increases the chance of encountering a stoma through which they enter (Wynn, 1976; Allen, *et al.* 1991). Certain fungal species such as *Mycosphaerealla graminicola* and *Ustilgao maydis* are dimorphic and need to switch from a yeast-like form to an infectious filamentous growth habit. This transition is regulated in part by the mitogen-activated protein kinases (MAPK) in *Mycosphaerealla graminicola* (Mehrabi *et al.* 2006) and by cyclin-dependant kinases, Rho-type guanylyltransferase (GTPase) and cyclic adenosine monophosphate (cAMP)-dependent protein kinases in *Ustilago maydis* (Gold *et al.*, 1994; Durrenberger *et al.,* 1998; Mahlert *et al.*, 2006; Castillo-Lluva *et al.*, 2007).

1.2.3 Penetration of the host

Penetration of the host occurs in various ways. Some fungi, *e. g. Puccinia* species, enter the host via natural openings such as wounds or stomata. In contrast, other species directly penetrate the cuticle and the cell wall or the host epidermis. Certain fungal species employing such methods rely on secreted cutinases and cell wall degrading enzymes (CWDEs) to breach the host surface *e. g. Blumeria* species. Alternatively, other fungi, *e. g. Magnaporthe* and *Colletotrichum* species, employ the physical force alone or in combination with hydrolytic enzymes to breach the host cuticle and cell wall. Necrotrophs such as *Fusarium graminearum* and *Botrytis cinerea* rely on a battery of CWDEs such as cutinases, lipases and polygalacturonases to breach the cuticle and the plant cell wall (van Kan, 2006). Plants maintain polygalacturonase inhibiting proteins which interact with the fungal secreted galacturonase enzyme preventing the enzyme from anchoring itself to the cell wall and degrading it (De Lorenzo and Ferrari, 2002). Additionally, the tip of the penetration peg of *Botrytis cinerea* generates hydrogen peroxide to assist in decomposition of the cuticle (van Kan, 2006). In contrast, *Magnaporthe* and *Colletotrichum* species, both hemibiotrophs, penetrate epidermal cells using mechanical force generated by a specialised structure called the appressorium. Appressoria are specialised infection structures formed at the tip of the germ tube of certain species. In these appressoria, turgour pressure required

for mechanical penetration of host surface by the penetration peg is generated. In most species, the appressorium is darkly pigmented by a layer of melanin in its cell wall. There, melanin plays a role in strengthening the appressorial wall to support high osmotic pressure, up to 8.0 MPa in appressoria of *Magnapothe grisea* (Howard *et al.,* 1991). Furthermore, the melanin layer determines the direction of growth of the penetration peg as it can only emerge from a zone lacking melanin, known as the penetration pore, found at the base of the appressorium (Howard and Valent, 1996). Additionally, the melanin layer in the cell wall also serves as a selectively permeable barrier which traps solutes inside the appressorium. The synthesis and accumulation of osmotically active compounds (*e. g.* glycerol) to high concentrations during appressorium maturation, is responsible for the generation of enormous internal turgour pressure due to osmosis (Howard *et al.,* 1991; de Jong *et al.*, 1997). Interestingly, some species such as *Blumeria* or rusts fungi which penetrate their host via stomata also form appressoria, although these are not pigmented (Pryce-Jones *et al.*, 1999; Iwamoto *et al.*, 2007). This suggests appressoria are not only important for mechanical penetration. Appressorial adhesins, composed of lipids, polysaccharides are essential for the exertion of mechanical force onto the cuticle without the appressoria becoming detached from the surface (Xiao *et al.*, 1994).

Many genes required for appressorium induction and morphogenesis have been identified in *Colletotrichum* and *Magnaporthe* species. They include MAPK, transcription factors and hydrophobins (Table). In *Magnaporthe grisea*, hydrophobins form hydrophobic rodlet proteins which coat the conidia and perceive the surface prior to appresorium formation (Talbot *et al.*, 1993; Talbot *et al.*, 1996). In addition, chemical signals from the host can also trigger appressorium formation. Thus, *Colletotrichum gloeosporioides* form appressoria in response to the plant ripening hormone ethylene (Flaishman and Kolattukudy, 1994) and from avocado wax (Podila *et al.*, 1993) whereas *Magnaporthe grisea* forms appressoria in response to the wax component 1,16-hexadecanediol (Gilbert *et al.*, 1996). Surface hardness and hydrophobicity are also both important stimuli for appressorium development in *Magnaporthe grisea* and *Colletotrichum* species (Jelitto *et al.*, 1994; Dean, 1997; Kim *et al.*, 1998). The putative extracellular chitin-binding protein CBP1 of *Magnaporthe grisea*, may be involved in sensing hydrophobic surface during appressorium penetration (Kamakura *et al.*, 2002) and in *Colletotrichum trifollii*, a lipid-induced protein

kinase (LIPK) involved in appressorium formation is induced by cutin (Dickman *et al.*, 2003).

The generation of turgour pressure in the appressorium relies on melanin biosynthesis enzymes, fatty acid metabolism and glycerol production (Wang *et al.*, 2003; Gupta and Chattoo, 2007). As for germination, environmental cues play an important role in triggering appressorium formation. Numerous genes for the synthesis of dihydroxyraphthalene (DHN)-derived melanin have also been identified in *Colletotrichum* and *Magnaporthe* species as melanisation is necessary for turgour pressure generation and therefore for appressorium-mediated penetration and pathogenicity (Table). Genes required for melanin synthesis include not only enzymes in the DHN pathway but also proteins necessary for the transfer of lipid bodies to the appressorium and lipases for rapid lipolysis of triacetylglycerol (Wang *et al.*, 2007) and the generation of the acetyl coenzyme A (acetyl-CoA) in the peroxisome (Kimura *et al.*, 2001; Idnurm and Howlett, 2002; Bhambra *et al.*, 2006; Divon and Fluhr, 2007; Wang *et al.*, 2007). Additionally, production of reactive oxygen intermediates by reduced nicotinamide adenine dinucleotide phosphate (NADPH) oxidases is also important for melanin synthesis (Egan *et al.*, 2007). Interestingly, the non-melanised appressoria of the powdery mildew *Blumeria graminis* f. sp. *hordei* also generate substantial turgour pressure during cuticle penetration (Pryce-Jones *et al.*, 1999). The appressorium also needs to be sealed off from the germ tube by a septum in order to generate sufficient turgour pressure for appressorium-mediated penetration (Howard and Valent, 1996). This septum is absent in species like *Botrytis cinerea* which do not rely on mechanical force for penetration but rather on hydrolytic enzymes, although they have a very weakly melanised appressorium (Doss *et al.*, 2003). Localisation of actin to the hyphal apex and rapid cell wall biosynthesis and remodelling have been found to be important for the formation of the penetration peg of *Magnaporthe grisea* (Tucker and Talbot, 2001). However, the role of CWDEs in appressorium-mediated penetration is unclear. Cutinases have been implicated in host penetration by *Magnaporthe grisea* (Skamnioti and Gurr, 2007) and a cellobiohydrolase and a cutinase are expressed during penetration by *Blumeria graminis* (Pryce-Jones *et al.*, 1999). A class of transmembrane proteins called tetraspanins are required for appressorium-mediated penetration by both *Botrytis cinerea* (Gourgues *et al.*, 2004) and *Magnaporthe grisea* (Clergeot *et al.*, 2001), possibly by re-establishing

polarised growth in the appressorium prior to emergence of the penetration peg (Veneault-Fourrey *et al.*, 2006).Recently, the formation of the appressorium in *Magnaporthe grisea* was shown to require the completion of mitosis, nuclear migration, spore autophagy and nuclear degeneration in the spore (Veneault-Fourrey *et al.*, 2006; Liu *et al.*, 2007).

1.2.4 Nutrition during pathogenesis

During germination and penetration, pathogens are in a state of starvation, relying on stored nutrients derived from the spore, including glycogen, trehalose, lipids and polyols such as mannitol (Carlile *et al.*, 2001). Prior to, during and after penetration, pathogens are exposed to changing nutritional environments. An important aspect of pathogenicity is how pathogens acquire nutrients from their host and how they adapt to the changing availability of nutrients. Nutrient availability is a major factor influencing gene expression during morphogenesis and pathogenicity.

Once inside the host, assuming the internal stores from the spore have been exhausted, the pathogen needs to rapidly take up adequate nutrients. Pathogenic fungi have adapted to utilise available nutrients in the apoplast or the plant cell, and in some cases to manipulate host physiology to optimise nutrient supply to the pathogen. Analysis of expressed sequence tags (ESTs) of the powdery mildew pathogen *Blumeria graminis* revealed that a large number of genes involved in amino acid metabolism, protein turnover and amino acid recycling are expressed during germination and appressorium formation, indicating the pathogen is already metabolically very active this early in infection (Thomas *et al.*, 2001). Likewise, the glutamine synthase of *Colletotrichum gloeosporioides* is upregulated during the early stages of infection (Stephenson *et al.*, 1997).

To obtain nutrients from a living host cell, biotrophs such as rust fungi and powdery mildew form a feeding structure called the haustorium, while hemibiotrophs may produce specialised intracellular hyphae as feeding structures. Although inside the cell lumen, these structures invaginate and expand the plasma membrane of the host cell but do not penetrate it and so remain within the plant apoplast. At the interface of nutrient transfer, the fungal cell and the host cell are alongside each other. The fungal cell wall and specialised cell membrane of haustoria of obligate biotrophs and intracellular hyphae is surrounded by an

interfacial matrix separating it from the invaginated plant plasma membrane (O'Connell, 1987; Green *et al.*, 1995; Perfect *et al.*, 1999). The interface forms a region of intimate contact between the plant and the fungus and may play important roles in the establishment and maintenance of biotrophy and the avoidance or suppression of host defences. Fungal glycoproteins in the interfacial matrix during the biotrophic phase may be particularly important for the establishment and maintenance of biotrophy and possibly for suppressing host defences (Perfect *et al.*, 1999). The haustorium and intracellular hypha appear to play an essential role in nutrient acquisition (Hahn and Mendgen, 2001) and there is evidence to suggest they are involved in the redirection of host metabolism and the suppression of host defences (Voegele *et al.*, 2001; 2005; 2006). The haustorium and intracellular hypha are functionally in the apoplast and nutrients need to pass both the fungal and the host plasma membrane to enter the fungus. Obligate biotrophs redirect assimilates away from the host sinks and towards the fungus, the feeding structure acting as a nutrient sink. Nutrients that enter the fungus are mainly the products of current photosynthesis. Fungal invertases and hexose transporters such as Hxt1p in *Uromyces fabae* haustoria play an important role in establishing the haustorium as a carbon sink (Voegele *et al.*, 2001). In addition to their own transporter, some biotrophs may employ the host nutrient transfer machinery to take up nutrients even more efficiently. For example, the biotroph *Erysiphe cichoracearum* exploits the monosaccharide transporter AtSTP4 and the invertase Atßfruct1 of its host *A. thaliana* to increase its sugar uptake (Fotopoulos *et al.*, 2003). The amino acid : proton symporter AAT1p of the rust *Uromyces fabae* has also been found to accumulate early in infection and a similar amino acid transporter AAT2p was found to be exclusively localised in haustoria (Hahn and Mendgen, 2001)

Hemibiotrophs switch from an initial biotrophic phase to a necrotrophic phase. Several genes involved in the switch between these two modes of growth have been identified. They include the zinc finger GAL4-like transcriptional activator CLTA1 in *Colletotrichum lindemuthianum* involved in the utilization on different nitrogen sources (Dufresne *et al.*, 2000 ;Pellier *et al.*, 2003), CLNR1 of *C. lindemuthianum* which encodes an Area-like regulator of nitrogen metabolism and the signal peptidase complex subunit CPR1 from *Colletotrichum graminicola* (Thon *et al.*, 2002). Nitrogen supply is therefore an important signal for the expression of genes involved in morphogenesis and virulence.

Nitrogen is required to synthesise proteins and other cell components such as nucleic acids and chitin. Fungi can assimilate a wide range of amino acids, amines and amides as well as proteins and other nitrogen-containing organic compounds to serve as nitrogen sources. As nutrient availability is one of the signals controlling the expression of genes involved in pathogenesis, the switch may be partly attributed to the relatively low nutrient uptake hemibiotrophs achieve during the brief biotrophic phase compared to the necrotophic stage. The secretion of a wide range of CWDEs is another characteristic of necrotrophy, causing maceration of host tissue and increasing the nutrient availability. The pH regulator pacC (KLAP2) of *Colletotrichum acutatum* is involved in the pH-regulation of CWDEs and proteolytic enzymes to initiate the necrotrophic stage (You and Chung, 2007).

Necrotrophs, such as *Botrytis cinerea* and *Cochliobolus carborum,* thrive of dead tissue, and obtain nutrients from their host shortly after penetration, aided by the rapid production of toxins and a battery of differentially regulated CWDEs including endopolygalacturonases, pectin methylesterases, cellulases, ß-1,4-xylanases and hemicellulases. These enzymes decompose cell wall components and break down proteins in the middle lamellae to separate plant cells from each other, softening the cell wall and causing cell death.

There is evidence that hemibiotrophs also employ CWDEs during necrotrophy, although in much smaller amounts and more localised than necrotrophs. Thus, the polygalacturonase ClPG2 which cleaves the linkages between D-galacturonic acid residues in non-methylated homogalacturonan (a major component of pectin) and the pectin lyase pel2 are upregulated in the necrotrophic phase of *Colletotrichum lindemuthianum* (Herbert *et al.*, 2004) and *Colletotrichum gloeosporioides* (Shih, J. *et al.* 2000), respectively. However, some CWDE are also expressed during the biotrophic stage, *e. g.* the pectin lyase pnl2 of *Colletotrichum gloeosporioides* (Wei *et al.*, 2002). Furthermore, the protein kinase Snf1 has been found to play an important role in the regulation of CWDEs in *Magnaporthe oryzae* (Tonukari *et al.*, 2000; Yi *et al.*, 2008). Obligate biotrophs also use CWDEs during pathogenesis although it is unclear to what extent. Disruption of the polygalacturonase genes cppg1 and cppg3 of the biotroph *Claviceps purpurea* resulted in decreased pathogenicity (Oeser *et al.*, 2002). However, genes encoding CWDEs such as endopolygalacturonases are also present in the genomes of non-pathogenic fungal species

such as *Saccharomyces cerevisae* and *Kluyveromyces marxianus*, suggesting that they are not always associated with infection and may also serve a nutritional function (Jia and Wheals, 2000).

Additionally, some necrotrophs such as *Sclerotinia sclerotiorum* and *Botrytis cinerea* also produce oxalic acid to stimulate secreted enzymes such as pectinases, proteinases and laccases that are active in acidic environment (Manteau *et al.*, 2003) and chelate calcium ions embedded in pectin, making it more accessible to CWDEs (van Kan, 2006). Necrotrophs not only actively kill the host by hydrolytic enzymes and secreted phytotoxic molecules, they also exploit the host defence response to facilitate cell death, for example by triggering an oxidative burst to elicit cell death during cuticle penetration (Govrin and Levine, 2000; Deighton *et al.*, 2001; Schouten *et al.*, 2008). Necrosis-related proteins causing cell lysis and death of host cells are also involved (van Kan, 2006).

1.2.5 Secondary metabolites

To facilitate plant colonisation, some fungi produce phytotoxic secondary metabolites. Plants may be resistant to a particular pathogen if they produce an enzyme(s) that catalyses the detoxification of this metabolite(s). Toxins of pathogenic fungi are sometimes proteins but typically secondary metabolites synthesised from precursors from different pathways of primary metabolism and are therefore chemically very diverse. For example, the AM-toxin of *Alternaria alternata*, a cyclic depsipeptide, causes death of leaf cells (Okuno *et al.*, 1974). Fusaric acid produced by several *Fusarium* species decreases plant cell viability by binding to metal ions, altering cell growth and mitochondrial activity and increasing permeability of the host cell membrane (Bouizgarne *et al.*, 2006). Toxin production is affected by the nutrient supply, the stage of the host life cycle and the fungal disease cycle. The HC toxin of *Cochliobolus carbonum* is developmentally regulated and expressed in appressoria (Weiergang *et al.*, 1996). The polyketide synthase ACE1 of *Magnaporthe grisea* is involved secondary metabolite synthesis and is expressed during penetration and early in infection (Collemare *et al.*, 2008). The isolates of *Pyricularia grisea* pathogenic on *Digitaria* plants produce and secrete pyrichalasin H. Pyrichalasin H belongs to class of a cytochalasin and may prevent actin polymerisation by binding to the plus end of actin

filaments (Tsurushima *et al.*, 2005). Interestingly, the production of this compound is not found among isolates pathogenic on other plant, suggesting it is responsible for genus-specific pathogenicity on *Digitaria* plants (Tsurushima *et al.*, 2005). Similarly to toxins, the Snodprot family includes small fungal secreted proteins with characterised members in *Magnaporthe grisea*, *Ceratocystis fimbirata* f. sp. *platini* and *Ophiostoma novo ulmi* having putative phytotoxic properties and may also be translocated into the host (Skinner *et al.*, 2001;Boddi *et al.*, 2004; Jeong *et al.*, 2007).

1.2.6 Overcoming plant defence responses

Fungal pathogens resort to several mechanisms to overcome the multilayered plant defence response confronting them inside the host, *e. g.* reactive oxygen species, phytoalexins and callose deposition in so-called papillae. Biotrophs need to avoid inducing host cell death and defence responses, or to suppress them. In contrast, during necrotrophy, pathogens actively trigger host defence responses involving host cell death, which they benefit from.

Necrotrophs must be able to protect themselves against the host defence responses that they trigger. In *Botrytis cinerea* and *Fusarium oxysporum*, chitin synthases are not only involved in maintaining cell wall integrity required for proper growth *in planta* (Soulie *et al.*, 2003), but are also required for resistance to the plant antimicrobial compounds α-tomatine and hydrogen peroxide (Madrid *et al.*, 2003). To protect themselves against reactive oxygen species, hyphae of *Botrytis cinerea* are covered with a sheath containing extracellular catalase, secreted superoxide dismutase and possibly laccases, polyphenol oxidase and alternative oxidases (Mayer *et al.*, 2001).

In biotrophs and hemibiotrophs, cell wall composition can play a role in evading detection by the host. Thus, the cell wall assembly regulator, ClaSSD1 of *Colletotrichum lagenarium,* is required for successful penetration as it avoids the formation of papillae by epidermal cells. Similarly, its orthologue in *Magnaporthe grisea,* MgSSD1, is needed for penetration as it prevents the accumulation of reactive oxygen species within host cells (Tanaka *et al.*, 2007). In *Colletotrichum graminicola*, chitin exposed on the hyphal surface is deacetylated, to avoid degradation of chitin by plant chitinases which would result in the recognition of chitin fragments by the plant and subsequent elicitation of defence responses

(El Gueddari *et al.*, 2002). Similarly, the proline-rich glycoprotein CIH1 found on the surface of biotrophic hyphae of *Colletotrichum* species and the secreted protein ECP6 of *Cladosporium fulvum,* have one or more LysM chitin-binding domains suggesting they may function in binding to chitin in the fungal cell wall (Perfect *et al.*, 1998; Rivas and Thomas, 2005; van Esse *et al.*, 2007). The secreted protein AVR4 of *Cladosporium fulvum* is also involved in chitin binding although it has no LysM domains and it may also function to shield chitin to avoid recognition by the host plant (Bolton *et al.*, 2008).

In the case that plant defence responses are triggered, biotrophic and hemibiotrophic pathogens need to rapidly protect themselves against them. To this end, the biotroph *Ustilago maydis* employs the transcription factor Yap1 to regulate the detoxification of host hydrogen peroxide by peroxidases (Molina and Kahmann, 2007). Likewise, *Colletotrichum lagenarium* has a transfer RNA modifier, APH1, involved in tolerance to hydrogen peroxide during penetration (Takano *et al.*, 2006). The rust *Uromyces fabae* produces mannitol which the host cannot metabolise and which therefore accumulates in the infected leaves where it serves as a scavenger of reactive oxygen species (Voegele *et al.*, 2005). *Colletotrichum gloeosporioides* uses CgDN3, a small secreted protein with weak homology to plant wall associated receptor-like kinases to avert HR-like responses and may act as a suppressor of host cell death during the biotrophic phase (Stephenson *et al.*, 2000).

Phytotoxins also play an important part in host defence. To protect themselves against these antimicrobial compounds, pathogens detoxify or compartmentalise the compounds or actively expel them from the cell. For example, *Botrytis cinerea* can break down the phytoalexin wyerone of the broad bean *Vicia faba* (Mansfield, 1980), *Nectria haematococca* can detoxify the phytoalexin pisatin (Wasmann and VanEtten, 1996) and *Gaeumannomyces graminis* possesses an avenacinase enzyme to detoxify the preformed antifungal compound avenacin present in oat roots (Bowyer *et al.*, 1995). The tomatinase of *Septoria lycopersicon* has a dual function in defence against host responses. It is involved in the detoxification of α-tomatine, a preformed phytoalexin and the degradation product of this hydrolysis suppresses induced defence responses such as cell death and ß-1,3-glucanase expression by interfering with fundamental signal transduction processes leading to disease resistance (Martin-Hernandez *et al.*, 2000). Pathogens also have efflux transporters such as the ATP-binding cassette (ABC) transporters Abc1 of *M. grisea* and BcartB of *Botrytis*

cinerea and major facilitator superfamily (MFS) transporter MgMFS1 of *Mycosphaerealla graminicola* to export plant defence compounds out of the fungal hyphae (Urban *et al.*,1999; Schoonbeek *et al.*, 2001; Roohparvar *et al.*, 2006).

Proteins delivered into the plant cell may also play roles in manipulating host cellular responses that suppress defence mechanisms and allow morphological changes to be elicited in the host cells. Such secreted effector proteins are being extensively studied in bacterial and oomycete pathogens where specialised delivery mechanisms have been identified. Bacterial effectors are directly delivered into the host cell by the type III secretion system (Galan and Wolf-Watz, 2006) whereas oomycete effectors have a conserved host cell-targeting motif RxLR-EER required for their translocation from biotrophic feeding structures and in some cases into the plant cytoplasm possibly using host endocytic machinery (Morgan and Kamoun, 2007; Whisson *et al.*, 2007). However, less is known at the molecular level of how fungal effectors enter the host cells and entrain host metabolism. The perception of Avr gene products appears to be mostly intracellular via cytoplasmic resistance proteins indicating that fungal proteins are translocated to the host cytoplasm during pathogenesis. For example, the *Magnaporthe grisea* metalloprotease Avr-Pita interacts directly with the corresponding R protein Pi-ta intracellularly (Jia *et al.*, 2000). Proteins of the rust fungi *Melamspora lini* AvrL567 and *Uromyces fabae* RTP1p have also been found in the host cytoplasm and nucleus in the case of RTP1p (Dodds *et al.*, 2004; Kemen *et al.*, 2005).

Recently, a P-type ATPase, APT2, encoding a putative golgi-localised aminophospholipid translocase, required for exocytosis of certain secreted proteins, was shown to be essential for pathogenesis in *Magnaporthe grisea,* supporting the importance of secretion in host-pathogen interactions (Gilbert *et al.*, 2006). Sequencing of whole fungal genomes has revealed that pathogens possess large suites of putative secreted proteins. In *Ustilago maydis*, 12 gene clusters encoding predicted secreted proteins were found (Kämper *et al.*, 2006). Similarly, genome analysis of the ectomycorrhizal fungus *Laccaria bicolor* revealed that mycorrhizae are also rich in secreted proteins, including mycorrhiza-induced small secreted proteins (MISSPs) that may have effector-like functions (Martin *et al.*, 2008).

1.2.7 Sporulation

An important step in the life cycle of any pathogen is reproduction and dissemination of propagules. Several genes involved in the induction of sporulation have been identified in pathogenic fungi. These include cAMP dependent protein kinases such as CtPKAC of *Colletotrichum trifolii* involved in the transition from vegetative growth to conidiation (Yang and Dickman, 1999). In *Ustilago maydis*, Hda1, a histone deacetylase (Reichmann *et al.*, 2002) and Rum1, a transcriptional repressor acting on chromatin structure (Quadbeck-Seeger *et al.*, 2000) have been found to be required for teliospore formation. In *Botrytis cinerea*, the adenylate cyclase Bac is required for conidiation (Klimpel *et al.*, 2002).

1.2.8 Signalling during pathogenesis

Many components of intracellular signalling pathways have been identified in pathogenic fungi as signal transduction is involved in perception of the environment and transmission of external signals leading to altered cell responses, gene expression and morphogenesis at all stages of pathogenesis, *e. g.* germination, appressorium formation, penetration, expression of CWDEs and sporulation. The signal transduction pathways in fungi include mitogen-activated protein kinases (MAPKs), cAMP-dependent pathways and calcium ions-mediated signal transduction and involves several regulatory proteins such as the G proteins.

A family of serine/threonine protein kinases known as MAPKs is involved in transducing extracellular signals by activating a cascade of conserved phosphokinases (MAPK kinase kinases, MAPK kinases and MAPKs) which in turn activate and mediate cellular responses to specific environmental stimuli resulting in the activation of transcription factors and changes in the expression of target genes (Nishida and Gotoh, 1993). In the cAMP-dependent pathway, adenylyl cyclase increases the cAMP level in response to a signal allowing cAMP to bind to the regulatory subunit of protein kinase A (PKA), triggering it to release active catalytic subunits which have multiple targets and controls the phosphorylation of transcription activators and repressors, kinases and metabolic enzymes. There is evidence for cross-talk among MAPKs and cAMP-dependent pathways, although the regulatory mechanism is not yet well understood. Calcium

signalling functions by the binding of free intracellular calcium ions to a small, acidic and conserved intracellular calcium receptor called calmodulin (Williams, 1992). Upon binding, conformational changes are induced in the calmodulin resulting in the activation of many enzymes including the multifunctional, calmodulin-dependent protein kinases and protein phosphatases (Williams, 1992). In addition, membrane receptors known as G-protein-receptors coupled to a monomeric Gα protein catalyse the exchange of GDP to GTP on their Gα protein partner. This dissociates the complex into Gα protein and Gβγ heterodimer which can then activate downstream effectors, leading to increased levels of secondary messengers (such as cAMP) or the stimulation of a protein kinase, resulting in changes in protein phosphorylation (Koelle, 2006). This in turn can affect metabolism, ion fluxes, gene expression, cell morphology, cellular differentiation, and many other developmental processes.

In fungal pathogenicity, there are numerous examples of the role of MAPK in responses to mating pheromones, nutrients and recognition of host surface. MAPKs in *Magnaporthe grisea*, *Botrytis cinerea*, *Colletotrichum lagenarium* have been found to be required for appressorium formation (Xu. and Hamer, 1996; Xu, 2000; Takano *et al.*, 2000; Zheng *et al.*, 2000; Kojima *et al.*, 2002). In the necrotroph *Fusarium graminearum*, the production of extracellular enzymes required for penetration is regulated by the MAPK Gpmk1 (Jenczmionka and Schafer, 2005). Furthermore, the formation of the penetration peg of *Magnaporthe grisea* is regulated by the MAPK pathway (Xu *et al.*, 1998). The MAPK of *Fusarium graminearum* is needed for cell wall strength and resistance to CWDEs (Hou *et al.*, 2002). In *Cochliobolus heterostrophus*, a MAPK has been identified which is involved in multiple stages of pathogenicity, including appressorium formation and conidiation (Lev *et al.*, 1999). Similarly, a MAPK has been found to be necessary for full virulence of *Ustilago maydis* (Mayorga and Gold, 1999). As with the MAPK pathway, cAMP signalling is also essential for appressorium penetration (Xu *et al.*, 1997; Yang and Dickman, 1999) and for the mobilisation of glycogen during appressorium formation (Thines *et al.*, 2000). In *Magnaporthe grisea*, adhesion might also be mediated by integrin-like receptor and modulated via a cAMP-dependent signalling mechanism (Bae *et al.*, 2007). Likewise, Gα proteins have been found to be important in numerous aspects of pathogenicity. The Gα protein BCG3 of *Botrytis cinerea* is needed for nutrient-induced

germination, penetration and sporulation (Doehlemann *et al.* 2006). The G-protein-coupled plasma membrane receptor PTH11 of *M. grisea* is required for sensing the environment and induction of appressorium formation (DeZwaan *et al.*, 1999; Kulkarni *et al.*, 2005). The calcium signalling system involving calmodulin-dependent protein kinases has also been implicated in appressorium-related morphogenesis of *Colletotrichum* species (Warwar and Dickman, 1996; Kim *et al.*, 1998; Warwar *et al.*, 2000; Uhm *et al.*, 2003; Sakaguchi *et al.*, 2008) and *M. grisea* (Liu and Kolattukudy, 1999; Viaud *et al.*, 2002) and hyphal branching in *F. graminearum* (Robson *et al.*, 1991).

1.3 Identifying fungal pathogenicity genes by random insertional mutagenesis

Several approaches have led to the identification of genes involved in fungal pathogenicity. These include investigating candidate pathogenicity genes, usually chosen by their homology to genes studied in other organisms, their expression correlating with pathogenicity, the identification of the gene product in infected tissue, the prediction of pathogenicity-related domains or motifs in the gene product or the predicted location of the gene product. A function in pathogenicity can then be confirmed by targeted gene disruption, silencing or overexpression of the candidate gene. However, a candidate gene approach can be biased for previously characterised genes or functions. A popular method which has led to the identification of many novel fungal pathogenicity genes involves generating a library of random mutants and screening them for loss of pathogenicity (Bolker *et al.*, 1995; Thon *et al.*, 2000; Seong *et al.*, 2005; Betts *et al.*, 2007; Jeon *et al.*, 2007).

Mutagenesis was first performed in fungi using radiation or chemicals as mutagens. Since the first genetic transformation of *Neurospora crassa* in 1973 (Mishra and Tatum, 1973), the heterologous integration of DNA has been improved and is now widely used to cause random gene disruption (insertional mutagenesis) in many of fungal species. An advantage of insertional mutagenesis is that the mutated gene is tagged by the transforming DNA and can subsequently be cloned. A good transformation method achieves a high frequency of random transformation events, as single copy integrations at a single locus in

the genome and avoids rearrangements or deletions of either the transferred DNA or the recipient genomic DNA (Michielse *et al.*, 2005). Several transformation techniques can be used to integrate heterologous DNA (Mullins and Kang, 2001; Weld *et al.*, 2006). These methods include particle bombardment (biolistic transformation), calcium chloride ($CaCl_2$)/polyethylene glycol (PEG) and lithium acetate (LiAc)/PEG transformation of protoplasts, electroporation, transposon-tagging and *Agrobacterium tumefaciens*-mediated transformation (ATMT). All methods have their own advantages and disadvantages which are summarised in Table 1.

Table 1. Summary of different transformation methods used for filamentous fungi

Method	Genera with examples of transformed species	Advantages of technique	Disadvantages of technique	References
Biolistics	*Cryptococcus, Gigaspora*, *Gliocladium, Phytophora, Pleurotus, Trichoderma, Venturia*	▪ Applicable to conidia ▪ High transformation frequency ▪ Mitotically stable	▪ Lesions in genomic DNA ▪ Tandem repeat integration ▪ Complex integration events	Forbes *et al.* 1998; Davidson *et al.* 2000; Cvitanich and Judelson, 2003; Lorito *et al.* 1993; Parker *et al.* 1995; Hazell *et al.* 2000; Sunawaga and Magae, 2002
Electroporation	*Aspergillus, Flammulina, Neurospora, Penicillium*, *Trichoderma*	▪ High transformation frequency ▪ Mitotically stable	▪ Requires protoplasts ▪ Lesions in genomic DNA ▪ Tandem repeat integration	Ward *et al.* 1989; Ozeki *et al.* 1994; Vijayaraghavan and Kapoor, 1996; Kuo *et al.* 2004; Reyes *et al.* 2002; Hazell *et al.* 2000
$CaCl_2$/PEG LiAc/PEG	*Aspergillus, Gliocladium*, *Venturia*, *Verticullum*	▪ High transformation frequency ▪ Mitotically stable	▪ Requires protoplasts (spores) ▪ Lesions in genomic DNA ▪ Tandem repeat integration	balance *et al.* 1983; Amey *et al.* 2002; Fitzgerald *et al.* 2003; Lorito *et al.* 1993
PEG transformation with REMI	*Ustilago, Magnaporthe, Colletotrichum*	▪ High transformation frequency ▪ Mitotically stable	▪ Requires protoplasts ▪ Lesions in genomic DNA ▪ Tandem repeat integration ▪ Multiple integration ▪ Untagged mutations ▪ Bias for highly transcribed regions	Sweigard *et al.* 1998; Kahmann and Basse, 1999; Thon *et al.* 2000
ATMT	*Aspergillus*, *Agaricus, Botrytis, Colletotrichum, Coniothyrium*, *Fusarium*, *Magnaporthe*, *Monilinia*, *Ophiostoma*, *Pythium, Phytophtora*, *Mycosphaerella, Verticillium*	▪ No protoplasts needed ▪ Very high transformation frequency ▪ Mitotically stable ▪ High proportion of single copy insertions ▪ Low complexity of integration events ▪ Applicable to wide range of fungi ▪ Random insertions	▪ Transformation of multinucleate fungi may not result in homokaryotic tissue ▪ Possible bias for insertion in transcribed and promoter regions ▪ Genomic rearrangement may occur ▪ Untagged mutations	De Groot *et al.* 1998; Michielse *et al.* 2005; Rolland *et al.* 2003; De Groot *et al.* 1998; Mullins *et al.* 2001; Rho *et al.* 2001; Tsuji *et al.* 2003; Rogers *et al.* 2004; Takahara. *et al.* 2004; Tanguay and Breuil, 2003; Lee and Bostock, 2006; Vijn and Govers, 2003; Zwiers and De Waard, 2001; Amey *et al.* 2002; Weld *et al.* 2006
Transposon-tagging	*Aspergillus, Mycosphaerella, Magnaporthe, Penicillium*, *Tolypocladium*	▪ high efficiency transformation system not required ▪rare genomic lesions and rearrangements	▪ Few systems available ▪ Transformants not stable ▪ Bias for non-coding regions	Giulia *et al.* 2001; Firon *et al.* 2003; Adachi *et al.* 2002; Hamer *et al.* 2001; Kempken and Kuck, 2000; De Queiroz and Daboussi, 2003

REMI: Restriction enzyme-mediated Integration, PEG: polyethylene glycol, ATMT: *Agrobacterium tumefaciens*-mediated transformation

Biolistic transformation of fungi involves shooting DNA-covered microparticles of colloidal gold or tungsten into fungal conidia or mycelium at high speed. However, the transformants may suffer genomic lesions and tandem integrations occur at high frequency (Weld *et al.,* 2006).

High concentrations of LiAC or $CaCl_2$ and brief exposure to a high amplitude electric field can be used to permeabilise protoplast membranes to allow uptake of foreign DNA and integration into the genome. PEG promotes cell agglomeration to facilitate DNA uptake. For certain species, PEG-mediated protoplast transformation yields a high frequency of transformants (Amey *et al.*, 2002). However, the main disadvantage of this method is the use of protoplasts. CWDEs used to prepare protoplasts are inconsistent and because the cell wall-free protoplasts are osmotically sensitive they must be handled with care and protected at all times by solutions providing osmotic support. Furthermore, the transformed protoplasts may still harbour multiple and/or tandem insertions or genomic lesions. For insertional mutagenesis, protoplast transformation was improved by the introduction of restriction enzyme-mediated integration (REMI), which significantly increases the frequency of transformation and the frequency of single-copy insertions (Bolker *et al.,* 1995). REMI involves the transformation of cells with a restriction enzyme(s) which generate cohesive ends in the genome. The double-stranded breaks recombine with the plasmid DNA linearised with the same restriction enzyme, resulting in the integration of the vector into the genome at the recognition site of the restriction enzyme (Riggle and Kumamoto, 1998). However, the genomic DNA can suffer damage, for example the chromosome may be digested by the restriction enzyme and imperfect DNA repair may follow during transformation, resulting in an untagged mutation (Sweigard *et al.,* 1998). A major disadvantage of REMI is the high proportion (up to one third) of mutations that are not tagged by the selectable marker, making cloning of the gene responsible for the mutant phenotype more complicated (Lu *et al.,* 1994; Yun *et al.,* 1998; Kahmann and Basse, 1999; Maier and Schafer, 1999; Redman *et al.,* 1999; Kuspa, 2006). Furthermore, depending on the fungal recipient, REMI can produce varying efficiency of integration events, proportions of single insertions, tandem insertions, deletions of flanking restriction sites, ectopic integration in the absence of an appropriate restriction site, and large genome deletions and inversions (Kahmann and Basse, 1999). It also seems that integration of the

transforming DNA is not completely random but biased towards highly transcribed genomic regions (Lu *et al.* ,1994).

Mobile elements such as transposons have also been used to make insertional mutants in fungi (Daboussi and Capy, 2003). Reliable heterologous transposon tagging techniques are still not well-established, but the recent development using the transposable elements *impala* from *Fusarium oxysporum* (Villalba *et al.,* 2001) and *restless* from *Tolypocladium inflatum* (Kempken and Kuck, 2000) has allowed the development of transposon-based insertional mutagenesis (Hamer *et al.* 2001; De Queiroz and Daboussi, 2003; Firon *et al.,* 2003). A transposon encodes a transposase which recognises inverted terminal repeats on the transposon and mediates its excision and reintegration in the recipient genome. An advantage of transposon-tagging is that genomic rearrangements caused by aberrant transposition are rare. However, the frequency of transpositions can vary widely, the extent to which integration is random is not known and stable integration is not very common. Furthermore, transposons have been found to integrate preferentially in non-coding regions of the genome (Firon *et al.,* 2003; Ladendorf *et al.,* 2003).

The Gram-negative soil bacterium *Agrobacterium tumefaciens* has been successfully exploited to transfer genes to a wide variety of hosts. As a pathogen, *A. tumefaciens* causes crown gall on a broad range of plants (Escobar and Dandekar, 2003). The mechanism of host manipulation used during infection is exploited for genetic engineering. The tumour-inducing (Ti) plasmid of *A. tumefaciens* contains transferred DNA (T-DNA) which is transferred to the host cell and integrated into the host genome during tumorigenesis and large number of *vir* genes. *vir* genes encode proteins involved in the formation, transport and integration of the T-DNA in the host genome via a conjugation-like process, the type IV secretion system (Felman. and Marks, 1987). Phenolic compounds found in plant wound exudates, such as acetosyringone, induce the *vir* regulon and the formation of single-stranded T-DNA and its transfer (Zupan *et al.,* 2000). The T-region is surrounded by a short border repeats, which act as cis-acting signals for DNA delivery. Apart from theses left and right borders (LB and RB), the T-DNA sequence can be deleted and replaced with the gene to be transformed in genetic engineering (Hooykaas and Beijersbergen, 1994). For genetic manipulation of the small T-DNA, a binary vector system, with the T-DNA and the virulence regions placed on separate plasmids, is used. In 1995,

the first fungal species, the yeast *Saccharomyces cerevisae,* was transformed by ATMT (Bundock *et al.,* 1995) and subsequently, ATMT has been applied to many filamentous fungi (De Groot *et al.,* 1998; Mullins and Kang, 2001; Michielse *et al.,* 2005). The principle advantages of ATMT over previous methods of transformation are the high efficiency of transformation, the frequency of single-copy integrations, the creation of fewer untagged mutations and the ability to transform intact cells (hyphae, spores, and even mycelial tissue and fruiting body) as well as protoplasts (De Groot *et al.,* 1998). The integration of the T-DNA appears to be approximately random, although there is evidence for bias towards transcribed regions and promoters in particular. Major truncations or rearrangements of transferred DNA are rare, although small deletions can occur at both borders of the T-DNA (Flowers and Vaillancourt, 2005; Bundock *et al.*, 1995). Integration of vector sequences from outside the T-DNA and genomic rearrangements varying from small genomic deletions (~100bp) to major chromosomal translocations have been reported (Flowers and Vaillancourt, 2005; Weld *et al.* 2006). Several recent studies have questioned the randomness of T-DNA integration into recipient fungal genomes (Choi *et al.,* 2007; Li *et al.,* 2007; Meng *et al.,* 2007). Nevertheless, ATMT has become the method of choice for insertional mutagenesis and has been successfully exploited for large-scale forward genetic screens in several pathogenic species, including *Magnaporthe grisea*, *Cryptococcus neoformans*, *Colletotrichum lagenarium* and *Leptosphaeria maculans* (Tsuji *et al.,* 2003; Walton *et al.,* 2005; Betts *et al.,* 2007; Blaise *et al.,* 2007; Jeon *et al.,* 2007).

In addition to generating random integrations, ATMT can also be exploited to obtain targeted gene disruption or replacement. In most fungal species, ectopic integrations of the transforming DNA are much more frequent than homologous integrations, resulting in a low frequency of targeted mutation. Strains with improved levels of gene replacement by homologous recombination can be obtained by disrupting the non-homologous DNA end-joining pathway by the targeted deletion of the Ku70 or Ku80 genes. This strategy has been used with success in several species (Kooistra *et al.,* 2004; Ninomiya *et al.* 2004; da Silva Ferreira *et al.,* 2006; Goins *et al.,* 2006; Krappmann *et al.,* 2006; Nayak *et al.,* 2006; Poggeler, and Kuck, 2006; Takahashi, *et al.*, 2006; Chang, 2008; Haarmann *et al,.* 2008; Villalba *et al.,* 2008).

1.4 *The* Arabidopsis thaliana-Colletotrichum higginsianum *pathosystem for studying plant-microbe interactions*

Colletotrichum higginsianum causes anthracnose disease on a wide range of cruciferous plants, including agronomically important species such as *Brassica* and *Raphanus*, as well as the model plant *Arabidopsis thaliana* (Narusaka *et al.,* 2004; O'Connell *et al.,* 2004). To invade host tissues, this hemibiotrophic fungus sequentially elaborates a series of specialised infection structures, as illustrated in Figure 1. Following attachment to the plant surface, conidia germinate to form dome-shaped, melanised appressoria that pierce the cuticle and cell wall directly by means of a narrow penetration peg. A swollen primary hypha then invades a living epidermal cell and invaginates the host plasma membrane, like the haustoria of obligate biotrophs (Bailey and Jeger, 1992). Both the biotrophic phase and the specialised primary hyphae of *C. higginsianum* are entirely restricted to the first epidermal cell, in contrast to other hemibiotrophic *Colletotrichum* species (Perfect *et al.,* 1999). Destruction of host tissue and macroscopic symptoms are not observed during this initial biotrophic stage. It is assumed the fungus uses different strategies to avoid eliciting host responses during biotrophy, possibly by masking invading hyphae to avoid host recognition or by actively suppressing host cell death and host defence responses. As in interactions with obligate biotrophs, host cells penetrated by the primary hyphae of *C. higginsianum* retain normal plasma membrane function during the biotrophic phase (O'Connell, *et al.* 2004). The primary hypha thus remains topologically outside the cell membrane, in the apoplast, so that nutrients must enter the fungus by crossing the plasma membrane of both partners. In addition, similar to haustoria, the primary hyphae of *Colletorichum* are surrounded by an interfacial matrix containing fungal glycoproteins that may be important for establishing and maintaining biotrophy and possibly suppressing host defences (Perfect *et al.,* 1998). There is also evidence that the primary hyphae locally modify the composition of the host plasma membrane, as reported for the extrahaustorial membrane of rusts and powdery mildews (Shimada *et al.,* 2006). Thus, the biotrophic primary hyphae of *C. higginsianum* may obtain nutrients from the plant apoplast in a similar way to the specialised haustoria of obligate biotrophs (Perfect *et al.,* 1998; 1999). Thereafter, the fungus switches to a necrotrophic mode of nutrition, associated with the

production of thin secondary hyphae which ramify within and between host cells and kill host cells ahead of infection. The asexual stage is completed by the production of acervuli on the surface of the dead host tissue. Acervuli consist of a mass of short conidiophores interspersed with long hair-like setae, which have darkly melanised cell walls like the appressoria.

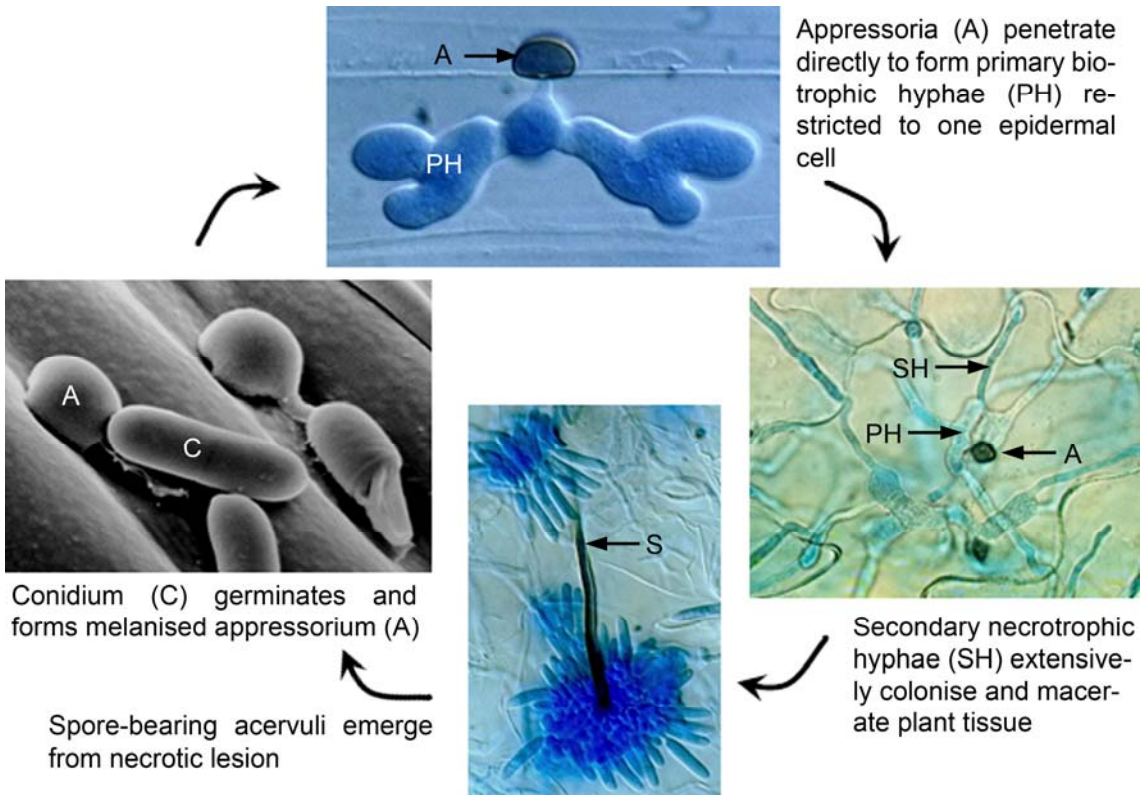

Figure 1. Life cycle of *Colltotrichum higginsianum*
A conidium (C) germinates on the plant surface, forms a short germ tube and differentiates an appressorium (A) in which the turgour pressure required for penetration is generated. A penetration peg penetrates the host epidermal cell directly. In the initial stage of the interaction, *C. higginsianum* forms a biotrophic primary hypha (PH) restricted to the first penetrated epidermal cell. The fungus then switches to a necrotrophic mode of growth, when long secondary hyphae (SH) grow extensively within and between host cells. *C. higginsianum* reproduces asexually by the production of conidia from acervuli containing melanised hair-like setae (S) which breach the cuticle and the host cell wall and erupt onto the surface of the dead tissue.

The *C. higginsianum-A. thaliana* pathosystem provides an attractive model for the molecular dissection of plant-fungal interactions. In addition to its interesting hemibiotrophic lifestyle and developmental transitions, *C. higginsianum* has haploid, uninucleate spores and can be cultured axenically and stably transformed, allowing the analysis of gene function by random mutagenesis and targeted gene disruption (O'Connell *et al.,* 2004), unlike many economically important crop pathogens which are obligate biotrophs. Moreover, in contrast to other *Colletotrichum* species, the plant host is also amenable to molecular manipulation and extensive genomic resources and genetic tools are available for analysing resistant and susceptible responses. However, although some candidate genes have been identified from the sequence analysis of stage-specific cDNA libraries (Kleemann *et al.,* 2008), no molecular determinants of pathogenicity or virulence have so far been isolated from *C. higginsianum*. In other *Colletotrichum* species, forward and reverse genetics approaches have identified many genes required for pathogenicity and infection-related morphogenesis (Table 2). However, most of these function at the early stages of infection, *e. g.* appressorium formation (Takano *et al.,* 2000; Kojima *et al.,* 2002), appressorium melanisation (Takano *et al.,* 1995; Perpetua *et al.*,1996; Tsuji *et al.,* 2000; Kimura *et al.,* 2001; Takano *et al.,* 2001) and host penetration (Veneault-Fourrey *et al.,* 2005; Asakura *et al.,* 2006; Hoi *et al.,* 2007). In contrast, relatively few factors required for post-penetration development and tissue colonization have been uncovered in *Colletotrichum* species. Examples include genes with putative functions in the avoidance or tolerance of host defence responses (Takano *et al.,* 2006; Tanaka *et al.,* 2007), establishment or maintenance or biotrophy (Dufresne *et al.,* 2000; Stephenson *et al.,* 2000) and the switch from biotrophy to necrotrophy (Thon *et al.,* 2002; Pellier *et al.*, 2003).

Table 2. Examples of the wide range of pathogenicity genes identified in *Colletotrichum* species

Gene	*Colletotrichum* sp.	Gene Product	Role	References
Germination				
CgCTR2	*C. gloeosporioides*	Putative vacuole copper transporter	Germination,copper homeostasis	Barhoom *et al.* 2008
CaMK	*C. gloeosporioides*	Putative calmodulin kinase	Germination and appressorium formation upon hard surface contact	Kim *et al.* 1998
Cam	*C. gloeosporioides*	Calmodulin	Germination and appressorium formation upon hard surface contact	Kim *et al.* 1998
Chip1	*C. gloeosporioides*	Ubiquitin-conjugating enzyme	Protein degradation during germination and appressorium formation	Liu and Kolattukudy, 1998
Appressorium morphogenesis				
CgMEK	*C. gloeosporioides*	MAPKK	Cell division, septum formation,	Kim *et al.* 2000
CMK1	*C. lagenarium*	MAPK	Germination, appressorium formation	Takano *et al.,* 200)
MAF1	*C. lagenarium*	MAPK	Appressorium differentiation	Kojima *et al.* 2002
ClaKEL2	*C. lagenarium*	Kelch repeat protein	Calcium signalling	Sakaguchi *et al.* 2008
LIPK	*C. trifolii*	Lipid-induced protein kinase	Appressorium formation triggered by cutin	Dickman *et al.* 2003
CgChsV	*C. gloeosporioides*	Chitin synthase class V	Appressorium formation	Werner *et al.* 2007
Appressorium melanisation				
PKS1	*C. lagenarium*	Polyketide synthase	Melanin biosynthesis	Takano, Y. *et al.* 1995
SCD1	*C. lagenarium*	Scytalone dehydrogenase	Melanin biosynthesis	Kubo *et al.* 1996
THR1	*C. lagenarium*	1,3,8-trihyroxynaphtalene reductase	Melanin biosynthesis	Perpetua *et al.* 1996
CMR1	*C. lagenarium*	Transcription factor	Control of melanin biosynthesis genes	Tsuji *et al.* 2000
Clap1	*C. lindemuthianum*	Copper-ATPase transporter	Melanin polymerisation	Pariso *et al.* 2002
ClaPEX6	*C. lagenarium*	Peroxin	Peroxisome function, appressorium melanisation	Kimura *et al.* 2001
Appressorial penetration				
ICL1	*C. lagenarium*	Isocitrate lyase	Glyoxylate cycle in peroxisome, penetration	Asakura *et al.* 2006
ClPLS1	*C. lindemuthianum*	Tetraspanin	Penetration peg development	Veneault-Fourrey *et al.* 2005
RPK1	*C. lagenarium*	Protein kinase A	Penetration, growth, conidiation	Takano *et al.* 2001
CST1	*C. lagenarium*	Transcription factor (Ste12-like)	Appressorial penetration	Tsuji *et al.* 2003
Chip6	*C. gloeosporioides*	Sterol glycosyl transferase	Penetration	Kim *et al.* 2002
Cac1	*C. lagenarium*	Adenylate cyclase	Appressorium-mediated penetration	Yamauchi *et al.* 2004
Cgsnf	*C. gloeosporioides*	sucrose non-fermenting (SNF1)-related protein kinase	Transmitting nutritional signals for penetration	Goodwin and Chen, 2002
CAP20	*C. gloeosporioides*	No homology	Appressorium-mediated penetration	Hwang and Kolattukudy, 1995
CbhII	*C. lindemuthianum*	Cellobiohydrolase (exo-1,4-ß-glucanase)	Degradation of cellulose	Acosta-Rodriguez *et al.* 2005
chsA	*C. graminicola*	Chitin synthase class V	Cell wall strength	Amnuaykanjanasin and Epstein, 2003

Necrotrophy				
CLNR1	*C. lindemuthianum*	Nitrogen regulator	Switch from biotrophy to necrotrophy	Pellier *et al.* 2003
CLPT1	*C. lindemuthianum*	Rab/GTPase	Secretion of proteins *e. g.* CWDEs	Siriputthaiwa *et al.* 2005
Pac1	*C. gloeosporioides*	Transcription factor	pH-signalling and regulation of CWDEs	Prusky *et al.* 2001
CPR1	*C. graminicola*	Signal peptidase	Secretion of CWDEs, switch to necrotrophy	Thon *et al.* 2002
PacKLAP2	*C. acutatum*	Transcriptional regulator	Regulation of CWDEs	You and Chung, 2007
CLPG1,	*C. lindemuthianum*	Endopolygalacturonases	Plant cell wall degradation	Centis *et al.* 1996
CLPG2	*C. lindemuthianum*	Endopolygalacturonases	Plant cell wall degradation	Centis *et al.* 1997
Pnl1	*C. gloeosporioides*	Pectin lyase	Maceration during necrotrophy	Shih *et al.* 2000
Pnl2	*C. gloeosporioides*	Pectin lyase	Maceration during necrotrophy	Shih *et al.* 2000
PME	*C. gloeosporioides*	Pectin methyl esterase	Maceration during necrotrophy	Ortega, 1996
Biotrophy				
CLTA1	*C. lindemuthianum*	GAL4-like protein	Establishment / maintenance of biotrophy	Dufresne *et al.* 2000
CIH1	*C. lindemuthianum*	Protein with LysM domain	Putative role in chitin binding	Perfect *et al.* 2000
Clk1	*C. lindemuthianum*	Serine/threonine kinase	Establishment / maintenance of biotrophy	Dufresne *et al.* 1998
Protection against host defence				
Cgcat1	*C. gloeosporioides*	Small-subunit peroxisomal catalase	Prevent damage from H_2O_2 during necrotrophy	Goodwin *et al.* 2001
CgDN3	*C. gloeosporioides*	Weak homology to plant wall associated RLKs	Suppression of host cell death	Stephenson *et al.* 2000
ClaSSD1	*C. lagenarium*	Weak homology to RNAse II related proteins	Avoid triggering host responses	Tanaka *et al.* 2007
APH1	*C. lagenarium*	transfer RNA modifier	Tolerance to plant defence responses	Takano *et al.* 2006
Conidiation				
ArpA	*C. gloeosporioides*	Actin-related protein	Conidiation	Li *et al.* 2001
CtPKAC	*C. trifolii*	cAMP-dependent protein kinase	Regulation of conidiation	Yang and Dickman, 1999

MAPK: Mitogen Activated Protein kinase; MAPKK: MAPK kinase; cAMP: cyclic AMP; RLK: Receptor-like Kinase, GTPase: guanylyltransferase

1.5 Aims and objectives

The overall aim of this study was to identify novel genes required for the pathogenicity of *C. higginsianum* on *Arabidopsis thaliana* using ATMT for random insertional mutagenesis. Specific objectives were to:

- Optimise the ATMT protocol for *C. higginsianum* to obtain a high transformation efficiency and a high proportion of single insertions.
- Generate a large library of T-DNA transformants.
- Screen the transformants for loss of pathogenicity on *Arabidopsis* plants using a high-troughput primary screen on seedlings and a second more stringent screen on mature plants.
- Classify the mutants according to the stage of infection at which their growth was arrested with the help of microscopic observations.
- Obtain genomic DNA flanking the T-DNA insertions by thermal-asymmetric interlaced (TAIL)-PCR and Inverse PCR.
- Isolate the tagged genes from a cosmic genomic library by PCR-screening using the sequence of flanking region obtained from TAIL-PCR and Inverse PCR:
- Perform detailed functional characterisation of selected tagged genes. These include, depending on the pathogenicity phenotype of the mutants, the ability to penetrate the host epidermis and insert substrates (cellophane membranes, killed tissue), invasive growth ability in wounded tissue, the ability to form primary hyphae and secondary hyphae, and the ability to induce host defence responses, such as HR or callose deposition.
- Confirm the gene(s) tagged by the T-DNA is responable for the pathogenicity defect, either by complementation with the wild-type copy of the gene or by targeted gene disruption.

2 Results

2.1 *Agrobacterium-mediated transformation of* C. higginsianum

2.1.1 *Optimisation of* Agrobacterium-*mediated transformation (ATMT) of* C. higginsianum

In preliminary experiments, efforts were made to optimise ATMT of *C. higginsianum* based on the methods of O'Connell *et al.*, Tsuji *et al.* and Cangelosi *et al.*) to maximise the transformation efficiency and the percentage of transformants with single T-DNA insertions, and thereby facilitate the subsequent identification of tagged genes.

Using the standart protocol (see section 4.9.2), transformants were not always obtained. Several conditions were modified from this protocol: i) presence of acetosyringone during pre-culture of *Agrobacteria* in AB broth, ii) length of the co-cultivation of *Agrobacteria* with the fungal conidia, iii) type of membranes used for the co-cultivation, iv) strains of *Agrobacteria*, v) ratio of *Agrobacteria* to fungal conidia and vi) concentration of hygromycin B in the selection plates. Due to the large variation of the transformation efficiency, it was difficult to determine whether modifications to any of these parameters resulted in a significant improvement in transformation efficiency. Observations made from 16 different transformation experiments are summarised in Table 3. In successful transformations, the number of hygromycin-resistant colonies obtained from 10^6 conidia varied from 75 to 125 (average = 102). The transformation efficiency was found to be highest when using *Agrobacterium* strain C58C1 harbouring either the pBIN-GFP-hph or pBIG2RHPH2 plasmid with induction of acetosyringone in the AB broth and with a co-cultivation time of at least 48 h. The co-cultivation on cellophane also gave more transformants than on paper, but paper membranes were much easier to handle. The *Agrobacterium* strain AGL-1 gave no transformants. Doubling the concentration of *Agrobacteria* had little effect on transformation efficiency. Stringent antibiotic selection may have favoured multiple insertions. Slightly more colonies were obtained when selecting with 70 µg/mL than with 100 µg/mL hygromycin B. However, a proportion of colonies selected on 70 µg/mL were false positives because thee wild-type strain could still

grow well at this concentration. Figure 2 shows the growth ability of the wild type and of a transformant harbouring three copies of the hygromycin B resistance gene on PDA ameneded with hygromycin B (0 to 500 µg/mL). A concentration of hygromycin B of 100 µg/mL allowed significantly less growth by the wild-type than 70 µg/mL and was therefore preferred for selection.

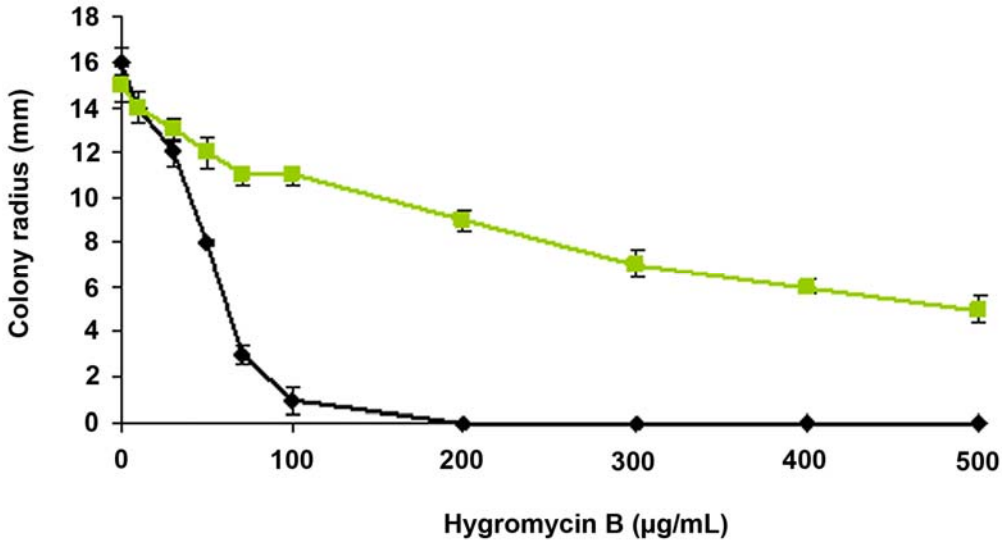

Figure 2. Sensitivity of *Colletotrichum higginsianum* to hygromycin B.
Plates of PDA amended with 0 to 500 µg/mL hygromycin B were inoculated with a 1x1 mm agar plug with growing mycelium. The radial growth was measured after 4 days. Graph shows average of 3 experiments and standard error (error bars) of the radial growth of the wild type (black) and a transformant carrying three copies of the pBIN-GFP-hph T-DNA (green).

2.1.2 Generation of random insertional transformants

A total of 8,850 random insertional transformants was generated, of which 5,100 had pBIN-GFP-hph insertions and 3,750 had pBIG2RHPH2 insertions. The majority were obtained from transformation using *Agrobacterium* strain C58C1, with a co-cultivation of 48 h, on either cellophane or paper and with 100 µg/mL of hygromycin B used for the selection.

2.1.3 Mitotic stability of transformants

Five randomly selected transformants of *C. higginsianum* were sub-cultured for five successive generations on Mathur's agar medium in the absence of hygromycin B and were subsequently screened for hygromycin resistance in the sixth generation. All fungal transformants were resistant to hygromycin B and the *hph* gene could be detected by PCR, confirming stable maintenance of the marker gene across successive generations (data not shown).

Table 3: Comparative analysis of different parameters influencing *Agrobacterium*-mediated transformation efficiency of *Colletotrichum higginsianum*

Experiment	Agrobacterium strain	Plasmid	Membrane for co-cultivation	Hygromycin B concentration (µg/mL)	Induction with AS in AB broth	Co-cultivation time (h)	Bacterial concentration for co-cultivation (OD_{600})	Average number of transformants per 10^6 conidia
1	AGL1	pBIN-GFP-hph	cellophane	100	yes	48	0.2	0
2	AGL1	pBIN-GFP-hph	paper	100	yes	48	0.2	0
5	C58C1	pBIN-GFP-hph	cellophane	100	yes	36	0.2	0
6	C58C1	pBIN-GFP-hph	cellophane	70	yes	48	0.2	112
7	C58C1	pBIN-GFP-hph	cellophane	100	yes	48	0.2	76
8	C58C1	pBIN-GFP-hph	cellophane	100	yes	58	0.2	124
9	C58C1	pBIN-GFP-hph	paper	100	no	48	0.2	46
10	C58C1	pBIN-GFP-hph	paper	100	yes	48	0.2	0
11	C58C1	pBIG2RHPH2	cellophane	100	no	48	0.2	94
12	C58C1	pBIG2RHPH2	cellophane	70	yes	48	0.2	115
13	C58C1	pBIG2RHPH2	cellophane	100	yes	48	0.2	85
14	C58C1	pBIG2RHPH2	paper	100	no	48	0.2	27
15	C58C1	pBIG2RHPH2	paper	100	yes	48	0.2	87
16	C58C1	pBIG2RHPH2	paper	100	yes	48	0.5	93

2.2 Screen for pathogenicity mutants

2.2.1 Primary screen for pathogenicity

All 8,850 hygromycin B-resistant *C. higginsianum* transformants were subjected to two rounds of testing in the primary pathogenicity mutant screen performed by droplet-inoculation of 10-day old seedlings of the susceptible *Arabidopsis thaliana* accession Landsberg *erecta* (L*er*-0) with conidial suspension of the transformants. Epi-fluorescence was used to visualise auto-fluorescing dead tissue 7 days after inoculation (dai) as shown in Figure 3. Seedlings inoculated with conidia of the wild-type strain and pathogenic transformants collapsed and showed extensive green auto-fluorescence. Transformants which produced only limited green-autofluorescent, necrotic lesions or no symptoms at all in both rounds of the primary screen were considered as putative pathogenicity mutants (Figure 3). A total of 265 transformants (3 % of all transformants) consistently produced no visible symptoms or reduced symptoms compared to the wild type.

2.2.2 Secondary screen for pathogenicity

To confirm the altered pathogenicity phenotype of these 265 transformants, they were subjected to two rounds of testing in a secondary screen on mature (3- to 4-week-old) *Arabidpsis* Ler-0 plants spray-inoculated with a standardised spore concentration. Of the 265 transformants screened, 40 (0.45 % of all transformants) consistently produced either no visible symptoms or very reduced symptoms, *e. g.* scattered necrotic specks or small lesions restricted to the oldest rosette leaves and were verified as pathogenicity mutants in the secondary screen (Figure 3). In contrast, the *C. higginsianum* wild-type strain extensively macerated host tissues and plants were completely collapsed 7 dai (Figure 3). These mutants were termed "*path*" (for pathogenicity). Macroscopic symptoms caused by the wild-type strain and the 40 pathogenicity mutants are shown in Supplementary Figure 1.

The altered pathogenicity phenotypes observed in these mutants were not specific to the interaction with *Arabidopsis,* because when inoculated onto seedlings of a highly susceptible *Brassica* host (*B. napus biennis*) they similarly produced very reduced

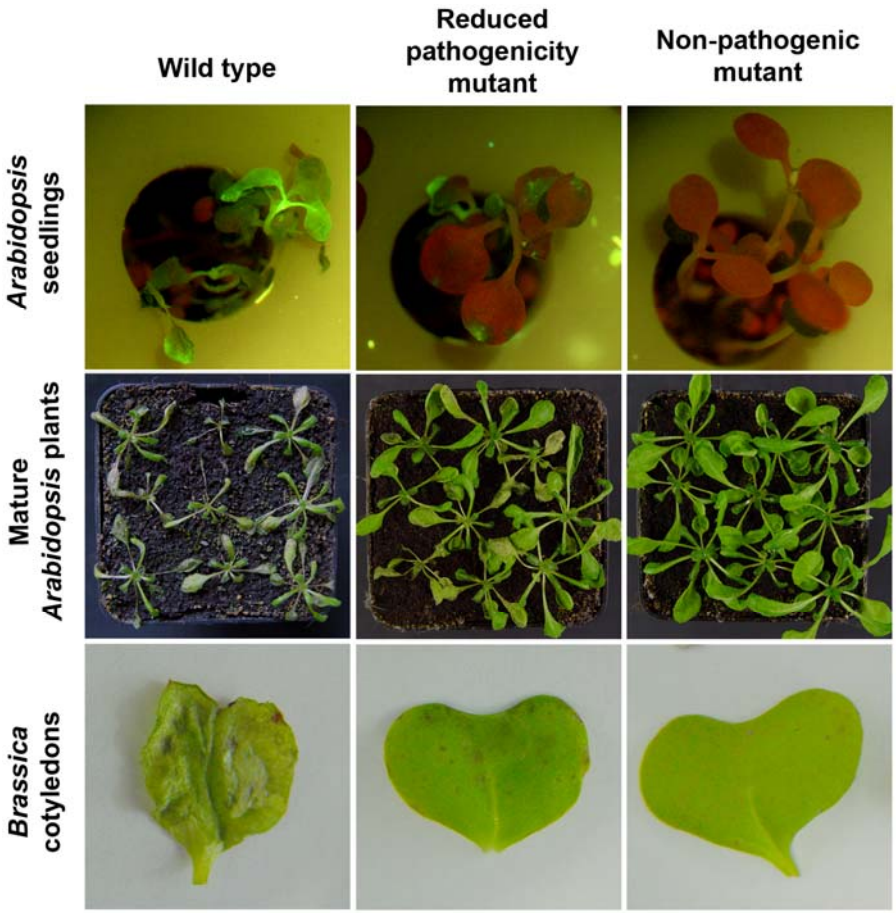

Figure 3. Pathogenicity assays used to select *Colletotrichum higginsianum* mutants.
Top row: In a primary screen, 10-day-old *Arabidopsis* seedlings grown in a 96-well format were droplet-inoculated with c suspension of *C. higginsianum* transformants obtained by irrigating 10-day-old colonies grown in 96-well plates on hygromycin B selection medium. Symptoms were scored at 7 dai by epi-fluorescence microscopy: dead tissue autofluoresced green while healthy tissue autofluoresced red due to chloroplasts autofluorescence. Seedlings inoculated with the wild-type strain collapsed and showed extensive green fluorescence. Transformants causing small green fluorescent necrotic lesions or no visible symptoms were selected as putative pathogenicity mutants. **Middle row:** In a secondary screen, mature *Arabidopsis* plants (3- to 4-week-old) were spray-inoculated with transformant spore suspension (5 x 10^5 conidia mL^{-1}) and examined for symptoms 7 dai. The wild-type strain caused extensive necrosis and maceration; transformants producing limited necrotic lesions were considered reduced pathogenicity mutants; those causing no symptoms were considered non-pathogenic. **Bottom row:** Pathogenicity assay on 8-day-old seedlings of *Brassica napus biennis*. The wild-type strain completely macerated cotyledons whereas pathogenicity mutants produced scattered brown necrotic flecks or no visible symptoms.

symptoms (*i. e.* few small necrotic spots) or no visible symptoms. In contrast, *Brassica* cotyledons were completely macerated by the wild-type strain 7 dai (Figure 3).

It was not possible to test about 20 % of the putative pathogenicity mutants in the secondary screen because they produced insufficient conidia for spray-inoculation at the

required spore concentration (5 x 10^5 conidia per mL). Such candidates appeared to be defective in conidiation rather than vegetative growth but were not characterised further. Other mutants were also eliminated from the secondary screen because their vegetative growth on rich medium (PDA) was severely reduced (>70 %) compared to the wild type The observed reduction in pathogenicity of these mutants would have been due to a severe reduction in general fitness and would not have les to the identification of a pathogenicity gene.

2.3 Phenotypical characterisation of pathogenicity mutants

Light microscopy was used to determine at which stage of host infection the development of the mutants was impaired. Assessments included appressorium morphology (size, shape, melanisation and penetration pore formation); appressorium penetration ability (on living host epidermis, dead leaf tissue or cellophane); ability to form biotrophic primary hyphae and necrotrophic secondary hyphae *in planta*; and induction of host cellular defence responses such as papillary callose deposition and hypersensitive cell death response (HR). Based on microscopic analysis of their infection phenotypes, the 40 pathogenicity mutants were classified into four groups: melanin deficiency, impaired penetration, induction of cellular host defence responses and failure to enter the necrotrophic phase (Table 4).

Table 4: Summary of *Colletotrichum higginsianum* pathogenicity mutant phenotypes.

Mutant ID	Growth on minimal medium [a]	Appressorium melanisation [b]	Penetration of epidermis [c]	Penetration of cellophane [d]	Secondary hyphae [e]	Induction of host defense responses [f]
Wild type	+	++	+++	+++	++	rare P
Melanin-deficient mutants						
path-1*	+	-	-	-	-	-
path-2*	+	+	-	-	-	-
path-3 *	+	+	-	-	-	-
path-4 *	+	-	-	-	-	-
path-5 *	+	-	-	-	-	-
path-6 *	+	+	+	-	+	-
Host penetration mutants						
path-7 *	+	++	+	+++	+	-
path-8 *	+	++	-	-	-	-
path-9 *	+	++	+	-	+	-
path-10 *	+	++	+	++	-	-
path-11 *	+	++	-	++	-	-
path-12 *	+	++	+	++	-	-
path-13 *	+	++	+	++	-	-
path-14 *	+	++	+	-	-	-
path-15 *	+	++	-	-	-	-
path-16 *	+	++	+	-	-	-
path-17 *	+	++	-	-	-	-
path-18 *	+	++	+	-	-	-
path-19 *	-	++	+	+	-	-
path-20 *	-	++	+	+	+	-
path-21 *	-	++	+	+	+	-
Mutants inducing host defense responses						
path-22 *	+	++	+++	+++	+	P and HR
path-23 *	+	++	-	+	-	large P
path-24 *	+	++	++	++	-	HR
path-25	+	+	+++	+++	+	HR
path-26	+	++	+++	+++	+	HR
path-27	+	+	++	+++	+	P and HR
path-28	+	+	+++	+++	+	P and HR
path-29 *	+	++	++	+++	+	HR
path-30 *	+	++	+++	+++	-	HR
path-31	+	++	+++	+++	-	HR
path-32 *	+	++	+	+++	-	P
path-33 *	+	++	+++	+++	+	HR
path-34 *	+	++	++	+++	-	HR
path-35 *	-	++	+	+	-	P
Mutants impaired in switch to necrotrophy						
path-36 *	+	++	+++	+++	+	-
path-37 *	+	++	+++	+++	-	-
path-38 *	+	++	+++	+++	-	-
path-39 *	+	++	+++	+++	-	-
path-40	+	++	+++	+++	+	-

Table 4 continued: Summary of *Colletotrichum higginsianum* pathogenicity mutant phenotypes.
* Mutants causing no symptoms or very reduced symptoms, with necrosis limited to oldest rosette leaves.
a. Radial growth rate was measured after 4 days on Czapek-Dox minimal medium. (+) wild-type growth rate; (-) reduced growth rate (<70 % of wild-type).
b. Melanisation was assessed at 3 dai. (-) albino appressoria; (+) weakly melanised appressoria; (++) darkly melanised appressoria similar to wild-type.
c. Penetration was quantified at 3 dai as percentage of appressoria producing a visible penetration peg or hypha in the underlying epidermal cell. (-) < 10 % penetration; (+) 11-35 % penetration; (++) 36-59 % penetration; (+++) >60% penetration similar to wild-type.
d. Penetration of cellophane was quantified after 36 h as percentage of appressoria which had produced a visible hypha inside the cellophane. (-) <10 % penetration; (+) 11-35 % penetration; (++) 36-70 % penetration; (+++) >70% penetration similar to wild-type.
e. Entry into the necrotrophic phase was quantified at 4 dai as percentage of appressoria giving rise to secondary hyphae. (-) < 30 % secondary hyphae; (+) 31-59 % secondary hyphae; (++) >60 % secondary hyphae, similar to wild-type.
f. Two host defence responses were quantified: deposition of callose papillae (assessed by Aniline Blue staining) and induction of hypersensitive cell death (HR, assessed by detecting H_2O_2 accumulation in dead cells with diaminobenzidine). The percentage of appressoria inducing callose deposition or HR in underlying epidermal cells was determined at 3 dai. Mutants inducing significantly more papillae or HR than the wild-type ($P<0.05$) are indicated by P or HR, respectively.
In all quantitative assays, at least 100 appressoria per mutant were counted in three independent experiments.

2.3.1 Mutants with non-melanised appressoria

Six pathogenicity mutants produced conidia which germinated normally and differentiated appressoria but the cell walls of the latter were either not melanised (*path*-1, -4 and -5) or very weakly melanised (*path*-2, -3 and -6), unlike the darkly pigmented appressoria of the wild-type strain (Figure 4). With the exception of *path*-6, appressoria of these mutants were completely unable to penetrate living host epidermal cells, ethanol-killed leaves or cellophane membranes (Table 4). Only 12 % of *path*-6 appressoria penetrated living host cells 3 dai (compared to 77 % in the wild type), but these went on to develop normal primary and secondary hyphae (Table 4). The appressoria of the melanin mutants also adhered less strongly to the leaf surface than those of the wild type because most became dislodged during processing of the tissue for microscopy (data not shown). Although unable to penetrate intact leaf surfaces, all the mutants formed necrotic lesions similar to the wild type on wounded tissue, except *path*-5 which produced smaller lesions (Figure 5). Thus the melanin mutants were capable of invasive growth *in planta* if the initial penetration step was circumvented.

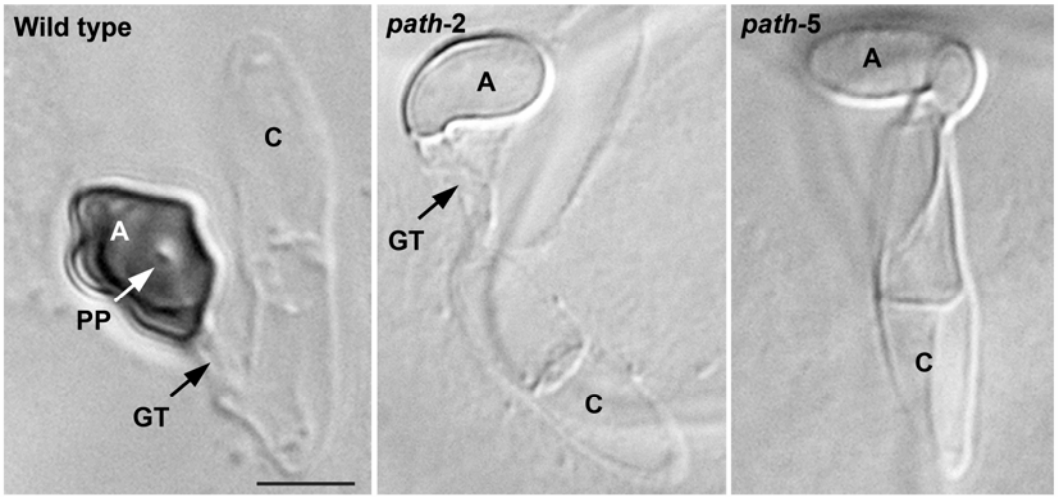

Figure 4. Appressorial morphology of two melanin-deficient *Colletotrichum higginsianum* mutants.
Arabidopsis plants were inoculated with spore suspension of the *C. higginsianum* wild-type strain and melanin-deficient mutants *path*-2 and *path*-5. After 2 days, leaf tissue was cleared and viewed with differential interference contrast microscopy. Both mutant and wild-type conidia (C) germinated to form germ-tubes (GT) and appressoria (A). However, the wild-type appressorium is darkly melanised and contains a basal penetration pore (PP) whereas the appressorium of *path*-2 and *path*-5 are weakly melanised and has no visible penetration pore. Scale bars = 5 µm.

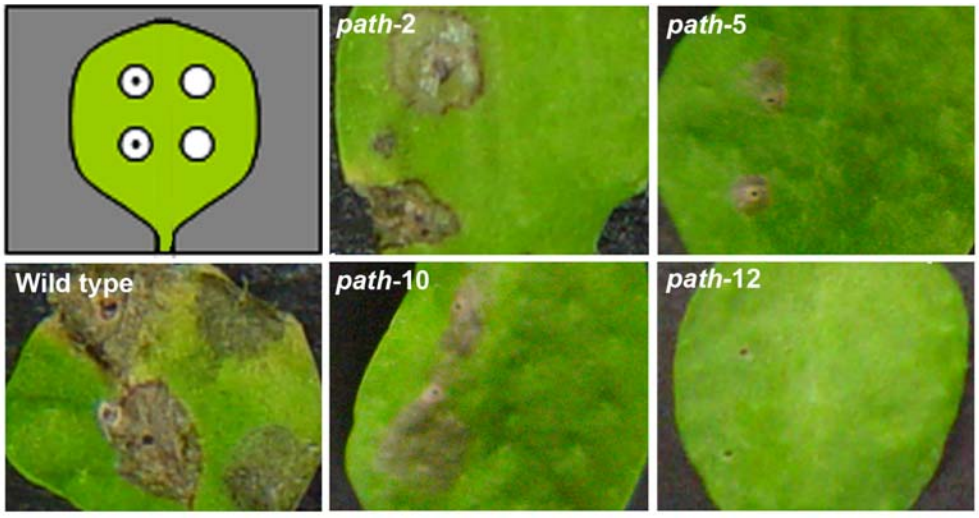

Figure 5. Invasive growth assay for melanin-deficient and penetration mutants.
Arabidopsis leaves were droplet-inoculated with *Colletotrichum higginsianum* conidial suspension. Top left panel: two sites on the left half of each leaf were wounded with a fine sterile needle prior to drop-inoculation (⊙), whereas two drop-inoculation sites on the right half were not wounded (○). After 7 days, the wild-type strain caused brown necrotic lesions on both wounded and intact tissue. Two melanin-deficient mutants (*path*-2 and *path*-5) and penetration mutant *path*-10 caused no symptoms on intact tissue, but were capable of invasive growth when drop-inoculated onto a wound, causing necrotic lesions similar to, or smaller than, the wild type. Penetration mutant *path*-12 lacked invasive growth ability as it failed to produce symptoms on both wounded and intact tissue.

2.3.2 Mutants defective in host penetration

Fifteen pathogenicity mutants (*path*-7 to -21) produced fully-melanised appressoria with visible penetration pores but either completely failed to penetrate living host cells or penetrated with lower frequency than the wild type (Table 2). These mutants produced no symptoms on *Arabidopsis* (Supplementary Figure 1).

Microscopic inspection of the epidermal cells underlying appressoria of these mutants revealed that neither callose papillae nor hydrogen peroxide accumulation occurred more frequently than with wild-type appressoria (Table 4). This suggests their failure to penetrate host tissue resulted from a defect in appressorial function rather than induction of host defence responses. Consistent with this view, seven of the host penetration mutants were also unable to penetrate either cellophane membrane (Table 4 and Figure 6A) and ethanol-killed leaf tissue (Figure 6B). However, the eight other penetration mutants could penetrate cellophane and dead leaf tissue, although less efficiently than the wild type (Table 4). With the exception of *path*-12, all penetration mutants retained invasive growth ability because they produced necrotic lesions similar to the wild type on wounded leaf tissue (Figure 5).

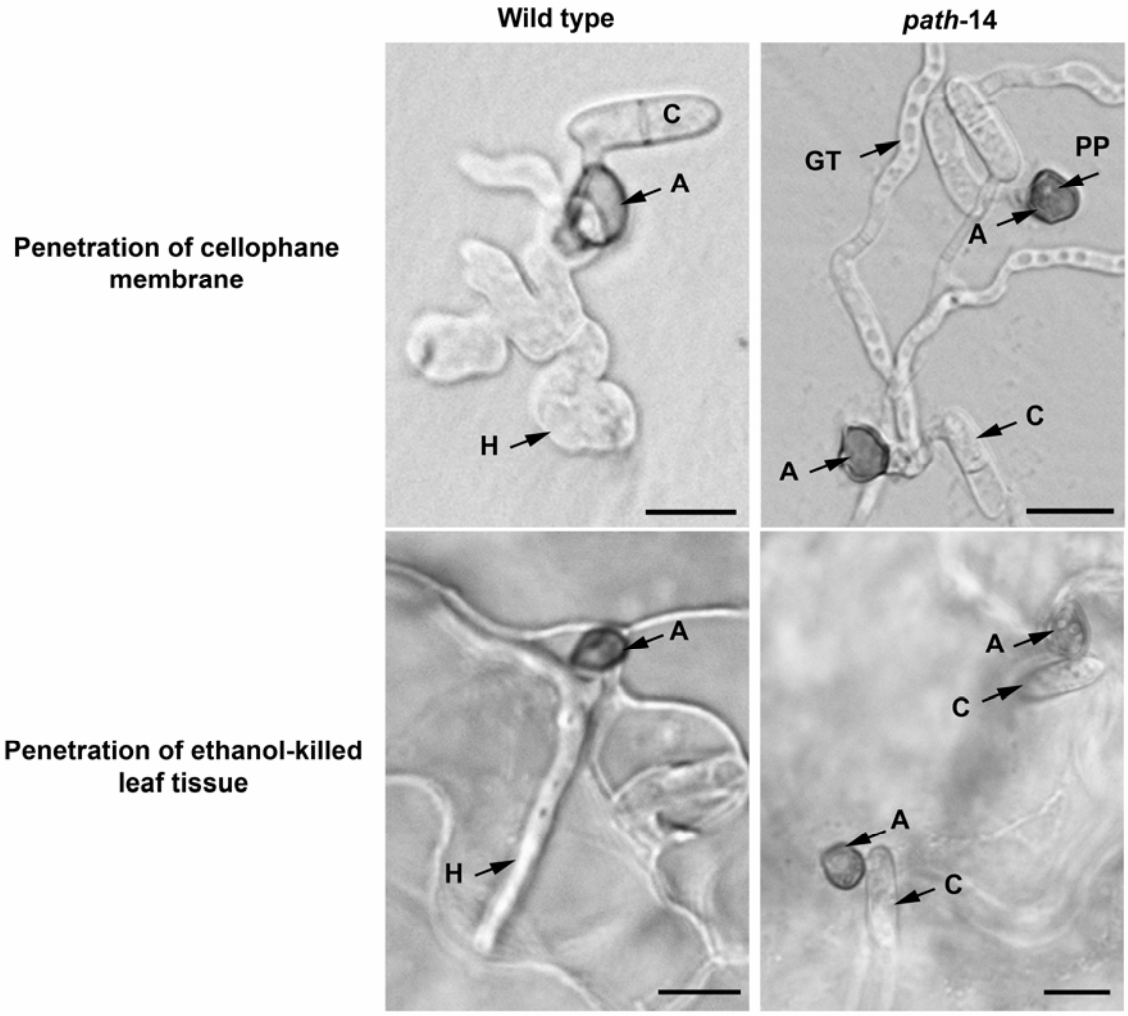

Figure 6. Appressorial penetration of inert substrata: cellophane and dead leaf tissue.
Light micrographs showing conidia (C) of *Colletotrichum higginsianum* wild-type strain and penetration mutant *path*-14 germinating on cellophane dialysis membrane after 36 h and ethanol-killed *Arabidopsis* leaves after 18 h. The wild-type appressorium penetrated the cellophane to form a hypha inside the membrane (H). Mutant *path*-14 formed melanised appressoria (A) with penetration pores (PP) but failed to penetrate the cellophane. Other conidia produced unusual long germ tubes (GT) over the surface of the cellophane. On ethanol-killed leaf tissue, both the wild type and mutant formed melanised appressoria (A), whereas the wild type rapidly penetrated to form thin hyphae inside the dead plant tissue, *path*-14 failed to penetrate. Scale bars = 10 μm.

2.3.3 Mutants inducing host defence responses

Fourteen pathogenicity mutants (*path*-22 to -35) formed appressoria that induced host cellular defence responses with higher frequency than the wild-type strain, *e. g.* deposition of callose papillae at fungal penetration sites, HR cell death or a combination of both (Table 4). These mutants caused very limited symptoms on *Arabidopsis* (Supplementary Figure 1).

The frequency with which appressoria induced HR in underlying epidermal cells was quantified at 3 dai by staining leaf tissue with DAB to detect hydrogen peroxide accumulation in the dead host cells. The efficiency of appressorial penetration was also scored according to whether a penetration peg or primary hypha was visible within the host cell. Figure 7A shows representative data for the *C. higginsianum* wild-type strain and four selected mutants. Appressoria of all four mutants induced HR in epidermal cells significantly more frequently than the wild type ($P<0.05$). In addition, the penetration efficiency of *path*-24 and *path*-29 was significantly less than the wild type ($P<0.05$), and thus appressoria of these mutants frequently induced HR without producing visible hyphae inside the affected cell. In contrast, two other mutants, *path*-31 and *path*-34, were unaffected in their penetration efficiency but their development became arrested at the penetration peg or primary hypha stage. Even after 7 dai they had not grown beyond one HR epidermal cell. In seven other mutants, a small proportion of appressoria did not induce an HR and these successfully developed to the point of forming necrotrophic secondary hyphae, especially on older rosette leaves, but overall they produced less severe necrotic symptoms than the wild type (Table 4 and Supplementary Figure 1). In most cases, host cell death was restricted to the penetrated epidermal cell (Figure 8A), but in the four mutants (*path*-26, -30, -31 and -33) HR also extended into one or more adjacent uninfected epidermal and mesophyll cells (Figure 8B).

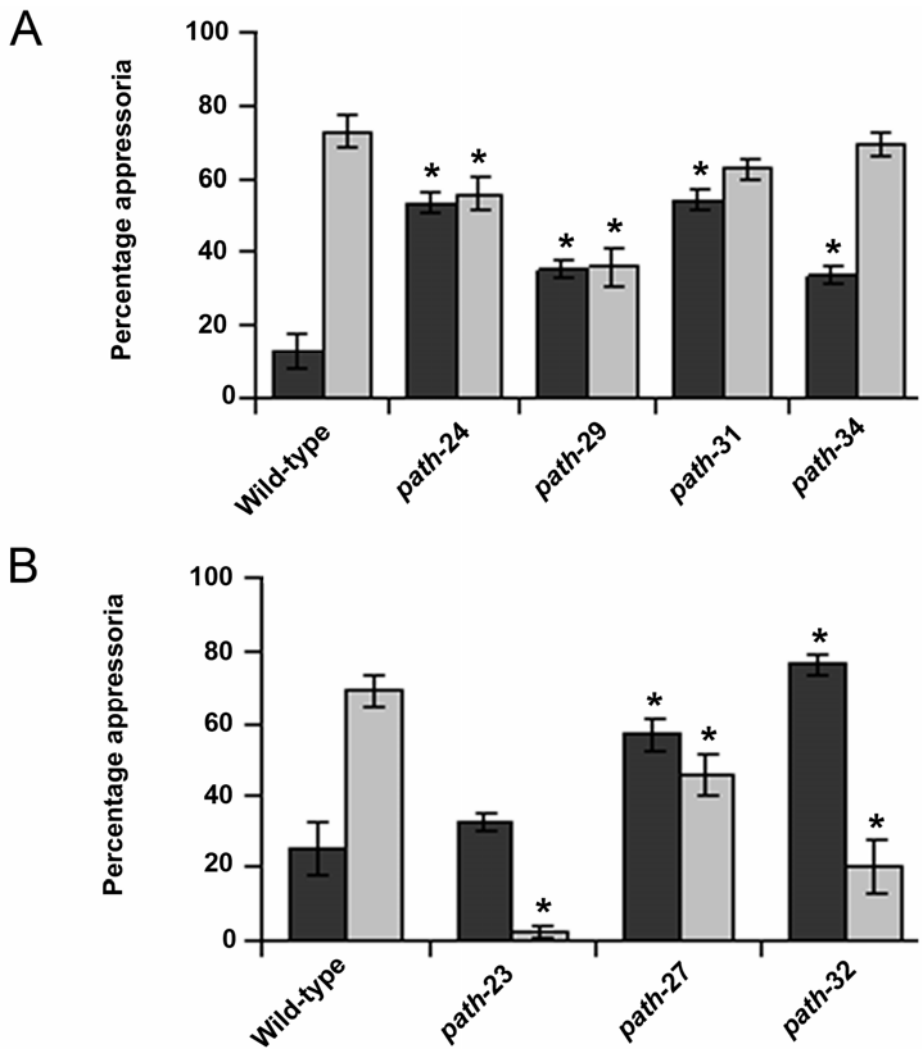

Figure 7. Quantification of appressorial penetration ability and induction of host defence responses by selected *Colletotrichum higginsianum* pathogenicity mutants.
Arabidopsis plants were spray-inoculated with *C. higginsianum* conidial suspension and penetration and host defence responses were quantified by microscopy at 3 dai. Penetration was scored according to whether hyphae were visible in epidermal cells underlying appressoria. Accumulation of hydrogen peroxide and deposition of callose papillae were detected by staining with diaminobenzidine (DAB) or Aniline Blue, respectively. At least 100 appressoria were scored for the wild type and mutants and values represent mean percentages and standard errors (error bars) calculated from three independent experiments. Asterisks indicate values significantly different to the wild type (Student t-test $P<0.05$). **A**, Graph showing percentage of appressoria penetrating epidermal cells (grey bars) and inducing hydrogen peroxide accumulation in host cells (black bars). Mutants *path*-24, -29, -31 and -34 all induced hydrogen peroxide accumulation significantly more frequently than the wild type. **B**, Graph showing percentage of appressoria penetrating epidermal cells (grey bars) and inducing papillary callose (black bars). Mutants *path*-27 and *path*-32 induced significantly more papillae than the wild type and their penetration efficiency was also significantly reduced.

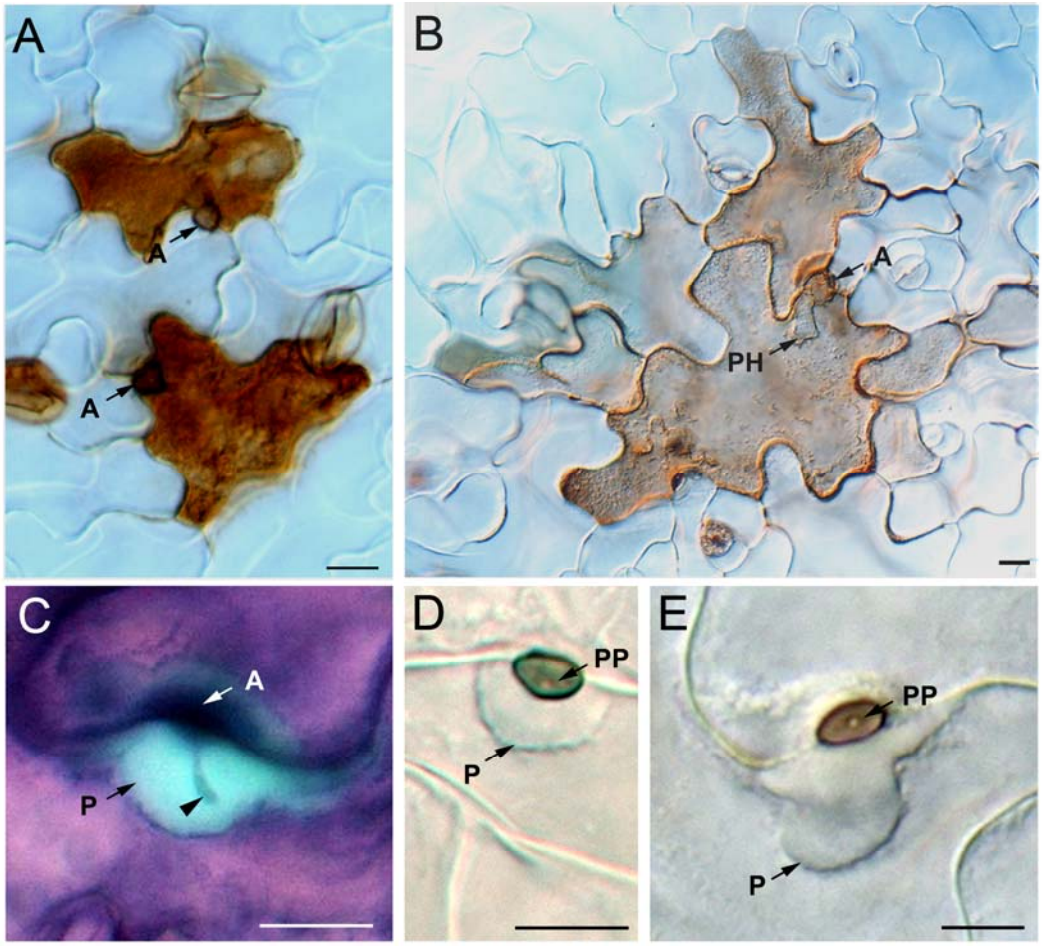

Figure 8. Accumulation of hydrogen peroxide and papillary callose at attempted penetration sites of *Colletotrichum higginsianum* pathogenicity mutants.
Light micrographs showing host defence responses to selected pathogenicity mutants. *Arabidopsis* plants were spray-inoculated and processed for microscopy at 3 dai. **A**, and **B**, Accumulation of hydrogen peroxide in host epidermal cells visualised with diaminobenzidine (DAB). **A,** Brown DAB staining was observed in single epidermal cells beneath appressoria of mutant *path*-29. **B**, Mutant *path*-31 induced DAB staining not only in the penetrated epidermal cell but also in adjacent uninfected cells. **C**, Papilla (P) formed beneath an appressorium (A) of mutant *path*-35 showing Aniline blue-induced fluorescence of callose. The fungal penetration peg (arrowhead) is visible within the papilla. **D**, and **E**, Papillae beneath appressoria of mutant *path*-27 (**D**) and *path*-23 (**E**) visualised by differential interference contrast microscopy. Scale bars = 10 µm.

The frequency with which callose papillae were deposited at appressorial penetration sites was quantified by staining leaf tissue at 3 dai with Aniline blue. Figure 7B shows representative data for the *C. higginsianum* wild-type strain and three selected mutants. In the wild type, callose was detected beneath only ~25 % of appressoria (Figure 7

and Table 4), and where callose was present most appressoria successfully penetrated and formed primary hyphae (Figure 7C and Figure 8B). However, in the three mutants (*path*-23, -27, -32), host callose deposition was associated with reduced penetration and failure to establish intracellular primary hyphae (Figure 7B). Thus, appressoria of the mutants *path*-27 and *path*-32 induced callose papillae significantly more frequently than the wild type ($P<0.05$) and their penetration efficiency was significantly less than that of the wild type ($P<0.05$) (Figure 7B). Mutant *path*-23 induced callose deposition production with similar frequency to the wild type but the papillae were abnormally large (Figure 8) and the penetration efficiency of this mutant was significantly less than the wild type (Figure 7B) suggesting these larger papillae were more efficient at preventing penetration than papillae found beneath wild-type appressoria.

To evaluate the contribution of plant defence responses to the infection phenotype of selected fungal mutants, *Arabidopsis* mutants impaired in different components of penetration resistance, namely the PEN1 syntaxin (Collins *et al.,* 2003), the PEN2 ß-glycosyl hydrolase (Lipka *et al.,* 2005), the PEN3 ABC transporter (Stein *et al.,* 2006) and the PMR4/GSL5 callose synthase (Nishimura *et al.,* 2003)were used. All mutants were in the Columbia (Col-0) background, an ecotype which is more resistant to *C. higginsianum* than Ler-0. Penetration ability by *path*-27 and *path*-28 was two- to three-fold higher on *pen2*-2 and *pen3*-3 mutants than on wild-type Col-0 plants, but was not enhanced on *pen1*-1 and *pmr4*-1 (Figure 9A). Consequently, symptoms caused on *pen2*-2 and *pen3*-3 plants by *path*-27 and *path*-28 were visibly more severe than on wild-type Col-0 plants, with necrosis of some leaves (Figure 9B). These findings suggest that toxic secondary metabolites synthesised by PEN2 and exported by PEN3 may impede penetration by *path*-27 and *path*-28, but callose deposition and PEN1-mediated secretion events do not compromise penetration by these mutants. To a lesser extent, the penetration efficiency of wild-type *C. higginsianum* was also significantly enhanced on the *pen2*-2 and *pen3*-3 mutants (Figure 9) suggesting that PEN2 and PEN3 also contribute to basal resistance of Col-0 to *C. higginsianum*.

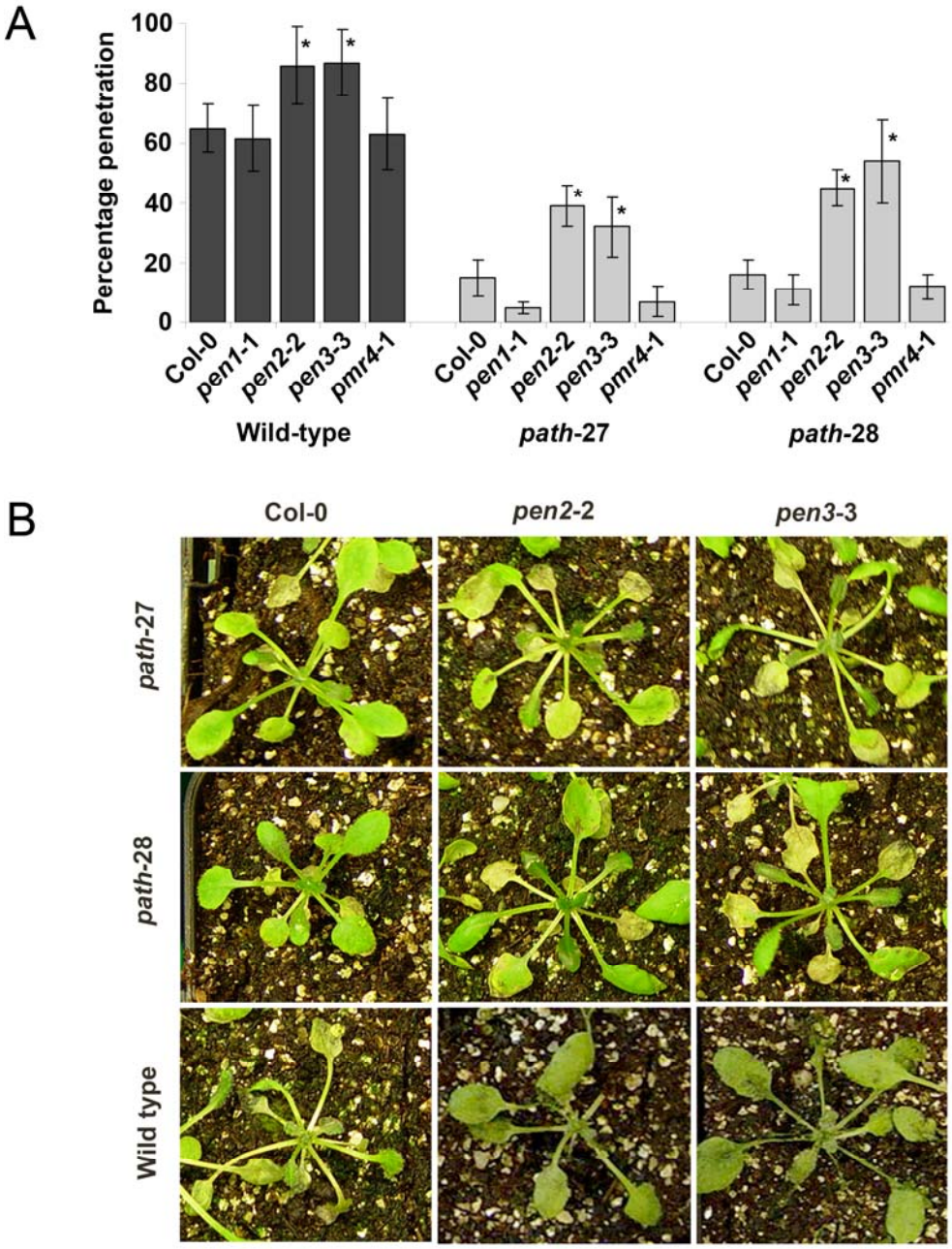

Figure 9. Contribution of plant defence responses to impaired penetration efficiency of *Colletotrichum higginsianum* mutants

Arabidopsis mutants impaired in components of penetration resistance (*pen1*-1, *pen2*-2, *pen3*-3 and *pmr4*-1, all mutants were in Columbia (Col-0) background) and Col-0 wild-type plants were spray-inoculated with conidial suspension of wild-type *C. higginsianum* and mutants *path*-27 and *path*-28.. **A.** After 3 days, penetration was quantified by microscopy according to whether hyphae were visible in epidermal cells underlying appressoria. At least 100 appressoria were scored and values represent mean percent penetration and standard error (error bars) calculated from three independent experiments. Asteriks indicate significant difference from the wild type (Student t-test $P<0.05$). Penetration by *path*-27 and *path*-28 was significantly higher on *pen2*-2 and *pen3*-3 mutants than on Col-0 wild-type plants, but not on *pen1*-1 and *pmr4*-1 mutants. To a lesser extent, penetration by wild-type *C. higginsianum* was also enhanced on *pen2*-2 and *pen3*-3 mutants. **B.** Mature *Arabidopsis* plants (3- to 4-week-old) were spray-inoculated with spore suspension (5 x 10^5 conidia mL^{-1}) and examined for symptoms at 7 dai.

2.3.4 Mutants defective in the switch to necrotrophy

A final group of five mutants (*path*-36 to -40) were affected in their ability to make the transition from biotrophy to necrotrophy. The penetration efficiency of these mutants was similar to that of the wild-type strain (Figure 10A and Table 2), and the timing and morphology of their development *in planta* was also indistinguishable from the wild type until the formation of biotrophic primary hyphae. Thereafter, they showed a strongly reduced ability to form secondary hyphae and rarely entered the destructive necrotrophic phase. Thus, even at 7 dai, fungal development was typically restricted to primary hyphae occupying single epidermal cells (Figure 10B). None of the mutants induced visible host defence responses such as HR or callose deposition with greater frequency than the wild-type strain. Some penetrated epidermal cells of hypocotyls were found to be still alive at 7 dai, as demonstrated by their continued ability to plasmolyse, suggesting these mutants successfully established and maintained a biotrophic relationship with host cells (Figure 10C). The proportion of live penetrated cells was not quantified due to the much lower penetration efficiency of *C. higginsianum* on *Arabidopsis* hypocotyls.

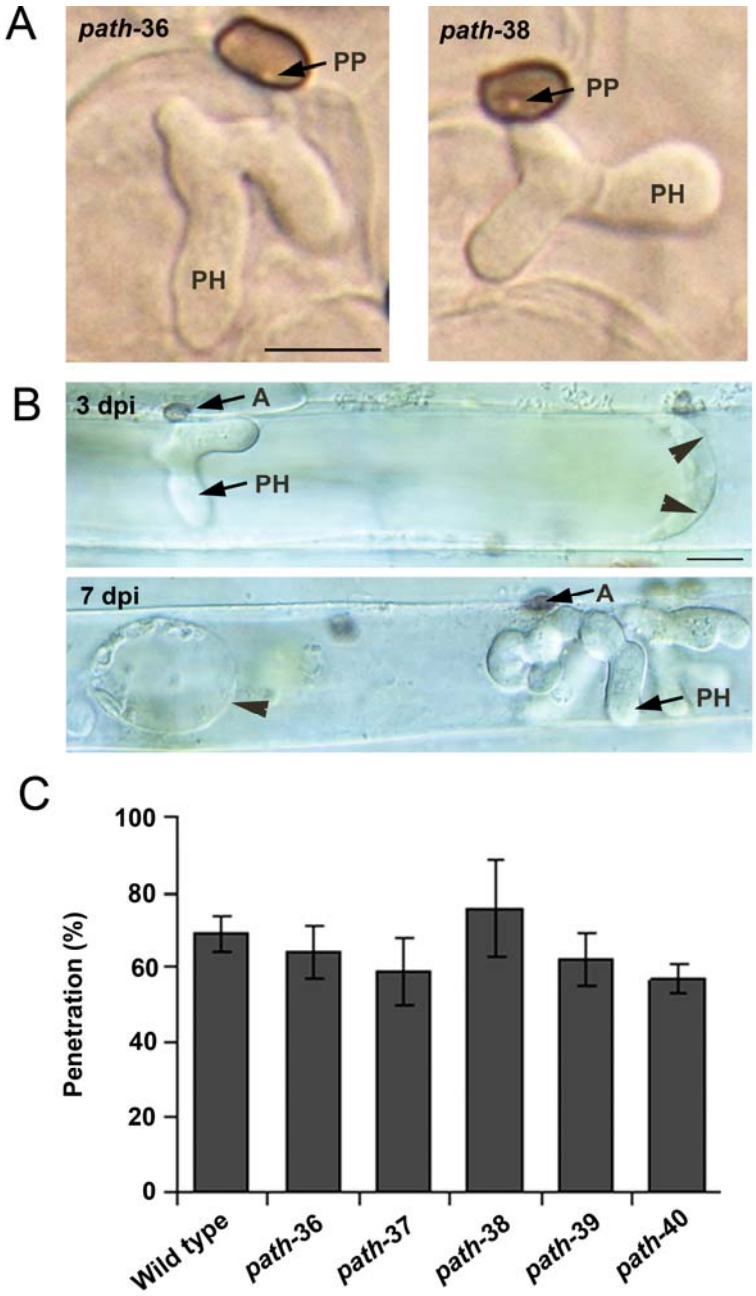

Figure 10. *Colletotrichum higginsianum* mutants impaired in the switch from biotrophy to necrotrophy. **A**, *Arabidopsis* plants were spray-inoculated with mutants *path*-36 and -38 and tissue was cleared for microscopy at 7 dai. Both mutants formed normal melanised appressoria with penetration pores (PP) and successfully established biotrophic primary hyphae (PH) in host epidermal cells, but necrotrophic secondary hyphae were rarely produced. Scale bars = 10 µm. **B**, Plasmolysis test for viability of penetrated epidermal cells. *Arabidopsis* seedlings were inoculated with mutant *path*-35 and hypocotyls were plasmolysed with 0.85M KNO_3. At 3 dai, biotrophic primary hyphae (PH) were visible beneath appressoria (A) and the penetrated epidermal cell remained alive, as shown by its ability to plasmolyse normally (arrows indicate the plasma membrane). At 7 dai, the primary hyphae were larger but secondary hyphae were not present and the penetrated host cells were still alive. Scale bars = 10 µm. **C**, Appressorial penetration ability of mutants impaired in the switch to necrotrophy was not significantly reduced (Student t-test $P<0.05$) compared to the wild type. At least 100 appressoria were scored for the wild type and mutants and values represent mean percentages and standard errors (error bars) calculated from three independent experiments.

2.3.5 Pathogenicity mutants with morphological defects

Morphogenesis can also play an important part in pathogenicity *e.g.* formation of specialised infection structures or cell wall integrity. While studying the pathogenicity phenotype of the mutants, some morphological defects were observed. The polysaccharide stain Congo Red was used to visualise the fungal cell wall and septa near the growing tips of hyphae grown on PDA (Figure 11A). Unlike the wild-type strain which showed regularly spaced septa, hyphae of mutant *path*-7 displayed very few septa and had numerous patches of cell wall thickening. Mutant *path*-37 showed regular septation, but more closely spaced than in the wild type. The shape and branching of the hyphae also showed some differences. Compared to the straight and branched hyphae of the wild-type strain, the hyphae of *path*-23 grew compacted together to form chords and the hyphae of *path*-8 were much more undulating than the wild type (Figure 11B). The conidia of three mutants also displayed alterations in their size and shape (Figure 11C). The conidia of the wild-type strain were on average 14.6 µm long and 3.3 µm wide. In comparison, conidia of *path*-8 (data not shown) and *path*-12 (Figure 11C) were much shorter, on average 9.8 and 10.2 µm in length respectively. Conidia of *path*-7 were slightly longer, on average 15.2 µm, and appeared fused together into short chains. Furthermore, conidia of mutant *path*-7 appeared to be interconnected with conidial anastamosis tubes (CATs). Such connections were not observed with conidia of the wild type (Figure 11D).

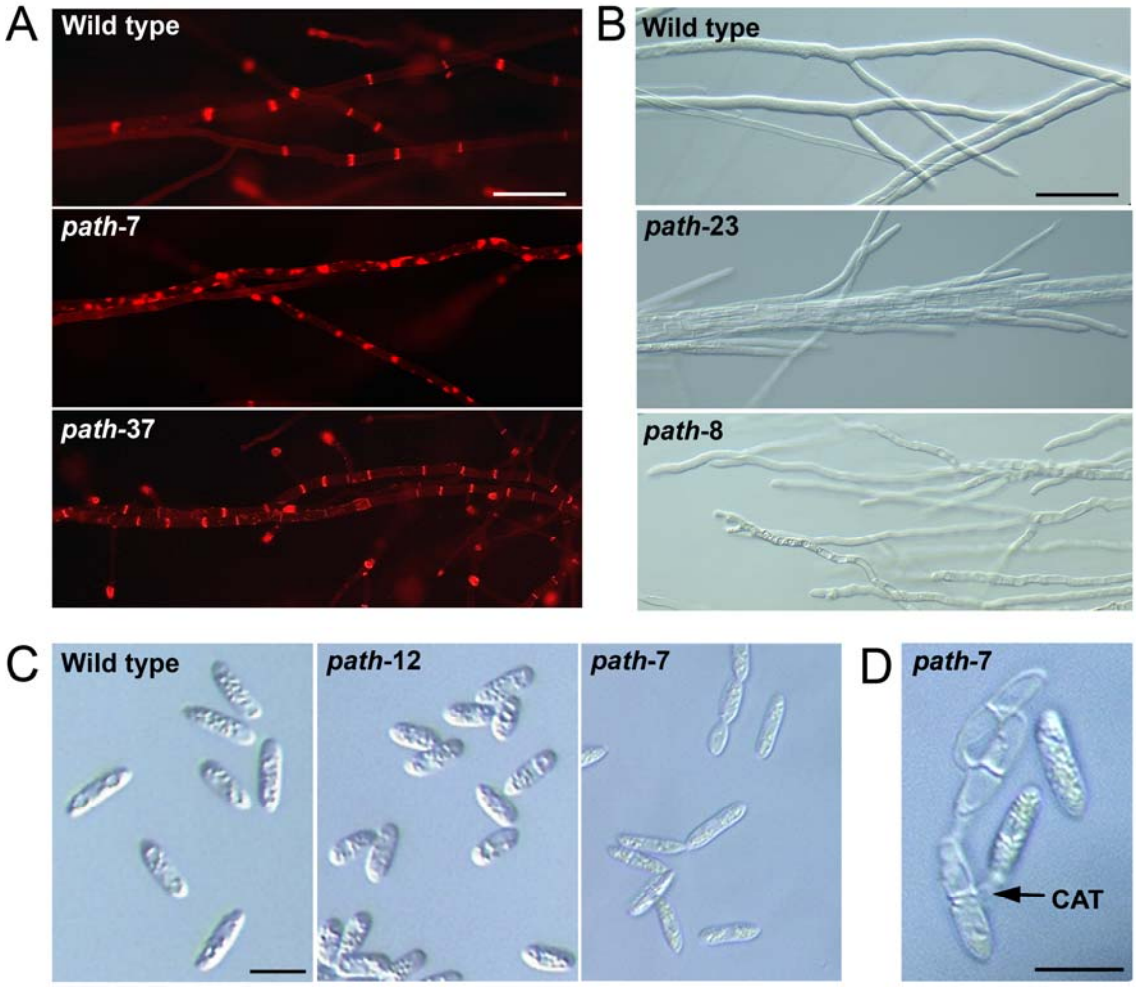

Figure 11. Morphological defects among pathogenicity mutants.
A, Congo Red staining of hyphae grown on PDA revealed regularly spaced septa in the wild type. Mutant *path*-7 sowed reduced septation and more patches of cell wall thickening and *path*-37 had more closely spaced septa. Scale bar = 50 µm. **B**, Bright field microscopy of hypha moprhology growing on PDA. Compared to the wild type, *path*-23 hyphae grew close together to form a chord-like structure and mutant path-8 hyphae were more undulated than the wild type. Scale bar = 50 µm. **C**, Conidia of wild-type strain and mutants *path*-12 and *path*-7. Scale bar = 10 µm. **D**, Anastamosis among conidia of *path*-7. Scale bar = 10 µm.

2.3.6 Auxotrophy mutants

The growth rate of the mutants was determined on minimal (CDA) media which has inorganic nitrogen as a sole nitrogen source and those showing severely reduced growth (<70 %) compared to the wild type were putative auxotrophs. Among the 40 verified pathogenicity mutants emerging from the secondary screen, four (*path*-19, -20, -21 and -35) were putative auxotrophs because they grew poorly or not at all on minimal medium but showed normal growth on rich media (PDA, Table 4 and Figure 12). All four mutants displayed significantly reduced penetration of the host epidermis, cellophane and ethanol-killed leaf tissue compared to the wild-type strain (Table 4). In addition, mutant *path*-35 also induced significantly more papillae than the wild-type strain (Table 4). The four auxotrophic mutants produced almost no symptoms when inoculated on *Arabidopsis*. In the case of *path*-37 and *path*-38, growth and penetration ability were rescued when exogenous arginine was provided, suggesting they were arginine auxotrophs (Takahara, personal communication).

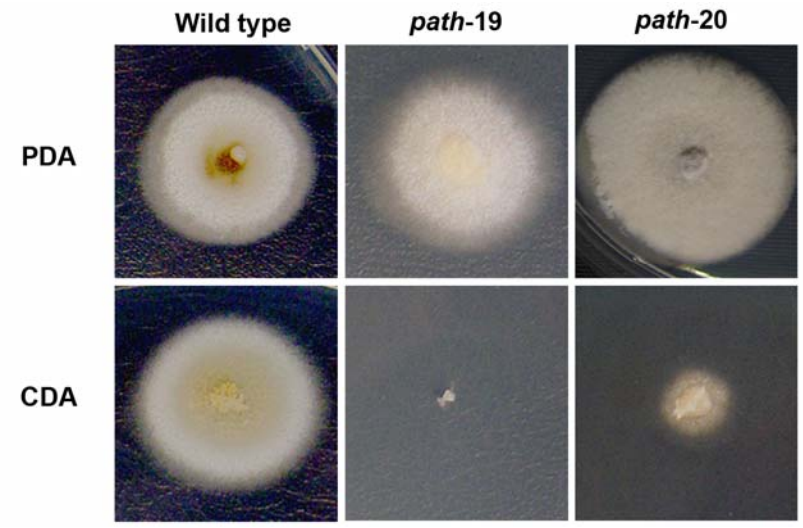

Figure 12. Radial growth assay for auxotrophic mutants.
To test for auxotrophy, the radial growth rate of transformants was compared to the *C. higginsianum* wild-type strain after 3 days incubation on rich nutrient medium (potato dextrose agar, PDA) or minimal medium (Czapek-Dox agar, CDA) containing inorganic nitrogen as the sole nitrogen source. Mutants such as *path*-19 and *path*-20 showing significantly reduced growth on CDA (Student t-test, $P<0.05$) but normal growth on PDA and were considered auxotrophs.

2.4 Confirmation and characterisation of T-DNA integration events

The 40 putative pathogenicity mutants were purified by single conidium isolation and maintained on PDA containing hygromycin B. To verify that the transformants had at least one T-DNA insertion, a region of the *hph* gene cassette of the T-DNA insertions was detected by PCR in all 40 mutants tested and was not detected in the wild-type strain.

Southern blot analysis (Figure 13A-B) was used to investigate the integration events in 95 mutants, including 55 randomly selected insertion transformants and the 40 pathogenicity mutants. Genomic DNA was digested with *Xba*I, which cuts inside the T-DNA of pBIG2RHPH2 on one side of the probe and the T-DNA of pBIN-GFP-hph on both sides, and with *Xho*I which cuts the T-DNA of pBIN-GFP-hph on one side of the probe and does not cut the T-DNA of pBIG2RHPH2. The number of hybridising bands with genomic DNA of pBIN-GFP-hph transformants digested with *Xho*I revealed the number of T-DNA insertions, while the size of the hybridising bands after hybridisation with *Xba*I revealed truncations. The number of hybridizing bands with genomic DNA of pBIG2RHPH2 transformants digested with either *Xba*I or *Xho*I indicated the number of T-DNA insertions. Southern blot analysis revealed that out of 55 randomly-selected transformants, 32 (58 %) had single T-DNA insertions, 16 (29 %) had two insertions and seven (12 %) had three or more insertions (Figure 13C). Among 14 T-DNA insertions sites from 12 mutants for which T-DNA flanking regions were analysed in detail, 11 contained two T-DNA insertions, of which eight had tandem insertions at a single site (Figure 13D). Tandem insertions could be differentiated from multiple insertions by Southern analysis (Figure 13B), but Southern blot analysis alone was not enough to differentiate between tandem insertions at a single locus and multiple insertions due to the large number of possible hybridisation patterns that can be obtained depending on the number of T-DNA copies, orientation of the repeats and truncations. Tandem insertions were only confirmed when sequence of the flanking region was obtained by thermal asymmetric interlaced (TAIL)-PCR or inverse PCR (Section 2.5.1). Seven of the tandem T-DNA integrations were direct (left border to right border) repeats, while only one comprised inverted left border to right border repeats.

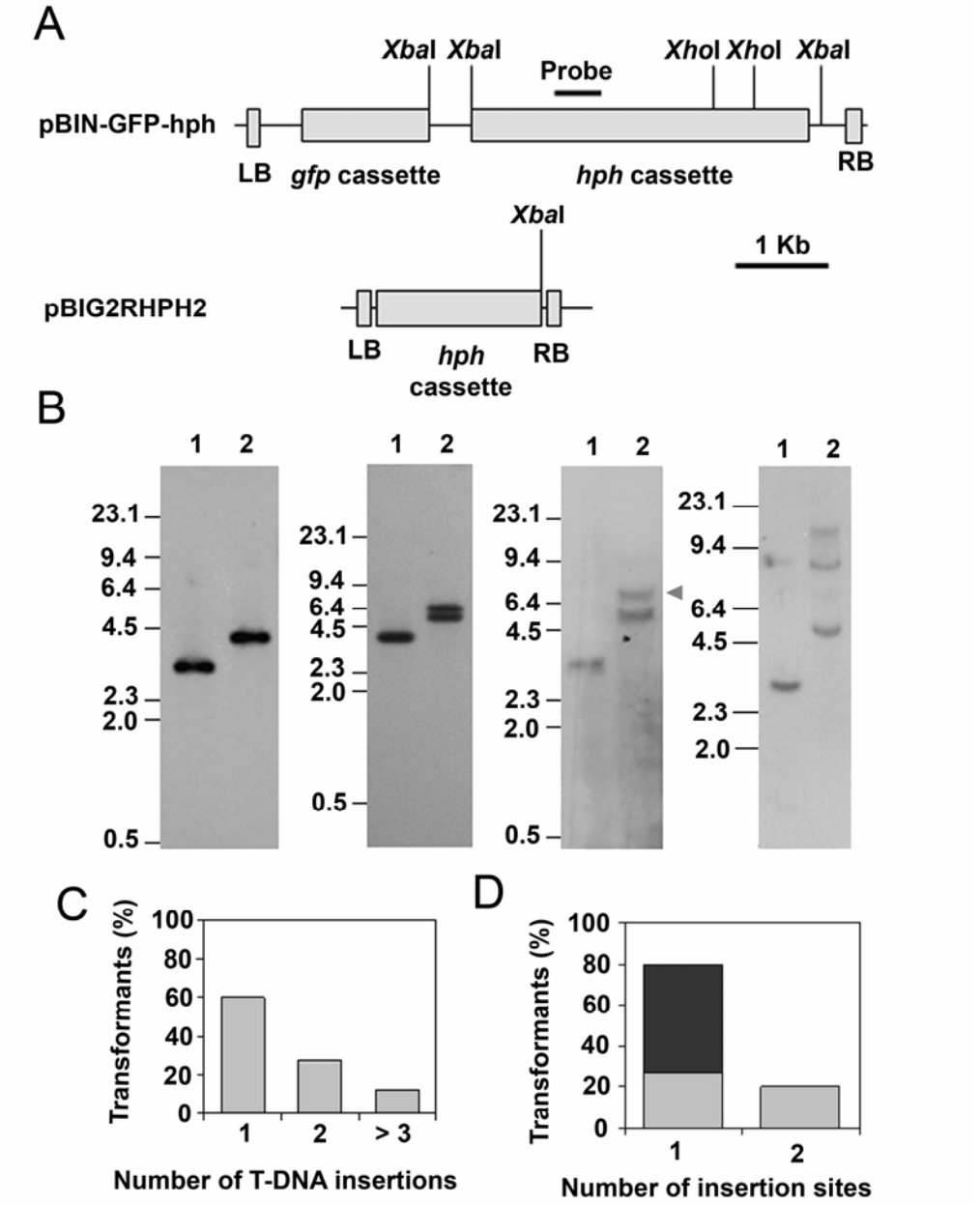

Figure 13. Analysis of T-DNA copy number in *Colletotrichum higginsianum* transformants
A, Physical map of transformation vector pBIN-GFP-hph containing the green fluorescent protein (*gfp*) and hygromycin resistance (*hph*) gene cassettes between the left (LB) and right (RB) T-DNA borders (O'Connell *et al.*, 2004) and vector pBIG2RHPH2 containing the *hph* gene cassette between the LB and RB. Positions of *Xba*I and *Xho*I restriction sites and a 578 bp *hph*-specific probe are indicated. **B**, Southern blot analysis of *C. higginsianum* transformants: genomic DNA from four representative p-BIN-GFP-hph transformants was digested with either *Xba*I (lane 1) or *Xho*I (lane 2) and hybridised with the digoxygenin (DIG)-labelled *hph* probe. The four panels show (from left to right) examples of transformants with a single insertion, two independent insertions, two T-DNA tandemly inserted at a single site, and three independent insertions. In the case of tandem insertions, a fragment of 6.6 kb was obtained upon digestion with *Xho*I (arrowhead). Molecular size is indicated in kilobases (kb). **C**, Number of T-DNA insertions in 55 randomly selected transformants of *C. higginsianum*, as determined by Southern blot analysis. **D**, Number of T-DNA insertion sites in 12 pathogenicity mutants, as determined by Southern blot and by sequencing genomic DNA flanking the T-DNA, obtained by TAIL-PCR or Inverse PCR.

2.5 Molecular characterisation of pathogenicity mutants

2.5.1 Obtaining genomic sequence of T-DNA flanking regions

C. higginsianum genomic sequence flanking the T-DNA right border was recovered from 12 pathogenicity mutants using inverse PCR and TAIL-PCR. TAIL-PCR was performed using nested right border-specific primers and a degenerate primer whereas Inverse PCR was performed with right border-specific nested primers and an *hph*-specific reverse primer on genomic DNA of the mutant digested with *Eco*RI, which cleaved in the T-DNA downstream of the *hph*-specific primer annealing site (Figure 14A). The right border sequences obtained by TAIL PCR were generally shorter (mean 955 bp, range 0.3-1.2 kb) than those from inverse PCR (mean 1994 bp, range 0.4 to 4.5 kb) (Figure 14B-C). When multiple amplification products were obtained, these were separated on a gel, extracted, cloned into *E. coli* and sequenced individually (Figure 14B-C). Sequencing of all the flanking regions obtained was done with right border-specific primer RBsp (Figure 14A). Inverse PCR was found to be a more reliable method for mutants with tandem insertions because the restriction digest removed the adjacent T-DNA insert.

For the remaining 28 pathogenicity mutants, no flanking sequence could be obtained using either TAIL-PCR or inverse PCR or the PCR products were less than 100 bp of genomic DNA and therefore insufficient to screen the genomic DNA library.

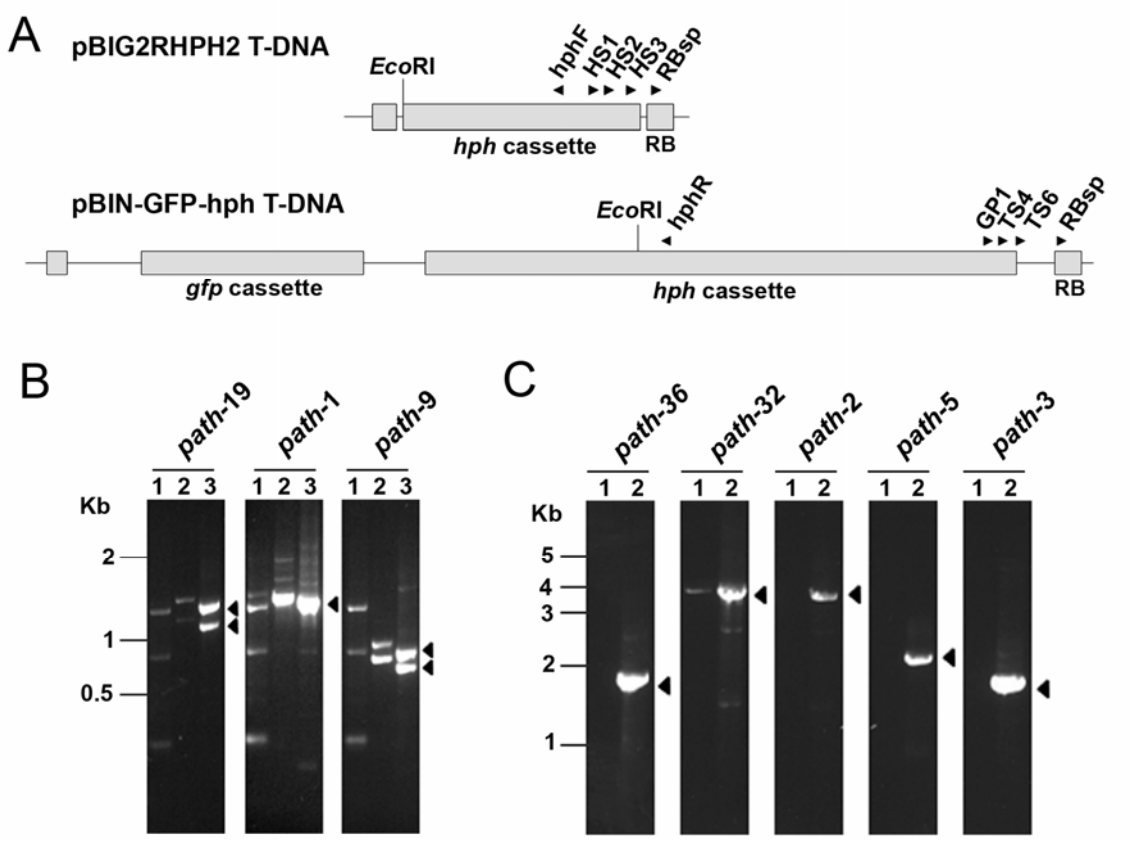

Figure 14. Identification of T-DNA flanking sequence by TAIL-PCR and Inverse PCR.
A, Location of annealing sites and restriction sites of primers and restriction enzymes used for TAIL-PCR and Inverse PCR. **B**. Agarose gel analysis of thermal asymmetric interlaced polymerase chain reaction (TAIL-PCR) products generated from mutants *path*-19, -1 and -9. Amplification was performed with the right border (RB) nest of primers (HS1, HS2 and HS3 for pBIG2RHPH2 transformants or GP1, TS4 and TS6 for pBIN-GFP-hph transformants) and with the arbitrary degenerate primer AD1. The first, second and third lane of each gel represent the primary, secondary and tertiary reactions, respectively of the protocol. **C.** Agarose gel analysis of inverse PCR products generated from mutants *path*-36, -29, -2, -5 and -3. Genomic DNA was digested with *Eco*RI, self-ligated and amplified with the right border nested primers (as used for TAIL-PCR) together with reverse primers hphF for pBIG2RHPH2 transformants or hphR for pBIN-GFP-hph transformants. Arrows label PCR products corresponding to a junction fragment containing a segment of the inserted T-DNA and associated flanking genomic DNA. Molecular size is indicated in kilobases.

2.5.2 Identification of tagged gene

To obtain full length sequences of predicted genes flanking the T-DNA insertion, it was necessary to obtain longer sequences flanking the T-DNA insertions. The cosmid *C. higginsianum* genomic DNA library was screened by PCR using primers specific to the flanking sequence obtained by TAIL-PCR and Inverse PCR. The genomic region of interest

in the cosmid harbouring the tagged locus was then sequenced by primer walking. Open reading frames (ORFs) were predicted using the algorithm FGENESH+ (Figure 15). Among the 14 T-DNA insertions analysed in these 12 mutants, nine were located inside a predicted ORF, while four were positioned upstream and one downstream, of a predicted ORF (Table 5). For these 14 T-DNA insertions, the sequence of the flanking regions obtained as well as the predicted ORFs are provided in Supplementary Data 2-14. The Blastx results for the predicted ORF are also provided in the Supplementary Data 15-26.

Seven ORFs showed high homology ($E \leq$ 1e-65) to known fungal proteins with annotated functions (Table 5). These include a Major Facilitator Superfamily (MFS) transporter (Supplementary Data 20), an ATP-binding endoribonuclease (Supplementary Data 24), a ß-1,3(4)-glucanase with a predicted signal peptide but no GPI-anchor (Supplementary Data 19), an ornithine decarboxylase (Supplementary Data 20), an importin ß2 (Supplementary Data 26), which was identified as the tagged gene in two independent mutants, and two genes involved in arginine biosynthesis, namely carbamoyl phosphate synthetase (Supplementary Data 25) and the ARG-6 precursor (Supplementary Data 22) which encodes N-acetylglutamate kinase and N-acetylglutamyl-phosphate reductase. Five tagged genes had significant similarity ($E \leq$ 1e-20) to fungal hypothetical proteins of unknown function (both tagged ORF in *path*-7, the predicted ORF tagged in *path*-8 and *path*-23, and the predicted ORF downstream of the T-DNA in *path*-9, Supplementary Data 15-18,23). A further two T-DNA insertions were located in predicted ORFs (tagged in *path*-5 and in *path*-23) without significant homology (E≤ 1e-5) to entries in the NCBI nr or COGEME EST databases (Table 5). However all three of these predicted ORFs matched trace files from the *C. graminicola* genome sequencing project. No functional motifs or conserved domains were identified using InterProScan or RPS-BLAST for the protein translations of predicted genes with no homology or resembling hypothetical proteins except for the putative ORF tagged in *path*-7 was found to have a hypothetical WD40 and a heme oxidase domains.

Table 5. Summary of *Colletotrichum higginsianum* genes identified from T-DNA flanking sequences.

Mutant ID	EMBL Accession No.	No. insertion sites [a]	Putative position of T-DNA insertion [b]	Best Blastx match with functional annotation		
				Putative function and NCBI accession number	Organism	*E*-value
path-5	FM201309	1	in predicted ORF [d]	Unknown	-	-
path-7	FM201311	2	in ORF	Hypothetical protein (FG06146.1)	*Gibberella zeae*	1e-116
	FM201310		1.5 kb upstream of ORF	Hypothetical protein (FG06145.1)	*Gibberella zeae*	2e-22
path-8	FM201314	1	in predicted ORF [e]	Hypothetical protein (MG_01130)	*Magnaporthe grisea*	1e-80
path-9	FM201308	1	1 kb downstream of ORF	Endo-1,3(4)-ß-glucanase (AFUA_1G05290)	*Aspergillus fumigatus*	4e-68
	FM201308		1 kb upstream of ORF	hypothetical protein (MG_05719)	*Magnaporthe grisea*	2e-18
path-12	FM201302	1	in ORF	MFS transporter (NFIA_086030)	*Neosartorya fisheri*	8e-170
path-16	FM201307	1	in ORF	Ornithine decarboxylase (AY602214)	*Glomerella lindemuthiana*	0.0
path-19	FM201305	1	in ORF	Arg-6 protein (EAA35492.1)	*Neurospora crassa*	0.0
path-23	FM201312	2	620 bp upstream of ORF	Hypothetical protein (FG02446.1)	*Gibberella zeae*	2e-102
	FM201313		in predicted ORF [d]	Unknown	-	-
path-29	FM201304	1	730 bp upstream of ORF	ATP-binding endoribonuclease (ACLA_048430)	*Aspergillus clavatus*	5e-110
path-35	FM201306	1[c]	in ORF	Carbamoyl-phosphate synthetase (EAA36214.1)	*Neurospora crassa*	0.0
path-36	FM201303	1	620 bp upstream of ORF	Importin ß2 subunit (AFUA_1G15900)	*Aspergillus fumigatus*	0.0
path-38	FM201303	1	in ORF	Importin ß2 subunit (AFUA_1G15900)	*Aspergillus fumigatus*	0.0

[a] Determined by Southern blot hybridization following *Xho I* digestion of genomic DNA. An *XhoI* site is present in the T-DNA but outside the *hph* probe.
[b] Distance upstream of predicted start codon or downstream of predicted stop codon.
[c] PCR and Southern blot data were consistent with a multiple insertion event comprising three T-DNA copies at a single site.
[d] ORF predicted by FGENESH using *Fusarium graminearum* and *Magnaporthe oryzae* matrices.
[e] ORF predicted by FGENESH using *Arabidopsis thaliana* matrix

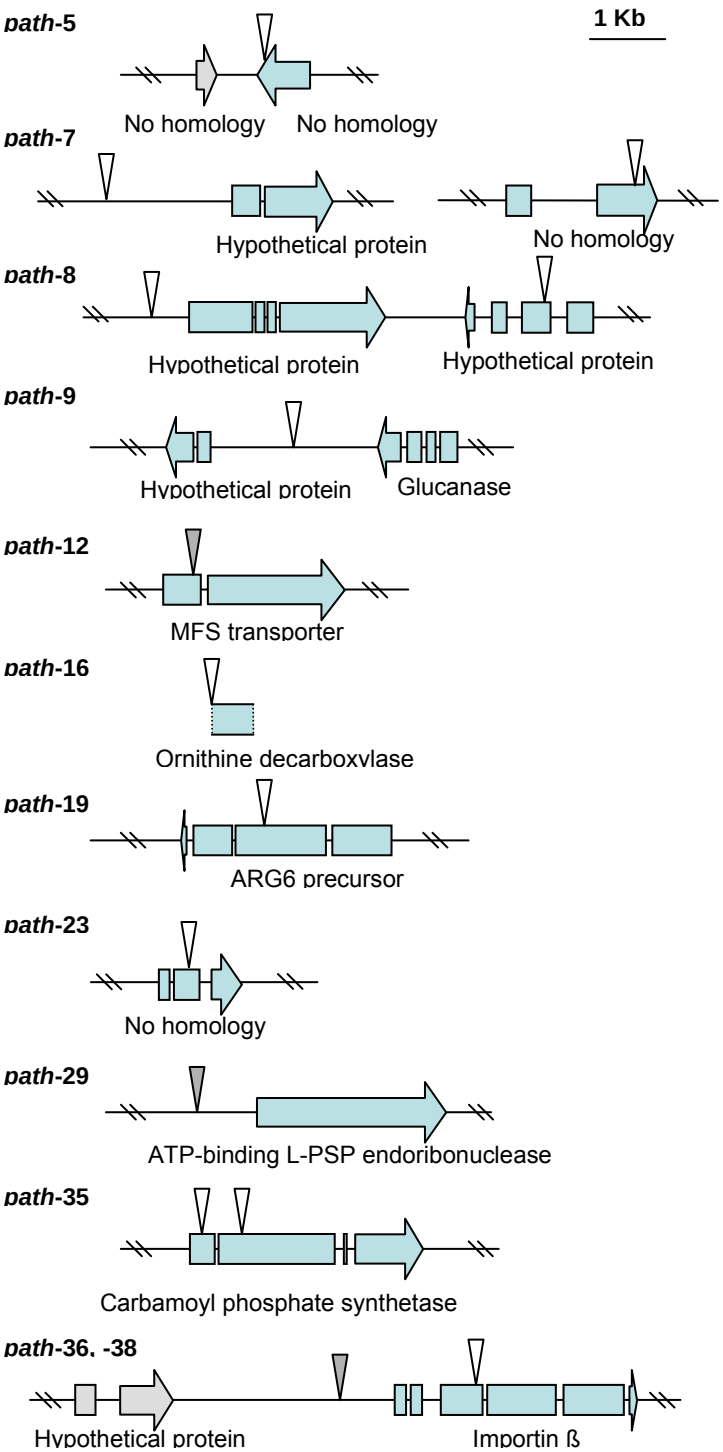

Figure 15. Predicted T-DNA insertions and putative ORFs tagged in 14 molecularly characterised pathogenicity mutants.
Blocks arrows indicate exons in open reading frames (ORFs) in the sense of transcription, as predicted by the FGENEH+ algorithm, for the flanking sequence obtained for the *Colletotrichum higginsianum* mutants. Putatively tagged ORFs are shown in blue. Sites of T-DNA insertions are marked by vertical arrowheads. White arrowheads are single insertions, grey arrowheads are tandem insertions.

2.5.3 Expression patterns of putative pathogenicity genes

For a selection of the putative pathogenicity genes, semi-quantitative reverse transcription (RT)-PCR was used to examine their expression in different fungal cell types and infection stages, namely i) *in vitro* mycelium, ii) conidia germinated *in vitro* on polystyrene forming mature appressoria at 20 h, iii) biotrophic primary hyphae isolated from inoculated *Arabidopsis* leaves by fluorescence-activated cell sorting (FACS), iv) leaves heavily colonised by necrotrophic hyphae at 72 hours after inoculation (hai) and v) non-inoculated leaves as a control (Figure 16A). Expression of four genes was studied in more detail and for these RT-PCR was additionally performed on cDNA obtained from i) ungerminated conidia, ii) conidia germinated *in vitro* conidia for 5 h, epidermal strips taken from inoculated leaves at iii) 3-7 hai (spore germination stage), iv) 20-22 hai (mature appressorium stage), and v) 40-42 hai (biotrophic stage) (Figure 16B). Most genes studied were constitutively expressed at all stages of fungal development including ungerminated conidia, namely the hypothetical protein tagged in *path*-8, the putative importin ß2, the putative ATP-binding L-PSP endoribonuclease and the putative endo-1,3(4)-ß-glucanase. The putative MFS transporter was expressed specifically in germinated spore and appressoria and the biotrophic stage, but not the necrotrophic stage or in mycelium. The tagged ORF in *path*-5 was most strongly expressed in appressoria and in the necrotrophic stage. Using *C. higginsianum* genomic DNA as template, yielded fragments that were larger than the cDNA amplicons when using primers annealing on different exons, indicated that the RNA extracts were free from DNA contamination.

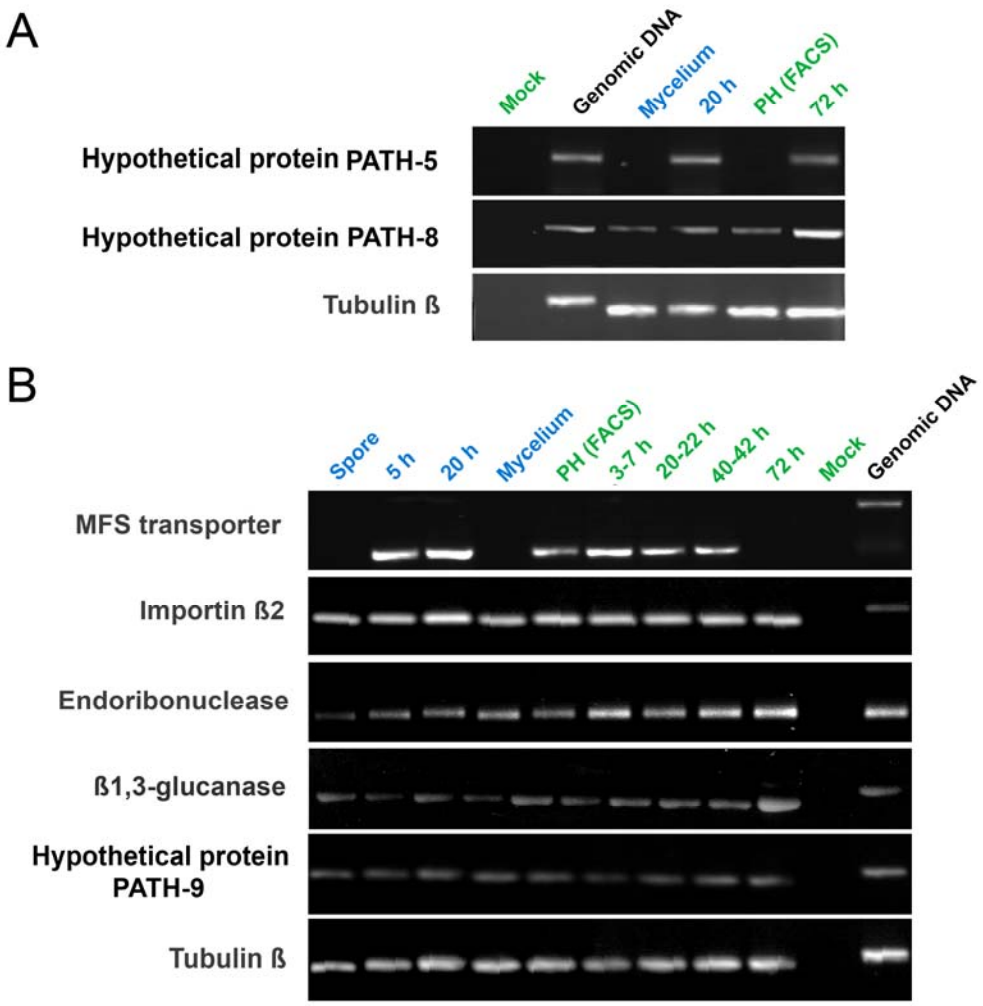

Figure 16. Expression analysis of candidate pathogenicity genes by reverse transcription (RT)-PCR. Expression analysis of selected genes was studied by RT-PCR in wild type *Colletotrichum higginsianum* in different conditions *in vitro* (labelled in blue) and *in planta* (labelled in green). **A**, Expression analysis of hypothetical proteins tagged in mutant *path*-5 (PATH-5) and *path*-8 (PATH-8). The templates used for the RT-PCR were obtained from mock-inoculated leaves (lane 1), genomic DNA (lane 2), saprophytic mycelium from liquid culture (lane 3), mature appressoria obtained on plastic after 20 hours of incubation (lane 4), biotrophic hyphae isolated by FACS from infected plants 40-42 hai (lane 5) and necrotrophically infected tissue obtained 72 hai. **B**, Expression analysis of the putative MFS transporter, the putative importin ß2, putative ATP-binding endoribonuclease and the putative ß1,3-glucanase and the hypothetical protein tagged in *path*-9 (PATH-9). The templates used for RT-PCR were cDNA from ungerminated conidia (lane 1), conidia germinated for 5 h (lane 2), mature appressoria obtained on plastic after 20 hours of incubation (lane 3), saprophytic mycelium from liquid culture (lane 4), isolated biotrophic hyphae obtained 40 to 42 hai (lane 5), conidia germinated on epidermal strips 3-7 hai (lane 6), mature appressoria on epidermal strips 20-22 hai (lane 7), primary hyphae in epidermal strips 40-42 hai (lane 8), necrotrophic hyphae in macerated leaf tissue 72 hai (lane 9) and mock-inoculated leaves sprayed with water only (lane 10). In addition, fungal genomic DNA was used as a template. The number of PCR cycles for each template was adjusted using the *C. higginsianum* tubulin ß as a constitutively expressed control gene.

2.6 Path-*12, a penetration mutant*

2.6.1 Phenotype of mutant path-*12*

Mutant *path*-12 is one of the mutants identified in the pathogenicity screen which gave very rare symptoms on *Arabidopis* at 7 dai compared to the extensive maceration of the whole plants caused by the wild-type strain (Figure 17). The mutant displayed strongly reduced appressorial penetration efficiency on living host tissue, and on cellophane, but not on ethanol-killed leaves (Figure 18A). Furthermore, the penetration ability of cellophane by this mutant was found to be delayed rather than permanently impaired since after 48 h, the penetration efficiency of *path*-12 on cellophane was equivalent with that of the wild-type strain (Figure 18A-B). A slight reduction of mycelial growth rate on both PDA and CDA was observed (77% of wild-type strain on PDA and 74 % on CDA) (Figure 19A). Mutant *path*-12 did not induce more host papillae or HR than the wild type (Table 4), suggesting the reduced penetration is not due to plant defence responses. Apart from severely reduced host penetration, the mutant was impaired in its growth *in planta* and when successful penetration was observed, only small biotrophic primary hyphae and no necrotrophic secondary hyphae were found.

Figure 1. Symptoms produced on mature *Arabidopsis* plants by selected pathogenicity mutants.
Mature (3-week-old) *Arabidopsis* plants were spray-inoculated with spore suspension (5 x 10^5 conidia mL^{-1}) and examined for symptoms at 7 dai. The wild type caused maceration and necrosis of the leaves whereas mutants *path*-12, -36, -38, -29, -19, -35 and -9 caused no symptoms at all or very limited necrotic spots.

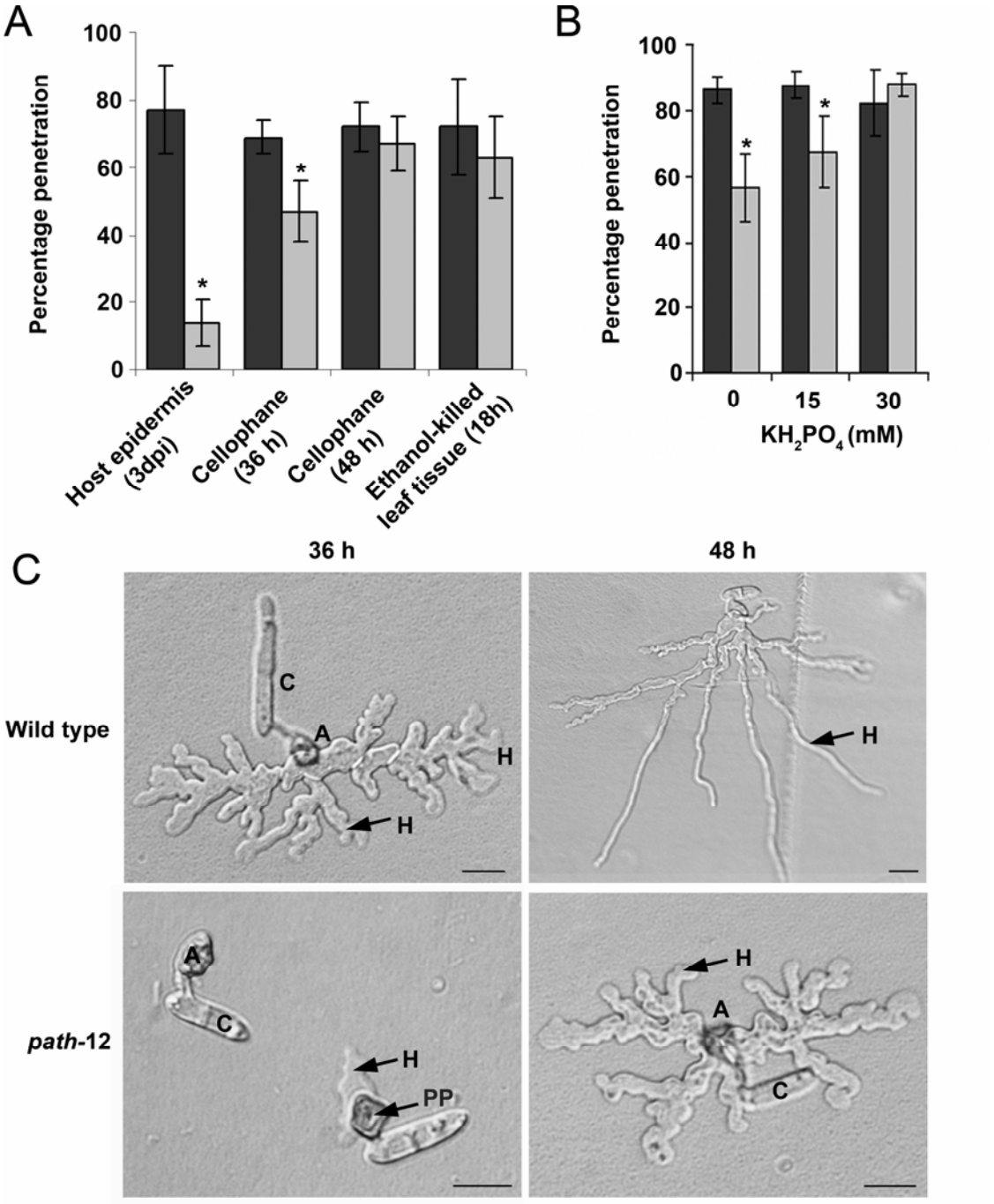

Figure 18. Appressorial penetration of *path*-12.
A, Percentage penetration of the wild-type strain (black bars) and the mutant *path*-12 (grey bars) of the host epidermis counted at 3 dai, cellophane after 36 and 48 hours and ethanol-killed leaves after 18 hours. **B,** Percentage penetration of the wild-type strain (black bars) and the mutant *path*-12 (grey bars) of cellophane after 36 hours with different concentrations of KH_2PO_4. **A**. and **B**. At least 100 appressoria were scored for the wild type and the mutant and values represent mean percentages and standard errors (error bars) calculated from three independent experiments. Asterisks indicate values significantly different to the wild type (Student t-test $P<0.05$). **C,** Light micrographs showing conidia (C) of *Colletotrichum higginsianum* wild-type strain and *path*-12 on cellophane at 36 and 48 hours. (A) Appressorium; (H) Hypha; (PP) Penetration pore. Scale bar = 10 μm.

2.6.2 Complementation of mutant phenotype by integration of cosmid harbouring wild type copy of T-DNA flanking region

Both the radial growth rate on PDA and the pathogenicity of the mutant were rescued to wild-type level when mutant *path*-12 was transformed with a cosmid harbouring the wild-type copy of the disrupted region (Figure 19). The cosmid consists of about 30 kb of genomic DNA flanking the T-DNA insertion. The complementation suggests the disruption of the putative MFS transporter by the T-DNA is indeed responsible for the severely reduced pathogenicity phenotype.

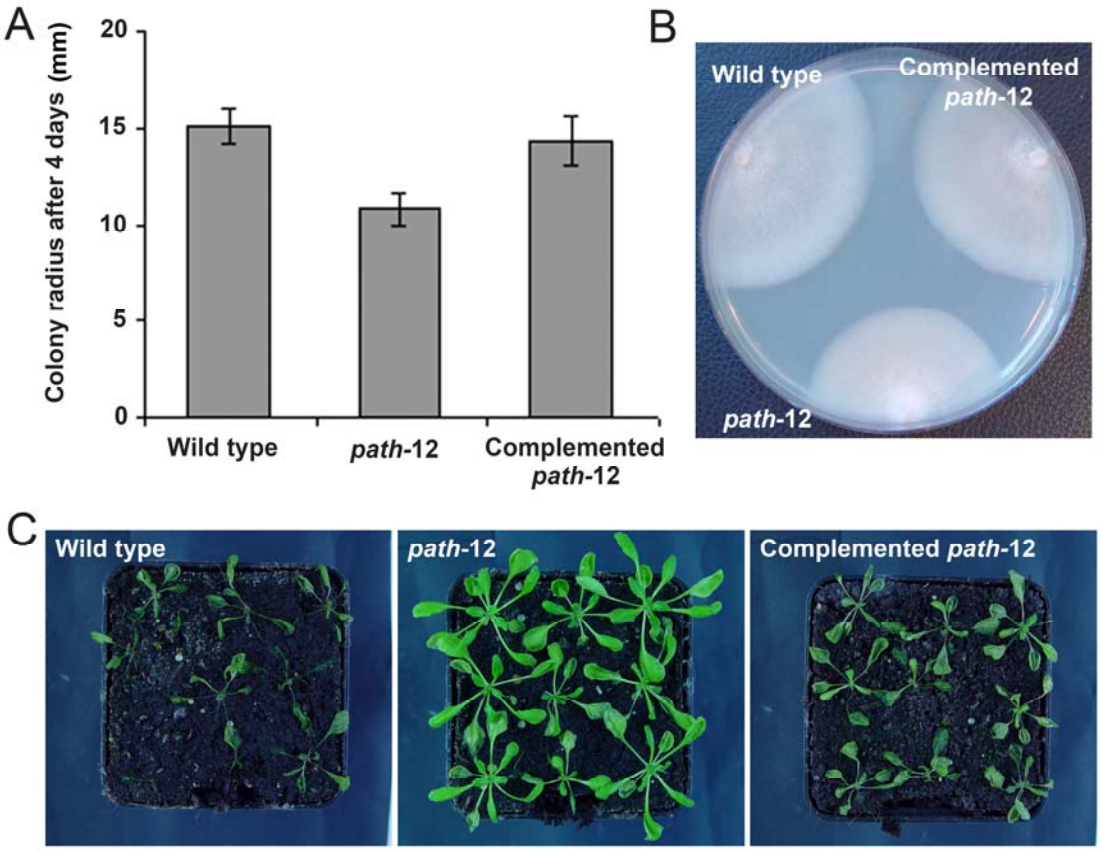

Figure 19. Complementation of the growth rate and pathogenicity of mutant *path*-12 by cosmid harbouring the wild-type copy of the gene.
A. Growth rate *Colletotrichum higginsianum* wild type, *path*-12 and *path*-12 complemented with a cosmid harbouring the full length wild-type copy of the putative major facilitator superfamily (MFS) transporter. The radius of 10 colonies was measured after 4 days. The mean of 3 experiments is shown, the error bars represent the standard error. **B**. PDA plates were inoculated with agar plugs of growing mycelium. Pictures were taken after 4 days. **C**. Mature (3-week-old) *Arabidopsis* plants were spray-inoculated with spore suspension (5 x 10^5 conidia mL^{-1}) of the wild-type strain, mutant path-12 and and *path*-12 complemented with full length wild-type copy of the putative MFS transporter . Macroscopic symptoms were examined at 7 dai.

2.6.3 Homology searches and phylogenetic of tagged gene

Southern blot analysis of genomic DNA from mutant *path*-12 indicated it possessed one tandem insertion of the pBIG2RHPH2 T-DNA inserted at a single site in the genome. The sequence for 2,576 bp of genomic DNA flanking the T-DNA insertion was obtained and submitted to homology searches (Blastx, tBlastx) and ORF prediction (FGENESH+). One ORF was predicted, containing 2 exons, one of 507 bp and a second of 1539 bp with an intron of 53 bp (Supplementary Data 7). The predicted protein product comprised 681 amino acid residues and a molecular weight of 76.670 kDa. The T-DNA was inserted in the first exon (Figure 15). Homology searches indicated that the genomic DNA has high homology (E = 0.0) to fungal hypothetical proteins or genes annotated as Major Facilitator Superfamily (MFS) transporters, proton : phosphate symporters, or high affinity phosphate transporter of filamentous fungi (Supplementary Data 20). Domain searches (ProDom, InterProScan, CDD) indicated the predicted amino acid sequence of the product of gene tagged in *path*-12 (Path-12p) and the homologous fungal sequences identified with Blast searches all possess high homology to transmembrane phosphate transporters (E < 6e-95) and transmembrane MFS (E < 4e-34) domains. Furthermore, the predicted ORF has 12 transmembrane domains predicted by TMHMM, HMMTOP and TMpred, characteristic of MFS transporters (Figure 21). Further down the list of homologous sequences obtained by tBlastx and Blastx are functionally characterised plant high affinity inorganic phosphate transporters. It is likely that most of the homology hits from fungal genomes were only annotated as phosphate transporters due to their homology to the characterised plant phosphate transporters. A function as high affinity phosphate transporter has not been confirmed experimentally for any of the homologues in filamentous fungi. The tBlastx and Blastx hits also included PHO84 of *Saccharomyces cerevisae* (E=4e-17), a very well-characterised high affinity inorganic phosphate : H+ symporter (Bun-Ya *et al.,* 1991). Together, domain predictions and homology searches indicate the ORF disrupted in mutant *path*-12 may encode an MFS transporter, possibly a phosphate transporter.

The putative *C. higginsianum* transporter is a single copy gene as demonstrated by Southern blot analysis using a probe specific for the disrupted locus (Figure 22). Interestingly, related filamentous fungi such as *Giberella zea*e, *Chaetomium globosum* or

Magnaporthe grisea, had one very high homology Blast hit to the putative transporter and a second hit of lower homology, probably with not enough sequence similarity to hybridise in the Southern analysis. A phylogenetic tree was constructed to investigate the relationship between the predicted gene product tagged in *path*-12, the high affinity phosphate transporters pho84p and pho89p of *S. cerevisae*, plant phosphate transporters, and the two best hits of *G. zeae*, *M. grisea* and *C. globosum*, as well as other fungal MFS transporters which have sugars, toxins or glycerophosphoinositol as cargoes (Figure 20). The phylogenetic tree revealed these three fungal species (*M. grisea*, *C. globosum* and *G. zeae*), as well as having a homologue of the *C. higginsianum* transporter, also had a putative transporter even more closely related to pho84p and plant high affinity phosphate transporter, than the predicted gene product tagged in *path*-12. The phylogenetic tree also revealed that the product of the tagged gene was more distantly related to pho89p, a high affinity phosphate : sodium symporter of *S. cerevisae*, or other MFS transporters such as sugar transporters, toxin transporters or GIT1 of *S. cerevisae* involved in the transport of glycerophosphoinositol and more recently found to be a low affinity phosphate transporter (Patton-Vogt and Henry, 1998; Almaguer *et al.,* 2004).

Alignments of the predicted product of the gene tagged in *path*-12, together with the most homologous sequences in *M. grisea*, *C. globosum* and *G. zeae* as well as the second best hit in the same fungi and Pho84p confirm what the tree indicates, that these lower hits were more homologous to Pho84p than to the *C. higginsianum* transporter tagged in *path*-12. The putative transporter tagged in *path*-12 is longer than pho84p and homology is restricted to certain regions only (Figure 21). This suggests filamentous these fungi have more than one transporter with homology to Pho84p, with varying degrees of conservation. The predicted transmembrane domain of Path-12p and of Pho84p (Lagerstedt *et al.,* 2004) are underlined in red in the alignment. The transmembrane domain share homology, but the conserved regions are distributed among transmembrane, and the extra- and intracellular loops. Path-12p has longer C- and N-terminal extensions (Figure 21).

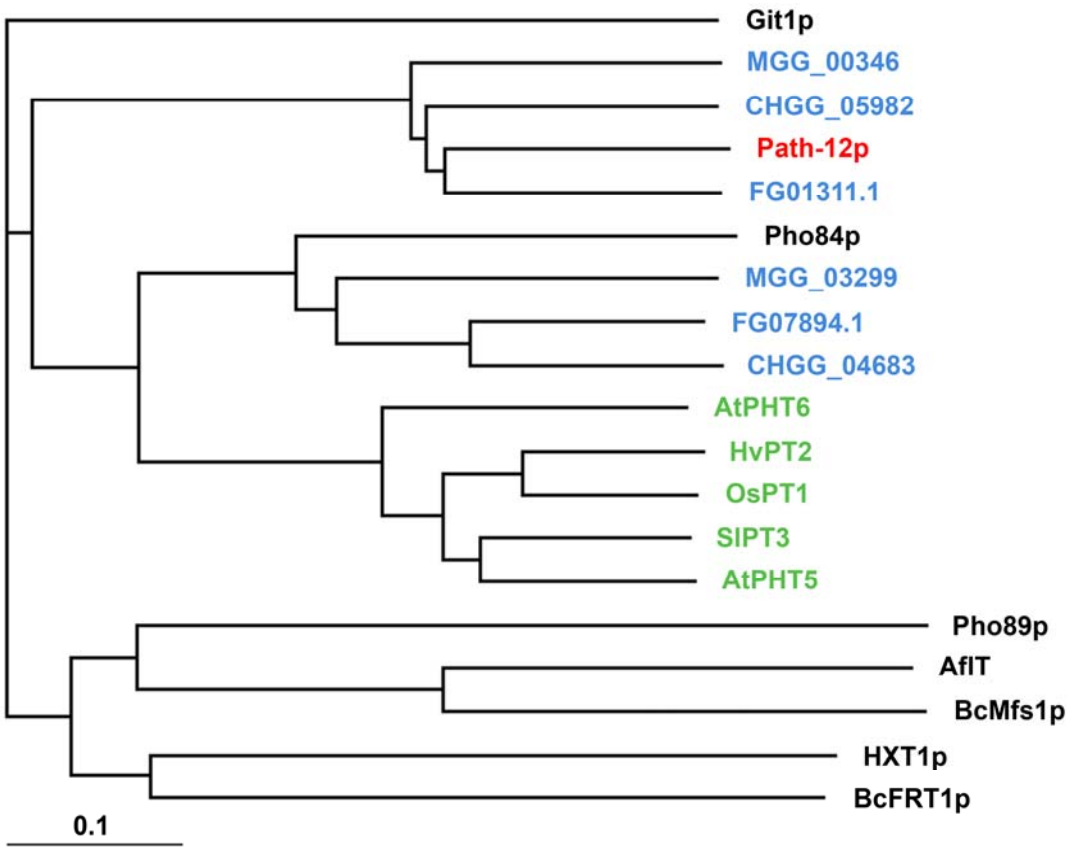

Figure 20. Phylogenetic tree showing relatedness of MFS transporters to gene tagged in *path*-12.
Neighbour-Joining tree based on the deduced amino acid sequence of the gene tagged in *Path*-12 (Path12p) and the complete sequences of the predicted protein of other major facilitator superfamily (MFS) transporters: the top hits to Path-12p from *Fusarium graminearum* (FG1311,1), *Chaetomium globosum* (CHGG_05982) and *Magnaporthe grisea* (MGG:00346), hits of lower homology to Path12p from *F. graminearum* (FG07894.1), *C. globosum* (CHGG_04683) and *M. grisea* (MGG_03299) (in blue), high affinity phosphate transporters of *Saccharomyces cerevisae* Pho84p and Pho89p, plant phosphate transporters HvPT2, OsPT1, SlPT3, AtPHT5, AtPHT6 (in green), phosphate and glycerophosphoinositol transporter of *S. cerevisae GIT1*, fungal sugar MFS transporters HXT1p of *Uromyces fabae*, *and* BcFRT1 of *Botrytis cinerea*, and fungal toxin MFS transporter AflT of *Aspergillus flavus*, and BcMfs1 of *B. cinerea.* Sequences were obtained from the NCBI database. The alignment and tree were performed by CLUSTALW. The bar indicates a distance of 0.1 substitution per site.

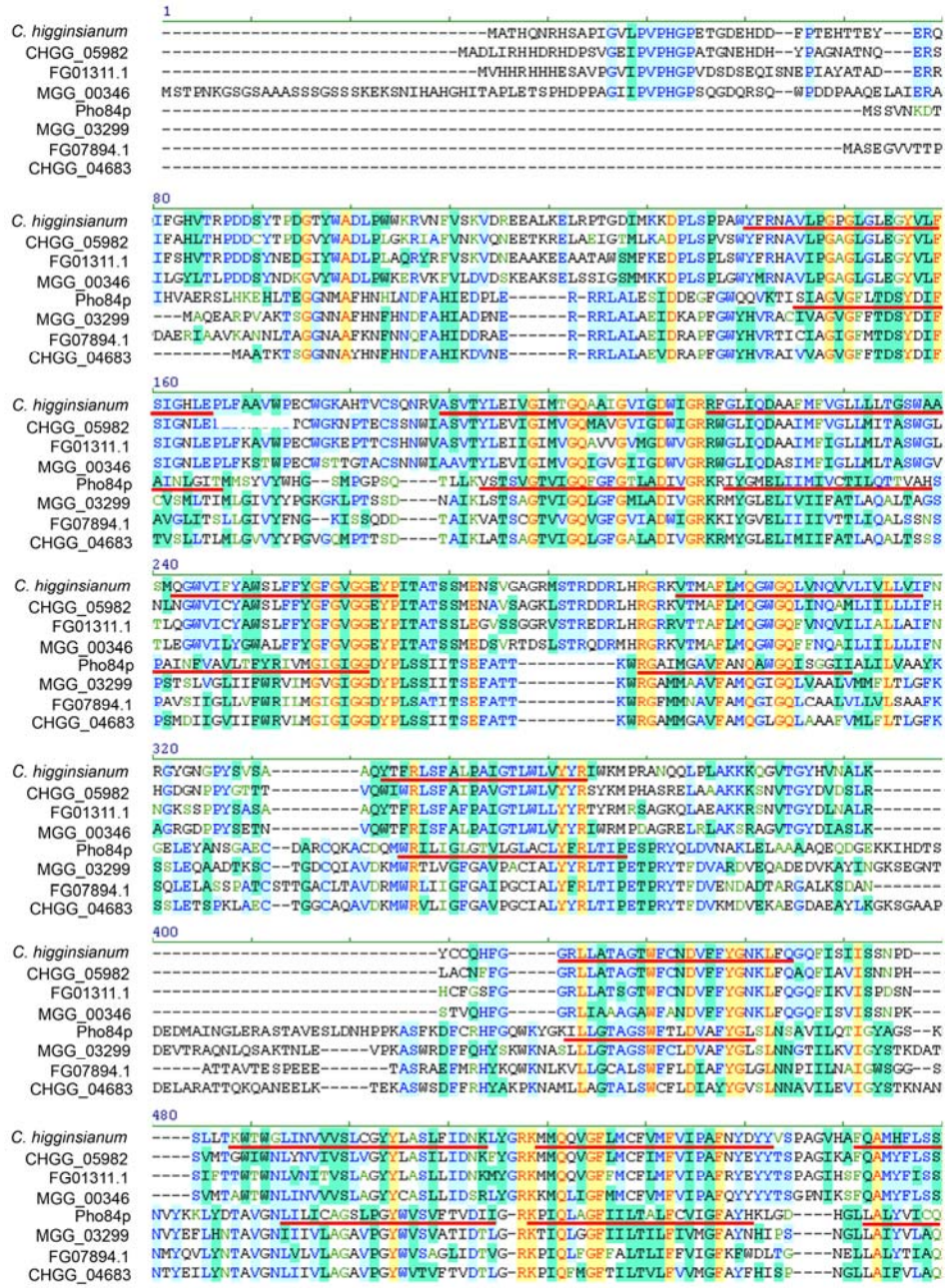

Figure 21. Alignment of sequences of the predicted transporter tagged in *path*-12 and homologous fungal transporters. Alignment of Path12p and top Blast hists from *Chaetomium globosum* (CHGG_05982), *Giberella zeae* (FG01311.1), *Magnaporthe grisea* (MGG_003346) and second best hits of the same organisms: *C. globosum* (CHGG_04683), *G. zeae* (FG07894.1), *M. grisea* (MGG_03299), as well as high affinity phosphate transporter of *Saccharomyces cerevisae* Pho84p. Residues in an alignment are coloured according to the following scheme: non-similar or weakly similar residues are in white, consensus residues derived from a block of similar residues at a given position are in blue, consensus residues derived from the occurrence of greater than 50 % of a single residue at a given position are in green, and consensus residues derived from a completely conserved residue at a given position are in yellow. The 12 transmembrane domains of the *Colletotrichum higginsianum* protein and Pho84p are underlined in red. The best hits aligned well with Path-12p whereas the second best hits align with Pho84p. Alignment made by VNTI.10, Invitrogen.

Figure 21 continued. Alignment of sequences of the predicted transporter tagged in *path*-12 and homologous fungal transporters.

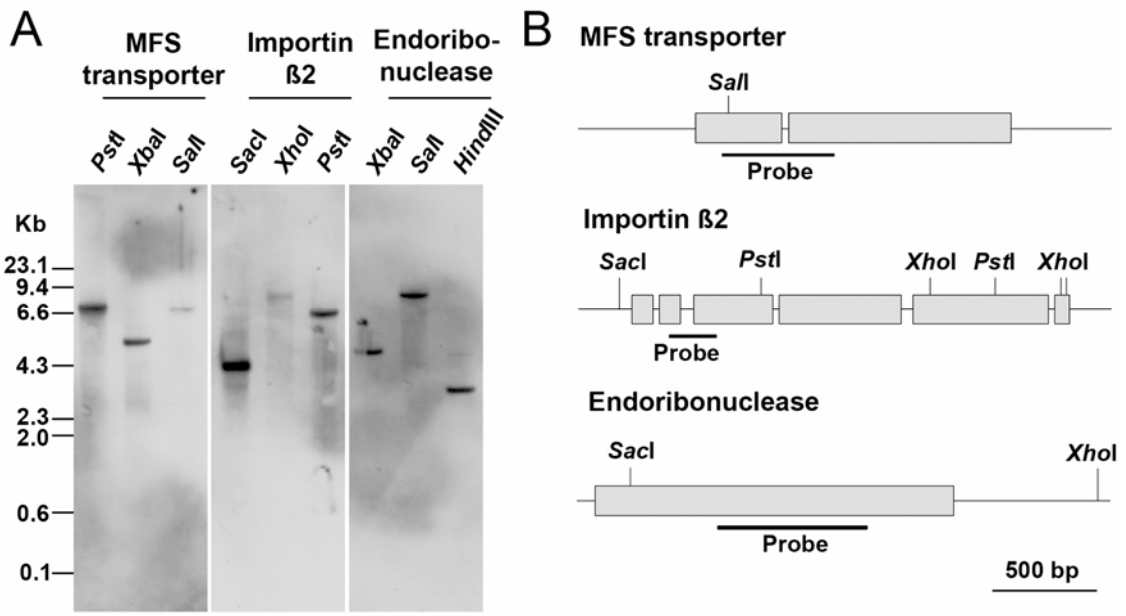

Figure 22. Determination of the copy number of selected tagged genes.
A, Southern blot analysis was performed with a gene-specific probe on genomic DNA of wild type *Colletotrichum higginsianum* digested with enzymes *Pst*I, *Xba*I, *Sal*I, *Sac*I, *Xho*I or *Hind*III. The major facilitator transporter (MFS) transporter tagged in *path*-12, the putative importin ß2 tagged in *path*-36 and *path*-38 and the putative endoribonuclease tagged in *path*-29 were all found to be present as a single copy. **B**, Sites of enzyme restriction and probe for each gene.

The *in vitro* growth defect of the *C. higginsianum path*-12 mutant could be rescued by the addition of high concentrations (75 mM KH_2PO_4) of phosphate to the growth medium (data not shown). Similarly, the ability to penetrate into cellophane membranes by *path*-12 appressoria was also restored by the addition of exogenous phosphate (30 mM KH_2PO_4) (Figure 18C). These findings suggest that the disrupted ORF indeed encodes for a phosphate transporter. Furthermore, the mutant *path*-12 was significantly more resistant ($P<0.05$) to the addition of toxic levels of arsenate, a toxic analogue of phosphate which is taken up by the same transporters (Lee *et al.,* 2003). The mutant was also significantly more resistant addition of the metal chlorides $MnCl_2$, $CuCl_2$, $ZnCl_2$ and $CoCl_2$ in the growth medium (Figure 23), which are known cargoes of the high affinity transporter pho84p of *S. cerevisase* (Jensen *et al.,* 2003). These observations support the hypothesis that the ORF disrupted in *path*-12 is involved in phosphate transport and may function in a similar way to the high affinity phosphate transporter pho84p of *S. cerevisae*.

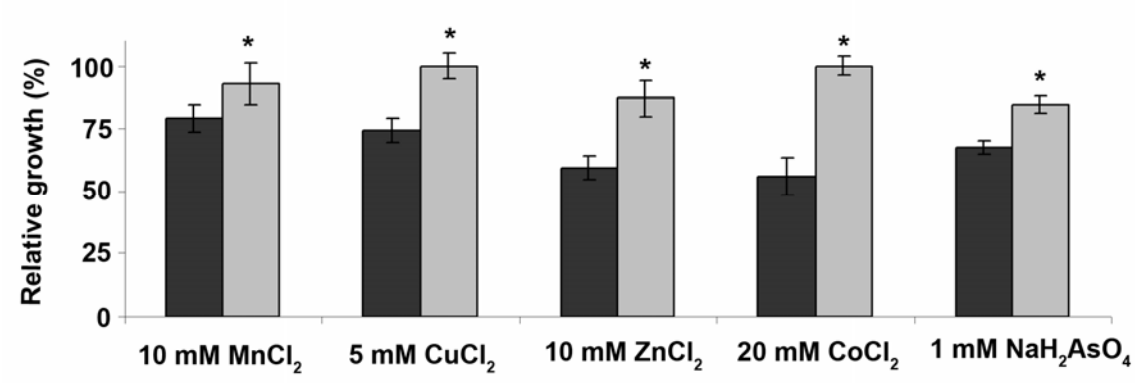

Figure 23. Resistance to arsenate and metals of the *path*-12 mutant.
Radial growth rate of the wild-type strain (black bars) and *path*-12 (grey bars) on PDA supplemented with $MnCl_2$, $CuCl_2$, $ZnCl_2$,$CoCl_2$ or NaH_2AsO_4 are shown as a percentage of the radial growth on unammended PDA, measured after 3 days. The radius of four colonies was measured and the experiment was performed three times. Mean percentages of three experiments are shown with the standard error (error bars). Asterisks indicate the mean growth on amended media as a percentage of growth on unammended medium is significantly different between mutant *path*-12 and the wild-type strain on the same medium (Student t-test $P<0.05$).

2.6.4 *Complementation of yeast quintuple phosphate transporter mutant with* C. higginsianum *gene tagged in path-12*

To demonstrate that the ORF disrupted in *path*-12 is indeed a phosphate transporter, a quintuple *S. cerevisae* knock-out strain lacking five phosphate transporter (*pho84Δ, 87Δ, 89Δ 90Δ 91Δ*) was used. This quintuple knock-out strain would not normally be viable but was rescued on galactose medium due to the presence of *PHO84* under the control of the galactose-inducible *GAL1* promoter. Introducing the yeast PHO84 cDNA or the full-length cDNA for the predicted *C. higginsianum* protein in *path*-12 under the control of the constitutive promoter *ADH1* similarly resulted in the rescue of yeast growth on glucose. The functional complementation of the yeast deletion strain by the *C. higginsianum* gene indicates that *path*-12 is involved in phosphate uptake and that its affinity for phosphate is similar to that of Pho84p (Figure 24).

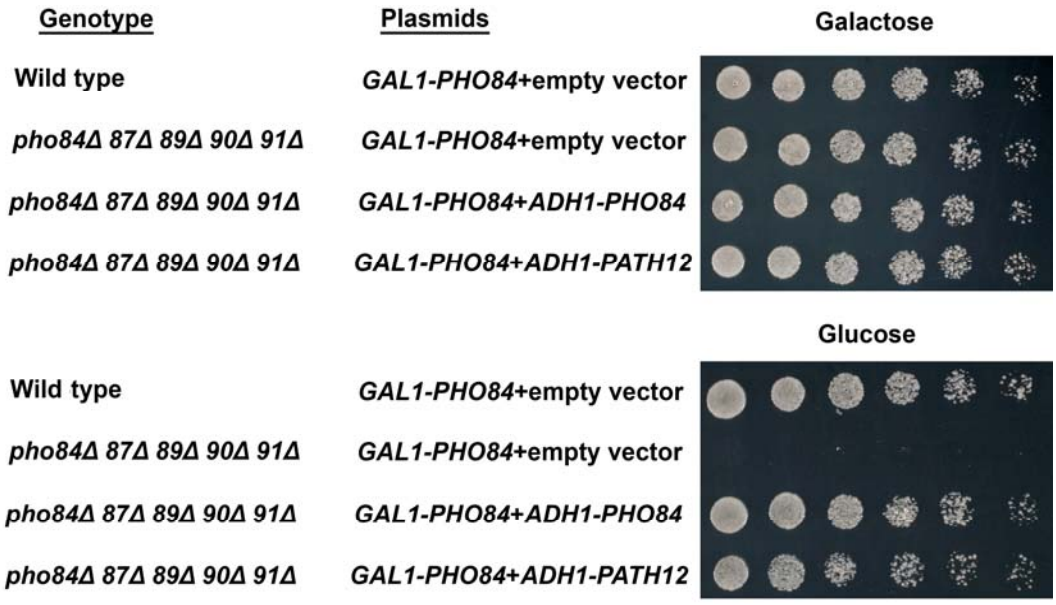

Figure 24. Complementation of the *Saccharomyces cerevisae* quintuple phosphate transporter mutant by *Colletotrichum higginsianum* MFS transporter *path*-12.
Row one is wild type yeast strain (EY57). Row two is the quintuple transporter deletion strain (EY917), row three is EY917 with an over-expression construct of pho84 under control of the constitutive promoter ADH1, row four is EY917 with an over-expression construct with path-12 under control of the constitutive promoter ADH1. The quintuple deletion is lethal and all strains contain EB1280 (p*GAL-PHO84*) allowing them to grow on galactose. Yeast cultures were grown to OD600 between 0.3 and 0.6 in YEP Galactose medium, diluted to OD600 = 0.3, and plated in a threefold dilution series on YEP Glucose and YEP Galactose media. The plates were incubated at 30 °C for 2 days.

2.6.5 Expression analysis of gene tagged *in* path-*12 by RT-PCR*

To understand at what stage of fungal infection phosphate uptake by the putative high affinity phosphate transporter is required, the expression of the transporter in the wild type was studied by semi-quantitative RT-PCR at different stages *in vitro* and *in planta*. The predicted transporter disrupted in *path*-12 was expressed during germination and appressorium formation in water, as well as during the intracellular bioptrophic stage. It was not expressed during the necrotrophic phase or when the fungus grew in rich medium (Figure 16). The expression of the transporter coincided with the stages of infection where the mutant *path*-12 was most affected: during appressorial penetration and biotrophy. It is possible that during germination, enough phosphate is available from internal stores within the conidium to develop appressoria but phosphate uptake may be required in a phosphate-limiting environment such as the plant surface and inside the plant apoplast for successful penetration and growth *in planta*.

2.6.6 Complementation of pathogenicity phenotype of path-*12 by supplementation of phosphate in and on plant tissue*

To study the importance of phosphate uptake during the pathogenesis of *C. higginsianum*, the effect of adding exogenous phosphate on the pathogenicity of the mutant and the wild type was observed. The *C. higginsianum* wild-type strain is pathogenic on *B. napus biennis* cotyledons, causing severe maceration of the host tissues (Figure 25). As on *Arabidopsis*, mutant *path*-12 showed reduced penetration and very reduced symptoms on *Brassica* cotyledons (Figure 25). The addition of phosphate (40 mM KH_2PO_4) on the plant surface by spraying the phosphate solution on the cotyledons prior to spray-inoculation, improved the host penetration by *path*-12 and resulted in the production of necrotic lesions (Figure 25). The addition of phosphate (40 mM KH_2PO_4) inside the leaf by vacuum-infiltration of the phosphate suspension into the cotyledons prior to spray-inoculation increased the pathogenic ability of *path*-12 to a level similar to that of the wild type (Figure 25). This suggests phosphate might be present in limiting concentrations on the plant surface and in the apoplast so that the addition of excess phosphate restores the pathogenicity of *path*-12.

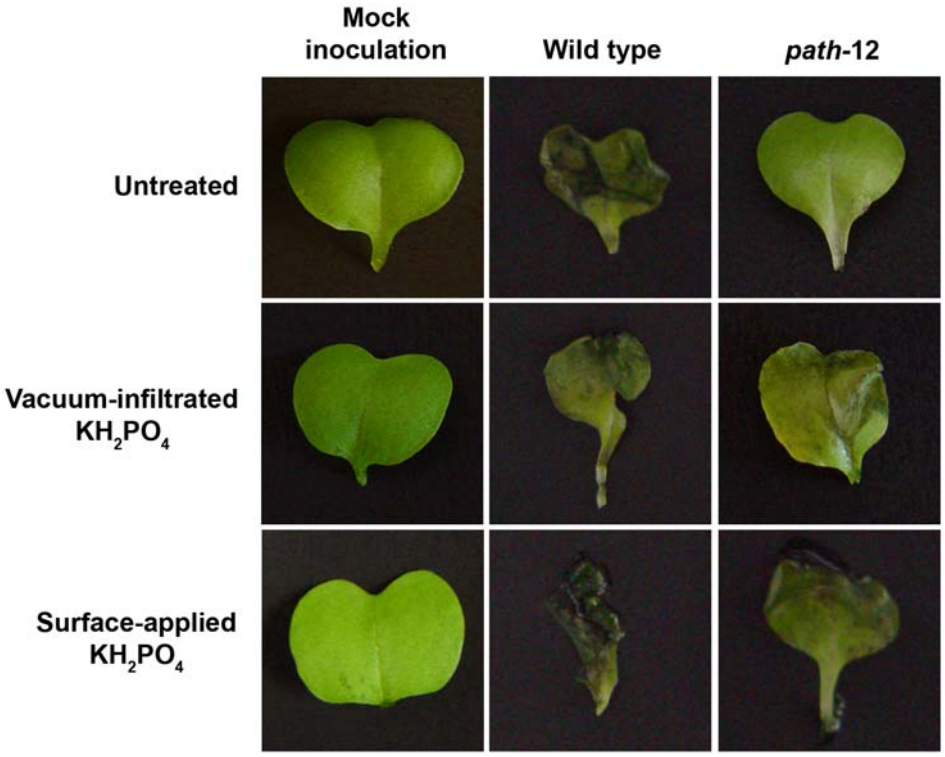

Figure 25. Pathogenicity of *path*-12 on *Brassica* cotyledons is restored by supplementation with phosphate.
Seven day-old cotyledons of *Brassica napus biennis* were detached and treated with 40 mM KH_2PO_4 either by spraying on the cotyledon surface or by vacuum infiltration prior to inoculation. The cotyledons were spray-inoculated with *Colletotrichum higginsianum* wild-type strain ($5x10^5$ conidia per mL) and symptoms were examined 5 at dai.

2.7 Mutants path-36 and path-38, impaired in switch to necrotrophy

2.7.1 Prediction of tagged gene and homology search

Two independent mutants, *path*-36 and *path*-38, both had T-DNA insertion(s) which tagged the same gene. Mutant *path*-36 had a single insertion of pBIN-GFP-hph T-DNA whereas *path*-38 had one tandem insertion of two copies of the pBIG2RHPH2 T-DNA integrated at a single site. By obtaining genomic DNA flanking the insertions of both mutants, the T-DNA insertion site in *path*-36 was found to be located 1,139 bp away from the *path*-38 insertion site. A total of 8 kb of genomic DNA sequence of the region around the inserts was obtained. An ORF with six exons was predicted using FGENESH+ which encoded a protein of 869 amino acids with a molecular weight of 96.881 kDa (Supplementary Data 14). The T-DNA in *path*-36 is 622 bp upstream of the first exon of the predicted ORF, but downstream of the predicted transcription start site (Figure 15). The tandem insertion in *path*-38 is located in the third exon. The region of genomic DNA was subjected to homology searches using Blastx and tBlastx and was found to have very high homology (*E*=0.0) to hypothetical protein and predicted importin ß2 of fungal species (Supplementary Data 26). All the hypothetical proteins without functional annotations as well as the predicted ORF tagged in *path*-36 and -38 were found to have functional domains characteristic of karyopherin or importin ß2 (InterProScan, ProDom, CDD). The *C. higginsianum* sequence also showed high homology (*E*<1e-120) to karyopherin ß2 of human and other animal species. An alignment performed with fungal sequences of the encoded putative importin ß2 supports the observation that they are highly conserved (Figure 26). The predicted *C. higginsianum* importin is a single copy gene as revealed by Southern blot analysis (Figure 22).

Figure 26. Alignment of sequences of the predicted importin ß2 tagged in *path*-36 and -38 with other fungal predicted importin ß2.

Alignment of the predicted importin ß2 and top Blast hits from *Giberella zeae* (FG01854.1), *Magnaporthe grisea* (MGG_009208) and *Botrytis cinerea* (BCG_11788) and the well characterised karyopherin ß2 of *Schizosaccharomyces pombe* Kap104p. The sequences display very high homology. Residues in an alignment are coloured according to the following scheme: non-similar or weakly similar residues are in white, consensus residues derived from a block of similar residues at a given position are in blue, consensus residues derived from the occurrence of greater than 50 % of a single residue at a given position are in green, and consensus residues derived from a completely conserved residue at a given position are in yellow. Alignment made by VNTI.10, Invitrogen.

Figure 26 continued. Alignment of sequences of the predicted importin ß2 tagged in *path*-36 and -38 with other fungal predicted importin ß2.

2.7.2 Phenotype of mutants path-*36 and* path-*38*

Both mutants had a similar pathogenicity phenotype: strongly reduced symptoms despite unaffected penetration efficiency (Figure 17 and Figure 10B). The growth rate *in vitro* was unaffected in both mutants (data not shown). The morphology and timing of formation of biotrophic hyphae was also similar to that of the wild type but necrotrophic secondary hyphae were rarely seen, usually on older leaves or at the leaf edge (Figure 10A, Table 4). The biotrophic hyphae appeared to be unable to enter the necrotrophic stage. Neither mutants produced significantly more hydrogen peroxide than the wild type (Table 4), suggesting that host defence responses were nor responsible for the reduced formation of necrotrophic hyphae. Untimely death of the host cell, *i.e.* while the fungus is still establishing the biotrophic stage, is one possibility for the failure to enter the necrotrophic phase because the fungus might not survive in a dead cell at his stage. However, with other mutants of the same phenotype (Section 2.3.4), penetrated host cells containing large primary hyphae of *path*-36 and *path*-38 retained the ability to plasmolyse, indicating they

were still alive at 7 dai (Figure 10C) and 9 dai (data not shown). However, due to the reduced frequency of penetration observed on *Arabidopsis* hypocotyls, it was not possible to quantify the percentage of penetrated cells which remained alive. To evaluate host cell viability in relation to the viability of the fungal hyphae showing arrested biotrophy, plasmolysis was combined with visualization of GFP expressed by primary hyphae of the mutant *path*-36. A variety of scenarios were observed at 7 dai: living primary hypha within a living host cell (Figure 27, first row), a living primary hypha in a dead host cell (Figure 27, second row) or a dead primary hypha in a living host cell (Figure 27, third row). Once again, due to the low frequency of penetration of hypocotyls, the occurrence of each interaction type could not be quantified.

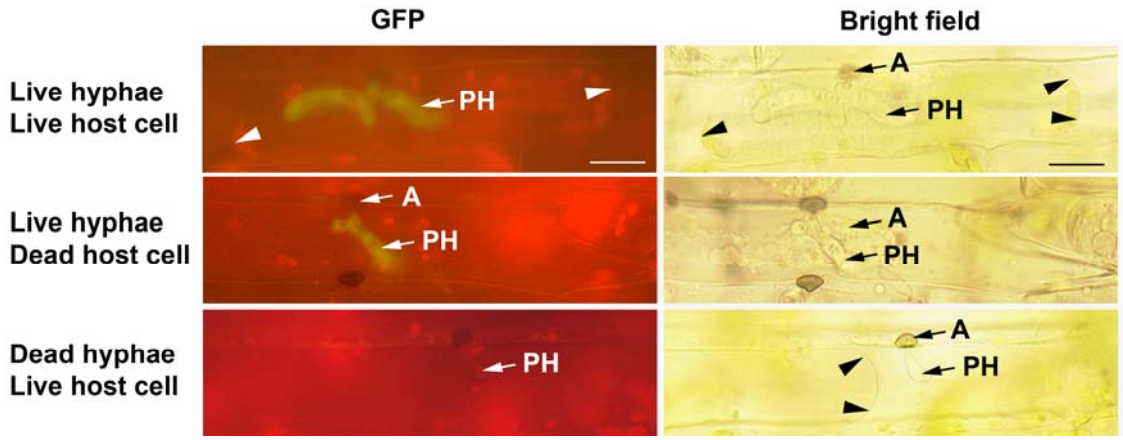

Figure 272. Viability of penetrated host cells and fungal hyphae of *path*-36.
Viability of penetrated hypocotyl epidermal cells of *Arabidopsis* 7 dai was determined by plasmolysis, involving contraction of the plasma membrane from the cell wall (arrowheads). The viability of fungal primary hyphae (PH) was estimated by its GFP fluorescence. Different scenarios were observed: first row, a living GFP-expressing hypha in a living host cell, second row: a living fungal hypha in a dead host cell, and third row: a dead, non-fluorescing primary hyphae in a living host cell. Scale bar = 10 µm.

2.7.3 Expression study of gene tagged in path-36 and -38 by RT-PCR

The expression of the putative importin was examined by RT-PCR in order to determine at what stage of pathogenicity the protein might be important. The putative *C. higginsianum* importin was found to be constitutively expressed at all stages of fungal development and plant infection (Figure 16).

2.8 Path-29, a HR-inducing mutant

2.8.1 Pathogenicity phenotype of mutant path-29

Mutant *path*-29 is a mutant which caused only reduced symptoms due to the low percentage of infections reaching the necrotrophic stage on *Arabidopsis* (Table 4). Its growth in vitro was not affected (Table 4). The mutant displayed a slightly reduced frequency of appressorial penetration of the host epidermis and a normal ability to form primary hyphae. However, unlike the wild-type strain, mutant *path*-29 had a severely reduced ability to form necrotrophic hyphae as previously described (Section 0, Table 4 and Figure 10). Consequently, very little symptoms were seen on *Arabidospis* at 7 dai (Figures 7 and 8A).

2.8.2 Identification of tagged gene and homology search

The mutant *path*-29 was found by Southern blot analysis to contain two copies of pBIN-GFP-hph T-DNA. The two inserts were integrated as a tandem at a single site. A 5,088 bp region of genomic DNA flanking the insertions was obtained and subjected to homology searches against tBlastx and Blastx. One ORF was predicted, with only one exon, encoding a putative protein of 826 amino acid residues with a molecular weight of 89.398 kDa (FGENESH+) (Figure 15, Supplementary Figure 12). The sequence was found to have high homology to putative ATP-binding endoribonucleases and hypothetical proteins of filamentous fungi but also of plants and animals (Supplementary Data 24). All the top Blast hits, as well as the predicted protein tagged in *path*-29, had the same domain architecture with an adenine nucleotide α-hydrolase close to the N-terminus and a liver-perchloric acid soluble protin (L-PSP) endoribonuclease in the C-terminal part of the protein (InterProScan,

CDD). An alignment of the predicted ATP-binding endoribonuclease of *C. higginsianum* and the most homologous sequences of *G. zeae*, *M. grisea*, *C. globosum* and *Neurospora crassa* indicate the proteins have very highly conserved regions as well as regions of no homology (Figure 28). The ATP-binding site and the putative L-PSP endoribonuclease site are among the conserved regions.

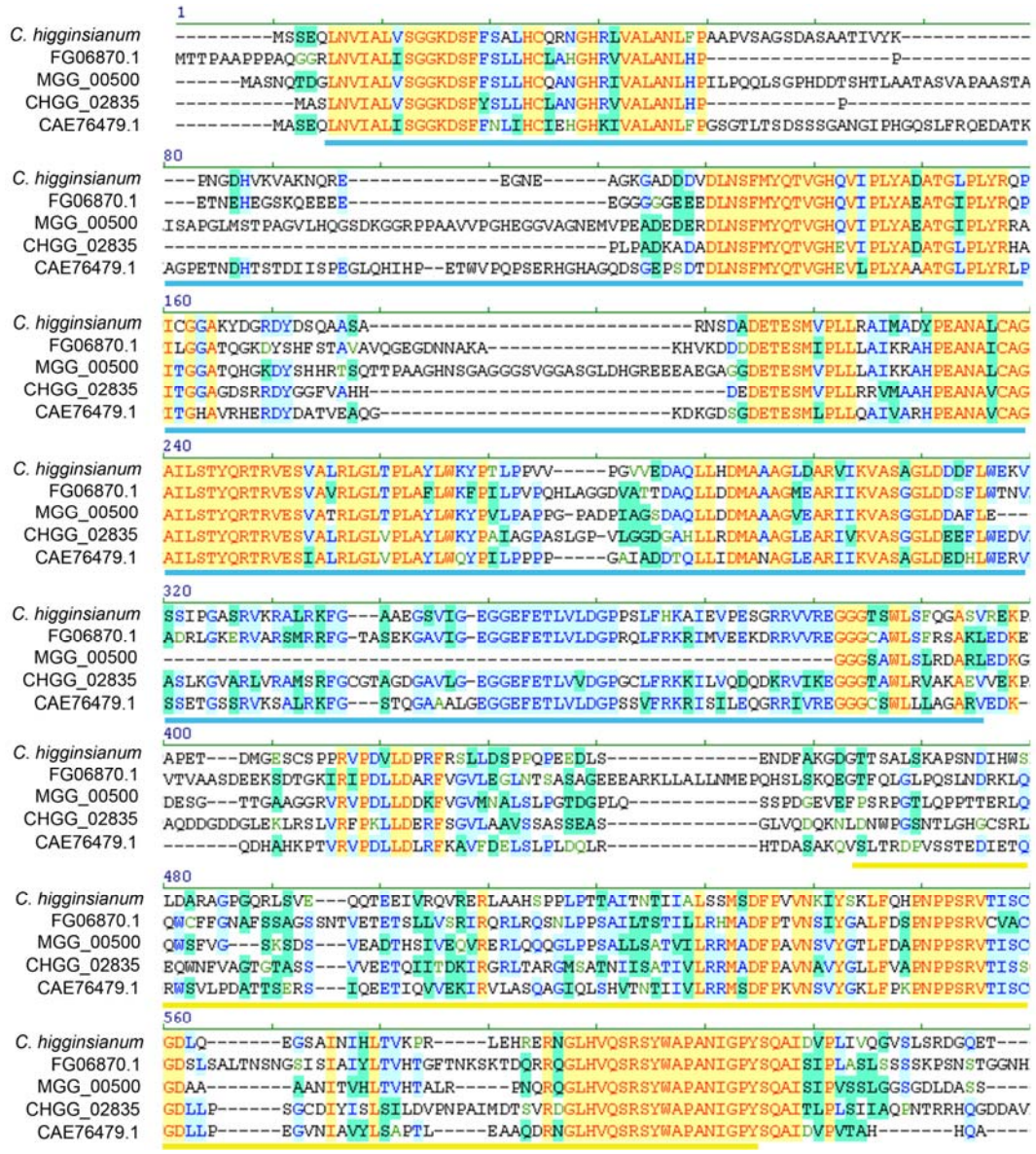

Figure 28. Alignment of sequences of the predicted *Colletotrichum higginsianum* ATP-binding liver perchloric acid-soluble (L-PSP) endoribonuclease and homologous fungal sequences.
Alignment of the C. higginsianum predicted ATP-binding endoribonuclease and top Blast hits from *Giberella zeae* (FG06870.1), *Magnaporthe grisea* (MGG_00500), *Chaetomium globosum* (CHGG_02835) and *Neurospora crassa* (CAE7649.1). The alignment indicates that the proteins have both very conserved regions and regions of no homology between them. The regions containing the predicted ATP-binding domain (underlined in blue) and the L-PSP endoribonuclease domain (underlined in yellow) contain conserved regions: Residues in an alignment are coloured according to the following scheme: non-similar or weakly similar residues are in white, consensus residues derived from a block of similar residues at a given position are in blue, consensus residues derived from the occurrence of greater than 50% of a single residue at a given position are in green, and consensus residues derived from a completely conserved residue at a given position are in yellow.

Figure 28 continued. Alignment of sequences of the predicted *Colletotrichum higginsianum* ATP-binding liver perchloric acid-soluble (L-PSP) endoribonuclease and homologous fungal sequences.

2.8.3 Expression study of gene tagged in path-29 by RT-PCR

The T-DNA insertion site was 735 bp upstream of the predicted ORF. No transcription start site or regulatory elements were found between the insertion site and the first exon, suggesting the T-DNA was inserted between the ORF and the transcription start site and the promoter (Proscan, FGENESH+). The expression of the putative ATP-binding endoribonuclease in the wild-type strain was found to be constitutively expressed at all stages of fungal development and plant infection (Figure 16B), suggesting that pathogenicity is only one of several functions in which this gene product might be involved. Because the T-DNA was inserted upstream of the ORF, an RT-PCR experiment was performed on cDNA from the mycelium of *path*-29. The predicted gene was found to be

expressed in the mutant but at a lower level than in the wild type (Figure 29). The putative endoribonuclease gene is a single copy gene (Figure 22).

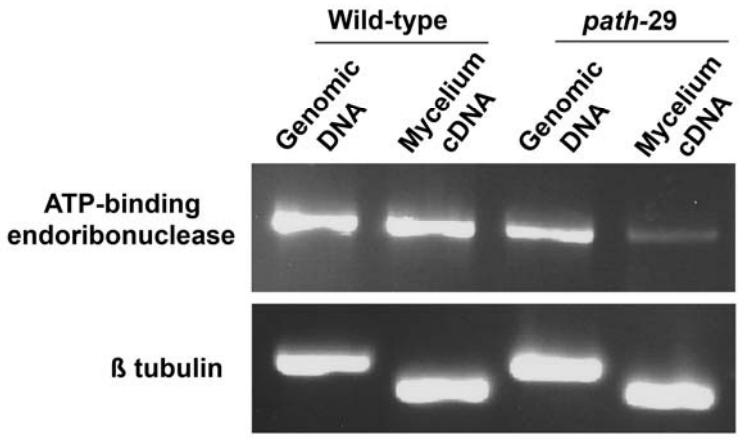

Figure 29. Expression of putative ATP-binding endoribonuclease in the *path*-29 mutant.
The expression of the predicted endoribonuclease, 735 bp downstream of a T-DNA insertion in *path*-29, was studied in the mycelium of the wild-type *Colletotrichum higginsianum* strain and of the *path*-29 mutant. The mutant showed some expression of the tagged gene, although lower than the wild type.

2.9 Path-9, a penetration mutant

2.9.1 Prediction of tagged genes in path-9

Mutant *path*-9 contains a single T-DNA insertion. A total of 4887 bp of genomic DNA was obtained and two ORFs were predicted using FGENESH+ (Figure 15, Supplementary Data 6). The T-DNA was found to be located approximately in the middle of two predicted ORF, about 1 kb upstream of a hypothetical protein (Blastx and tBlastx) (Supplementary Data 18) and the other 1 kb downstream of a predicted ORF with homology to glucanases, particularly endo1,3(4)ß glucanases of fungal species (Supplementary Data 18). Interestingly, several species appear to have more than one homologous gene, *e.g. G. zeae*, *M. grisea*, *Sclerotinia sclerotium*, *Neosartorya fischeri, Puccinia tritici-repentis, Botryotinia fuckeliana* and *Coccidoides immitis* (Supplementary Data 19). Using SignalP to predict N-terminal signal peptides, the putative glucanase was predicted to be secreted. This may be a soluble extracellular protein because it was not predicted to contain either

transmembrane domains using the TMHMM algorithm or a C-terminal glycosylphosphatidylinisotol (GPI) anchor that would link it to the plasma membrane or cell wall using the Fungal big-PI algorithm. The ORF encoding a predicted glucanase has four exons and encodes a protein of 295 amino acids with a molecular weight of 31.628 kDa.

The hypothetical protein downstream of the T-DNA insertion encodes two exons to yield a protein of 241 amino acids, with a molecular weight of 24.434 kDa (Figure 15). The gene product has a predicted signal peptide and is predicted to be secreted (Signal P, InterProScan), but has no conserved domains (InterPRoScan, CDD). The predicted protein is very rich in lysine and alanine (Supplementary Figure 6). Similarly to the predicted glucanase, the hypothetical protein is constitutively expressed (Figure 16).

2.9.2 Phenotype of mutant path-*9*

Mutant *path*-9 produced extremely reduced symptoms due to its very limited capacity to penetrate epidermal cells (Figure 17 and Table 4). The mutant was also impaired in its ability to penetrate cellophane (Table 4). The mutant did not show physiological defects such as colony morphology, hyphae size and branching, septation pattern and conidia size and shape. One possibility is that the glucanase is required for penetration of the plant cell wall or callose papillae. Another possibility is that the glucanase is required for remodelling the fungal cell wall during formation of the penetration peg. Likewise, the secreted protein may have a role in penetration.

2.9.3 Expression of genes putatively tagged in path-9

The study of the expression by RT-PCR revealed that both the hypothetical protein and the putative ß-1,3(4)-glucanase are constitutively expressed at all stages of fungal developmental and plant infection (Figure 16). If one of these genes is involved in penetration, it is likely that it is also involved in other phases of the *C. higginsianum* life cycle as well.

2.10 Path-*19 and* path-*35: auxotroph mutants*

2.10.1 Identification of tagged genes

For two of the four auxotrophs, the tagged gene has been identified. Mutant *path*-19 had a single insertion of pBIN-GFP-hph T-DNA. A total of 4007 bp of genomic DNA of the region of the insertion were obtained. This region has one predicted ORF with four exons, encoding a protein of 849 amino acids using FGENESH+ (Figure 15, Supplementary Data 9). The predicted ORF was subjected to a homology search and was found to have high homology to ARG6 precursor of fungal species (Supplementary Data 22), a gene which encodes N-acetylglutamate kinase and N-acetylglutamyl-phosphate reductase, involved in arginine biosynthesis in the mitochondria.

Mutant *path*-35 has two T-DNA insertions integrated about 500 bp from each other. A total of 5,534 bp of genomic DNA in the region of the insertion was obtained and two ORFs were predicted using FGENESH+ (Figure 15, Supplementary Data 13). Both insertions are in the same ORF, containing four exons encoding a 925 amino acids protein with high homology to a carbamoyl phosphate synthetase of fungal species (Supplementary Data 25), also involved in arginine biosynthesis.

2.10.2 Pathogenicity and auxotrophy phenotype

Both mutants showed very reduced pathogenicity, resulting from their strongly impaired penetration of host epidermal cells (Table 4), however, they could penetrate cellophane. Interestingly, mutant *path*-38 induced deposition of more papillae than the wild-type strain (Table 4 and Figure 8C). The mutants were found to be arginine auxotrophs and their growth on CDA minimal medium was rescued when arginine was added (Dr. Hiroyuki Takahara, personal communication)

2.11 Path-*14, a penetration mutant*

2.11.1 Identification of tagged genes

Mutant *path*-14 contained two insertions of pBIG2RHPH2 T-DNA. Flanking sequence was only obtained for one insertion site (Figure 15, Supplementary Data 9). It showed high homology to ornithine decarboxylase enzymes of several fungal species (Supplementary Data 22), a key enzyme in the synthesis of polyamines. Although the 556 bp of sequence flanking the T-DNA insertions was too short to predict an ORF, due to its very conserved homology to ornithine decarboxylase encoding genes of other fungi, it is very likely that the T-DNA insertion is inside the coding region for the putative ornithine decarboxylase.

2.11.2 Pathogenicity and auxotrophy phenotype of path-*14*

Mutant *path*-14 is defective in penetration of host, cellophane and ethanol-killed leaves. Because of the homology of one of the tagged gene to ornithine decarboxylase, involved in polyamine synthesis, it was suggested this mutant may be an auxotrophs. However, mutant *path*-14 did not have a growth rate defect *in vitro* after 4 days on either PDA or CDA (Table 4). However, when trying to revive cultures from glycerol stocks, the cultures were not viable suggesting they were more sensitive to freezing or impaired in some aspect of vegetative growth.

2.12 Path-5, a melanin mutant

2.12.1 Identification of genes tagged in mutant path-*5*

Mutant *path*-5 had two insertions of pBIN-GFP-hph T-DNA. For one of the T-DNA insertions, the flanking region could not be amplified by either TAIL-PCR or Inverse PCR and the tagged gene was therefore not identified. Furthermore, Southern blot analysis suggested that this T-DNA insertion was truncated. For the second T-DNA insertion, a total of 2,236 bp of genomic DNA flanking the insertion were obtained. When subjected to homology searches, no Blast hits were obtained for the available flanking sequence, but

when searched against the trace files of the *Colletotrichum graminicola* sequencing project, hits of moderate homology were found (*E*= 8e-12). It appears that this gene is present in these two *Colletotrichum* species, but not in other filamentous fungi, including *M. grisea*. However, using the FGENESH+ algorithm of gene prediction with the dicot matrix, two ORFs, with one exon each, were predicted (Figure 15). The T-DNA insertion is located in one of the two predicted ORFs. No functional domains were predicted for either of the predicted proteins. Semi-quantitative RT-PCR was performed to determine whether the tagged ORF was expressed in the wild-type strain. Interestingly, it was found to be expressed exclusively in appressoria and during the necrotrophic phase (Figure 16).

2.12.2 Phenotype of mutant path-5

Mutant *path*-5 formed appressoria but these were not melanised and consequently failed to penetrate living host tissue, cellophane or ethanol-killed leaves (Table 4). The mutant entirely failed to produce symptoms on *Arabidopsis* (Figure 17) but retained a capacity for invasive growth from wounds (Figure 5). The observation that the tagged gene is expressed during stages of pathogenesis where melanin synthesis is important, namely during the formation of the melanised appressorium and melanised setae during sporulation, supports the possibility that the tagged gene may be responsible for the albino and non-pathogenic phenotype.

3 Discussion

In this study, a high-throughput forward genetic screen, based on *Agrobacterium tumefaciens*-mediated transformation (ATMT)—mediated insertional mutagenesis, was developed with the aim of identifying pathogenicity genes in *C. higginsianum*. From a library of 8,850 random insertional transformants, 40 pathogenicity mutants displaying a wide range of defects in their pre- and post- penetration development were obtained. Sequence analysis of flanking regions for 14 T-DNA insertions has allowed the identification of candidate pathogenicity genes. The tagged genes include a phosphate transporter, putative importin ß2, glucanase, endoribonuclease, ARG6 precursor, carbamoyl phosphate synthetase, ornithine decarboxylase and several hypothetical proteins. Further analysis of these putative pathogenicity factors should give new insights into molecular interactions between *C. higginsianum* and *Arabidopsis*.

3.1 Effectiveness of ATMT for random insertional mutagenesis of C. higginsianum

A transformation method was adapted from protocols previously applied for ATMT of *Colletotrichum* species (Tsuji *et al.,* 2003; O'Connell *et al.*, 2004) based on the co-cultivation of *Agrobacterium* with germinating conidia of *C. higginsianum* and from a study on *Agrobacteria* as a vehicle for transformation (Cangelosi *et al.,* 1991). Many studies on the optimisation of ATMT of filamentous fungi have been published (Bundock *et al.,* 1995; Piers *et al.,* 1996; De Groot *et al.,* 1998; Bundock *et al.,* 1999; Mullins *et al.,* 2001; Takahara *et al.,* 2004). All these reports found that the transformation efficiency was improved by increasing the ratio of *Agrobacterium* cells to fungal conidia and by prolonging the co-cultivation time, but not so long that the fungal mycelium covers the support membrane because this appears to suppress bacterial growth. In contrast, inducing *Agrobacteria* cells with acetosyringone prior to co-cultivation did not always affect the transformation efficiency. Based on these reported observations, efforts were made in this study to optimise the transformation of *C. higginsianum* by varying parameters such as co-cultivation time, ratio of *Agrobacteria* to conidia during co-cultivation, bacterial strain,

transformation vector, type of co-cultivation membrane, and addition of acetosyringone to the induction broth. However, due to the poor reproducibility of these experiments, it was not possible to determine whether any of these parameters made a significant contribution to transformation efficiency. The transformation efficiency obtained in this study ranged from 20 to 125 transformants per 10^6 conidia (average of 102 transformants per 10^6 conidia) depending on various modifications to the protocol.

Although higher transformation efficiencies (up to 17,000 per 10^6 conidia) have been reported for some other *Colletotrichum* species (Flowers and Vaillancourt, 2005; Maruthachalam *et al.,* 2008; Talhinhas *et al.,* 2008), as indicated in Table , the transformation efficiency obtained in this study was high enough to quickly generate a library of many thousands of transformants. Furthermore, if the transformation efficiency had been higher the number of fungal conidia and *Agrobacteria* used for co-cultivation would have had to be reduced because the transformants would have been too densely packed on the selection plates. Moreover, obtaining large numbers of conidia of *C. higginsianum* for the transformation was not a limitation. The variation in transformation efficiency observed with ATMT of different *Colletotrichum* species and other fungi can be accounted for by biological differences between the recipient organisms since the transformation protocols for the transformations described in Table 6 use similar approaches. Structural differences such as properties of the cell wall through which the T-DNA is transported or physiological differences, in particular in the optimal temperature or pH for the fungus and *Agrobacteria* during co-cultivation, might be key determinants of transformation efficiency.

In fungi lacking a sexual stage, such as *C. higginsianum*, multiple T-DNA insertions cannot be separated through genetic segregation. To facilitate the recovery of tagged genes from such fungi, it is therefore desirable that the majority of transformants should contain insertions at a single site in the genome. Improvements in transformation efficiency are theoretically correlated with an increased occurrence of multiple insertions (Tsuji *et al.,* 2003; Michielse *et al.,* 2005). Thus, a greater proportion of transformants with single insertion may be obtained by compromising with a lower transformation efficiency. In an attempt to increase the proportion of single insertions, the co-cultivation time and the

concentration of hygromycin B used in the selection medium were reduced. However, these modifications resulted in a higher frequency of false positives.

Table 6. Transformation efficiency of ATMT in fungal pathogens

Species	Transformants per 10^6 conidia	Percentage single insertions	Reference
Colletotrichum higginsianum	20-100	58	This study
Colletotrichum gloeosporioides	50-130	-	De Groot *et al.* 1998
Colletotrichum lagenarium	150-130	86	Tsuji *et al.* 2003
Colletotrichum trifolii	20-30	75	Takahara *et al.* 2004
Colletotrichum graminicola	3000-17000	16	Flowers and Vaillancourt, 2005
Colletotrichum falcatum	300-500	62	Maruthachalam *et al.* 2008
Colletotrichum acutatum	400-500	65	Maruthachalam *et al.* 2008
Colletotrichum acutatum	15600	72	Talhinhas *et al.* 2008
Pseudozyma antartica	60-160	0	Marchand *et al.* 2007
Helminthosporium turcicum	3000-5000	80*	Degefu and Hanif 2003
Sclerotinia sclerotorum	80	33*	Weld *et al.* 2006
Helbeloma cylindrosporum	-	61	Combier *et al.* 2003
Calonectria morganii	8-13	100*	Malonek and Meinhardt 2001
Coniotharium minitans	76	40	Rogers *et al.* 2004
Ascochyta rabiei	-	100*	White and Chen, 2006
Botrytis cinerea	15	50*	Rolland *et al.* 2003
Aspergillus giganteus	5-79	100*	Meyer *et al.* 2003
Coccidioides immitis	1-10	76	Abuodeh *et al.* 2000

Number of transformants analysed ≤ 10

In this study, Southern blot analysis suggested that 58% of *C. higginsianum* transformants contained single-copy T-DNA insertions, which is greater than the frequency reported for *C. gramininola*, and similar to *C. falcatum* but less than *C. acutatum*, *C. lagenarium* and *C. trifolii* (Table ; De Groot *et al.,* 1998; Tsuji *et al.,* 2003; Takahara *et al.,* 2004; Flowers and Vaillancourt, 2005; Maruthachalam *et al.,* 2008; Talhinhas *et al.,* 2008). Following ATMT of other fungal species, the ratio of single insertion can vary from 0 to 100 % (Table 6). Such differences may be due to the ability of the fungus to take up T-DNA and the mode of integration. Among the *C. higginsianum* transformants found to harbour multiple T-DNA insertions in this study, the majority (70 %) had T-DNA integrations at a single site, mostly as tandem repeats in head-to-tail orientation, which did not prevent amplification of the right border flanking sequences by TAIL-PCR and identification of tagged genes. Tandem insertion could have arisen from homologous recombination among plasmids resulting in integration of multiple copies. Alternatively, a single plasmid may increase the homology

with copies of the plasmid making a second integration event easier (Finchman, 1989). The transformation protocol described in the materials and methods of this study was found to yield an adequate number of transformants with a sufficient proportion of single insertions and therefore was not modified any further.

No integration of plasmid DNA from outside the T-DNA was detected, in contrast to *C. graminicola*, where 70 % of ATMT transformants contained tandem integrations of the entire Ti-plasmid (Flower and Vaillancourt, 2005), and *C. lagenarium*, where binary vector backbone DNA was detected in 43 % of flanking sequences (Tsuji *et al.,* 2003). Systemic analysis of T-DNA integration events in *M. grisea* showed that insertions is often associated with small target site deletions, and occasionally induces larger deletions of host DNA or chromosomal rearrangements such as inversion and translocations (Choi *et al.,* 2007; Li *et al.,* 2007; Meng *et al.,* 2007). The extent to which such events may have occurred during the ATMT of *C. higginsianum* could not be evaluated because only right border flanking sequences were obtained, and no attempts were made to obtain left border flanking sequences. Consistent with studies on other fungi (Mullins *et al.,* 2001; Tsuji *et al.,* 2003; Choi *et al.,* 2007), we found no evidence of truncations of the T-DNA right border. The right border of the T-DNA tends to be more conserved than the left border, presumably due to the attachment of VirD2 proteins to the right border (Bundock and Hooykaas, 1996). However, the left border integrity was not determined in this study and Southern analysis indicated that some T-DNA insertions were indeed truncated.

Several recent studies provide evidence that T-DNA integration into fungal genomes is not entirely random. For example, large scale analyses of randomly-selected transformants in *M. grisea* revealed a significant bias for promoter regions, while insertions into coding regions occurred less often than expected (Choi, *et al.* 2007; Li *et al.,* 2007; Meng *et al.,* 2007). Preferential insertion of T-DNA into promoter regions was also detected in *Cryptococcus neoformans* melanisation mutants (Walton *et al.,* 2005). In *Arabidopsis* and rice, transcriptionally active regions are preferred, particularly 5'untranslated regions of genes and polyadenylation sites (Barakat *et al.,* 2000; Alonso *et al.,* 2003; Forsbach *et al.,* 2003; Pan *et al.,* 2005; Schneeberger *et al.,* 2005; Li *et al.,* 2006; Zhang *et al.,* 2007). The differences in chromatin organisation may affect accessibility of the host DNA to incoming T-DNAs and result in regions of preferential integration (Meng

et al., 2007). In eukaryotes, promoters and gene-coding regions are well conserved as AT- and GC-rich regions, respectively (Hurst *et al.,* 2004), and these could account for the low GC content found in regions flanking the T-DNA insertions in these studies. Our analysis of 14 integration events in *C. higginsianum* was based on mutants showing altered pathogenicity phenotypes and, as expected, most T-DNA insertions were located in regions likely to affect gene function. However, insertions into gene coding regions were more frequent (nine) than insertions into putative regulatory regions (five). Other methods of insertional mutagenesis of filamentous fungi are not more random than ATMT. Transposon mutagenesis preferentially affects non-coding regions (Firon *et al.,* 2003; Ladendorf *et al.,* 2003) whereas restriction enzyme-mediated integration (REMI) has a bias for transciptionally active regions similarly to ATMT (Lu *et al.,* 1994; Sweigard *et al.,* 1998).

This study also suggests that there might be "hotspots" for T-DNA integration within the *C. higginsianum* genome. Thus, out of only 12 mutants for which flanking sequence was obtained, the same gene (an importin ß2 homologue) was tagged in two different mutants (*path*-36 and *path*-38). Furthermore, two independent insertions were located only 4 kb apart in mutant *path*-7, while in *path*-23 two tagged genes were identified within the same cosmid clone and must therefore be no more than about 30 kb apart, *i.e.* the average insert size in the cosmid library. Similarly, there is evidence that some rice genes are T-DNA tagged more frequently than would be expected by random integrations (Zhang *et al.,* 2007). Acquisition of T-DNA flanking sequences from more transformants is required to determine the extent of non-random T-DNA insertion in *C. higginsianum.* If insertions are indeed not randomly distributed in the recipient genome, it would be more difficult and take a lot more transformants to saturate the genome with mutations.

3.2 Identification of tagged genes by Inverse and TAIL-PCR

An important aspect of random insertional mutagenesis for gene identification is the ability to isolate tagged genes from the mutants. Right border flanking sequences from 12 out of 40 pathogenicity mutants (30 %) were recovered using TAIL- and Inverse PCR. This relatively low success rate was similar to that reported for similar mutant library projects with the pathogen *Leptosphaeria maculans* (34 %) but less than that obtained with *M.*

grisea (46 %) and *F. oxysporum* (90 %) (Mullins *et al.,* 2001; Blaise *et al.,* 2007; Meng *et al.,* 2007). In the present study, amplification of right border flanking sequences may have failed due to truncation of the T-DNA right border beyond the primer annealing site, insertion of inverted (right border to right border) tandem repeats or, in the case of Inverse PCR, absence of a restriction site close enough to the T-DNA insertion. It may therefore be possible to recover flanking regions from these recalcitrant mutants using more internal border primers, left border primers, or different restriction enzymes.

Another concern with the use of ATMT for insertional mutagenesis is the occurrence of untagged mutations. Such mutations can be small or large deletions or duplications occurring during ATMT that do not result in T-DNA insertion but still cause the observed phenotype. Thus, in *Arabidopsis*, T-DNA insertion was linked to a mutant phenotype in only 35-40 % of ATMT mutants (Azpiroz-Leehan and Feldmann, 1997) while in both *L. maculans* and *C. neoformans* only 50 % of mutations were T-DNA tagged (Walton *et al.,* 2005; Blaise *et al.,* 2007). In *C. higginsianum*, it is not possible to analyse co-segregation of the T-DNA and mutant phenotype because the sexual stage of this fungus is not known. It is therefore necessary to validate T-DNA tagging by complementation with a cosmid carrying a wild-type gene copy or by targeted gene disruption.

3.3 Identification of 40 pathogenicity mutants

To efficiently pre-screen large numbers of ATMT transformants, with minimal handling of fungal cultures, a miniaturised pathogenicity assay was devised. By growing both the fungal transformants and *Arabidopsis* seedlings in a 96-well format, subculturing and plant inoculation could be performed using a multichannel pipetter to transfer conidial suspension. Subsequent examination of disease symptoms by fluorescence microscopy also facilitated the rapid scoring of infection phenotype, whereby the green autofluorescence of necrotic tissues contrasted with the red chlorophyll fluorescence of healthy tissues. In this way, several hundred transformants could be screened in one experiment. The selection of false positives in the primary screen probably resulted from plants receiving insufficient inoculum, *e. g.* when the inoculation droplet contained insufficient conidia or did not contact, or rolled off the seedlings. However, false positives were efficiently eliminated by

two rounds of selection in the secondary screen, where adult plants were spray-inoculated with a standardised conidia concentration. An advantage of this stringent secondary screen was that all the selected mutants had robust, reproducible phenotypes. However, mutants with only minor reductions in pathogenicity were probably missed.

After screening 8,850 transformants, 40 (0.45 %) were either non-pathogenic or strongly reduced in their pathogenicity on both *Arabidopsis* and *Brassica* plants. A similar proportion of pathogenicity mutants were identified after insertional mutagenesis of other fungal species using ATMT or REMI (Table 7). Microscopic analysis of infected leaf tissues allowed classification of the mutants according to the stage at which fungal development was arrested and the extent to which host defence responses were induced. Overall, nearly equal numbers of mutants affected in their pre-penetration on the plant surface (18 mutants) and post-penetration development inside host cells (22 mutants) were obtained. None of the 40 pathogenicity mutants were impaired in conidiation or germination, probably because the use of conidium suspension for sub-culturing and infection assays would have eliminated such mutants from the screen. Moreover, apart from appressorial melanisation defects, none of the mutants showed significant morphological abnormalities in their infection structures formed *in planta* or vegetative hyphae growing *in vitro*.

Table 7. Mutant screens in other fungal pathogens

Pathogen	Number of transformants	Percentage of pathogenicity mutants	Reference
Colletotrichum higginsianum	8850	0.45	This study
Colletotrichum acutatum	1500	0.33	Talhinhas *et al.* 2008
Colletotrichum lindemuthianum	600	0.67	Dufresne *et al.* 1998
Colletotrichum graminicola	660	0.30	Thon *et al.* 2000
Magnaporthe grisea	33943	0.38	Betts *et al.* 2007
Magnaporthe grisea	3527	0.14	Balhadére *et al.* 1999
Magnaporthe grisea	5538	0.49	Sweigard *et al.* 1998
Magnaporthe oryzae	21070	0.96	Jeon *et al.* 2007
Ustilago maydis	1000	1-2	Bolker *et al.* 1995
Fusarium graminaerum	6500	0.17	Seong *et al.* 2005
Leptosphaeria maculans	1388	3.9 *	Blaise *et al.* 2007
Coniotharium minitans	4000	0.23	Rogers *et al.* 2004
Ascochyta rabiei	550	1.45	White and Chen, 2006

*In at least half of the transformants, the phenotype was not tagged by the DNA insertion

Although potentially, 40 loci affecting fungal pathogenicity were mutated in this study, a mutant screen involving 8,850 transformants is far from being a saturating genome-wide screen. In the large scale ATMT of the rice blast fungus *M. oryzae,* which as a genome of 39,4 Mb with 12,841 predicted genes, Jeon *et al.* generated 21,070 transformants and estimated that this covers 61 % of the genome (Jeon *et al.,* 2007). The genome size of *C. higginsianum* is not known. However, optical mapping of the *C. graminicola* genome indicates a size 57,44 Mb (Dr. Lisa Vaillancourt, personal communication). This is similar to the genome of *Nectria haemococca,* which contains 16,237 predicted genes (Xu *et al.,* 2006). Assuming a genome utilisation similar to that of *M. oryzae* and *N. haematococca*, a maximum of about 17 % of the *C. higginsianum* genome was covered with 8,850 transformants in this study.

3.4 Identification of 14 putatively tagged genes and candidate pathogenicity genes

The tagged *C. higginsianum* genes identified which are putatively involved in pathogenicity included two predicted ORFs with no homology to any known sequences in the public databases, five hypothetical proteins containing no recognisable functional domains, and seven genes with homology to proteins with annotated functions. These include an Major facilitator superfamily (MFS) phosphate transporter, genes with high homology to importin ß2, ATP-binding endoribonuclease, carbamoylphophate synthetase, ARG 6 precursor, ornithine decarboxylase and putatively secreted ß1,3(4)-glucanase.

3.5 Melanin mutants

In both *Colletotrichum* and *Magnaporthe*, a large number of genes involved in the induction and morphogenesis of appressoria have been identified using forward and reverse genetic approaches (Deising *et al.,* 2000). Surprisingly, none of the pathogenicity mutants obtained in the present study were affected in their ability to form appressoria on leaf surfaces. However, a relatively large number of appressorium melanisation mutants were identified (6/8850), based on their complete loss of pathogenicity on *Arabidospis*. This

proportion is comparable to more targeted screens for melanin mutants in *C. neoformans* (Walton *et al.,* 2005) and *C. lagenarium* (Tsuji *et al.,* 2003). All the *C. higginsianum* melanin mutants produced albino or weakly-melanised appressoria that were incapable of penetrating intact host epidermis or cellophane, as expected given the crucial role of melanin in generating turgour pressure for penetration (Deising *et al.,* 2000). The appressoria of these mutants appeared to be only weakly attached to host surfaces. This phenotype was not previously found in melanin mutants of *Colletotrichum* or *Magnaporthe*, although treatment with melanin biosynthesis inhibitors was reported to reduce adhesion of *M. grisea* appressoria (Inoue *et al.,* 1987).

In the appressorial cell wall of *Colletotrichum* and *Magnaporthe* species, melanin is necessary for penetration as it is involved in blocking the leakage of osmolytes such as glycerol and strengthening the cell wall to generate the enormous turgour pressure required for host penetration (Howard *et al.*, 1991). Interestingly, the appressoria of barley powdery mildew *Blumeria graminis* are not pigmented yet still generate substantial turgour pressure, although much less than *Colletotrichum* and *Magnaporthe* species. (Iwamot *et al.,* 2007). In the melanised hair-like setae produced in *Colletotrichum* acervuli, melanin could also function to strengthen the cell wall. Other fungal species do not produce melanised appressoria but rather melanised conidia *e.g. Cochliobolus* species and *Alternaria* species (Takano *et al.,* 1997; Carzaniga *et al.,* 2002). From the recent literature, it is starting to emerge that pigments such as melanin are important factors for virulence in both plant and human pathogenic fungi. In the cell walls of spores of mammalian pathogens such as *A. fumigatus*, melanin is in direct contact with the immune system of the host and contributes to protection against light, lysing enzymes and extreme temperature but also acts as an electron acceptor against reactive oxygen species and reactive nitrogen species produced by macrophages during the oxidative burst (Brakhage and Liebmann, 2005). In the cell wall of opportunistic mammalian pathogen *Paracoccidiodes brasiliensis* conidia, melanin also protects against digestion by proteases and hydrolases and other fungicidal host proteins such as defensins and protegrins of animal origins (Rosas and Casadevall, 2001). Furthermore, the melanised spores of *C. neoformans* are also more resistant to toxins (drugs and antibiotics) than spores of melanin mutants (Ikeda *et al.,* 2003).

3.5.1 A Colletotrichum-specific protein of no homology or a yet unidentified tagged gene is required for melanin biosynthesis

Mutant *path*-5 is one of the *C. higginsianum* mutants affected in its ability to form melanised appressoria and to penetrate the host, but it does retain invasive growth ability through wounds. It is therefore probable that one of the two tagged genes in this mutant is responsible for the melanin deficiency phenotype and the consequent incapability to penetrate the host surface. Flanking sequence was obtained for only one of the two T-DNA insertions of *path*-5. This was in a predicted ORF with no homology to any known proteins and without any recognisable functional domains, but which matched to trace files from the *C. graminicola* genome sequence. It is therefore conceivable that this may be a novel *Colletotrichum*-specific gene that is required for some aspect of melanin biosynthesis or its regulation. RT-PCR revealed that the predicted ORF is expressed during appressorium formation and during the necrotrophic phase but not in mycelium grown *in vitro* or in isolated primary hyphae. The expression corresponds to the developmentally regulated production of melanin in *Colletotrichum* species: in appressoria during appressorium formation and in setae during sporulation in the necrotrophic phase. It is therefore possible that the protein encoded by the predicted ORF is indeed involved in melanin biosynthesis. However, complementation of the mutant with a wild-type copy of the gene or a targeted gene disruption is necessary to determine whether the identified predicted ORF or the gene(s) tagged by the second insertion or even an untagged mutation is responsible for the observed melanin-deficient phenotype and defective penetration.

3.6 Penetration mutants

A total of fifteen pathogenicity mutants elaborated melanised appressoria with normal morphology but were unable to penetrate living host cells, and in some cases also inert substrates, *i.e.* cellophane and dead leaf tissue. Such mutants may be defective in appressorium-mediated mechanical penetration, degradation of the host cuticle and cell wall, signalling for induction of penetration, formation of the penetration peg itself or the synthesis or acquisition of essential nutrients after stored resources from the conidium have been exhausted. Among the five characterised penetration mutants, the putatively tagged

genes identified showed high homology to an MFS phosphate transporter, an ornithine decarboxylase, the ARG6 precursor, a carbamoyl phosphate synthetase, a putative a ß-1,3(4)-glucanase and a hypothetical protein conserved among fungi with no homology to known functional domains.

3.6.1 Phosphate uptake during penetration and the biotrophic phase

In mutant *path*-12, the tagged gene was highly homologous to conserved MFS transporters of other fungi and plants, and in particular plasma membrane proton symporters involved in the uptake of inorganic phosphate. One of them is the well-characterised MFS transporter of *S. cerevisae,* PHO84. This gene encodes a high affinity proton and inorganic phosphate symporter localised at the plasma membrane (Petersson *et al.* 1999; Wykoff and O'Shea, 2001). Similarly, the tagged gene was predicted to be localised at the plasma membrane and contained 12 transmembrane domains, typical of MFS transporters.

The pathogenicity phenotype of mutant *path*-12 could be complemented by the ectopic insertion of the cosmid harbouring the wild-type copy of the gene. This suggests that the mutation responsible for the phenotype is indeed the T-DNA insertion in the phosphate transporter. Further confirmation could be obtained by performing a targeted gene disruption.

Homology with characterised fungal and plant phosphate transporters is an indication that the tagged gene may be involved in phosphate uptake. The observation that the host penetration efficiency and consequently pathogenicity, of mutant *path*-12 were restored by the addition of exogenous phosphate on the plant surface, or by infiltration into the plant apoplast support the hypothesis that the mutant is impaired in phosphate transport and that phosphate uptake plays a role in host penetration and pathogenicity of *C. higginsianum*.

Evidence that the tagged gene encodes a functional phosphate transporter was obtained from the functional complementation of a *S. cerevisae* mutant lacking five phosphate transporters. This quintuple mutation is lethal but the mutant was maintained alive on galactose medium because it harbours a copy of the *S. cerevisae* high affinity transporter PHO84 under the control of a galactose-inducible promoter. The growth of the

quintuple disruption strain on glucose medium was rescued by a complementation with a copy of the cDNA of the *C. higginsianum* putative MFS transporter under the control of a constitutive promoter. Interestingly, the *C. higginsianum* sequence restored growth on glucose as efficiently as the yeast PHO84 cDNA, suggesting that the gene tagged in *path*-12 might also encode transporter with a comparable affinity for phosphate to Pho84p.

Homology searches revealed that filamentous plant pathogenic fungi for which the whole genome has been sequenced typically have two to three genes with high homology to *S. cerevisae* PHO84. Although using a gene-specific probe for Southern analysis, the MFS tagged in *path*-12 appeared to be a single copy gene, it is possible that *C. higginsianum* also has multiple genes homologous to PHO84, but with enough sequence discrepancy to not be detectable by stringent Southern analysis. Interestingly, among the PHO84 homologues present in other filamentous fungi, those most similar to the gene tagged in *path*-12 did not have the highest homology to yeast PHO84. It is possible that these phosphate transporters differ in their pH optima, ionic current and expression patterns. Yeasts also have two high affinity transporters: Pho84p and Pho89p, which differ in their affinity for phosphate, optimal pH and the ion they transport together with phosphate. Thus, Pho84p is a proton and phosphate symporter with a Michaelis constant ($K_{m)}$ for external phosphate of 1 – 15 µM and an optimal pH of 5.0 (Bun-Ya *et al.,* 1991; Wykoff and O'Shea, 2001). In contrast, Pho89p relies on sodium for phosphate symport, has a K_m for external phosphate of 0.5 µM and is maximally active at pH of 9.5 (Martinez and Persson, 1998; Martinez, P. *et al.* 1998). In yeast, the low affinity transport system is constitutively expressed whereas the high affinity transporters are de-repressed in low external phosphate conditions. The observation that the tagged gene in *path*-12 encodes a phosphate transporter does not exclude the possibility that it also functions as a carrier for other molecules. For example, the *S. cerevisae* transporter of glycerophosphoinositol, Git1p, was recently found to also be a high affinity transporter of phosphate, although it has a significantly lower affinity for phosphate than Pho84p (Patton-Vogt and Henry, 1998; Wykoff and O'Shea, 2001). Git1p can therefore take up both organic and inorganic phosphate. Similarly, the gene tagged in *path*-12 could encode a transporter of phosphate-related substrates and a broad substrate specificity may help the fungus to better scavenge phosphate when it is limiting.

Phosphate is an indispensable nutrient for all organisms; it is necessary for the biosynthesis of nucleic acids, proteins, phospholipids and cellular metabolites and is therefore an essential ion for fungal growth. Hence, it is conceivable that efficient phosphate uptake is important for fungal pathogenicity. The gene tagged in *path*-12 was found to be specifically expressed during germination, appressorium formation and during biotrophy but not in mycelium growing in rich media or during the necrotrophic phase. The expression pattern corresponds to the stages of fungal development when available phosphate might be limiting: on the host surface and in the apoplast, before host cells lose their integrity during the necrotrophic phase. Experiments with barley leaves indicate the apoplast concentration of free phosphate is low, 2.5 mM compared to 16.8 mM in total leaf samples (Mimura *et al.,* 1992). Similarly, the concentration of phosphate in the apoplast of sugar beet was estimated to be 2.5 mM (Lopez-Millan *et al.,* 2000).

Plasma membrane phosphate transporters have not previously been described as playing a role in fungal pathogenicity. However phosphate acquisition has been demonstrated to be important for pathogen survival. In a previous study with the obligate biotroph *Erisyphe graminis hordei,* acid phosphatases were found in relatively high concentrations in haustoria in barley epidermis (Atkinson and Shaw, 1955). The fungal acid phosphatases were suggested to play an important role in the transfer of metabolites between host and fungus. More recently, the expression of two putatively secreted phosphatases of *C. graminicola* (phytase 1 and acid phosphatase PHO1) was upregulated after two days of growth *in planta* compared to conidia germinated *in vitro,* corresponding to the biotrophic phase (Tang *et al.,* 2006). Additionally, a putatively secreted phosphatase was identified in the proteome of germination fluids of conidia of *C. higginsianum* germinating and forming appressoria *in vitro* (Jochen Kleemann, personal communication). Phytases are a class of phosphatases and are enzymes involved in the degradation of phytic acid (inositol hexaphosphate), one of the forms in which phosphate is stored in plants. Thus, the induction of fungal phytases *in planta* could be a response to a low free-phosphate environment. Furthermore, deletion strains of Pho84p homologue $phoD^{PHO84}$ in the mammalian pathogen *Aspergillus fumigatus* were fully pathogenic, despite the fact that the serum concentration of phosphate is 1 mM, ten times less than that required by *A. fumigatus* (Tekaia and Latge, 2005). Sufficient phosphate uptake from serum by *A. fumigatus* is

believed to involve a battery of extracellular phosphatases and phospholipases (Tekaia and Latge, 2005). Interestingly, in bacterial pathogens of mammals such as *Fransiscella tularensis*, *Mycobacerium tuberculosis*, *Coxiella burnetii*, *Legionella micdadei* and *Salmonella enterica*, acid phosphatases are suggested to play an important role in bacterial survival by inhibiting the respiratory burst response produced by macrophages and neutrophils (Saha *et al.,* 1985; Baca *et al.,* 1993; Reilly *et al.,* 1996; Saleh and Belisle, 2000; Eriksson *et al.,* 2003; Rengarajan *et al.*, 2005). Whether fungal pathogens also use such a method to inhibit host production of reactive oxygen species remains to be studied.

Since phosphate uptake appears to play an important role in pathogenicity, further insights in the role of phosphate uptake during biotrophy and necrotrophy could be obtained by looking at the expression of homologous putative phosphate transporters in the genome of *C. higginsianum*. Apart from their expression profile, their affinity for phosphate, optimal pH and substrate might also be different and worth investigating. Similarly, the study of other enzymes involved in phosphate uptake, such as phosphatases, and in the break down of polyphosphate, the form in which phosphate is stored in the cell, may also reveal roles in pathogenicity and possibly during specific stages.

3.6.2 A ß-1,3(4)-glucanase or a hypothetical secreted protein is required for host penetration

One of the penetration mutants, *path*-9 had a T-DNA insertion between a predicted hypothetical protein, conserved in fungal species, with a signal peptide and an ORF encoding a putative endo-ß-1,3(4)-glucanase which cleaves both β-1,3-, β-1,4- and β-1,3-β-1,4-glucans (Kim *et al.* 2001). The T-DNA is upstream of the hypothetical protein and downstream of the putative glucanase. Both genes are putatively tagged by the T-DNA insertion: the expression of either of these genes could be affected by the T-DNA insertion if upstream of downstream regulatory elements of the genes are affected.

The predicted hypothetical protein possesses no conserved domain to help deduce a possible function for it. Interestingly, it is predicted to be secreted. Many examples of secreted proteins involved in pathogenicity have been identified in fungal pathogens, for example, enzyme involved in adhesion, cell wall degradation, suppression of host defences,

toxins. The expression of the hypothetical protein is constitutive, suggesting it may not be specific to penetration, however, since the mutant was unable to penetrate the host, defects at later stages of pathogenicity could not be studied.

ß-1,3-glucan is a major component of fungal cell wall and plant callose papillae, in contrast to plant cell walls which are composed of cellulose, a ß-1,4-linked glucose. It is therefore plausible that a ß-1,3(4)-glucanase is involved in fungal pathogenicity, particularly in penetration. Interestingly, the putative ß1,3(4)-glucanase gene was found to be constitutively expressed.

A possible function of the ß-1,3(4)-glucanase in penetration may be to hydrolyse the callose in papillae present beneath the appressoria or cellulose of the plant cell wall. Papillary callose occurs beneath about 25 % of appressoria of the wild-type strain, but the papillae are not successful at preventing penetration, possibly because the *C. higginsianum* possesses the ability to hydrolyse them using a glucanase. The mutant was not only unable to penetrate the host, it was also defective at penetrating cellophane membranes composed of cellulose. This suggests the mutant may be affected in its ability to degrade cellulose. The putative glucanase has a predicted signal peptide, but unlike most of the top Blast hits to which it is highly homologous, it is not predicted to have a GPI anchor that would bind it to the fungal cell wall or plasma membrane. If the glucanase is indeed secreted, it would support the possibility that it is involved in the hydrolysis of cellulose in the host cell wall or of papillary callose.

The fungal cell wall is a complex structure composed typically of chitin, ß-1,3- and ß-1,6-glucans, mannans and proteins. It is also highly dynamic and subject to constant modification, for example during apical expansion, conidium germination, hyphal branching and septum formation. It is possible that cell wall polymers change in their branching and cross-linking in order to maintain cell wall plasticity during morphogenesis, including infection structure formation. Glucanases, along with other hydrolytic enzymes, may be required for this and such enzymes have been found intimately associated with the fungal cell wall, often glycosylphosphatidylinositol (GPI)-anchored (Adams, 2004). Interestingly, apart for the penetration defect, the mycelium of the *path*-9 mutant showed no difference in appearance compared to that of the wild-type strain, i.e. a normal septation pattern and no abnormal cell wall thickening in the cell walls of spores and hyphae of *path*-

9. Because mutant *path*-9 is affected in its ability to penetrate, the glucanase may be important for remodelling the cell wall in the base of the appressorium where the penetration peg will emerge, similarly to branching or yeast budding. The glucanase may also play a role as a cell wall-loosening factor during extension of hyphal tip, but radial growth and hyphal morphology were not affected.

Likewise, the glucanase may play an important role in eliminating ß-1,3-glucans from the cell wall of the penetration peg because ß-1,3-glucan in the fungal cell wall of C. higginsianum may act as a PAMP. ß-glucans of fungal pathogen are recognised as PAMPs by the Dectin-1 receptor in animals (Gow *et al.,* 2007). There is good evidence for this in pathogens of animals where ß-1,3-glucans are replaced by α-1,3-glucans to avoid recognition (San-Blas *et al.,* 1977; Klimpel and Goldman, 1988; Hogan and Klein, 1994). Furthermore, a receptor for glucans has been identified in *Arabidopsis* (Dr. Chian Kwon, personal communication). It would be interesting to see the pathogenicity phenotype of mutant *path*-9 on *Arabidopsis* mutants disrupted in this glucan receptor.

Alternatively, the glucanase could be important for autolysis. Autophagic cell death of the spore is important in *M. grisea* for successful appressorium-mediated penetration (Veneault-Fourrey *et al.,* 2006) and endo-ß-1,3-glucanases have been found in the autolysate of *A. fumigatus* (Mouyna *et al.,* 2002), raising the possibility that cell wall hydrolysis by glucanase may play a role in fungal autophagy. The role of autophagy in pathogenicity of *Colletotrichum* species still remains to be determined but an analysis of expressed sequence tag (EST) libraries of *C. higginsianum* appressoria and isolated primary hyphae, revealed the expression of several autophagy-related genes during these stages of fungal development (Jochen Kleemann and Dr. Hiroyuki Takahara, personal communication).

Alternatively, hydrolysis of the fungal cell wall could contribute to generating an adhesive to strongly attach the appressorium which is essential for the exertion of mechanical force during penetration. However, the appressoria of this mutant did not appear to be more easily dislodged, although the strength of their adhesion was not studied.

Glucanases have been well-studied in the yeast *S. cerevisae* which has a wide range of 15 endo- and exo-ß-1,3-glucanases (Baladron *et al.,* 2002). The characterised glucanases of *S. cerevisae* have been found to play roles in cell separation (Baladron *et al.,* 2002), ß-

1,3-glucan cross-linking in the cell wall (Popolo and Vai, 1999) and septum formation (Adams, 2004). Interestingly, the putative glucanase tagged in *path*-9 showed high homology to proteins of filamentous fungi but only weak homology to any *S. cerevisae* proteins. This suggests it may be a specific class of glucanase unique to filamentous fungi.

To determine which of the two genes, the putative glucanase or the predicted secreted hypothetical protein, is responsible for the pathogenicity phenotype, complementation with the wild-type copy of each genes or targeted gene disruptions will be necessary.

3.6.3 Sucessful penetration requires arginine and polyamine biosynthesis

Other mutants with reduced ability to penetrate are mutant *path*-16 tagged in a putative ornithine decarboxylase and *path*-19 and *path*-35 tagged in genes with high homology to the ARG-6 precursor and carbamoyl phosphate synthetase, respectively, both of which are involved in arginine biosynthesis.

Mutant *path*-16 has two T-DNA insertions: one is located in a gene encoding a putative ornithine decarboxylase (ODC) but the other tagged gene was not identified. ODC catalyses the conversion of ornithine to putrescine, the first and rate-limiting step in biosynthesis of all polyamines in most organisms (Figure 30). It was expected that mutant *path*-16 would be a polyamine auxotroph, unable to grow on the minimal medium CDA, which contains inorganic nitrogen as the sole nitrogen source. Auxotrophy for putrescine has been observed in ODC null mutants in *U. maydis* (Guevara-Olvera *et al.,* 1997) and less severely with *Stagonospora nodorum* (Bailey *et al.,* 2000). Surprisingly, *path*-16 was not significantly affected in its growth ability on CDA. The lack of auxotrophy among ODC mutants may be species-specific because the extent of growth inhibition caused by the specific ornithine decarboxylase inhibitor α-difluoromethylornithine (DFMO) varies widely, from 0 % to 80 % growth reduction, depending on the fungus investigated (Walters, 1995). Unfortunately, it was not possible to rescue viable conidia of mutant *path*-16 from the glycerol stocks. The lack of viability of the *path*-16 mutant after storage may indicate a malfunction in basic metabolism.

The main polyamines found in fungi are putrescine, spermidine and spermine. They are known to be required for cell growth and play roles in DNA stabilization (Marton *et al.* 1991), membrane structure, resistance to oxidative stress and differentiation (Minguet *et al.*, 2008). In fungal pathogens, polyamines are known to be important for differentiation, including germination and morphogenesis of infection-related structures. Consequently, polyamines are involved in pathogenicity. Thus, ODC is required for spore germination and sporulation in Mucorales (Martinez-Pacheco *et al.,* 1989) and for the dimorphic transition in *Ustilago maydis* (Guevara-Olvera *et al.,* 1997). ODC is also required for full virulence in the necrotrophic wheat pathogen *Stagonospora nodorum* (Bailey *et al.,* 2000) and treatment with the specific ODC inhibitor DFMO inhibited appressorium formation by the rust fungus *Uromyces viciae-fabae* (Reitz *et al.,* 1995). Although polyamine biosynthesis was not previously implicated in appressorial penetration, it may be required for differentiation of the penetration peg and the transition to invasive growth.

Ornithine is also known to be involved in plant stress responses and it has been suggested that pathogens could exploit plant-derived ornithine for their nutritional benefit, as some pathogens do with other plant defence compounds such as uric acid and γ-amino butyric acid (GABA; Divon and Fluhr, 2007). During *Fusarium oxysporum* infection, plants produce uric acid as a scavenger of reactive oxygen species (Becker *et al.,* 1989) and *F. oxysporum* induces a fungal uricase which catalyses the conversion of plant uric acid to allantoin, a major metabolic intermediate in fungi (Divon *et al.,* 2005). Similarly, *Cladosporium fulvum* induces the tomato glutamate decarboxylase, resulting in increased levels of GABA in the tomato apoplast during infection (Solomon and Oliver, 2002; Dickman *et al.,* 2003). The fungus can then use apoplastic GABA as a nitrogen source and as a scavenger of reactive oxygen species (Solomon and Oliver, 2002).

To study the effect of the polyamine starvation on pathogenicity and more specifically differentiation of infection structures such as appressoria or sporulation, using the T-DNA insertion mutant disrupted in the ORF encoding a putative ornithine decarboxylase, is not ideal as the mutant has two insertions the second tagged gene is not known and may cause effects on pathogenicity. An alternative would be to apply inhibitors of the ornithine decarboxylase: di-fluoromethylornithine (DFMO; Walters, 1995) or diaminobutanone (Rajam *et al.,* 1985; Tabor and Tabor, 1985; Reyna-Lopez and Ruiz-

Herrera, 2004). Furthermore, ODC is one of the most highly regulated enzymes of eukaryotes (Davis *et al.,* 1992) and it would therefore be interesting to study the expression of the ODC gene during the different stages of pathogenesis.

The gene tagged in *path*-19 has high homology to the ARG-6 precursor, which encodes both N-acetylglutamate kinase and N-actetylglutamyl-phosphate reductase while the gene tagged in *path*-35 show high homology to carbamoyl phosphate synthetase. All three enzymes are involved in arginine biosynthesis in mitochondria (Figure 30) and accordingly, both mutants were arginine auxotrophs, unable to grow on minimal medium. Both mutants also displayed reduced host penetration, probably due to the depletion of stored arginine during spore germination and appressorium formation. In addition, mutant *path*-35 also induced significantly more host papillae than the wild type, which may have further impeded their penetration of living epidermal cells. It is not surprising that mutants unable to synthesise primary metabolites are non-pathogenic, however it is remarkable that out of only twelve characterised pathogenicity mutants, two were affected in the same biochemical pathway, suggesting that the ability to synthesise arginine is critical for early stages of host infection by *C. higginsianum*. Mutation of *arg1*, encoding argininosuccinate lyase, showed that arginine biosynthesis is also required for pathogenicity of *Fusarium oxysporum* on melon (Namiki *et al.,* 2001). Taken together, these observations suggest arginine biosynthesis is important for pathogenicity. Arginine is also one of the least abundant amino acids in the plant apoplast (Solomon and Oliver, 2001).

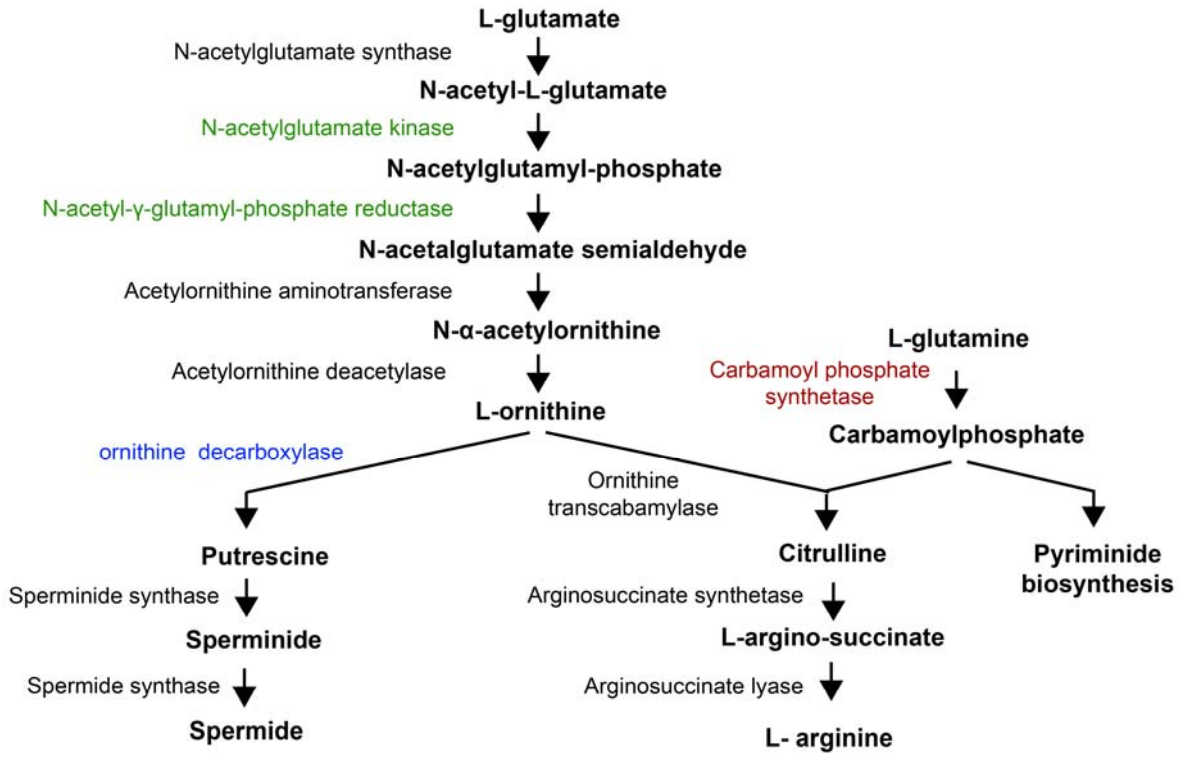

Figure 30. Metabolic relationship between arginine and polyamines metabolism in fungi.
The enzymes N-acetylglutamate kinase and N-acetyl-glutamyl-phosphate encoded by the ARG6 precursor tagged in *path*-19 are indicated in green and both encode enzymes required for ornithine synthesis and consequently the synthesis of arginine and of polyamines. The carbamoyl phosphate synthetase tagged in *path*-35 is indicated in red and is involved in arginine and pyriminide biosynthesis. The gene product of the gene tagged in *path*-16 is the ornithine decarboxylase, indicated in blue, and constitutes the first step in the synthesis of the polyamines putrescine, sperminide and spermide. (Diagram simplified from KEGG ornithine cycle and metabolism of amino acids, http://www.genome.jp/kegg/).

Two pathogenicity mutants were identified in *M. grisea*, that are affected in amino acid biosynthesis, namely *pth3* disrupted in a gene encoding imidazole glycerol phosphate dehydratase involved in the sixth step of histidine biosynthesis, and *met1* a methionine auxotroph for which the tagged gene has not yet been identified (Sweigard *et al.,* 1998; Balhadére *et al.,* 1999). These results, together with the non-pathogenicity phenotypes of *C. higginsianum* mutants tagged in arginine and polyamine synthesis genes show the potential importance of genes involved in basic metabolism for penetration and production of disease symptoms by fungal plant pathogens. Furthermore, a study of ESTs derived from isolated primary hyphae showed that many genes encoding amino acid biosynthetic enzymes and

amino acid transporters are expressed during the biotrophic phase of *C. higginsianum* (Dr. Hiroyuki Takahara, unpublished).

3.7 Mutants induction plant defence responses

Fourteen mutants induced cytologically-detectable defence responses (*i.e.* HR or papillae) upon penetration of host epidermal cells. Such mutants may be affected in genes required for evading host recognition or suppressing host cell death or defence responses during the intracellular biotrophic phase. Examples from other *Colleotrichum* species include *CgDN3*, encoding a secreted protein required in *C. gloeosporioides* to suppress HR (Stephenson *et al.,* 2000), *ClaSSD1*, a regulator of cell wall assembly in *C. lagenarium* required to avoid papilla induction (Tanaka *et al.,* 2007) and possibly CIH1 which may mask chitin in the fungal cell wall of biotrophic hyphae (Perfect *et al.*, 2000).

3.7.1 Regulation of translation may be important to avoid HR induction

In the HR-inducing mutant *path*-29, the T-DNA was inserted upstream of an ORF that is homologous to other fungal proteins which have high homology to an ATP-binding domain and to a small endoribonucleases identified as liver perchloric acid-soluble protein (L-PSP). L-PSP belongs to a new class of small proteins named the YER057C/YJGF family (Schmiedeknecht *et al.,* 1996). This poorly characterised protein family is conserved in prokaryotes and eukaryotes and has been implicated in diverse cellular processes, including inhibition of protein synthesis and the biosynthesis of purines and isoleucine (Morishita *et al.,* 1999; Christopherson *et al.,* 2008). It is important to note that despite having an endoribonuclease domain, the encoded protein product is not predicted to be secreted and is not homologous to small secreted endoribonucleases of fungi such as α-sarcin of *Aspergillus gigangteus*, also known as ribotoxins or cytotoxins. The top Blast match against *Magnaporthe* sequences was to a hypothetical protein (MGG_00500) with the same predicted ATP-binding endoribonuclease domain conformation. This gene was tagged in a large scale ATMT insertional mutagenesis programme of *M. oryzae* (http://atmt.snu.ac.kr/; (Jeon *et al.,* 2007). Interestingly, the *M. grisea* mutant also showed reduced pathogenicity

on rice but, unlike the *C. higginsianum* mutant, it was impaired in appressorium formation (less than 50 %).

The domain architecture of an ATP-binding domain followed by one or two L-PSP ribonuclease domains is well-conserved among eukaryotes. However, for none of the many proteins with this conformation has a function as endoribonuclease been proven. L-PSP is rat liver perchloric acid-soluble protein and has been demonstrated to be an endoribonuclease acting on single-stranded mRNA to inhibit protein synthesis by preventing elongation of translation (Morishita *et al.,* 1999). Homologous translational inhibitors have been characterised only in human monocytes and mouse liver, called p14.5 and PSP, respectively (Schmiedeknecht *et al.,* 1996). Interestingly, L-PSP, p14.5 and PSP are up-regulated during cellular differentiation, *i.e.* p14.5 is up-regulated during the differentiation of macrophages whereas PSP levels increase in kidneys during post-natal development of rat, and is down-regulated in renal tumour cells (Schmiedeknecht *et al.,* 1996).

The expression of the putative ATP-binding endoribonuclease was found to be constitutive. It is therefore possible that it is a substrate, or interactor of the putative endoribonuclease which might be differentially regulated during pathogenesis. Interestingly, the T-DNA insertion of *path*-29 was upstream of the predicted ORF and expression of the predicted ORF was still detected in saprothytic mycelium of the mutant, although at much lower level than in the wild type.

One can speculate that the inhibition of translation of particular proteins may be required at certain stages during pathogenesis. Because the mutant is impaired in pathogenicity and induces more HR than the wild type, it is possible that inhibition of the translation of certain proteins might be involved in avoiding recognition by the host or suppressing HR. Determining the targets and downstream effects of the endoribonuclease might reveal interesting candidates for the avoidance of recognition or suppression of host cell death.

To confirm that the putative ATP-binding L-PSP endoribonuclease is responsible for the observed pathogenicity phenotype and the HR induction, complementation with a wild-type copy of the gene or targeted gene disruption is required. Furthermore, mutant *path*-29 is not a null mutant and small amounts of transcripts were detected in the mutant. A

targeted knock out is therefore necessary to investigate the function of the predicted protein tagged in *path*-29 in pathogenicity. It is also important to investigate whether the protein encoded by the tagged open reading frame has ribonuclease activity. Its localisation in the cell during pathogenesis may also yield further hints to its function. A proteomics approach might also be a promising approach to identify downstream effects of the mutation if it is indeed involve din the inhibition of protein translation.

3.8 Biotrophy-necrotrophy switch mutants

Five mutants were identified which successfully established intracellular biotrophy but became arrested at the primary hypha stage, and only rarely entered the necrotrophic phase or formed secondary hyphae. Although fundamental to the infection process of all hemibiotrophic *Colletotrichum* species, the regulation of this major life-style transition is poorly understood. To date only three genes were implicated in the switch from biotrophy to necrotrophy: CLNR1 and CLTA1 from *C. lindemuthianum*, which encode an AreaA-like regulator of nitrogen metabolism and a GAL4-like transcriptional activator, respectively, and CPR1 from *C. graminicola*, which encodes a subunit of the signal peptidase complex (Dufresne *et al.,* 2000; Thon *et al.*, 2002; Pellier *et al.,* 2003).

3.8.1 Proper mRNA processing may be important for maintaining biotrophy

In two pathogenicity mutants, *path*-36 and *path*-38, both affected in the transition from biotrophy to necrotrophy, the tagged gene showed high homology to conserved importin ß2 proteins, including the human karyopherin ß2 (Kapß2) and yeast Kap104p. This class of importins has not been studied in filamentous fungi, but in mammals, yeast and plants they are known to mediate the nuclear import of pre-mRNA processing proteins, *e.g.* human heterogeneous nuclear ribonucleoprotein A1 (hnRNP A1), which regulates pre-mRNA spice-site selection (Bonifaci *et al.,* 1997), human HuR, which stabilises mRNA 3' untranslated regions (Fan and Steitz, 1998), human TAP, a nuclear RNA export factor (Truant *et al.,* 1999) and yeast hnRNP-like proteins Nab2 and Nab4, required for poly(A)

tail cleavage site selection (Anderson *et al.*, 1993; Lee and Aitchisin, 1999; Lee *et al.,* 2006). However, a more recent bioinformatics approach based on prediction of the specific nuclear localisation signal (NLS) characteristic of Kapß2 cargoes (the M9 NLS, composed of 38 amino acid residues) suggests this human karyopherin may have 81 new candidate substrates, and not they are not exclusively involved in transport of mRNA processing proteins (Lee *et al.,* 2006). The same computational approach identified over 100 new ligands for Kap104p of *S. cerevisae* (Chook, 2007; Lange *et al.,* 2008). The maturation of mRNA is a prerequisite for its export into the cytoplasm. Before its export, mRNA is packaged and undergoes modifications such as splicing, polyadenylation and capping. All these processes require the association of mRNA with specific proteins within the nucleus (Nakielny and Dreyfuss, 1997).

Karyopherins belong to a conserved family of proteins and are composed of helical molecular motifs called HEAT or Armadillo repeats which are stacked on top of each other to form a highly flexible, superhelical structure (Mosammaparast and Pemberton, 2004). Karyopherin ß proteins mediate the nuclear transport of cargo proteins by binding their substrates and targeting them to the nuclear pore complex by interacting with nucleoporins. Two pathways are used by karyopherin ß proteins. In the classical pathway, karyopheirn ß forms a heterodimer with a karyopherin α protein bound to the nuclear localisation signals of target proteins. Karyopherin ß then binds the nuclear pore complex to guide the dimer into the nucleus. Karyopherin ß2 uses a different pathway for nuclear import (Aitchisinson *et al.* 1996; Bonifaci *et al.,* 1997). Unlike the other karyopherin ß proteins, karyopherin ß2 binds directly to the nuclear localisation signal of its substrate and imports it into the nucleus; without interaction with karyopherin α protein being required.

The *S. cerevisae* karyopherin ß2 Kap104 disruption mutant is neither non-viable nor reduced in fitness (Mosammaparast and Pemberton, 2004). This is in accordance with the observation that both mutant *path*-36 and *path*-38 do not show any differences from the wild-type strain except for the observed pathogenicity defect, despite the fact that the gene encoding the putative importin is a single copy gene in *C. higginsianum*. Both mutants showed the same pathogenicity phenotype: a reduced ability to enter the necrotrophic phase, resulting in a prolonged biotrophic phase, although the extent of fungal cell death or host cell death has not been quantified. No induction of HR was observed in response to

penetration by either of the mutants, although it is possible that other host defence responses are elicited that were not visible by microscopy, *e.g.* pathogenicity–related (PR) gene expression. It is possible that a mutation in a karyopherin ß2 homologue may cause inappropriate pre-mRNA processing, splicing or export and thus result in incorrect or misregulated gene expression. It would therefore be interesting to study effects of the mutation on downstream gene expression and splicing in *C. higginsianum*. To date, there is only one example of a fungal gene displaying alternative splicing during pathogenesis: the transcription factor CLSTE12 of *C. lindemuthianum,* for which a splice variant lacking the third short exon (out of four exons) is up-regulated during germination and appressorium formation compared to conidia germinated in glucose (Hoi *et al.,* 2007). It is possible that the STE12 homologue in *C. higginsianum* also undergoes alternative splicing and it would be interesting to see if the ratio of the two splice variants is affected in the importin disruption mutants. Thus, STE12 could provide a useful indicator to determine whether alternative splicing is impaired in the importin mutants.

Two independent mutants with T-DNA insertions tagging the same predicted gene and sharing the same pathogenicity phenotype is indication that the insertions are responsible for the phenotype. However, to confirm tthat the phenotype is due to the T-DNA insertion in the putative importin, complmementation with the wild-type copy of the importin and its flanking region, or a targeted gene disruption of the importin is necessary. To identify targets of the substrates of the importin, a proteomics approach might be useful if the mRNA is not properly processed and results in different protein profile.

3.9 Conclusion

Using ATMT for insertional mutagenesis, 14 genes with potential roles in appressorial pigmentation, host penetration, avoidance or suppression of host defences, nutrition *in planta*, and the switch from biotrophy to necrotrophy were identified. None of these genes have been previously implicated in the pathogenicity of any *Colletotrichum* species, and only ODC and the L-PSP endoribonuclease were reported as pathogenicity genes on other fungi. So far, three mutations (the carbamoyl phosphate synthetase, the ARG 6 precursor and the phosphate transporter) have been validated by complementation with the

corresponding cosmid clones (this study and Dr. Hiroyuki Takahara, unpublished). Verification of the remaining candidate pathogenicity genes by complementation and targeted gene disruption is now required. Overall, despite revealing some evidence for non-random T-DNA integration, this study demonstrates that insertional mutagenesis by ATMT has great potential for the large-scale discovery of novel pathogenicity genes and future genome annotation in *C. higginsianum*.

3.10 Outlook

3.10.1 Confirming a role in pathogenicity for candidate pathogenicity genes

All the tagged genes identified from the screen of random insertional mutants remain candidate pathogenicity genes. It is important now to confirm that these are involved in pathogenicity, by either complementation of the mutant with a wild-type copy of the gene or targeted gene knock out of the desired gene in the wild-type background.

Complementation can be done by random ectopic integration of the entire cosmid harbouring the selected gene. The cosmids used as vectors for the genomic DNA library also have a bialaphos resistance (BAR) gene as selection marker and can therefore be used to select for complemented strains. However, in complementation experiments performed in this study, bialaphos was found to give only weak selection, even at high concentrations, and it might be useful to engineer a different selection marker into the cosmid to use in complementation, for example the phleomycin resistance gene.

Targeted gene disruption would also allow verification that the altered pathogenicity phenotype is linked to the T-DNA insertions. Particularly in the case of mutants with multiple insertions, or where the tagged genes is still weakly expressed, independent targeted disruption of each gene would allow the determination of which gene is responsible for the observed phenotype. Targeted gene disruption via homologous recombination is well established in fungi. In this study, attempts were made to obtain targeted knockout mutants by split-marker method in which protoplasts are transformed by overlapping linear DNA fragments containing part of the target gene fused to the

hygromycin resistance gene. However, this approach was not successful and yielded only ecotpic integrations, probably because the efficiency of homologous recombination in *C. higginsianum* may be as low as 1 % (Dr. Gento Tsuji, personal communication). Alternatively, targeted disruption mutants can be obtained in *C. higginsianum* using *Agrobacterium*-mediated transformation to introduce the hygromycin resistance cassette into the target gene. However, it will be important to use a *C. higginsianum* mutant strain lacking the Ku70 gene responsible for non-homologous end-joining in order to increase the frequency of targeted over ectopic insertions (Ninomiya *et al.,* 2004; da Silva Ferreira *et al.,* 2006; Goins *et al.,* 2006; Krappmann *et al.,* 2006; Nayak *et al.,* 2006; Poggeler and Kuck, 2006; Takahashi *et al.,* 2006; Chang, 2008; Haarmann *et al,.* 2008; Villalba *et al.* ,2008).

3.10.2 Investigating the role of an importin ß2 and a putative L-PSP endoribonuclease in pathogenicity

Due to their pathogenicity phenotypes: the incapability to switch to the necrotrophic phase and the induction of HR, respectively, the putative importin ß and the putative ATP-binding L-PSP endoribonuclease are promising candidates for factors involved in pathogenicity, particularly the establishment and maintenance of biotrophy.

For genes which putatively affect pathogenicity by modifying gene expression, for example the importin ß and the ATP-binding L-PSP endoribonuclease, it would be interesting to look at the effect the mutation has on downstream gene expression. Expression of candidate genes such as STE12 could be looked at by RT PCR and real-time PCR. Additionally, alternative splicing of STE12 or other candidate genes could be looked at in the importin mutant. A protemics analysis of the fungus proteome during pathogenesis or penetration or cellophane compared to growth *in vitro* may also bring to light changes of abundant proteins which may be important for pathogenicity.

For the mutant *path*-29, tagged in the putative ATP-binding L-PSP endoribonuclease, the occurrence of fungal primary hyphae which appear dead after 7 days and whether these are in live or killed host cells should be quantified using fluorescein diacetate (FDA) staining as a better determinant of cell viability than the GFP fluorescence of the hyphae, combined with plasmolysis.

4 Materials and methods

4.1 Materials

4.1.1 Chemicals

Laboratory grade chemicals and reagents were purchased from Roth (Karl Roth, Karlsruhe, Germany), Boehringer (Mannheim, Germany), Merck (Darmstadt, Germany), and Sigma (Deisenhofen, Germany) unless otherwise stated.

4.1.2 Antibiotics

Solutions described in Table 8 were stored at -20° C. Aqueous solutions were sterile filtered.

Table 8. Stock solution of antibiotics used in this study

Antibiotic	concentration (mg/ml)	solvent	Source
Ampicillin	100	ddH_2O	Sigma
Bialaphos	10	ddH_2O	Wako Pure Chemicals
Cefotaxime	50	ddH_2O	Sigma
Chloramphenicol	25	ddH_2O	Sigma
Hygromycin	100	ddH_2O	Invivogen
Kanamycin	100	ddH_2O	Sigma
Rifamicin	10	ethanol	Sigma
Streptomycin	100	ddH_2O	Sigma
Spectinomycin	10	ddH2O	Sigma

4.1.3 Organisms and growth conditions

Fungal pathogen strains and growth conditions

The fungal strain of *Colletotrichum higginsianum* used in this study as recipient for the *Agrobacterium tumefaciens* mediated mutagenesis was the strain IMI349061 which was originally isolated from *Brassica campestris*. Cultures were maintained in Mathurs's agar medium at 25 °C under constant light and conidia were harvested from 7- to 10-day old cultures by irrigation (O'Connell *et al.* 2004).

Yeast strains and growth conditions

The *Saccharomyces cerevisae* strain EY57 (MATa) and the quintuple deletion mutant EY917 (MATα *pho84Δ::HIS3 pho87Δ:: CgHIS3 pho89Δ::CgHIS3 pho90Δ::CgHIS3*

pho91Δ::ADE2) both harbouring the plasmid EB1280 containing the full length *PHO84* cDNA under the control of the *GAL1* promoter (Wykoff and O'Shea, 2001). Strains were provided by Dr. Freimoser, ETH Zurich. All strains were grown in synthetic media with either 2 % glucose (SD) of 2 % galactose (SG) at 30 °C.

Bacterial strains and growth conditions

Escherichia coli strain used of molecular purposes was DH5α (genotype F^- *sup*E44 Δ*lac*U169 *hsd*R17 *rec*A1 *end*A1 *gyr*A96 *thi*-1 *rel*A1). The strain grew on LB agar at 37 °C. *Agrobacterium tumefaciens* strains used for transformation were C58C1 and AGL-1. The strains grew on LB or YEB at 28 °C.

Plants and growth conditions

The susceptible host plants used for inoculation experiments were *Arabidopsis thaliana* ecotypes Landsberg *erecta* (Ler-0) and wild rape kale, *Brassica napus biennis* (Horticulture Research International Genetic Resource Unit, Accession No. 5671). The *Arabidopsis* mutants *pen1*-1 (Collins *et al.* 2003), *pen2*-2 (Lipka *et al.* 2005), *pen3*-3 (Stein *et al.* 2006) and *pmr4*-1 (Nishimura *et al.* 2003) were all in the Columbia (Col-0) background.

Plants were grown in a soil-less compost. Seeds were and stratified for two days at 4 °C in darkness to allow for synchronous germination. Germination was induced by transfer of the plants to controlled environment chambers under a regime of a 10-h light period at 150 to 200 mE m^{-2} s^{-1}, 65% relative humidity, with 22 °C during the day and 20°C during the night. Mature *Arabidopsis* plants and *Brassica* seedlings were grown in 9-cm pots, nine plants per pot. For experiments on *Arabidopsis* seedlings, pipette boxes filled with soil were used to grow 15-20 seedlings in each of the 96 well of the pipette box inlay, for 10 days. Cabbage cotyledons were obtained by growing the seedlings for 7-10 days in a 9 x 9 cm pot.

4.1.4 Enzymes

Restriction enzymes

Restriction enzymes were purchased from New England Biolabs (Frankfurt, Germany) and unless otherwise stated 10 X buffers and BSA for restriction enzymes were supplied with the enzymes by manufacturer.

Polymerases

Standard PCR reactions were performed using Amplicon *Taq* DNA polymerase (VWR-Bie & Berntsen, Copenhagen, Denmark) while for Inverse and TAIL PCR, LA polymerase (Bio, Saint-Germain-en-Laye, France) was used with GC buffer II.

For the synthesis of Southern Blot probes, the PCR DIG Probe Synthesis Kit (Roche, Mannheim, Germany) was used according to the manufacturer's instructions.

T4 DNA ligase was obtained from Roche (Mannheim, Germany)

Other enzymes

For cDNA synthesis, the SuperScript enzyme from the Superscript double-stranded cDNA synthesis Kit and the LR and BP clonase were from Invitrogen (Karlsruhe, Germany) was used. Pronase E was obtained from Sigma (Deisenhofen, Germany), DNase for RNA treatment was obtained from Qiagen (Hildern, Germany), the DNA alkaline phosphotase CiP was obtained from New England Biolabs (Frankfurt am Main, Germany).

4.1.5 Oligonucleotides

Listed below are primers used in this study obtained from Isogen or Invitrogen. Lyophilised primers were resuspended in ddH_2O to a final concentration of 100 pmol/µl. Working solutions were diluted to 10 pmol/µl (=10 µM).

Table 9. Primers used in this study

Name	Sequence 5'-3'	Use
M13R	GTAAAACGACGGCCAGT	Sequencing in pGEM T-Easy
M13R	GGAAACAGCTATGACCATG	
RBsp	TCAGATTGTCGTTTCCCGCC	Sequencing of flanking region
RHP	GGGGCTCGAGNNNNNN	First strand cDNA synthesis
HS1	GGCCGTGGTTGGCTTGTATGGAGCAGCAGA	TAIL- and Inverse PCR
HS2	TGGTCTTGACCAACTCTATCAGAGCTTGGT	
HS3	TCTGGACCGATGGCTGTGTAGAAGTACTCG	TAIL- and Inverse PCR
TS4	TACAGATGCATGACGGCC ATCATGCCAACG	
TS5	AACTGGCCCTTATCGTACTCCATGTTGGTA	
TS6	AGCAGGCTCGACGTATTTCAGTGTCGAAAG	
AD1	NGTCGASWGANAWGAA	TAIL-PCR
hphF	ACTCACCGCACGTCTGTCG	Inverse PCR and *hph* probe
hphR	TGCGGCCATTGTCCGTCAGG	
2D4U	TGTGCTGGGTGTGCTTGTAT	Library screen for ORF tagged in *path*-36
2D4L	CGGGGAGGAATGCGAAAGA	
G11U	AACCGGGTGTTTGAATTTGGTCTA	Library screen for ORF tagged in *path*-5
G11L	CGCTGTTACGTCGGTGGAG	

Table 9 cont. Primers used in this study

M1F	GAGGAGGCCCTCAAGGAG	Library screen for ORF tagged in *path*-12
M2R	GGCGGCGTCCTGAATGAG	
I28F	CTCGCCCCTCTCCTGCCAACC	Library screen for ORF tagged in *path*-38
I28R	GAATGGTGGCACTCAGCAGGTC	
F12U	GCCAGGCAGGTCGTCGTC	Library screen for ORF tagged in *path*-29
F12L	GTGGCCGGTCCGTTTGTGT	
XIF	GCTCAGCGGCTTCGACAAGAATG	RT-PCR putative importin ß2
XIR1	ATTCGGGCCAGCTCAGAATACCA	
pl2F	ACAGGCCGCCAGTCAGTCAATC	RT-PCR predicted ORF tagged in *path*-5
pl2R	AGGCCCCCAGTTAAAGGTCATAGC	
M1D	ACCACAGAGTATGAACGCCAGATTT	RT-PCR putative MFS transporter tagged in *path*-12
M2D	AGAAGAGGGACCAGGCGTAGAAGATGA	
GF1	GCGCAGCAAAAGTACGTCCTCCAC	RT-PCR putative glucanase tagged in *path*-9
GR1	TCGTCGTTCTGCTCCCACACTTTC	
hxF	AGGCCAAGCTTCTATCTGTC	RT-PCR hypothetical protein tagged in *path*-9
hxR2	GCTGGAGCTTGAGGCACTTGTT	
prMF	ATTTGCCCTGGTGGAAGCGTGTCA	DIG-labelled probe synthesis for predicted MFS transporter tagged in *path*-12
prMR	AAGGGCGAAGGAGAGGCGGAAAGT	
prIF	CCTCCCCCGACATCAACAACTACC	DIG-labelled probe synthesis for predicted importin tagged in *path*-36, -38
prIR	GAGAGCGGCGGCAGAGCACTT	
prEF	TCGACGGCCCTCCCAGTTTGTTCC	DIG-labelled probe synthesis for predicted endoribonuclease tagged in *path*-29
prER	GCCCGCCTTCGTTATCCGCATCCT	
cMF[1]	**GWYF**ATGGCGACCCATCAGAATCGC	Amplification of MFS cDNA with Gateway® extension
McR[2]	**GWYR**TTAACCCCGCTTCTCATCCAG	
Pcf	**GWYF**ATGAGTTCCGTCAATAAGA	Amplification of PHO84 cDNA with Gateway® extension
PcR	**GWYR**TTATGCTTCATGTTGAAGTT	

[1] GWYF: forward attB1 primer Gateway® compatible
[2] GWYR: reverse attB2 primer Gateway® compatible

4.1.6 Vectors

pBIG2RHPH2: Binary vector used for fungal transformation harbouring the hygromycin B phosphotransferase (*hph*) gene cassette under the control of *Aspergillus nidulans* trpC promoter and terminator between the right and left border (Tsuji, G. *et al.* 2003).

pBIN-GFP-hph: Binary vector used for fungal transformation carrying green fluorescent protein (*gfp*) gene under the control of the *A. nidulans* trpC constitutive promoter and *hph* under the GPDA promoter from *A. nidulans*, between the right and left borders (O'Connell, R. J. *et al.* 2004).

pGEM®-T Easy: Plasmid obtained from Promega (Mannheim, Germany), used for cloning of multiple PCR products from the TAIL- PCR. The multiple cloning site (MCS) inside and in-frame the α-peptide coding regions of the ß-galactosidase enzyme so that insertion of DNA results in inactivation of the α-peptide.

pDONR™: Invitrogen Gateway®-adapted vectors designed to generate *att*L-flanked entry clones containing your gene of interest following recombination with an *att*B expression clone or an *att*B PCR product.

pRS416-ADH1-HA: Plasmid obtained from Dr. Freimoser, ETH Zürich, used to transform yeast. The plasmid has a MCS driven by the ADH1 constitutive promoter.

pRS416-ADH1-PHO84-HA: Plasmid obtained from Dr. Freimoser, ETH Zürich, used to transform yeast. The plasmid has the yeast phosphate transporter PHO84 driven by the ADH1 constitutive promoter.

4.1.7 Media

Unless otherwise indicated all media were sterilized by autoclaving at 121°C for 20 mins. Heat labile solutions were filter-sterilised and added to cooled autoclaved components.

Fungal media:

- ***Mathur's medium***

2.80	g	Glucose
1.22	g	$MgSO_4 \cdot 7H_2O$
2.72	g	KH_2PO_4
2.18	g	Mycological peptone
30	g	Agar (for solid medium only)
1	L	ddH_2O

- ***Other media***

Potato dextrose agar (PDA) and Czapek Dox medium (CD) were supplied as ready medium from Merck, Darmstadt, Germany). For Czapek Dox agar medium (CDA), 1.5 % agar was added to CD.

Yeast media

- ***2X YPAD***

12	g	Yeast extracts
24	g	Peptone
24	g	Glucose
120	mg	Adenine hemisulphate
600	mL	ddH_2O

- ***Synthetic media with glucose (SD) or galactose (SG)***

6.7	g	Yeast nitrogen base w/o amino acids
2.0	g	Glucose or galactose
As needed		Supplements
1	L	ddH_2O
10	g	Agar (for solid medium)

Media for E. coli

- ***Luria Benturia (LB) broth***

1	% (w/v)	Tryptone peptone
0.5	% (w/v)	Yeast extracts
0.5	% (w/v)	NaCl
2	% (w/v)	Agar (for solid medium only)

- ***SOC***

20	g	Tryptone
5	g	Yeast extract
10	mM	NaCl
2.5	mM	KCl
10	mM	$MgCl_2$
10	mM	$MgSO_4$
20	mM	Glucose (sterile-filtered)

Fill to 1L with ddH_2O and adjust pH to 7.0 if necessary.

Media for Agrobacterium tumefaciens-mediated transformation

- ***Agrobacterium broth (AB)***

10	mL	AB salts I
10	mL	AB salts II
10	mL	AB phosphate (pH 7.0)
10	mL	AB glucose
60	mL	ddH_2O

- ***Glycerol Induction (GI) broth***

10	mL	AB salts I

10	mL	AB salts II
10	mL	GI carbon
10	mL	GI MES
60	mL	ddH_2O
200	µM	acetosyringone

- ***Glycerol Induction (GI) agar***

50	mL	AB salts I
50	mL	AB salts II
50	mL	GI phosphate
50	mL	GI carbon
50	mL	GI MES
250	mL	6 % agar
200	µM	acetosyringone

Components are added to cooled agar (55° C).

4.1.8 Buffer and solutions

- ***Diethylpyrocarbonate (DEPC)-H_2O***

0.1	%	DEPC in H_2O

Shake vigorously, let stand overnight and autoclave 30 mins

- ***Agarose gel***

1	g	Agarose
100	mL	TAE buffer (10x)
2	µl	Ethidium bromide stock (10 mg/mL)

- ***TE (Tris/EDTA) buffer***

10	mM	Tris/HCl (pH 8.0, 7.5)
1	mM	EDTA (pH 8,0)
1	mM	Tris/HCl
121	g	Tris-Base
1	L	H_2O

Dissolve 121 g Tris base in 800 mL, adjust to desired pH with concentrated HCl, adjust volume to 1 L with H_2O, filter sterilise if necessary, can be stored up to 6 months at 4° C or at room temperature.

- ***EDTA (ethylenediaminetetraacetic acid)-stock (0.5 M, pH 8.0)***

186.1	g	Na_2EDTA
1	L	H_2O

Dissolve 186.1 g Na_2EDTA in 700 mL water, adjust pH to 8.0 with 10 M NaOH (~50 mL; add slowly), add water up to 1 L. Filter sterilise.

- ***Lysis buffer***

100	mM	Tris-HCl (pH 8.0)
100	mM	EDTA (pH 8.0)
50	mM	NaCl
0.5	%	SDS

Dissolve in distilled water and autoclave.

- ***TAE (Tris/acetate/EDTA) buffer (10x)***

24.2	g	Tris base
5.71	mL	glacial acetic acid
3.72	g	$Na_2EDTA \cdot 2H_2O$
994	mL	H_2O

- ***TFB1***

1.18	g	KAc
2.52	g	$MNCl_2$
4.80	g	RbCl
0.58	g	$CaCl_2$
60	mL	glycerol
340	mL	ddH_2O

Adjust to pH 5.8 with HCl

- ***TFB2***

0.42	g	MOPS
2.20	g	$CaCl_2$
0.24	g	RbCl
30	mL	glycerol
170	mL	ddH_2O

Filter-sterilise

- ***AB salts I***

5	g	NH_4Cl
1.5	g	$MgSO_4 \cdot 7H_2O$
0.75	g	KCl
500	mL	ddH_2O

- ***AB salts II***

50	mg	$CaCl2 \cdot H_2O$
12.5	mg	$FeSO_4 \cdot 7H_2O$
0.75	g	KCl
500	mL	ddH_2O

Filter-sterilise.

- ***AB phosphate***

19.7	g	$K_2HPO_4 \cdot 3H_2O$
5.0	g	$NaH_2PO_4 \cdot H_2O$
500	mL	ddH_2O

Adjust pH to 7.0

- ***GI MES***

48.8	g	MES
500	mL	ddH_2O

Adjust pH to 5.2 with NaOH and filter-sterilise.

- ***GI phosphate***

3.45	g	$NaH_2PO_4 \cdot H_2O$
500	mL	ddH_2O

- ***3,3′-Diaminobenzidine (DAB) staining solution***

10	mL	ddH_2O, adjust pH 3.8 with HCl
10	mg	DAB

Boil for 1 h

- ***Anilline Blue solution***

0.07	M	KH_2PO_4
0.01	% (w/v)	Aniline Blue in H_2O

- ***Toluidine Blue solution***

0.05	M	Sodium citrate buffer, pH 3.5
0.05	% (w/v)	Toluidine Blue

4.2 Methods

4.2.1 DNA isolation

Cosmid and plasmid DNA isolations

Cosmid and plasmid DNA was isolated by alkaline lysis method (Birnboim, H. and Doly, J. 1979). High quality DNA for PCR and DNA sequencing was isolated using Qiagen or peqlab or MACHEREY-NAGEL(MN) Mini-prep kits.

Fungal DNA isolation

Mycelim from 2 days old cultures grown in liquid Mathur's medium was collected and blotted dry using a paper towel. The mycelium was homogenized in liquid nitrogen using a mortar and pestle. 1.5 mL of lysis buffer and 20 µl of pronase E were added to the mycelium in a 2 mL tube. After incubation of 30 mins at 65° C, the lysed mycelium was pelleted by centrifugation at 8000 rpm for 5 mins. The supernatant was transferred to a new tube and mixed vigorously with an equal volume of phenol-chloroform-isopropanol. The tube was then centrifuged at 13000 rpm for 5 mins. The supernatant was transferred to a new tube and mixed vigorously with an equal volume of chloroform-isoamyl alcohol. The tube was centrifuged 5 mins at 13000 rpm. The upper layer was transferred to a new tube with an equal volume of isopropanol. After a 2 mins incubation a room temperature, the DNA was pelleted by centrifugation at 8000 rpm for 30 secs. The pellet was washed with 1 mL of 70 % ethanol, dried and resuspended in 200 µl TE. The DNA was treated with 1 µl RNase (final concentration 20 µg/mL) for 1-2 hrs at 37° C. The DNA was then extracted once with phenol and once with chloroform as described previously and washed once with 70 % ethanol. The DNA pellet was then resuspended in 200 µl TE and stored at -20° C.

Isolation of DNA fragments from agarose-gel

The Nucleospin Extract-Kit (Macherey-Nagel GmbH, Düren, Germany) was used to extract DNA fragments from agarose-gels according to the manufacturer's protocol.

4.2.2 RNA isolation

RNA isolation was carried out using Trizol® reagent (Invitrogen) according to the manufacturer's instructions including the supplementary RNA precipitation protocol for samples with high polysaccharide contents. RNA pellets were dissolved in 140-180 µl RNase-free water. RNA was purified from traces of genomic DNA by column purification using the RNeasy Plant Mini Kit (Qiagen) following the manufacturer's instructions including the optional drying step prior to elution. Polyadenylated RNA was stored at -80 °C until cDNA synthesis.

4.2.3 Nucleic Acid Manipulations

Standard Polymerase Chain Reaction

Standard PCR was used to for cosmid, plasmid or genomic PCR *(Taq* polymerase) and gene expression. For colony PCR performed on either bacterial colony or fungal mycelium, the template consisted of 1 µl of 10µL ddH_2O into which the colony had been picked and vortexed. The initial denaturation step was extended to 10 mins. Tables 11-12 indicate the components of a typical PCR reaction mix and the thermal conditions.

Table 11: Reaction mix for standard PCR

Components	Amount
Template DNA (genomic or plasmid)	20 ng
10x PCR amplification buffer	5 µL
2.5 mM dNTPs mix (dATP, dCTP, dGTP, dTTP)	5 µL
Forward oligo (50 pmol or 10 µM)	1 µL
Reverse oligo (50 pmol or 10 µM)	1 µL
Amplicon *Taq* DNA polymerase	1 µL
H_2O	To 50 µL

Table 12: Thermal profile for standard PCR

Stage	Temperature (°C)	Time	N° of cycles
Initial denaturation	94	5 minutes	1 x
Denaturation	94	50 seconds	
Annealing	50-58	50 seconds	25-35 x
Extension	72	1-2 minutes	
Final extension	72	5 minutes	

Restriction enzyme digestion of DNA

All restriction digests were performed using the manufacturers recommended conditions. Typically, reactions were carried out in 1.5 mL eppendorf tubes. For southern blot use, typically, 5.20 ng of genomic DNA was digested to completion using 10-20 Units of restriction enzyme for 100 µL of reaction volume. For Inverse PCR use, 10 µ of genomic DNA were partially digested with 3 Units of restriction enzymes. All digests were carried out overnight at 37° C. The digested DNA is then precipitated by incubating the restriction digestion in 10 µl of 3 M sodium acetate (pH 5.2) and 200 µl ethanol for 30 mins at -20° C. The digested DNA is pelleted by centrifugation for 15 mins at 13000 rpm then rinsed once with 70 % ethanol and pelleted again by centrifugation for 5 minutes at 13000 rpm. The pellet is air-dried and resuspended in TE buffer. For use on inverse PCR, the digested DNA was treated with 1 µl RNAse for 1-2 hrs at 37° C, was extracted once with phenol, once with chloroform and precipitated with ethanol. The digested DNA was then resuspended in 20 µl ddH_2O.

DNA ligation

Ligation of constructs to vectors or self ligation of genomic DNA was conducted with T4 ligase from Invitrogen. In a reaction volume of 10 µl, 2 µl of 5X buffer were used with 1µl of the T4 ligase and appropriate concentrations of DNA.

DNA dephosphorylation

DNA was dephosphorylated using CiP and buffer 3 from New England Biolabs. A reaction volume of 150 µl contained 7.5 µg of DNA, 15µl buffer 3, 2.25 µl CiP. The reaction was conducted for 1 hr at 37 °C.

DNA sequencing

DNA sequences were determined by the Automatische DNA-Isolierung und Sequenzierung (ADIS-Unit) at the MPIZ on Applied Biosystems (Weiterstadt, Germany) Abi Prism 377 and 3700 sequencers using Big Dye-terminator chemistry (Sanger *et al.*, 1997). PCR products were purified with the Nucleospin Extract-Kit (MACHEREY-NAGEL) or Qiagen Extract Kit, ensuring sufficient amount at appropriate concentration to be directly sequenced.

4.2.4 Obtaining genomic sequence flaking T-DNA insertion

Inverse PCR

10 µg of mutant genomic DNA which had been partially digested by *Eco*RI (3 Units) in 20 µl final volume, overnight at 37 °C. The digestion reaction was treated with RNase and cleaned by phenol-chloroform extraction and ethanol precipitation. The digested DNA was re-suspended in 10 µl ddH_2O and 250-400 ng of digested DNA was self-ligated with T4 ligase (2 Units) in 100 µl final volume overnight at 4 °C. The self-ligated DNA was again phenol-chloroform extracted and ethanol precipitated and resuspended in 10 µl ddH_2O. For the Inverse PCR, 0.5 µl of the self-ligation were used as template for the first reaction. Inverse PCR were performed with LA *Taq* and corresponding GC buffer II (Takara Bio, Saint-Germain-en-Laye, France) or Ampliqon Taq and buffer (VWR-Bie & Berntsen, Denmark). The second reaction used 1 µl of a 1/100 dilution of the product of the first reaction as a template and was performed using a nested primer. Table 13 summarises the thermal profile for inverse PCR.

Table 13. Thermal profile for Inverse PCR

Stage	Temperature (°C)	Time	N° of cycles
Initial denaturation	94	5 minutes	1 x
Denaturation	94	50 seconds	
Annealing	50-58	50 seconds	25-35 x
Extension	72	1-2 minutes	

Thermal Asymmetrical Interlaced-PCR

The thermal asymmetrical interlaced-polymerase chain reaction (TAIL-PCR) was used to amplify the genomic DNA fragment flanking T-DNA from fungal transformants using nested gene specific primers and a degenerate primer, as in the protocol from Tsuji and colleagues with slight modifications (Tsuji *et al.* 2003). TAIL PCR were performed with LA *Taq* and GC buffer II with genomic DNA as template. A first reaction was performed as shown in Table 13. The second reaction used 1 µl of a 1/100 dilution of the product of the reaction as a template and was performed using a nested primer. The third reaction was again, performed using 1 µl of a 1/100 dilution of the product of the reaction as a template and with a nested primer. The thermal profile is summarised in Table 13.

Table 141. Thermal profile for TAIL-PCR

Stage	Temperature (°C)	Time	N° of cycles
Primary reaction			
Initial denaturation	94	5 minutes	1 x
Denaturation	94	20 seconds	5 x
Annealing	65	5 seconds	
Extension	72	30 seconds	
Denaturation	94	20 seconds	1 x
Annealing	30	30 seconds	
Annealing	41	55 seconds	
Annealing	52	55 seconds	
Annealing	63	55 seconds	
Extension	72	30 seconds	
Denaturation	94	20 seconds	13 x
Annealing	68	5 seconds	
Extension	72	30 seconds	
Denaturation	94	20 seconds	
Annealing	68	5 seconds	
Extension	72	30 seconds	
Denaturation	94	20 seconds	
Annealing	44	5 seconds	
Extension	72	30 seconds	
Final extension	72	2 minutes	
Secondary and tertiary reactions			
Stage	Temperature (°C)	Time	N° of cycles
Initial denaturation	94	5 minutes	1 x
Denaturation	94	20 seconds	10 x
Annealing	68	5 seconds	
Extension	72	30 seconds	
Denaturation	94	20 seconds	
Annealing	68	5 seconds	
Extension	72	30 seconds	
Denaturation	94	20 seconds	
Annealing	44	5 seconds	
Extension	72	30 seconds	

4.2.5 Gene expression analysis by semi-quantitative RT-PCR

Gene expression was analysed by semi-quantitative RT-PCR. First-strand cDNA was synthesized from 1 µg of RNA after DNAse treatment by reverse transcription. The reaction mix and the thermal profile are summarised in Table 15 and Table 16. The product was then diluted 1:20 in TE and used for gene specific amplification.

Table 15: Reaction mix for cDNA first-strand synthesis

Components	Amount
Template (RNA) *	1-5 µg
5 x first strand buffer	4 µL
10 mM dNTPs mix (dATP, dCTP, dGTP, dTTP)	1 µL
0.1 M DTT	2 µL
OligodT-adaptor primer (20 pmol/µl)	0.2 µL
RNAse inhibitor (40 U / µL)	0.25 µL
SuperScript reverse transcriptase 200 U	1 µL
DEPC-treated H_2O	To 20 µL

*The RNA template was first denatured in 11µl DEPC water by incubation at 80 °C for 3 minutes.

Table 16: Thermal profile for cDNA first-strand synthesis reaction

Temperature (°C)	Time
23	5 minutes
42	1 hour
50	10 minutes
80	3 minutes

cDNA was converted from 1 µg polyadenylated RNA using the Superscript Double-Stranded cDNA Synthesis Kit (Invitrogen) according to the manufacturer's instructions excluding the steps for radioactive labelling. First strand synthesis was carried out using 100 ng random hexamer primer (RHP) (Sigma; Genosys). The final extraction and purification steps after the second strand synthesis were extracted with phenol, supplemented with 100 µl DEPC-H_2O and re-extracted with chloroform. After centrifugation at 14000 rpm for 5 mins, the aqueous phase was added to 120µl 7.5 M NH_4OAc and precipitated in 900 µl ice-cold ethanol. The mixture was vortexed and pelletted by centrifugation (14000 g, 60 mins at room temperature). The pellet was washed with 900 µl ice-cold 70 % ethanol, dried at 37° C and dissolved in 18 µl DEPC-H_2O.

4.2.6 Southern Blotting

5-20 ng of DNA digested to completion was separated on a 1 % (w/v) agarose gel run at 90-110 V. The gel was then incubated 10 minutes in 0.25 N HCl, washed once with ddH_2O and incubated in denaturing solution (0.5 M NaOH, 1.5 M NaCl) for 30-60 mins. The gel was then placed directly on top of an Hybond N++ membrane, on 5 pieces of Whatman filter paper of the size of the gel and of a stack of paper towel. The gel was covered with 3 pieces of Whatman filter paper and 2 more pieces of filter paper which were dipped in alkaline

transfer solution (8 mM NaOH, 0.5 M NaCl) in a tank higher than the gel. The digested DNA transferred to the membrane overnight. The membrane was then incubated in 0.2 M Na_2PO_4 buffer, pH 6.8 for 5 mins and air-dried for 2-3 hrs. The DNA was cross-linked on the membrane by exposure to UV light for 1 min. Synthesis of DIG-labelled probe, hybridisation and detection with CDP-*Star* were performed using the DIG High Prime DNA Labelling and Detection Starter Kit II (Roche, Manheim, Germany) according to the manufacturer's instructions.

4.2.7 Transformation of Escherichia coli

Production of heat-shock competent cells

E. coli DH5 α strain is grown overnight in LB liquid. 10 ml of the overnight culture is used to inoculate 1 L of LB and shaken 250 rpm at 37° C until an OD_{600} of 0.4 - 0.5 is reached. The bacteria are then pelleted by centrifugation (4000 rpm for 15 mins at 4° C) and resuspended in 300 ml ice-cold sterile TFB1. The cells are incubated on ice for 5-10 mins, re-pelleted by centrifugation and resuspended in 40ml of ice-cold sterile TFB2. Competent cells are frozen in liquid nitrogen and stored in 50 µl aliquots at -80° C.

Transformation of heat-shock competent cells

100 to 250 ng of plasmid DNA is mixed with 50 µl of heat-shock-competent *E. coli* DH5α cells in a 1,5 ml reaction tube and incubated on ice for 10 mins. The tube is then transferred to 42° C for 90 secs and immediately transferred to ice for 10 mins. Then 450µl SOC medium is added and cells are incubated shaking at 37°C for 45 mins. Cells are then plated on agar containing the appropriate antibiotics.

4.2.8 *Transformation of* Agrobacterium tumefaciens

Production of heat-shock competent Agrobacteria cells

Agrobacteria are grown overnight in 2 mL YEB supplemented with the appropriate antibiotics at 28 °C, shaking at 250 rpm. 1 mL of the culture is then transferred to 50 mL fresh YEB with rifampicin and kanamycin and allowed to grow to an OD_{600} of 0.5. From

then on, the cells are kept on ice. The cells are centrifuged (15 mins, 4000 rpm, 4 °C). The cell pellet is resuspended in 1 mL of ice cold 20 mM $CaCl_2$. Aliquots of 50 µl are frozen in liquid nitrogen and stored at -80 °C.

Heat-shock transformation of Agrobacteria

2 µl of DNA are added to 50 µl of frozen competent cells. The frozen DNA-bacteria mixture is then placed at 37 °C to thaw for 5 minutes under occasional shaking. The cells are then chilled on ice. 450 µl of YEB medium without antibiotics are added. The cells are allowed to grow for 2 hours at 28 °C and are then spread on YEB agar plates supplemented with the appropriate antibiotics.

4.2.9 Agrobacterium-mediated transformation of C. higginsianum

A pre-culture of *Agrobacterium tumefaciens* with the appropriate binary vector or cosmid was grown for 18-24 hours in LB broth with the appropriate antibodies at 28° C shaking at 200 rpm. 10 mL of AB broth, with the appropriate antibiotics, was inoculated with 250 µl of the pre-culture and incubated for 18-24 hours at 28° C shaking at 200 rpm. The bacteria were then pelleted by centrifugation (3500-4000 rpm, 10 mins, room temperature) and re-suspended in 1 mL GI broth. The bacterial suspension was then diluted to an OD_{600} of 0.4-0.5 with GI broth. A suspension of *C. higginsianum* spores diluted to 10^7 conidia per mL in GI broth was prepared. Equal volumes of the conidial and the bacterial suspensions were mixed and 200 µl aliquots were spread onto either paper (Blotting paper 3MM, Schleicher & Schiell Bioscience) or cellophane membranes of cellophane membrane (MAXI gel-drying cellophane, Carl Roth, Karlsruhe, Germany) supported on GI agar plates using a glass rod. The *Agrobacteria* and the fungal conidia were co-cultivated for 2 days at 22° C in constant darkness. The membranes were then transferred, inoculated side down, on PDA supplemented with 50 µg per mL cefotaxime and 50 µg per mL spectinomycin to kill the *Agrobacteria* and with the required antibiotic for selection of transformants (70-100 µg / mL hygromycin B for insertional mutagenesis or 5-10 µg / mL bialaphos for complementation transformation) and incubated at 25° C for 3 days. The membranes were then removed and antibiotic-resistant colonies were picked and transferred to PDA plates

with hygromycin B. After 2 days, resistant colonies were transferred to PDA with the required antibiotics in 96 well plates.

4.2.10 Yeast Complementation

Yeast transformation

Yeast strain was inoculated into 5 mL of liquid 2 X YAPD and incubated overnight at 30 °C shaking at 200 rpm. 50 mL of pre-warmed 2X YAPD was transferred to a pre-warmed culture flask and add 2.5 x 10^8 cells. The cells were then incubated at 30 °C shaking at 200 rpm for about 4 hours until the cell concentration reached 2 x 10^7 cells /mL. The cells were harvested by centrifugation (3000*g*, 5 mins) washed in 25 mL sterile water and resuspended in 1 mL of sterile water. Salmon sperm (SS) carrier DNA (1 mL) was boiled for 5 mins and chilled on ice. The cell suspension was transferred to a 1.5 mL microcentrifuge tube, centrifuged for 30 secs and the supernatant was discarded. Water was added to a final volume of 1 mL. For the transformation, an aliquot of 100 µl was taken and centrifuged briefly. The supernatant was removed and the remaining cells were used for the transformation. To the cells (about 34 µl), a transformation mix composed of 240 µl PEG 3500 50 % w/v, 36 µl 1 M LiAc and 50 µl boiled SS-carrier DNA was added and the mixture was used to resuspend the cells by vigorous vortexing. The mixture was incubated at 42 °C for 40 seconds and was microcentrifuged to remove the mix. The cell pellet was then resuspended in 1 mL of sterile water by vortexing. Dilutions of the cell suspension were plated on SC selection medium. The plates were incubated for 4 days at 30 °C.

Construction of Gateway compatible construct for yeast complementation

The plasmid pRS416-ADH1-HA (5µg) was opened by restriction with *Sma*I for 3 hrs. The Gateway construction vector TOPOB (10µl) was digested with EcoRI for 3 hrs and the 1.7 Kb was gel-extracted with a column (Macherey-Nagel) and dephosphorylated. Both the TOPOB and the linearised pRS416 vectors were cleaned by column purification (Macherey-Nagel) and ligated together. The construct of TOPOB in pRS416-ADH1-HA was transformed in DB3.1 cells, amplified and extracted with plasmid DNA mini-preparation kit (Macherey Nagel). The cDNA of the yeast PHO84 and putative transporter

tagged in *path*-12 were amplified using Pfu (Fermentas) with primers with the appropriate Gateway extensions. The PCR products were cloned into pDONR^{TM} with BP clonase (Invitrogen) overnight at room temperature. The product was cloned and amplified into DH5α. and plasmid DNA was extracted using a kit (Machery Nagel). The LR reaction was performed with the BP product (pDONR^{TM} empty or with yeast PHO84 or *C. higginsianum* transporter) and the TOPOB ligated to pRS416-ADH1-HA using the LR clonase (Invitrogen) overnight at room temperature. The reaction was then cloned and amplified in DH5α and extracted by plasmid DNA extraction kit (Machery Nagel).

4.2.11 Plant inoculations

Spray inoculations

For inoculations with *C. higginsianum*, spores were harvested by irrigation of 7-10 days old cultures growing in flask with Mathur's medium. The spore concentration was counted using a haemocytometer and adjusted to the wanted concentration with deionised water ($5x10^5$ spores per mL unless otherwise stated). Mature plants were spray-inoculated using an atomizer and inoculated plants were placed in sealed propagator boxes to maintain 100 % humidity and incubated in a controlled environment chamber at 24 °C (16-h light period, 20-60 µmol m^{-2} s^{-1}, 24 °C). For inoculation experiments where exogenous KH_2PO_4 was added, the pH was kept the same in control inoculations by the addition of KCl.

Drop inoculations

For the primary screen, Arabidopsis seedlings were inoculated with a 20µl drop of conidial suspension of undefined concentration using a multichannel pipettor.

To test invasive growth ability of transformants, 4 weeks-old L*er*-0 plants were used. On one side on the leaf, a 4 µl drop of spores suspension was applied in triplicates and on the other side of the leaf, the drops were applied on a small wound made using a fine needle. Inoculated plants were kept in same controlled environment as mentioned above.

Inoculated material for gene expression study

To obtain epidermal strips for gene expression, fully expanded rosette leaves were excised from 5-week-old *A. thaliana* Col-gl-1-1 plants and the abaxial surface was inoculated with approximately 100 µL conidial suspension (5 x 10^6 conidia ml^{-1}) using a paint brush and nylon mesh to spread the suspension over the entire leaf surface. Inoculated leaves were incubated in sealed boxes in complete darkness at 25° C.

4.2.12 Microscopic analysis

Clearing of leaf tissue

Leaf tissue was cleared in ethanol-chloroform (3:1) mixture overnight and in lactophenol overnight. The cleared samples were then mounted in glycerol. Alternatively, leaf tissue was cleared in methanol overnight and in chloral hydrate overnight and mounted in glycerol.

3,3 diaminobenzidine (DAB) staining for hydrogen peroxide accumulation

At 48 hpi three leaves of each plant were harvested and stained with DAB (Thordal-Christensen *et al.* 1997). Leaves were harvested and placed with the petiole in 200 µl DAB solution in a multiwell plate. The plate was put in a box with moist paper towel to maintain high humidity and closed with aluminium foil to allow for complete darkness. The leaves then were cleared overnight in methanol and overnight in chloral hydrate and mounted in glycerol.

Aniline Blue staining of callose

For staining of callose deposition, leaves were harvested at 2, 3 and 4 days post inoculation, cleared in ethanol-chloroform and subsequently with lactophenol. The leaves were re-hydrated gradually in 75 %, 50 %, 25 % lactophenol and pure water for 15 mins each. The plant phenolic compounds were then blocked by overnight treatment of Toluidine blue solution. The leaves were rinsed three times 20 mins in distilled water and then transferred to aniline blue solution. After 12 hrs in Aniline Blue, the leaves were mounted in Aniline Blue and callose deposition was analysed by light microscopy with UV excitation.

Congo Red

A small piece of mycelium was used to inoculate a thin layer of medium on a microscope slide and grown for 3 days. Drop of Congo Red solution (1% w/v Congo Red in H_2O) were applied to the mycelium and rinsed with cleared water. Polysaccharides in the cell wall were visualised with bright field microscopy.

Plasmolysis

Etiolated hypocotyls of *Arabidopsis* or *Brassica* were vacuum-infiltrated with a Neutral Red plamolysis solution (0.01 % Neutral Red, 0.85 M KNO_3, 5 mM phosphate buffer pH 7.5). Vacuoles and cytoplasm plasmolyse and are stained in living cells.

4.2.13 Software, databases, and other internet resources

- ***Sequence alignment***
  ClustalW http://www.ebi.ac.uk/Tools/clustalw2/index.html
  Vector NTI
- ***Translation of DNA into protein sequences***
  Vector NTI
- ***Analysis and alignment of sequencing chromatograms***
  SeqMan (Lasergene)
- ***Primer design***
  Primer3 (http://frodo.wi.mit.edu/)
- ***Sequence analysis and comparison***
  NCBI blast http://www.ncbi.nlm.nih.gov/BlAST/
  COGEME http://cogeme.ex.ac.uk/
  Blast against Colletotrichum graminicola *draft genome sequence*
  http://www.ncbi.nlm.nih.gov/BLAST/Blast.cgi
- ***Gene prediction***
  SOFTBERRY http://softberry.com/berry.phtml FGENESH+ algorithm
- ***Search for pathogenicity genes***
  PHI-BASE http://www.phi-base.org/
  ATMT database http://atmt.snu.ac.kr

- ***Phylogenetic tree construction***
  CLUSTALW http://www.ebi.ac.uk/Tools/clustalw2/index.html
  PHYLIP version 3.68 http://evolution.genetics.washington.edu/phylip.html

- ***Promoter scan***
  Proscan http://www-bimas.cit.nih.gov/molbio/proscan/

- ***Transmembrane domain prediction***
  DAS http://www.sbc.su.se/~miklos/DAS/
  HMMTOP http://www.enzim.hu/hmmtop1.1/server/submit.html
  TMpred http://www.ch.embnet.org/software/TMPRED_form.html

- ***Protein domain predictions***
  ProDom http://prodom.prabi.fr/prodom/
  ProSite http://ca.expasy.org/prosite/
  InterProScan www.ebi.ac.uk/Tools/InterProScan/

5 Supplementary Data

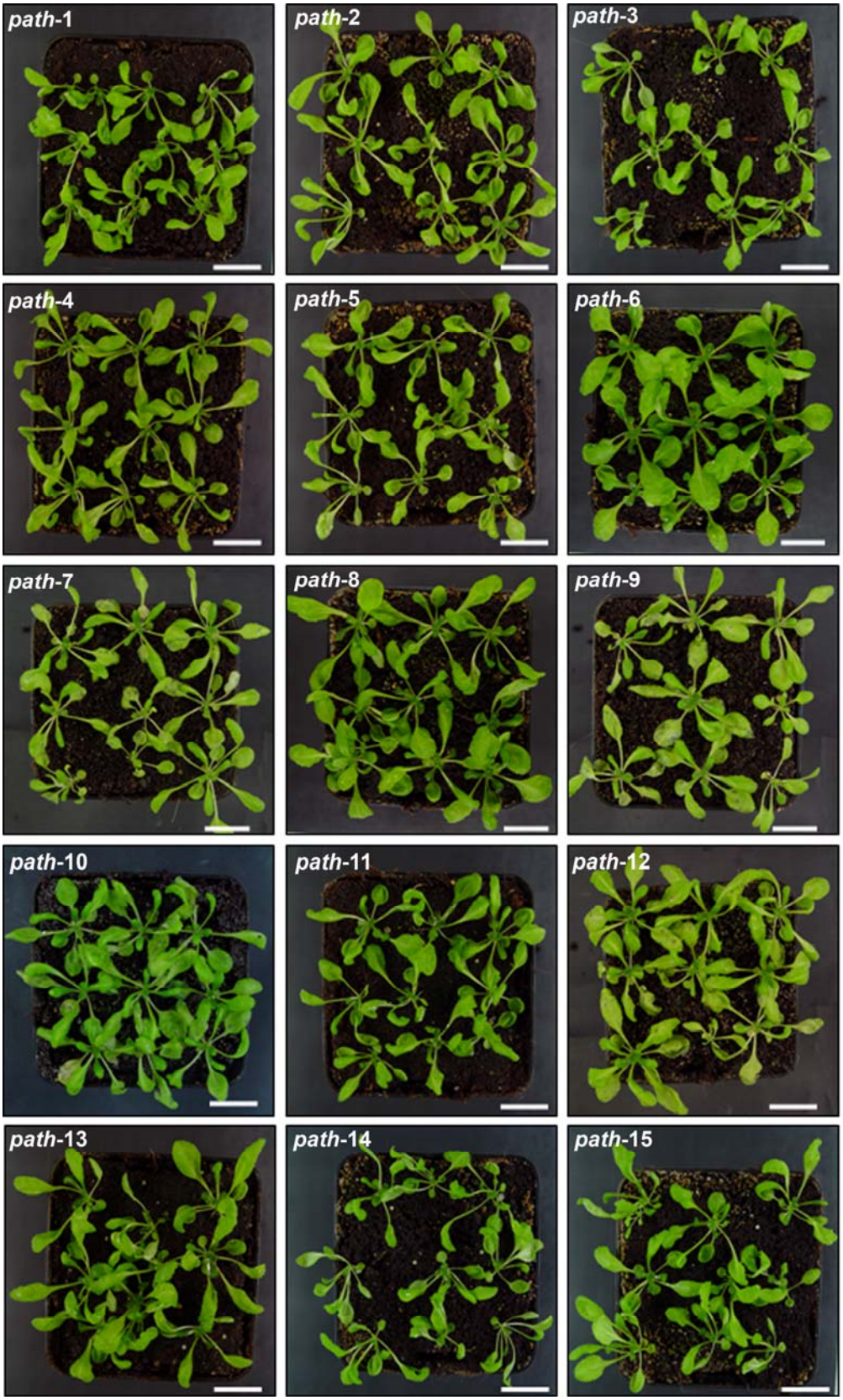

Supplementay Data 1. Symptoms of wild type *Colletotrichum higginsianum* and all 40 pathogenicity mutants.

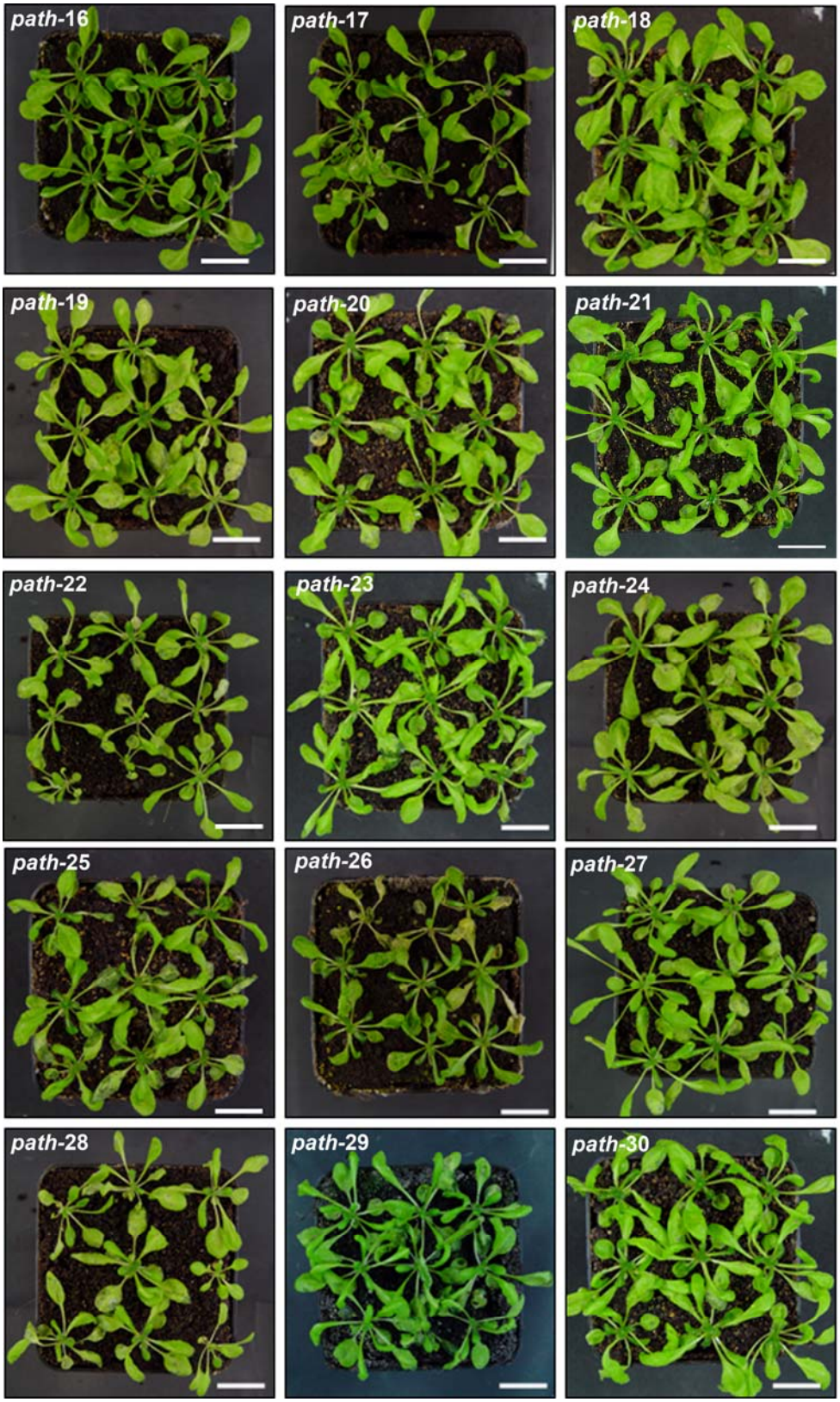

Supplementay Data continued 2. Symptoms of wild type *Colletotrichum higginsianum* and all 40 pathogenicity mutants.

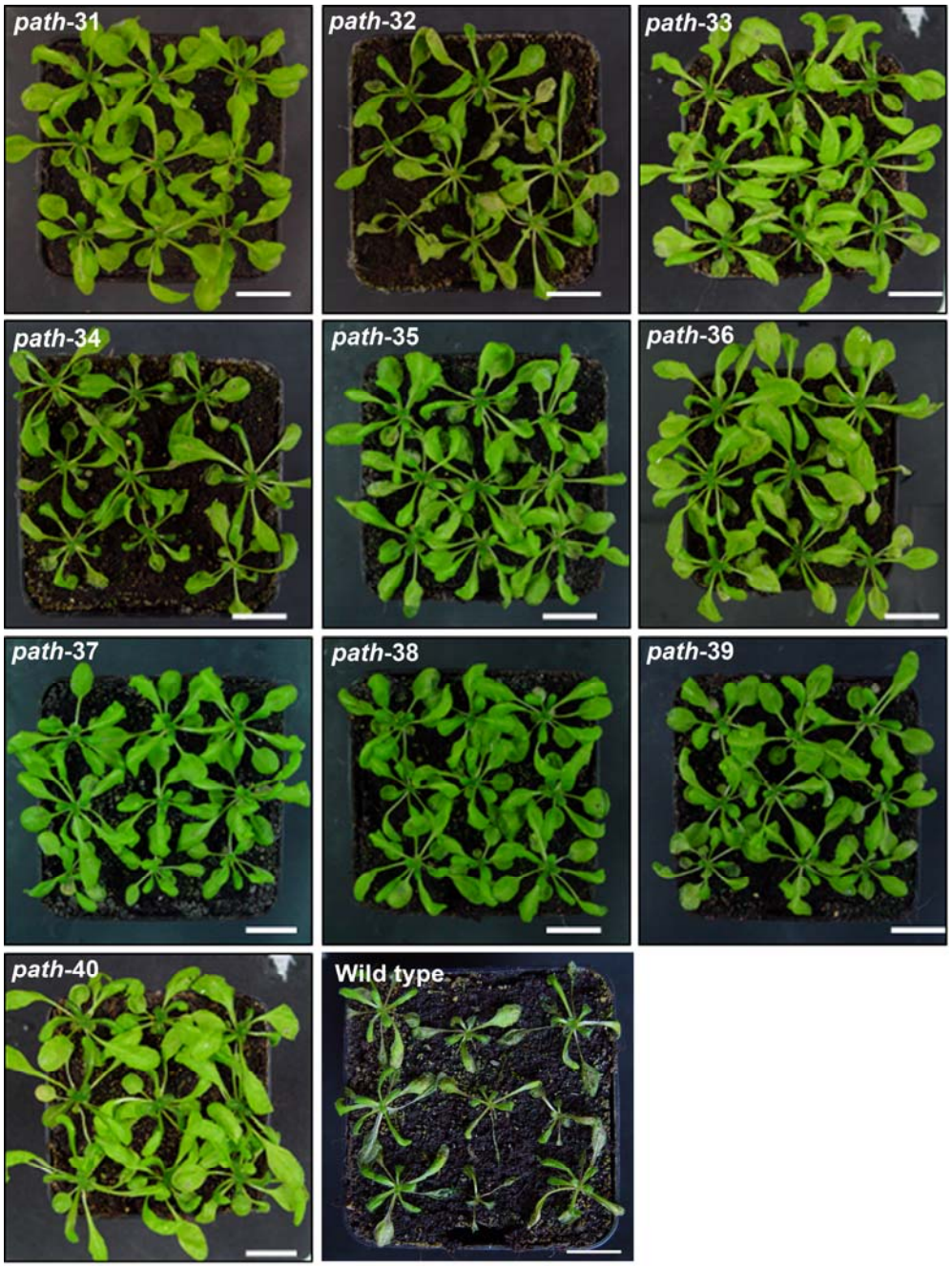

Supplementay Data 3. Symptoms of wild type *Colletotrichum higginsianum* and all 40 pathogenicity mutants.
Mature *Arabidopsis* Ler-0 plants (3- to 4-week-old) were spray-inoculated with transformant spore suspension (5×10^5 conidia ml^{-1}) and examined for symptoms 7 dai. The wild-type strain caused extensive necrosis and maceration; transformants producing limited necrotic lesions were considered reduced pathogenicity mutants; those causing no symptoms were considered non-pathogenic.

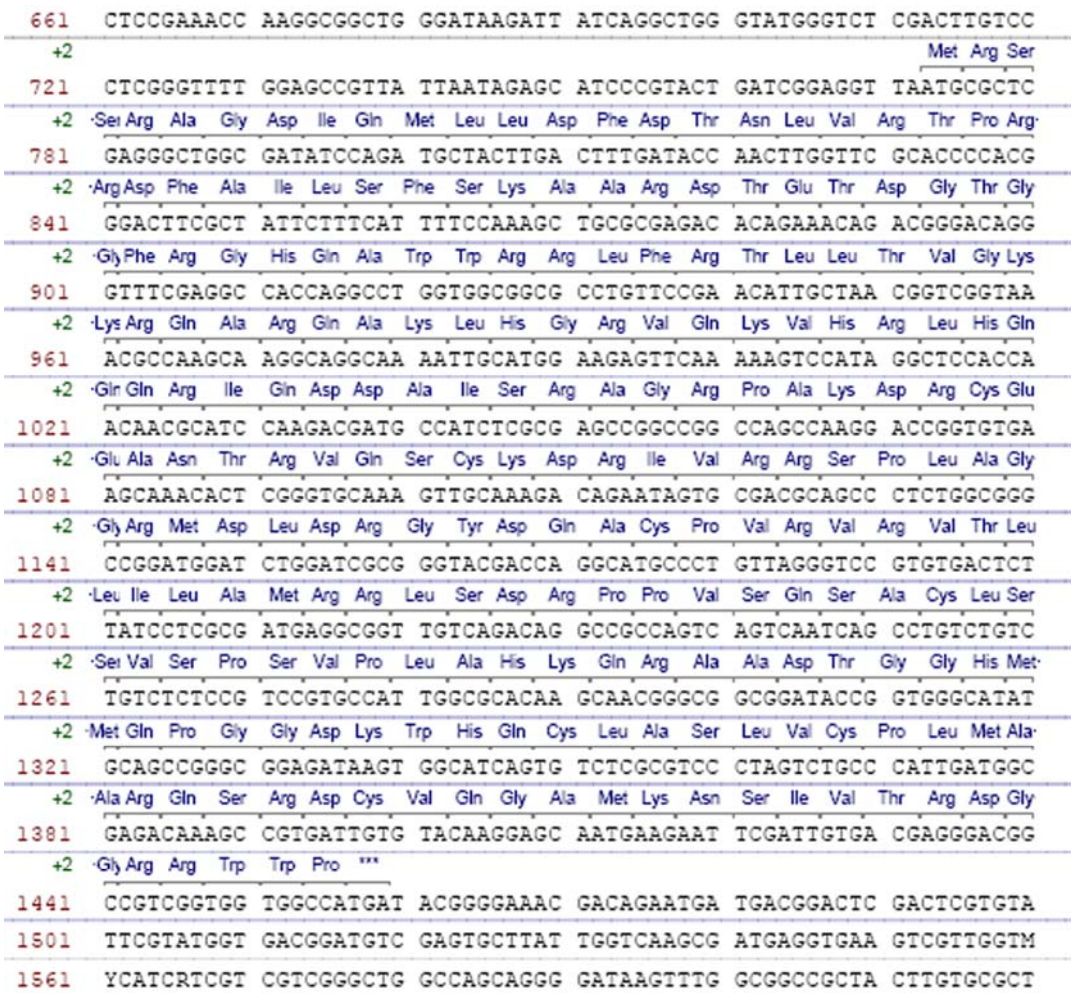

Supplementary Data 4. Genomic sequence and translation of predicted ORF tagged in *path*-5.
ORF prediction was performed by FGENEH+ and translation was performed by Vector NTI.

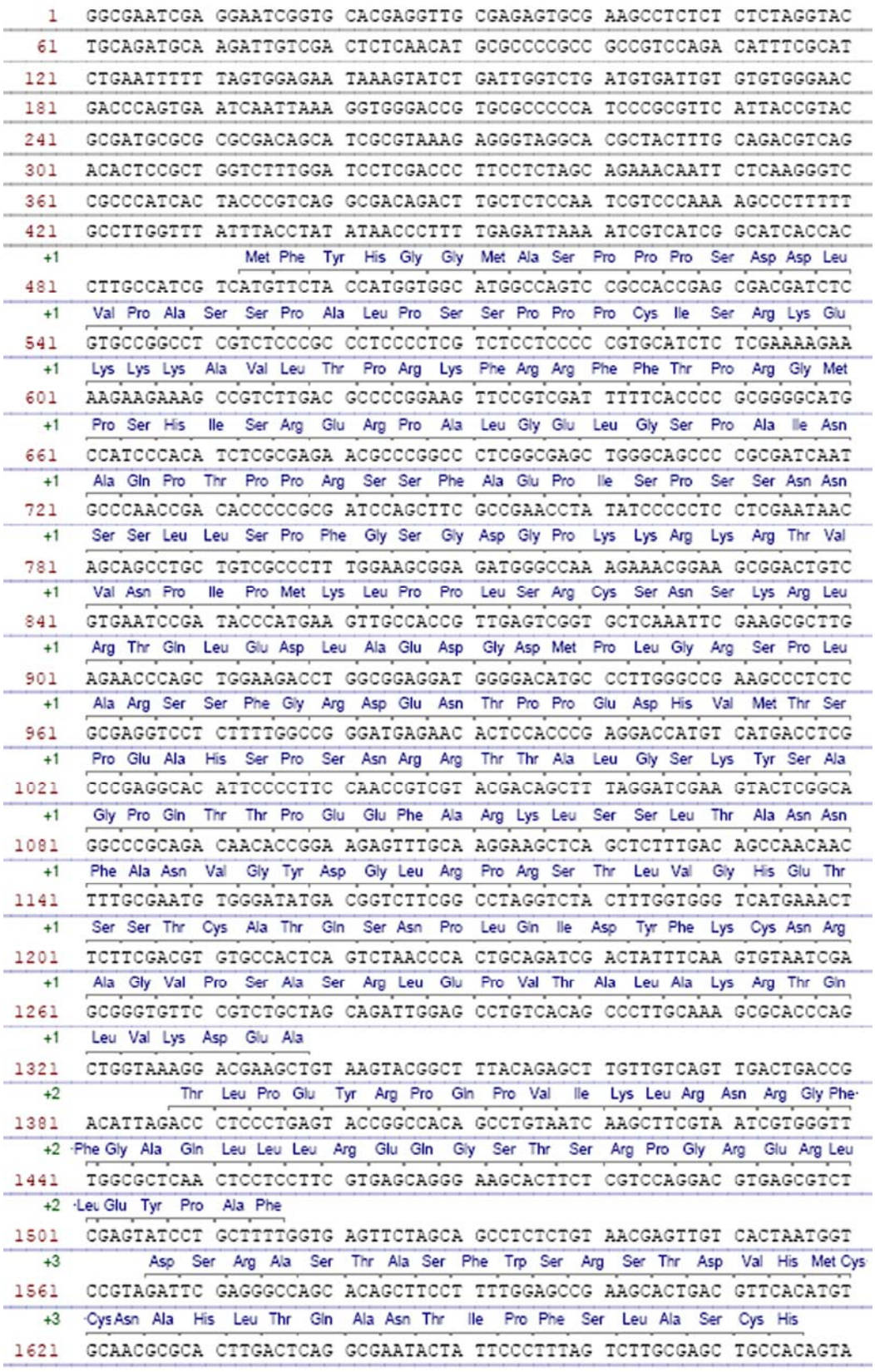

Supplementary Data 5. Genomic sequence and translation of predicted ORF (1) tagged in *path*-7

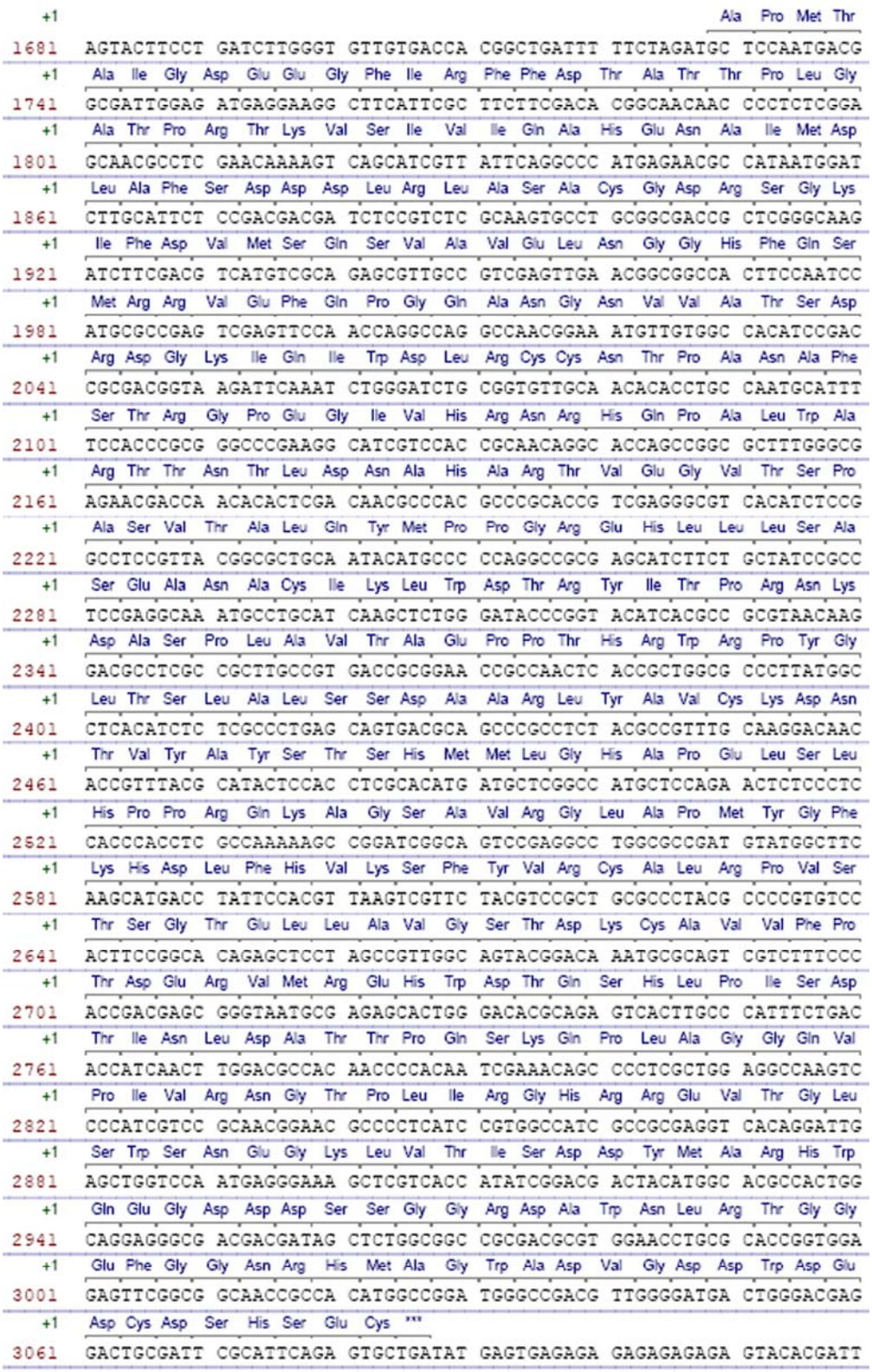

Supplementary Data 6 continued. Genomic sequence and translation of predicted ORF (1) tagged in *path*-7

ORF prediction was performed by FGENEH+ and translation was performed by Vector NTI.

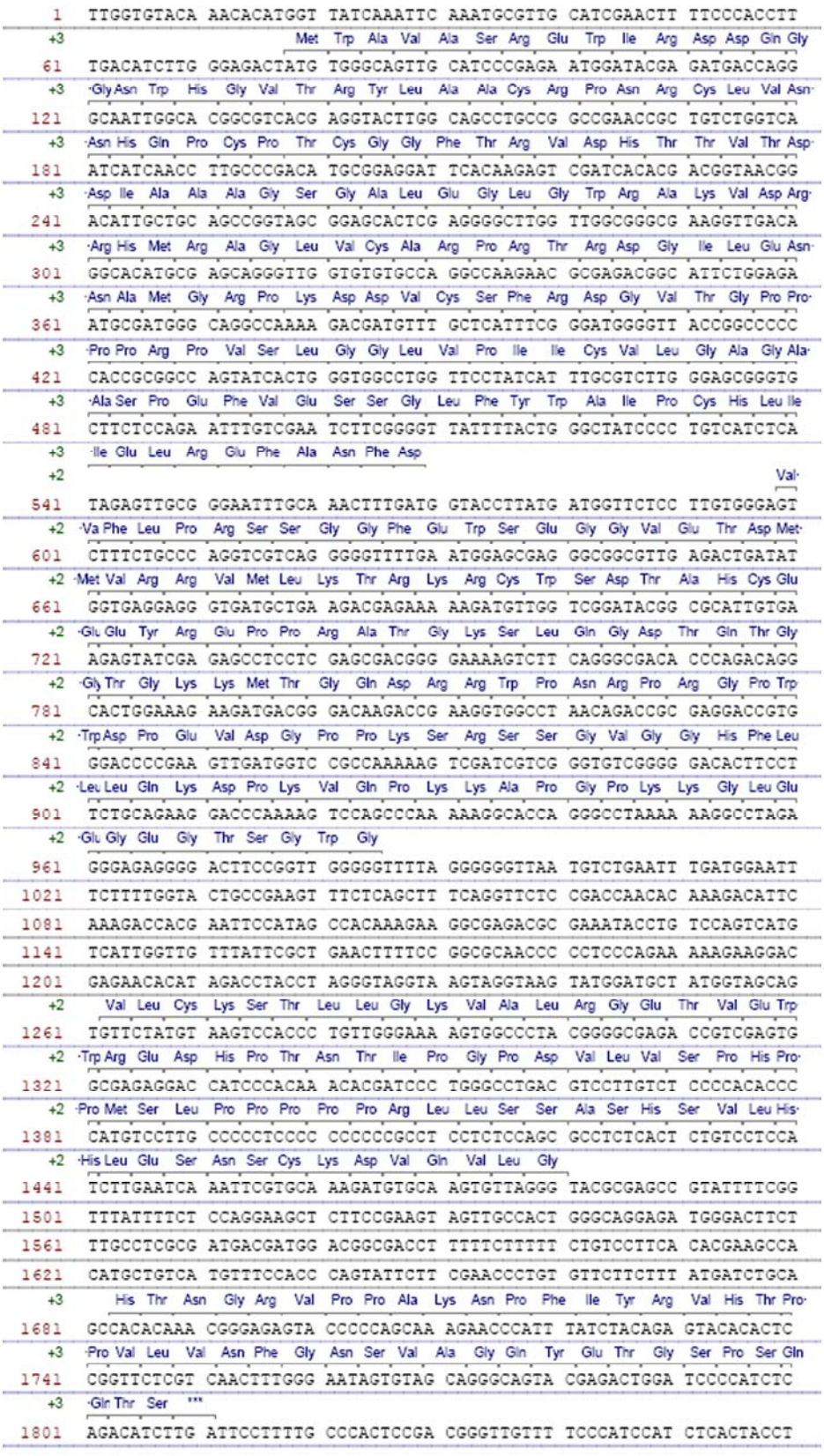

Supplementary Data 7. Genomic sequence and translation of predicted ORF (2) tagged in *path*- 7.
ORF prediction performed by FGENEH+ and translation performed by Vector NTI.

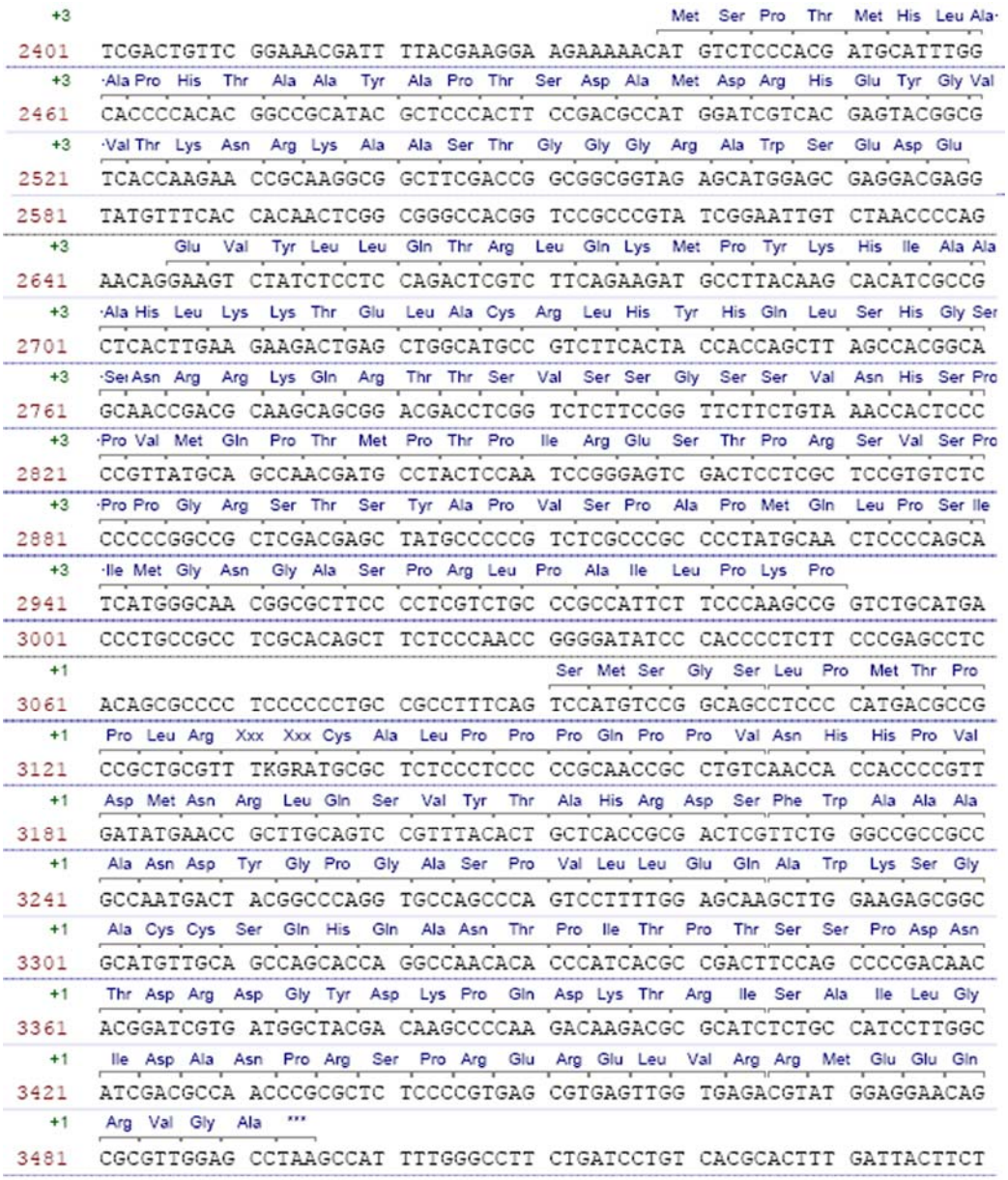

Supplementary Data 8. Genomic sequence and translation of predicted ORF tagged in *path*-8
ORF prediction was performed by FGENEH+ and translation was performed by Vector NTI.

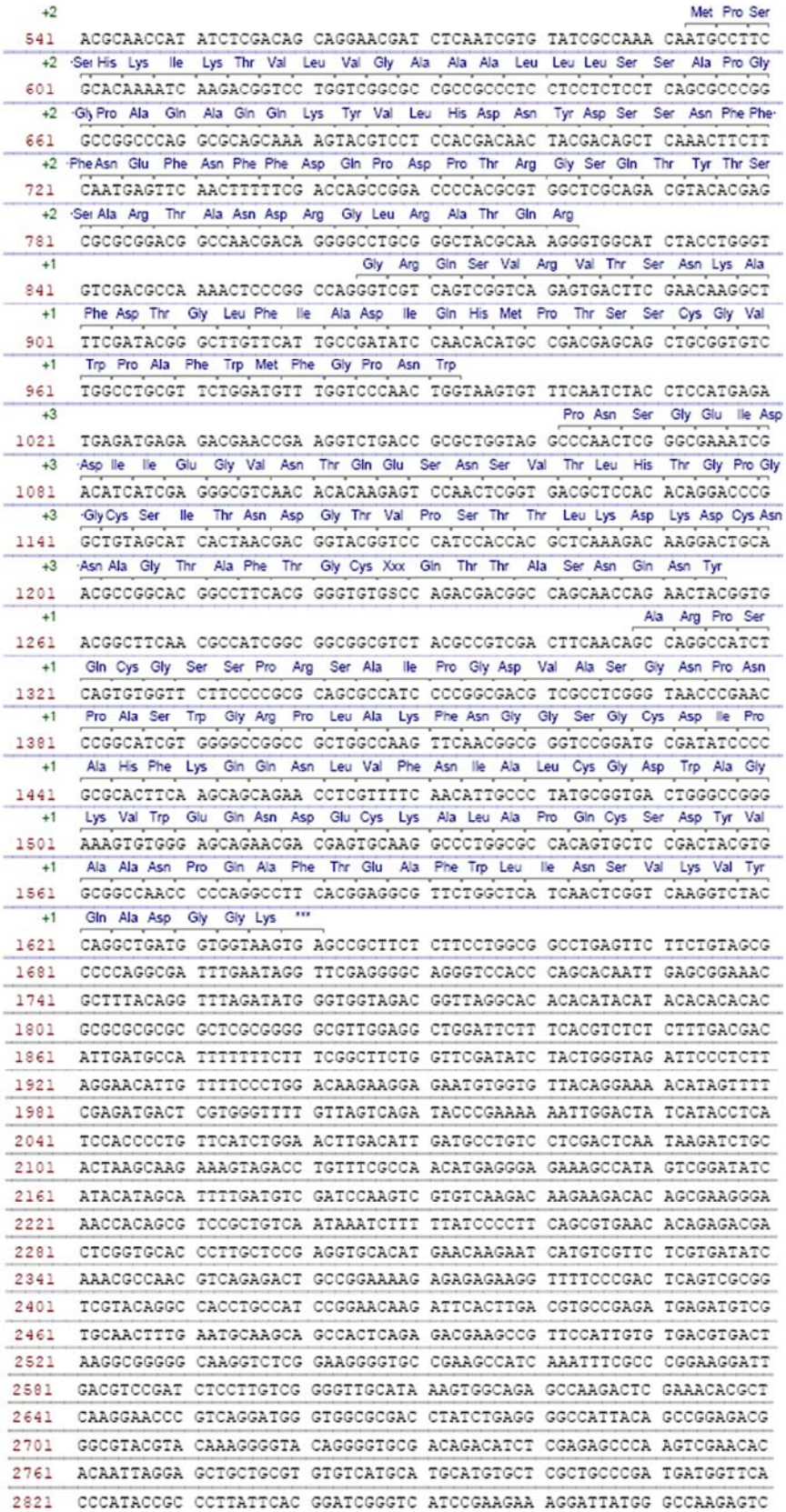

Supplementary Data 9. Genomic sequence and translation of predicted ORF encoding a putative glucanase tagged in *path*-9.

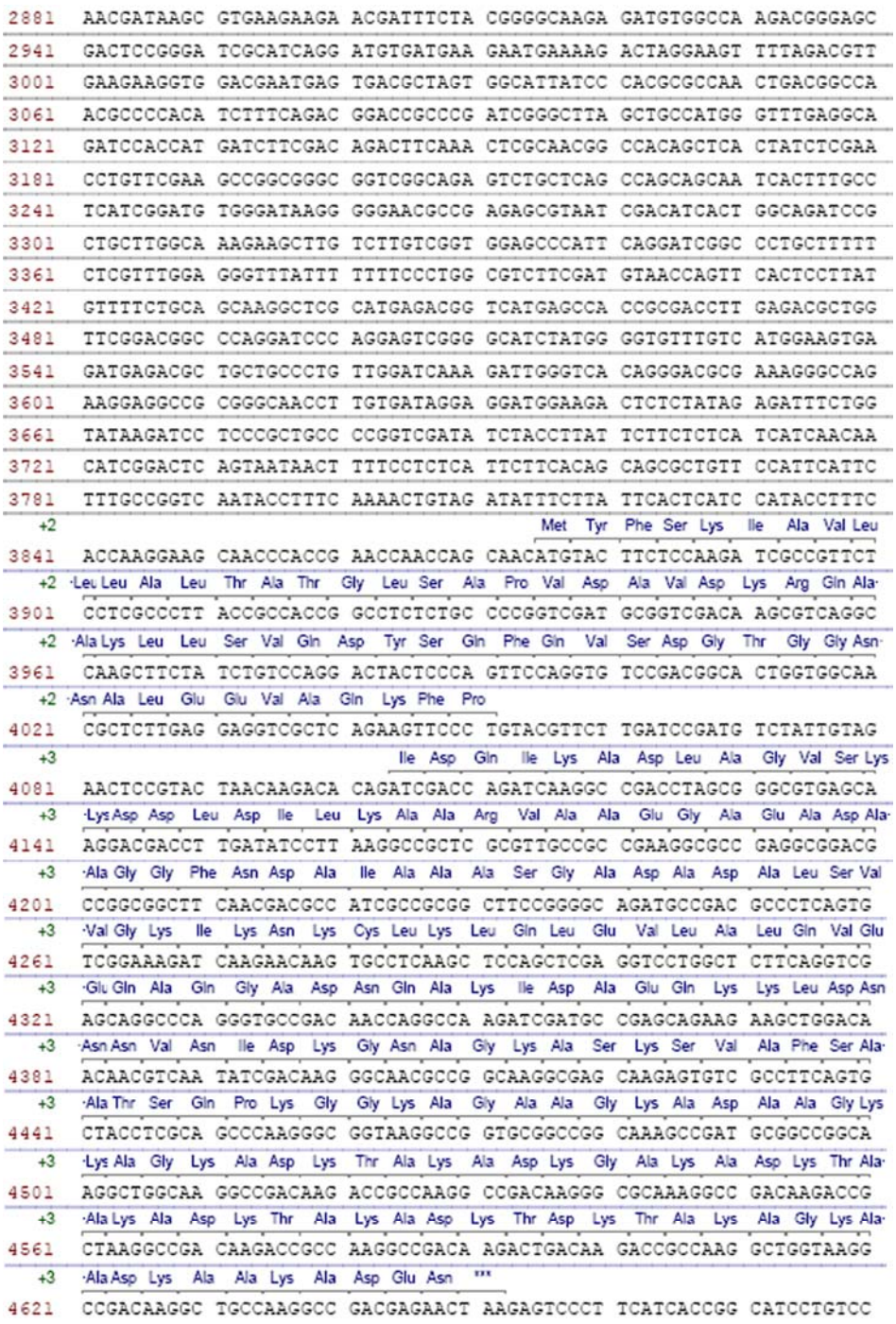

Supplementary Data 10. Genomic sequence and translation of predicted ORF encoding a putative glucanase tagged in *path*-9.
ORF prediction was performed by FGENEH+ and translation was performed by Vector NTI.

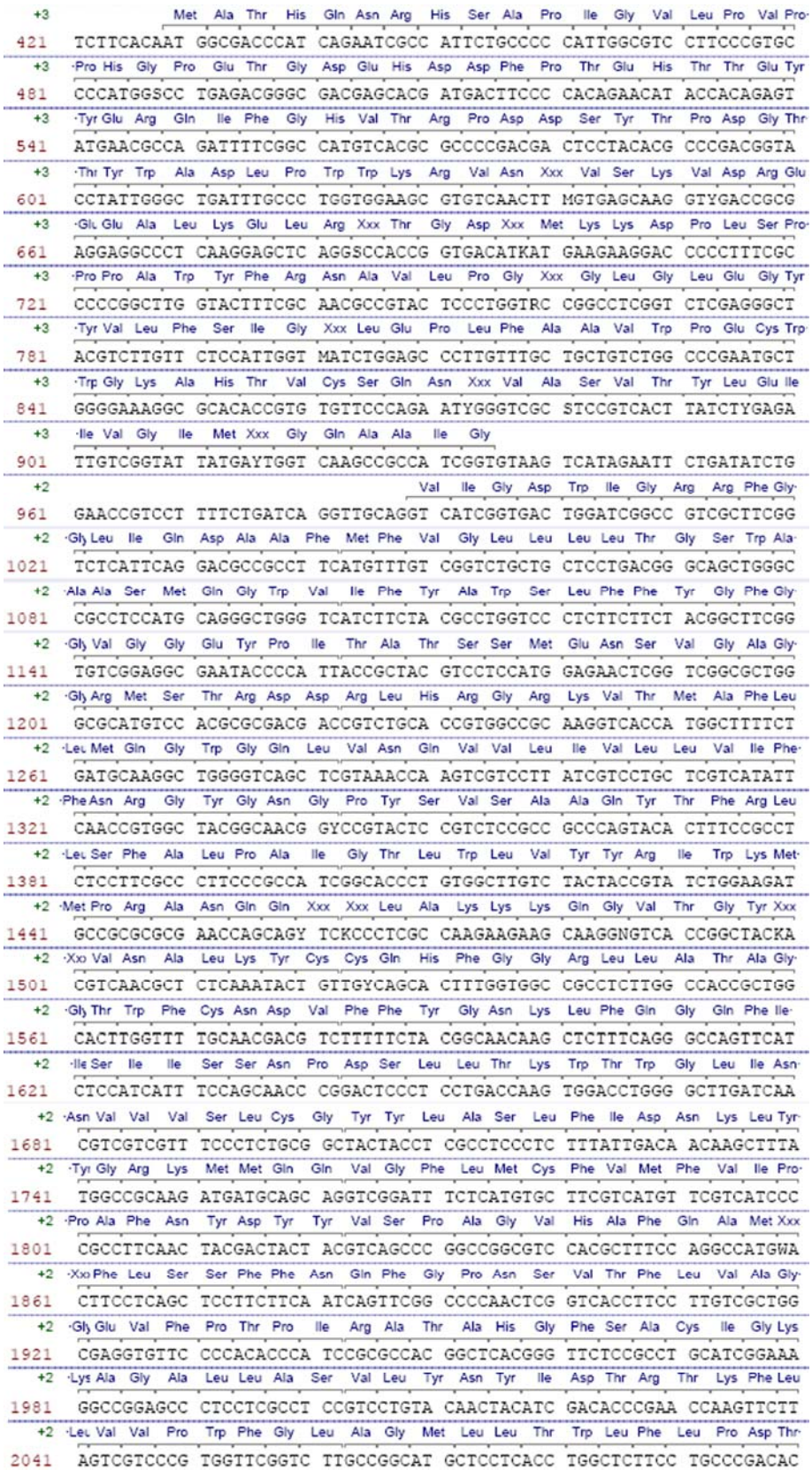

Supplementary Data 7. Genomic sequence and translation of predicted ORF encoding a hypothetical protein tagged in *path*-12.

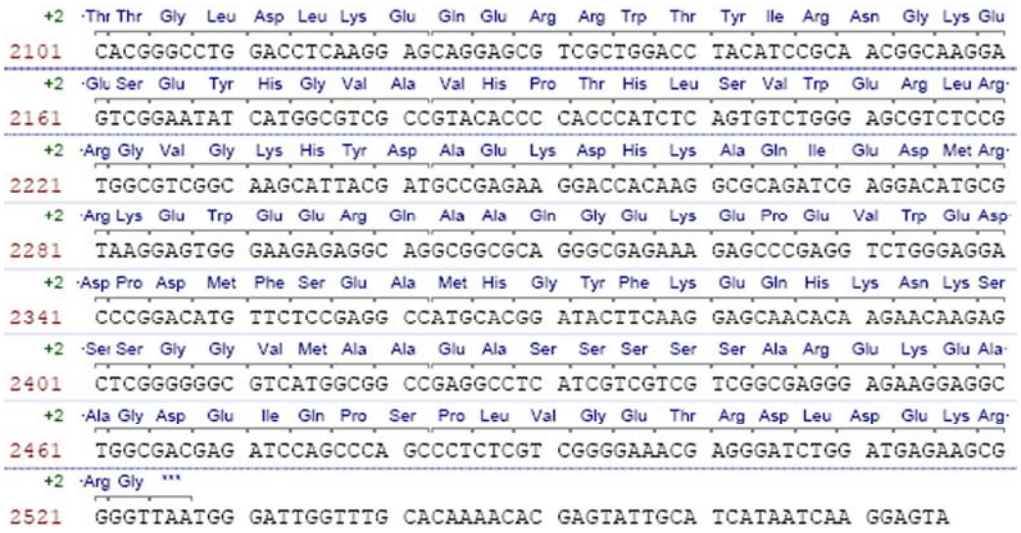

Supplementary Data 7 continued. Genomic sequence and translation of predicted ORF encoding a hypothetical protein tagged in *path*-12.
ORF prediction performed by FGENEH+ and translation performed by Vector NTI.

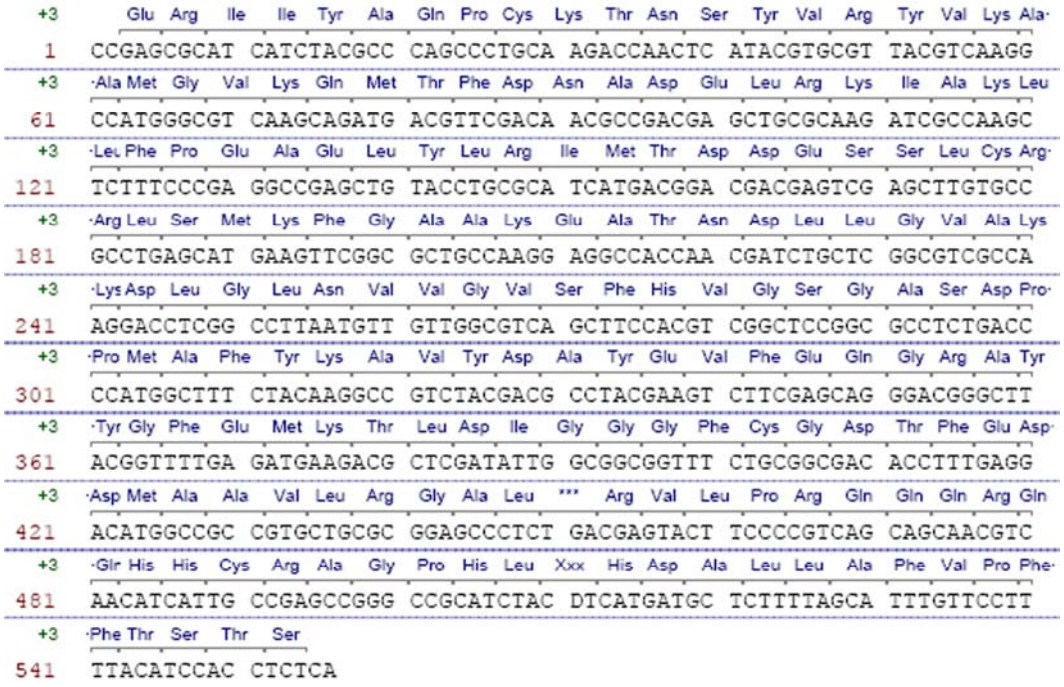

Supplementary Data 8. Genomic sequence and translation of predicted ORF encoding a hypothetical protein tagged in *path*-14.
ORF prediction was performed by FGENEH+ and translation was performed by Vector NTI.

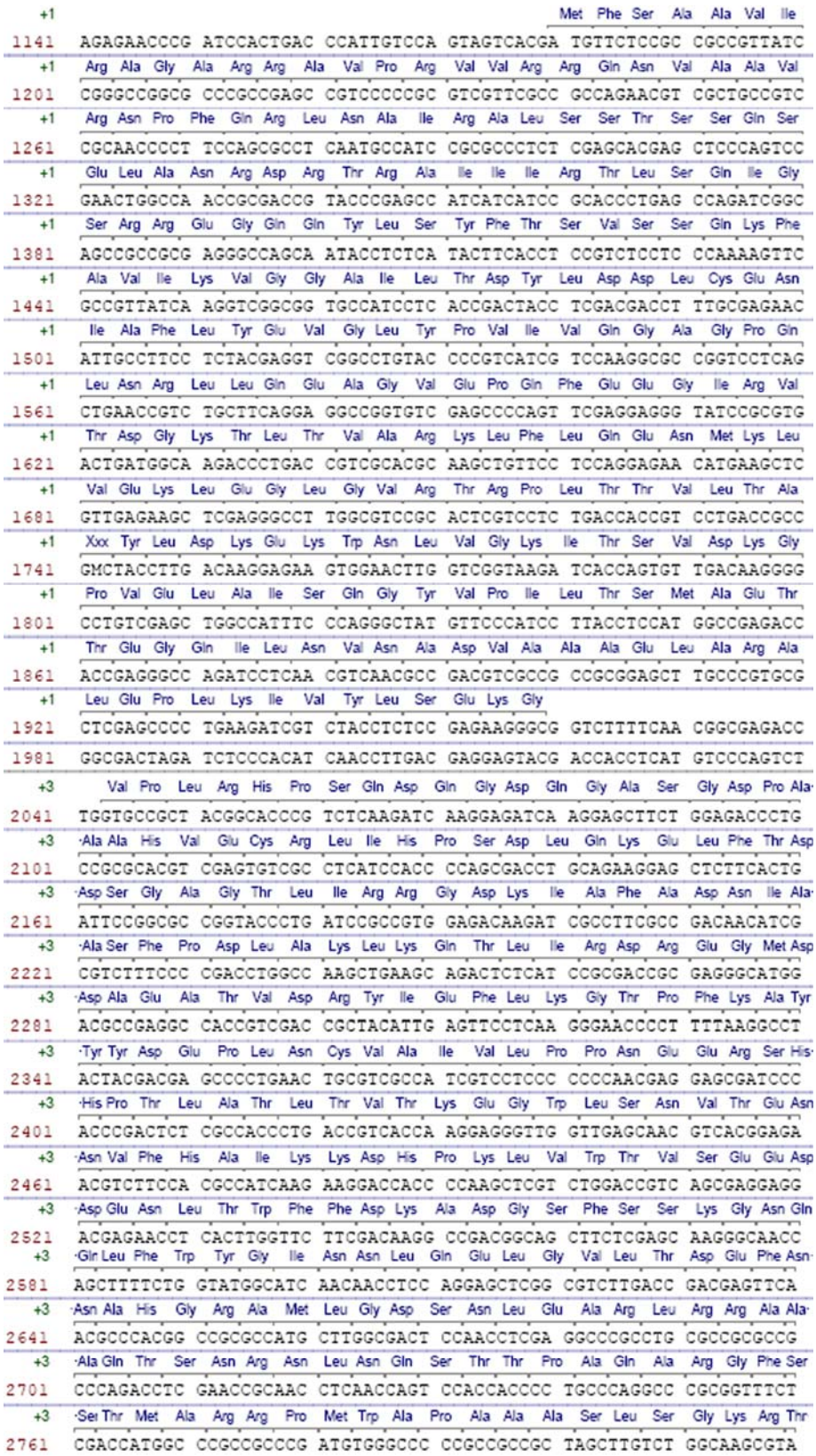

Supplementary Data 9. Genomic sequence and translation of predicted ORF tagged in *path*-19.

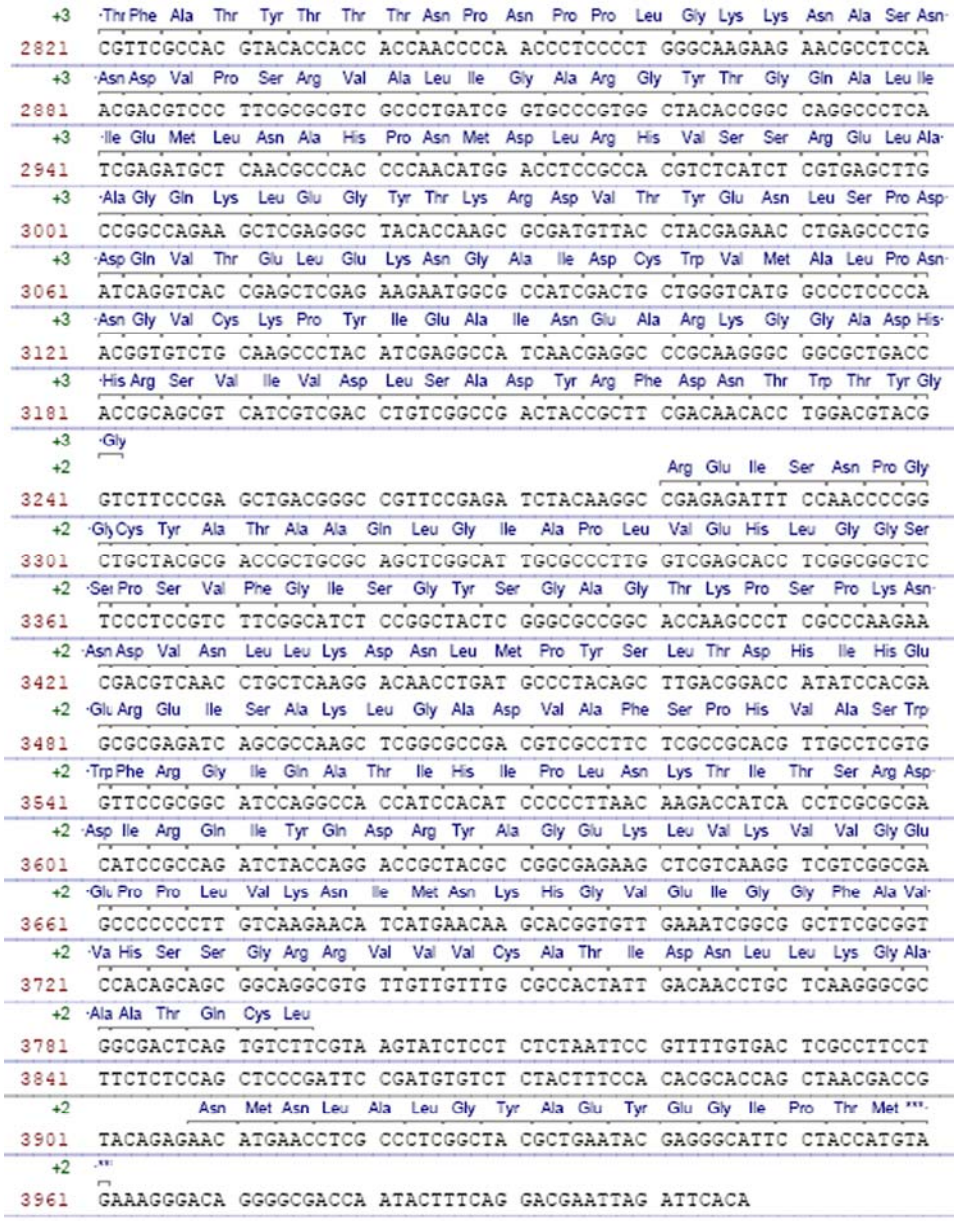

Supplementary Data 9. Genomic sequence and translation of predicted ORF tagged in *path*-19.
ORF prediction was performed by FGENEH+ and translation was performed by Vector NTI.

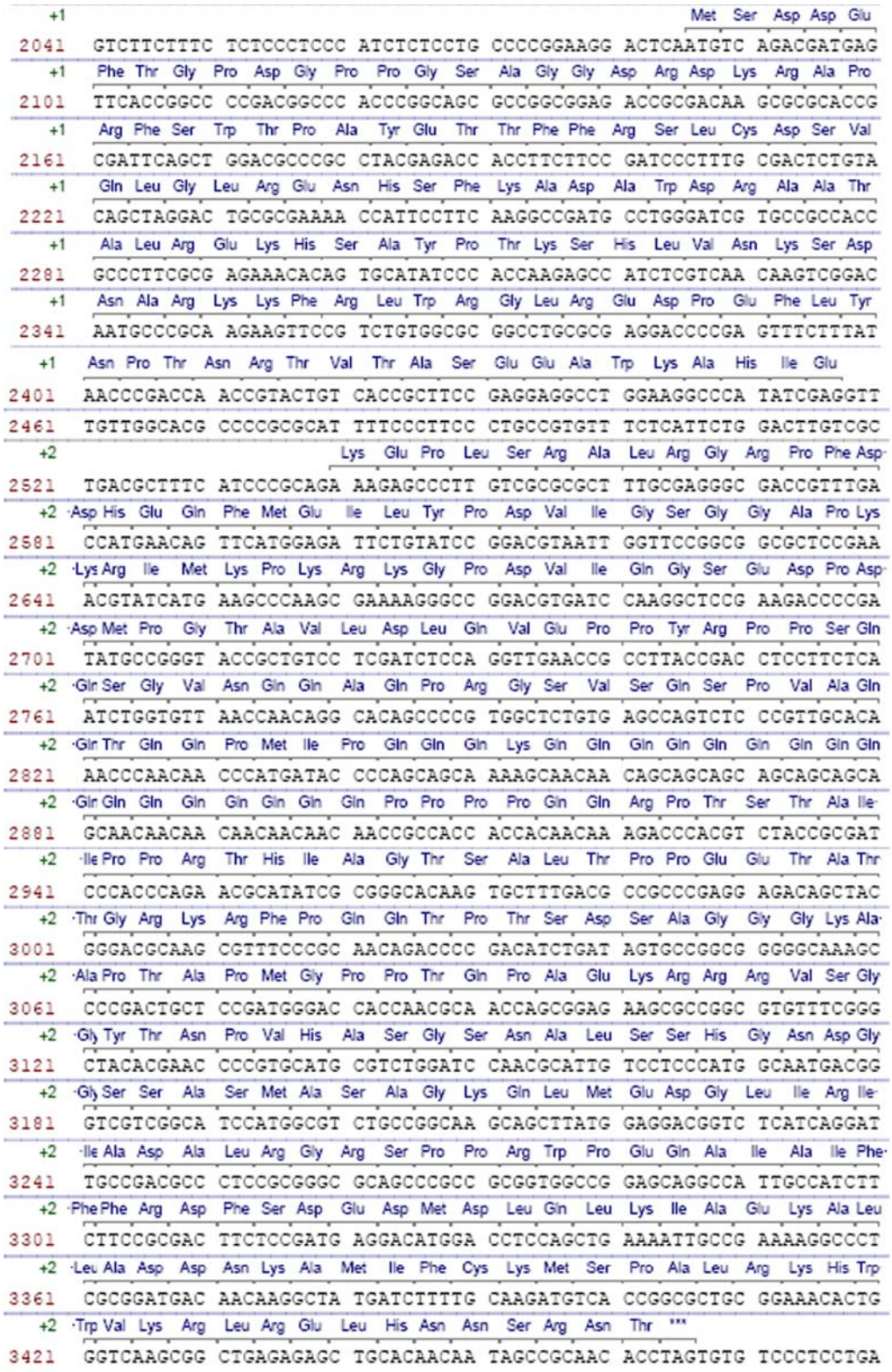

Supplementary Data 10. Genomic sequence and translation of predicted ORF encoding a hypothetical protein tagged in *path*-23.
ORF prediction was performed by FGENEH+ and translation was performed by Vector NTI.

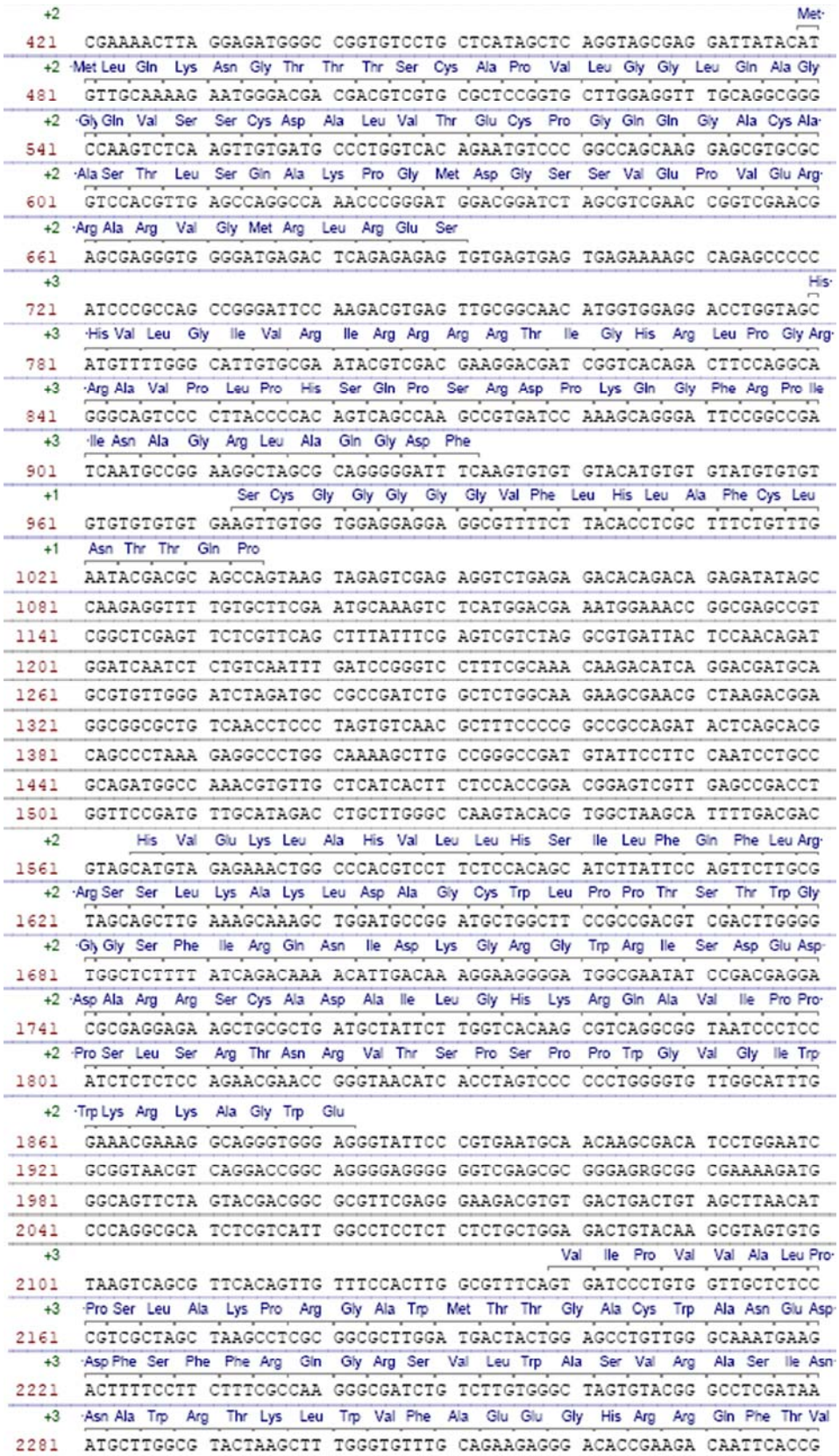

Supplementary Data 11. Genomic sequence and translation of predicted ORF encoding a putative protein with no homology tagged in *path*-23.

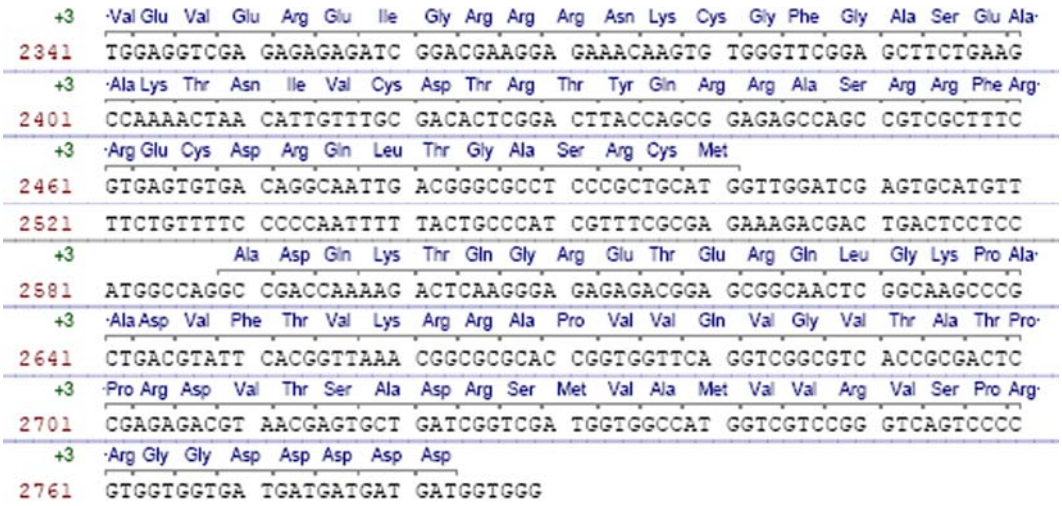

Supplementary Data 12 continued. Genomic sequence and translation of predicted ORF encoding a putative protein with no homology tagged in *path*-23.
ORF prediction performed by FGENEH+ and translation performed by Vector NTI.

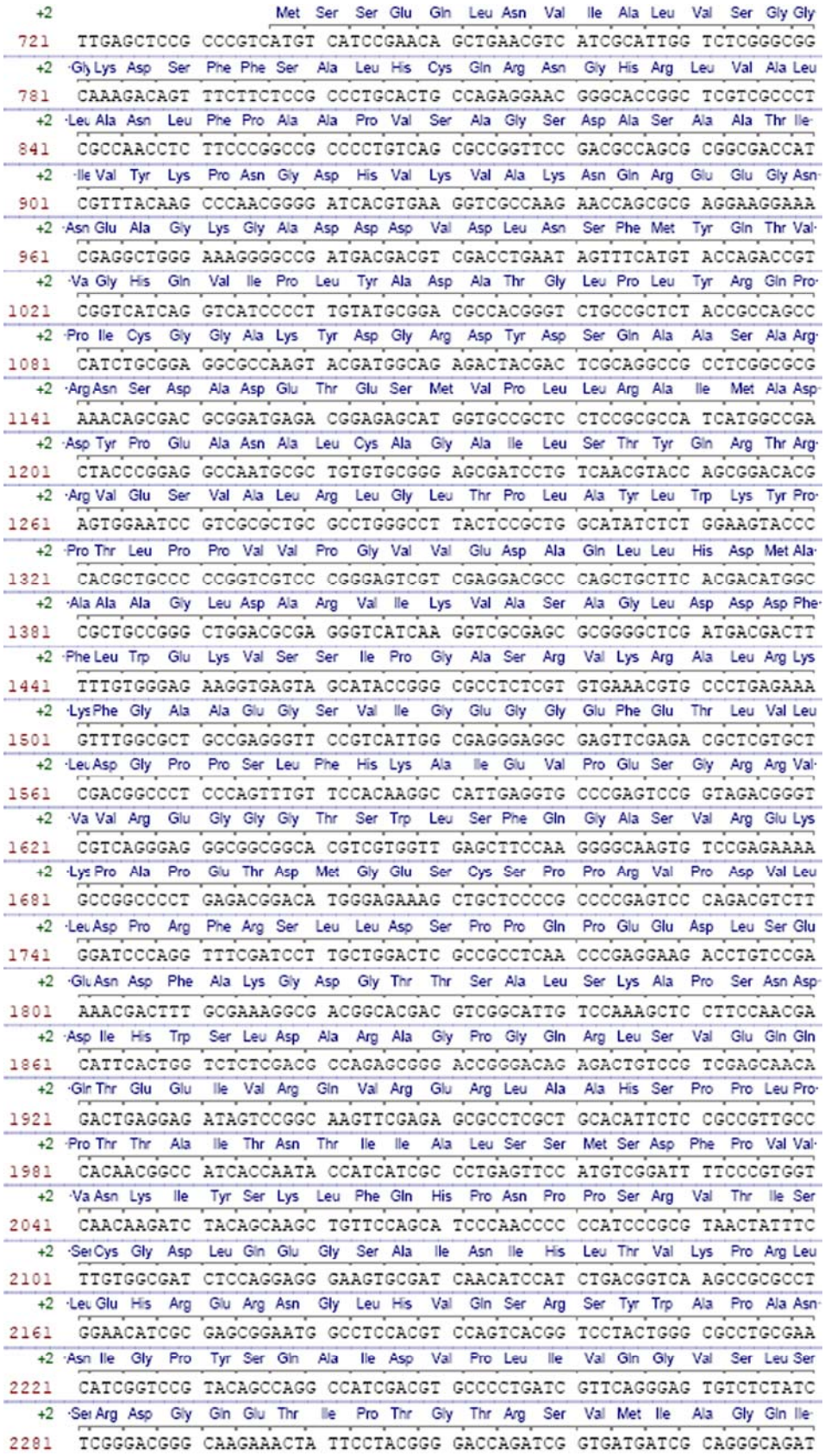

Supplementary Data 13. Genomic sequence and translation of predicted ORF tagged in *path*-29.

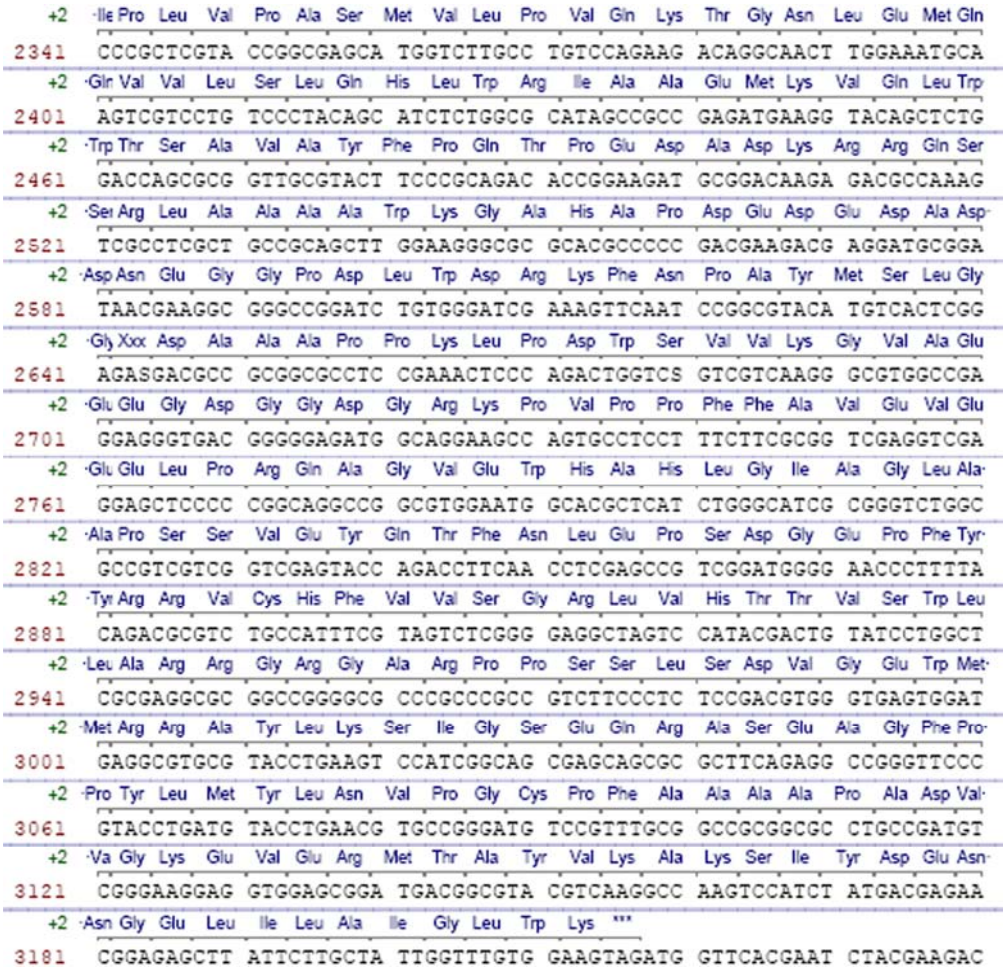

Supplementary Data 14 continued. Genomic sequence and translation of predicted ORF tagged in *path*-29.
ORF prediction was performed by FGENEH+ and translation was performed by Vector NTI.

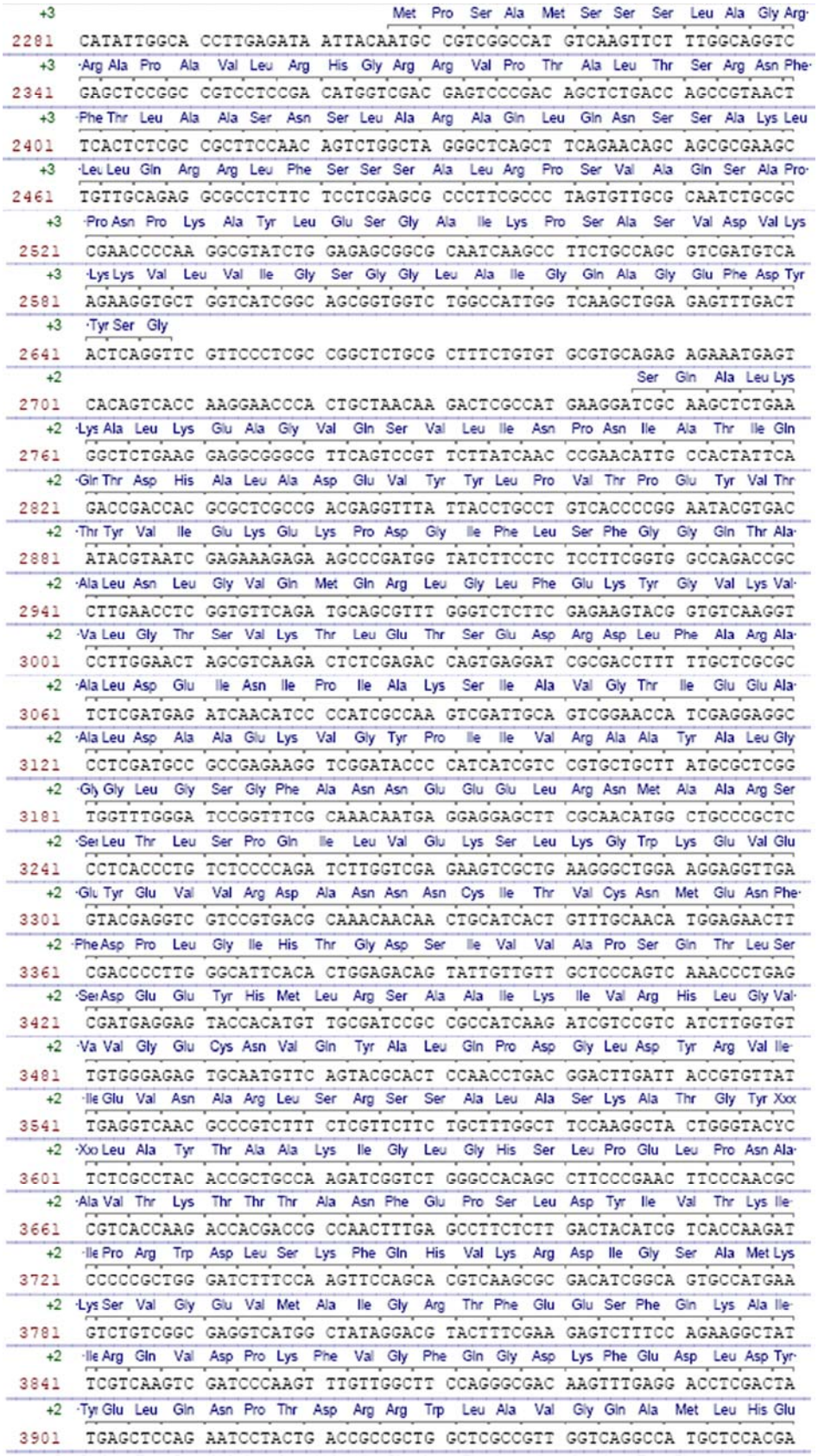

Supplementary Data 15. Genomic sequence and translation of predicted ORF tagged in *path*-35.

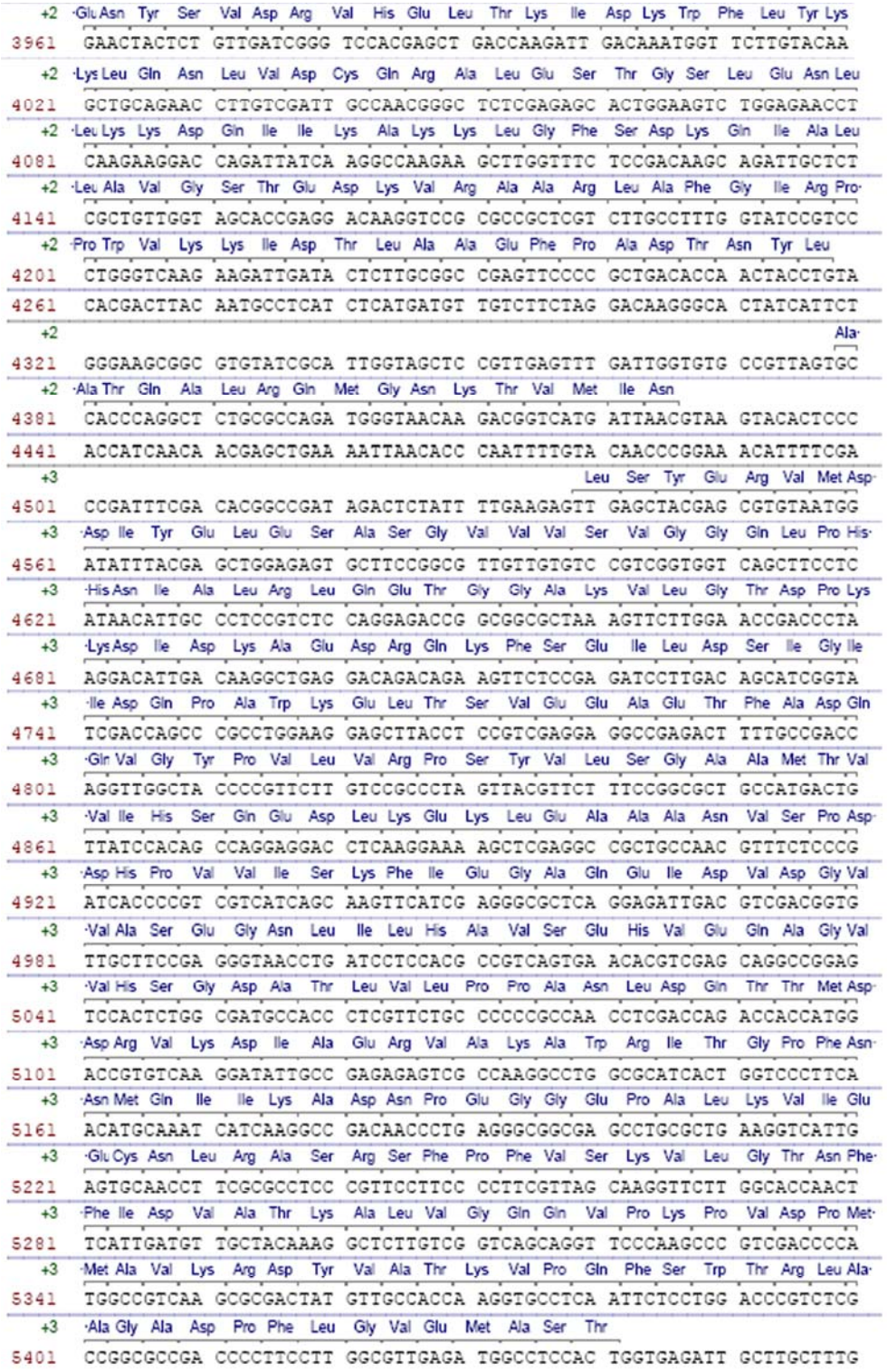

Supplementary Data 16 continued. Genomic sequence and translation of predicted ORF tagged in *path*-35.

ORF prediction was performed by FGENEH+ and translation was performed by Vector NTI.

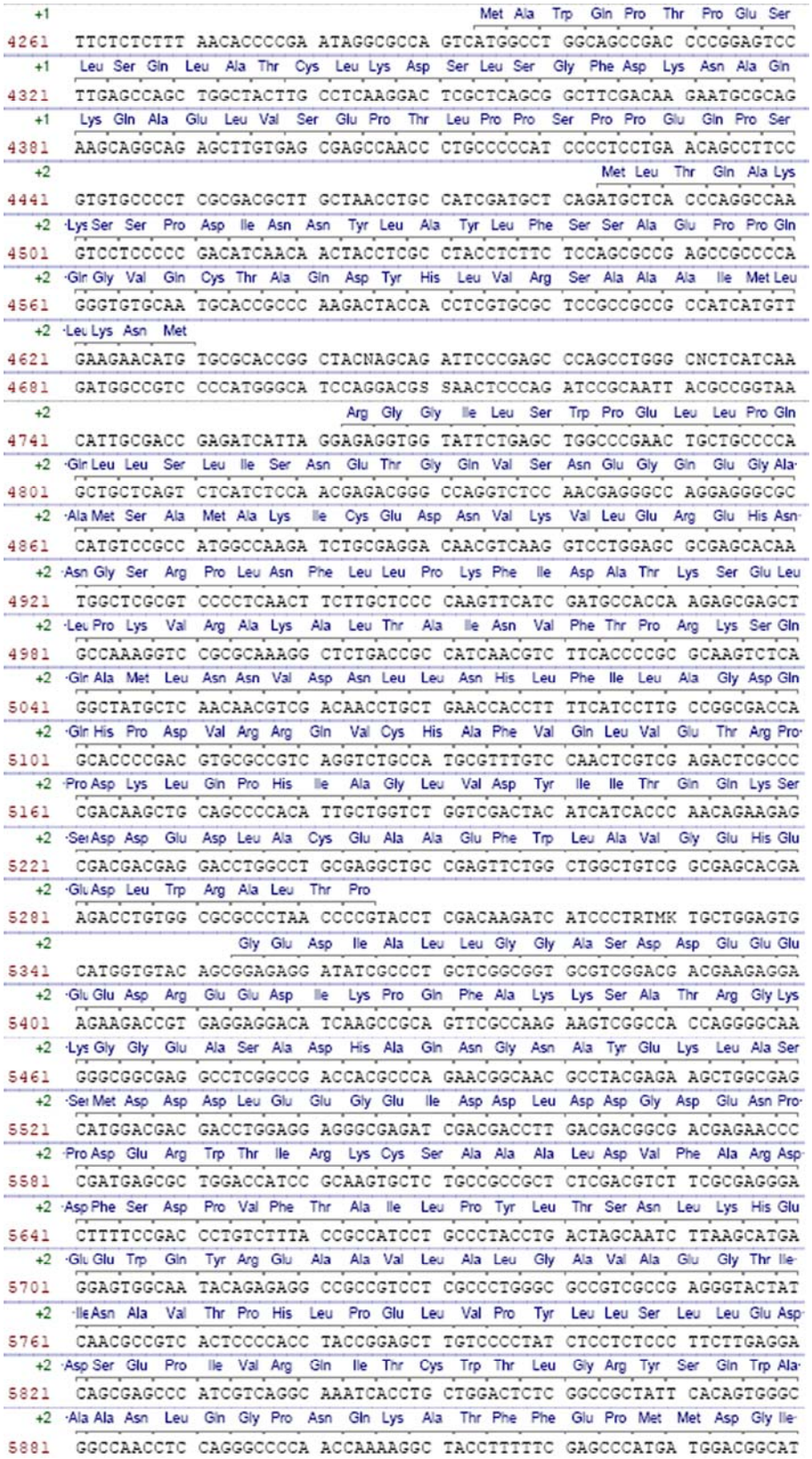

Supplementary Data 17. Genomic sequence and translation of predicted ORF tagged in *path*-36 and *path*-38.

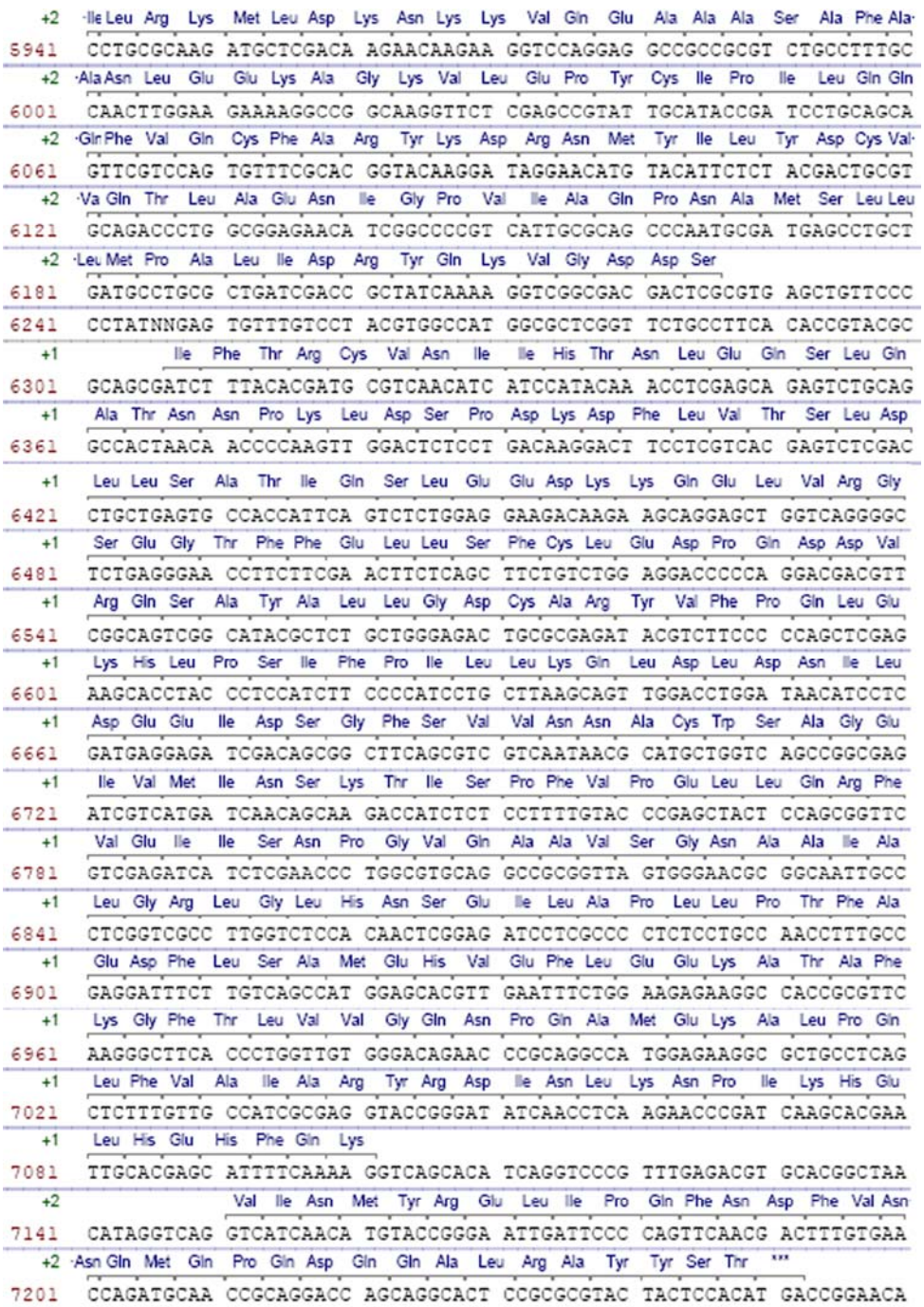

Supplementary Data 18 continued. Genomic sequence and translation of predicted ORF tagged in *path*-36 and *path*-38.
ORF prediction performed by FGENEH+ and translation performed by Vector NTI.

Supplementary Data 15. Blastx hits to predicted ORF (1) tagged in *path*-7

Organism	Annotation	Locus Accession	E-value
Gibberella zeae	hypothetical protein	FG06146.1	5e-117
Neurospora crassa	hypothetical protein	NCU03668	2e-101
Aspergillus clavatus	WD domain protein	ACLA_075000	1e-92
Aspergillus nidulans	hypothetical protein	AN2148.2	5e-92
Aspergillus fumigatus	WD repeat protein	AFUA_2G16030	1e-91
Neosartorya fischeri	WD domain protein	NFIA_091290	3e-91
Podospora anserina	unnamed protein product	PODANSg8135	7e-90
Aspergillus oryzae	unnamed protein product	AO090012000198	1e-88
Pyrenophora tritici-repentis	Lethal(2)denticleless protein	PTRG_05899	2e-87
Sclerotinia sclerotiorum	hypothetical protein	SS1G_03119	7e-87
Aspergillus niger	unnamed protein product	An15g06380	1e-86
Botryotinia fuckeliana	hypothetical protein	BC1G_07599	8e-86
Coccidioides immitis	hypothetical protein	CIMG_00323	8e-86
Magnaporthe grisea	hypothetical protein	MGG_08141	2e-84
Phaeosphaeria nodorum	hypothetical protein	SNOG_10282	7e-82
Chaetomium globosum	hypothetical protein	CHGG_02552	1e-79
Ajellomyces capsulatus	conserved hypothetical protein	HCAG_07281	9e-79
Exophiala dermatitidis	WD domain protein	ABZ91902.1	4e-59
Aspergillus terreus	conserved hypothetical protein	ATEG_02341	6e-43
Schizosaccharomyces pombe	WD repeat protein Cdt2	AAA85478.1	5e-23
Nasonia vitripennis	conserved hypothetical protein	LOC100118766	1e-21
Vitis vinifera	unnamed protein product	CAO14712.1	2e-20
Apis mellifera	similar to lethal-(2)-denticleless	LOC412472	4e-20
Nematostella vectensis	predicted protein	EDO44039.1	1e-19
Caenorhabditis elegans	protein T01C3.1	T01C3.1	5e-19
Ornithorhynchus anatinus	similar to denticleless (Drosophila)	LOC100078604	2e-18
Monodelphis domestica	similar to denticleless (Drosophila)	LOC100016445	2e-18
Drosophila melanogaster	lethal-(2)-denticleless	L2DTL_DROME	4e-18

Fungal sequences are in blue, animal sequences are in purple and plant sequences in green.

Supplementary Data 16: Blastx hits to predicted ORF (2) tagged in path-7

Organism	Annotation	Locus Accession	E-value
Gibberella zeae	hypothetical protein	FG06145.1	2e-24
Sclerotinia sclerotiorum	hypothetical protein	SS1G_03135	2e-20
Botryotinia fuckeliana	hypothetical protein	BC1G_07597	3e-20
Phaeosphaeria nodorum	hypothetical protein	SNOG_10381	3e-16
Magnaporthe grisea	hypothetical protein	MGG_08142	1e-14
Neurospora crassa	hypothetical protein	NCU03709	2e-13
Podospora anserina	hypothetical protein	PODANSg8142	2e-12
Pyrenophora tritici-repentis	conserved hypothetical protein	PTRG_09743	4e-12
Ajellomyces capsulatus	predicted protein	HCAG_06424	9e-04

Supplementary Data 17. Blastx hits to predicted ORF tagged in *path*-8

Organism	Annotation	Locus Accession	E-value
Magnaporthe grisea	hypothetical protein	MGG_01130	1e-80
[Gibberella zeae	hypothetical protein	FG02718.1	2e-80
Chaetomium globosum	hypothetical protein	CHGG_05369	2e-77
Podospora anserina	unnamed protein product	PODANSg2517	1e-55
Neurospora crassa	hypothetical protein	NCU05681	4e-42
Sclerotinia sclerotiorum	hypothetical protein	SS1G_02497	1e-35
Botryotinia fuckeliana	hypothetical protein	BC1G_04953	7e-35
Coccidioides immitis	hypothetical protein	CIMG_04581	1e-19
Pyrenophora tritici-repentis	conserved hypothetical protein	PTRG_10690	5e-18
Ajellomyces capsulatus	predicted protein	HCAG_04566	4e-17
Phaeosphaeria nodorum	hypothetical protein	SNOG_09796	5e-14

Supplementary Data 18. Blastx hits to predicted ORF downstream of T-DNA in *path*-9

Organism	Annotation	Locus Accession	E-value
Magnaporthe grisea	hypothetical protein	MGG_05716	2e-18
Neurospora crassa	hypothetical protein	NCU03294	7e-16
Podospora anserina	unnamed protein product	PODANSg09981	3e-15
Chaetomium globosum	hypothetical protein	CHGG_01564	3e-15
Botryotinia fuckeliana	hypothetical protein	BC1G_13158	2e-11
Phaeosphaeria nodorum	hypothetical protein	SNOG_13939	7e-10
Gibberella zeae	hypothetical protein	FG03454.1	9e-08
Pyrenophora tritici-repentis	hypothetical protein	PTRG_09091	3e-06
Botryotinia fuckeliana	hypothetical protein	BC1G_11080	4e-06
Magnaporthe grisea	hypothetical protein	MGG_08300	9e-05

Supplementary Data 19. Blastx hits to predicted ORF upstream of T-DNA in *path*-9

Organism	Annotation	Locus Accession	E-value
Gibberella zeae	hypothetical protein	FG06888.1	9e-85
Podospora anserina	unnamed protein product	PODANSg5926	2e-75
Botryotinia fuckeliana	hypothetical protein	BC1G_13847	8e-75
Chaetomium globosum	hypothetical protein	CHGG_00798	5e-73
Sclerotinia sclerotiorum	hypothetical protein	SS1G_13872	9e-71
Aspergillus oryzae	hypothetical protein	BAE57957.1	8e-63
Aspergillus clavatus	endo-1,3(4)-ß-glucanase, putative	ACLA_029360	4e-62
Pyrenophora tritici-repentis	mixed-linked glucanase precursor	PTRG_07078	7e-62
Aspergillus fumigatus	endo-1,3(4)-ß-glucanase, putative	EDP55864.1	5e-61
Aspergillus niger	hypothetical protein	An01g04560	8e-59
Neosartorya fischeri	endo-1,3(4)-ß-glucanase, putative	NFIA_019460	1e-58
Aspergillus nidulans	hypothetical protein	AN0245.2	1e-58
Botryotinia fuckeliana	hypothetical protein	BC1G_13534	7e-58
Cochliobolus carbonum	mixed-linked glucanase precursor	AAC49904.1	5e-55
Ajellomyces capsulatus	predicted protein	HCAG_04806	3e-53
Coccidioides immitis	hypothetical protein	CIMG_06566	9e-53
Aspergillus fumigatus	GPI anchored endo-1,3(4)-ß glucanase, putative	AFUA_2G14360	4e-52
Gibberella zeae	hypothetical protein	FG09755.1	1e-51
Phaeosphaeria nodorum	hypothetical protein	SNOG_04451	2e-51
Neosartorya fischeri	GPI anchored endo-1,3(4)-ß glucanase, putative	NFIA_089530	6e-51
Magnaporthe grisea	hypothetical protein	MGG_11652	8e-51
Coccidioides immitis	hypothetical protein	CIMG_04844	1e-50
Aspergillus clavatus	GPI anchored endo-1,3(4)-ß glucanase, putative	ACLA_073210	3e-49
Aspergillus niger	hypothetical protein	An02g00850	2e-48
Aspergillus oryzae	hypothetical protein	AO090023000083	2e-46
Phaeosphaeria nodorum	hypothetical protein	SNOG_00968	4e-46
Schizosaccharomyces pombe	glycosyl hydrolase family 16	SPBC21B10.07	4e-45
Pyrenophora tritici-repentis	1,3(4)-ß-glucanase	PTRG_07961	1e-44
Rhizopus oryzae	1,3(4)-ß-glucanase	AAQ20798.1	4e-44
Phaeosphaeria nodorum	hypothetical protein	SNOG_12175	5e-44
Pyrenophora tritici-repentis	mixed-linked glucanase precursor	PTRG_03370	1e-43
Aspergillus terreus	conserved hypothetical protein	ATEG_02561	2e-42
Cryptococcus neoformans	endo-1,3(4)-ß-glucanase, putative	CNC04770	2e-41
Botryotinia fuckeliana	hypothetical protein	BC1G_09991	3e-41
Coprinopsis cinerea	hypothetical protein	CC1G_01665	4e-41
Gibberella zeae	hypothetical protein	FG07772.1	6e-41
Phaffia rhodozyma	endo-1,3(4)-ß-glucanase	AAC17104.1	2e-40
Aspergillus clavatus	endo-1,3(4)-ß-glucanase, putative	ACLA_002970	2e-39
Phanerochaete chrysosporium	putative laminarinase	BAC67687.1	5e-39
Laccaria bicolor	glycoside hydrolase family 16	EDR14587.1	6e-39
Magnaporthe grisea	hypothetical protein	MGG_07473	3e-38
Chaetomium globosum	hypothetical protein	CHGG_00648	4e-38
Sclerotinia sclerotiorum	hypothetical protein	SS1G_06401	1e-37

Supplementary Data 20. Blastx hit to predicted ORF tagged in *path*-12

Organism	Annotation	Locus Accession	E-value
Chaetomium globosum	hypothetical protein	CHGG_05982	0.0
Giberella zeae	hypothetical protein	FG01311.1	0.0
Magnaporthe grisea	hypothetical protein	MGG_00346	0.0
Neosartorya fischeri	MFS phosphate transporter, putative	NFIA_086030	0.0
Aspergillus fumigatus	MFS phosphate transporter, putative	EAL933643.1	0.0
Aspergillus oryzae	MFS permease	AO090011000572	0.0
Aspergillus niger	hypothetical protein	An02g02480	0.0
Aspergillus clavatus	MFS phosphate transporter, putative	ACLA_069680	0.0
Aspergillus nidulans	hypothetical protein	AN5935.2	0.0
Coccidioides immitis	hypothetical protein	CIMG_08126	0.0
Botryotinia fuckeliana	hypothetical protein	BC1G_08011	0.0
Sclerotinia sclerotiorum	hypothetical protein	SS1G_01696	0.0
Pyrenophora tritici-repentis	phosphate transporter HvPT2	EDU50500.1	0.0
Ustilago maydis	hypothetical protein	UM05260.1	1e-159
Cryptococcus neoformans	Pi-transporter A-1	CNH01210	2e-158
Aspergillus terreus	hypothetical protein	ATEG_01506	9e-98
Ajellomyces capsulatus	predicted protein	HCAG_07189	3e-90
Phaeosphaeria nodorum	hypothetical protein	SNOG_04294	1e-67
Oryza sativa	high affinity phosphate transporter 2	AAQ01157.1	1e-29
Hordeum vulgare	phosphate transporter HvPT2	AAO72433.1	1e-29
Hordeum vulgare	phosphate transporter 1	AAN37900.1	1e-29
Triticum aestivum	phosphate transporter 8	AAP49822.1	2e-29
Capsicum frutescens	phosphate transporter PT3	ABK63962.1	1e-28
Nicotiana tabacum	phosphate transporter PT3	ABK63964.2	1e-28
Hordeum vulgare	putative phosphate transporter HvPT7	AAO63133.1	3e-28
Arabidopsis thaliana	PHT6 (phosphate transporter 6)	BAA97413.1	3e-28
Arabidopsis thaliana	AtPht1;2 (H(+)/Pi cotransporter)	BAA97416.1	4e-28
Lupinus albus	phosphate transporter 2	AF305624_1	6e-28
Solanum melongena	phosphate transporter PT3	ABK63963.1	7e-28
Cryptococcus neoformans	phosphate transporter, putative	CNC03960	7e-28
Yarrowia lipolytica	hypothetical protein	YALI0D08382g	2e-27
Oryzae sativa	putative phosphate transporter OsPT12	AAN39053.1	3e-27
Solanum lycopersicum	phosphate transporter 3	AAV97729.1	4e-27
Zea mays	phosphate transport protein	AAT51690.1	6e-27
Triticum monococcum	putative phosphate transporter	|AAQ06280.1	6e-27
Zea mays	inorganic phosphate transporter 4	AAY42388.1	6e-27
Arabidopsis thaliana	inorganic phosphate transporter PHT3	BAA97415.1	6e-27
Zea mays	inorganic phosphate transporter 2	AAY42386.1	8e-27
Oryzae sativa	putative phosphate transporter OsPT3	AAN39044.1	1e-26
Hordeum vulgare	phosphate transporter HvPT4	AAO72438.1	2e-26
Zea mays	inorganic phosphate transporter 1	AAY42385.1	2e-26
Ustilago maydis	hypothetical protein	UM06490.1	8e-26
Arabidopsis thaliana	PHT5 (phosphate transporter 5)	BAA24280.1	2e-25
Aspergillus niger	hypothetical protein	An16g06190	1e-25
Arabidopsis thaliana	AtPht1;7 (H(+)/Pi cotransporter)	CAB77590.1	2e-25
Sclerotina sclerotium	hypothetical protein	SS1G_09313	4e-25
Sclerotina sclerotium	hypothetical protein	SS1G_11184	1e-24
Botryotinia fuckeliana	hypothetical protein	BC1G_08663	3e-24
Gibberella zeae	hypothetical protein	FG07894.1	5e-24
Saccharomyces cerevisae	Inorganic phosphate transporter PHO84	CAA89157.1	2e-21
Botryotinia fuckeliana	hypothetical protein	BC1G_04126	1e-19
Magnaporthe grisea	hypothetical protein	MGG_03299	2e-19
Neosartorya fischeri	phosphate:H+ symporter	NFIA_029820	2e-19

Fungal sequences are in blue and plant sequences are in green.

Supplementary Data 21. Blastx hits to sequence flanking T-DNA insertion in *path*-16.

Organism	Annotation	Locus Accession	E-value
Glomerella lindemuthianum	ornithine decarboxylase	AAT99013.1	2e-82
Gibberella zeae	hypothetical protein	FG05903.1	3e-66
Epichloe festucae	ornithine decarboxylase	ABM55741.1	9e-66
Metarhizium anisopliae	Ornithine Decarboxylase	AAQ91788.1	1e-64
Magnaporthe grisea	ornithine decarboxylase	MGG_02441	2e-62
Fusarium solani	ornithine decarboxylase	ABC47117.1	3e-62
Podospora anserina	unnamed protein product	ODANSg8052	3e-62
Neurospora crassa	ornithine decarboxylase	NCU01271	6e-62
Chaetomium globosum	hypothetical protein	CHGG_02594	8e-61
Botryotinia fuckeliana	hypothetical protein	BC1G_01799	5e-57
Sclerotinia sclerotiorum	hypothetical protein	SS1G_12207	2e-56
Tapesia yallundae	ornithine decarboxylase	AAK38838.1	5e-54
Prunus persica	ornithine decarboxylase	BAD97830.1	8e-53
Pyrenophora tritici-repentis	ornithine decarboxylase	PTRG_02854	7e-52
Phaeosphaeria nodorum	ornithine decarboxylase	SNOG_03643	3e-51
Aspergillus oryzae	ornithine decarboxylase	AO090023000771	3e-51
Coccidioides immitis	ornithine decarboxylase	CIMG_08778	4e-51
Aspergillus terreus	ornithine decarboxylase	ATEG_05404	4e-51
Neosartorya fischeri	ornithine decarboxylase	NFIA_108190	2e-50
Aspergillus fumigatus	ornithine decarboxylase	AFUA_4G08010	2e-50
Paracoccidioides brasiliensis	ornithine decarboxylase	AF212867_1	3e-50
Ajellomyces capsulatus	ornithine decarboxylase	HCAG_06269	3e-50
Yarrowia lipolytica	ornithine decarboxylase (YlODC)	CAG83002.1|	3e-49
Aspergillus nidulans	hypothetical protein	AN3846.2	6e-49
Aspergillus niger	hypothetical protein	CAL00729.1	3e-48
Aspergillus clavatus	ornithine decarboxylase	ACLA_047370	1e-47
Coccidioides immitis	ornithine decarboxylase	AF179245_1	2e-47
Schizosaccharomyces pombe	ornithine decarboxylase Spe1	CAB59684.1|	9e-41
Cryptococcus neoformans	ornithine decarboxylase	CNC04890	1e-40
Danio rerio	ornithine decarboxylase 1	AF290981_1	9e-40
Monodelphis domestica	similar to ornithine decarboxylase	LOC100027936	2e-39
Xenopus tropicalis	Ornithine decarboxylase 1	AAH74547.1	2e-39
Rattus norvegicus	ornithine decarboxylase 1	AAA66286.1	3e-39

Fungal sequences are in blue, animal sequences are in purple.

Supplelementry Data 22. Blastx hits to predicted ORF tagged in *path*-19

Organism	Annotation	Locus Accession	E-value
Neurospora crassa	arg-6 protein, mitochondrial precursor	NCU00567	0.0
Phaeosphaeria nodorum	hypothetical protein	SNOG_15544	0.0
Schizosaccharomyces pombe	arg1	ARG56_SCHPO	0.0
Botryotinia fuckeliana	hypothetical protein	BC1G_07180	0.0
Saccharomyces cerevisiae	ARG5,6, mitochondrial precursor	ARG56_YEAST	0.0
Sclerotinia sclerotiorum	hypothetical protein	SS1G_05107	0.0
Aspergillus fumigatus	acetylglutamate kinase	AFUA_6G02910	0.0
Podospora anserina	hypothetical protein	PODANSg3930	0.0
Neosartorya fischeri	acetylglutamate kinase, putative	NFIA_049240	0.0
Aspergillus niger	hypothetical protein	An12g07580	0.0
Aspergillus terreus	protein arg-6, mitochondrial precursor	ATEG_07160	0.0
Aspergillus clavatus	acetylglutamate kinase, putative	ACLA_097520	0.0
Candida glabrata	hypothetical protein	CAGL0J03124g	0.0
Coccidioides immitis	hypothetical protein	CIMG_10081	0.0
Ajellomyces capsulatus	protein arg-6, mitochondrial precursor	HCAG_05073	0.0
Cryptococcus neoformans	arg-6 protein, mitochondrial precursor	CNF02250	0.0
Laccaria bicolor	acetylglutamate kinase ARG6	EDR13256.1	0.0
Magnaporthe grisea	hypothetical protein	MGG_02690	0.0
Pyrenophora tritici-repentis	hypothetical protein	PTRG_05652	0.0
Coprinopsis cinerea	hypothetical protein	CC1G_06506	0.0
Chaetomium globosum	arg-6 protein, mitochondrial precursor	CHGG_06224	0.0
Pichia guilliermondii	conserved hypothetical protein	EDK37745.2	3e-171
Yarrowia lipolytica	unnamed protein product	YALI0B17666g	2e-170
Pichia stipitis	predicted protein	PICST_55623	2e-170
Debaryomyces hansenii	unnamed protein product	DEHA0F11726g	3e-168
Candida albicans	Protein ARG5,6, precursor	CAA67383.1	1e-166
Kluyveromyces lactis	unnamed protein product	KLLA0C07997g	3e-156

Supplentary Data 23. Blastx hits to predicted ORF tagged in *path*-23

Organism	Annotation	Locus Accession	E-value
Gibberella zeae	hypothetical protein	FG02446.1	5e-103
Magnaporthe grisea	hypothetical protein	MGG_09350	2e-94
Chaetomium globosum	hypothetical protein	CHGG_05189	4e-90
Podospora anserina	unnamed protein product	PODANSg286	1e-85
Neurospora crassa	hypothetical protein	NCU04954	7e-84

Supplementary Data 24. Blastx hits to predicted ORF tagged in *path*-29.

Organism	Annotation	Locus Accession	E-value
Gibberella zeae	hypothetical protein	FG06870.1	0.0
Neurospora crassa	conserved hypothetical protein	CAE76479.1	3e-166
Magnaporthe grisea	hypothetical protein	MGG_00500	2e-157
Chaetomium globosum	hypothetical protein	CHGG_02835	2e-135
Aspergillus terreus	hypothetical protein	ATEG_05309	6e-125
Aspergillus nidulans	hypothetical protein	AN1653.2	6e-123
Aspergillus clavatus	putative ATP binding L-PSP endoribonuclease family protein	ACLA_048430	7e-121
Aspergillus oryzae	unnamed protein product	BAE59170.1	1e-118
Neosartorya fischeri	putative ATP binding L-PSP endoribonuclease family protein	NFIA_107100	9e-118
Aspergillus fumigatus	putative ATP binding L-PSP endoribonuclease family protein	EDP50284.1	2e-117
Aspergillus niger	hypothetical protein	An04g03970	9e-116
Coccidioides immitis	hypothetical protein	CIMG_08216	2e-112
Pyrenophora tritici-repentis	meiotically up-regulated gene	PTRG_02804	1e-103
Phaeosphaeria nodorum	hypothetical protein	SNOG_03779	4e-96
Sclerotinia sclerotiorum	hypothetical protein	SS1G_04410	5e-92
Botryotinia fuckeliana	hypothetical protein	BC1G_00522	4e-89
Ajellomyces capsulatus	predicted protein	HCAG_07093	3e-72
Podospora anserina	hypothetical protein	PODANSg2030	6e-70
Yarrowia lipolytica	hypothetical protein	YALI0F14553g	7e-62
Pichia guilliermondii	hypothetical protein	PGUG_03693	1e-57
Pichia stipitis	hypothetical protein	PICST_43636	7e-57
Candida albicans	hypothetical protein	CaO19.839	2e-56
Pichia guilliermondii	hypothetical protein	PGUG_03693	6e-56
Vanderwaltozyma polyspora	hypothetical protein	Kpol_1036p86	4e-55
Schizosaccharomyces pombe	endoribonuclease (predicted)	SPBC577.12	4e-55
Debaryomyces hansenii	hypothetical protein	DEHA0B04763g	5e-55
Candida glabrata	hypothetical protein	CAGL0M04521g	5e-53
Lodderomyces elongisporus	hypothetical protein	LELG_01257	5e-52
Ustilago maydis	hypothetical protein	UM04996.1	1e-50
Saccharomyces cerevisiae	Putative protein, GFP-tagged protein localizes to the cytoplasm;	YLR143W	2e-49
Coprinopsis cinerea	hypothetical protein	CC1G_00411	2e-48
Apis mellifera	similar to ATP binding domain 4	LOC411591	1e-46
Ashbya gossypii	AGL164Wp	AGL164Wp	2e-46
Tribolium castaneum	hypothetical protein	LOC663632	7e-46
Kluyveromyces lactis	unnamed protein product	KLLA0D16984g	7e-46
Nasonia vitripennis	hypothetical protein	LOC100116698	1e-45
Strongylocentrotus purpuratus	hypothetical protein	LOC576024	2e-45
Xenopus laevis	MGC83562 protein	MGC83562	6e-45
Drosophila pseudoobscura	GA13952 gene product	GA13952-PA	1e-44
Aedes aegypti	hypothetical protein	EAT38761.1	1e-41
Gallus gallus	ATP binding domain 4	XP_421214.2	2e-40
Physcomitrella patens	predicted protein	EDQ75374.1	2e-38
Acyrthosiphon pisum	similar to GA13952-PA	LOC100162183	3e-38
Arabidopsis thaliana	endoribonuclease	AT3G04480	2e-37
Ostreococcus tauri	endoribonuclease L-PSP protein	CAL55488.1	2e-36
Trichoplax adhaerens	hypothetical protein	EDV29840.1	3e-35
Laccaria bicolor	predicted protein	EDR12916.1	2e-34
Cryptococcus neoformans	cytoplasm protein, putative	CNJ02960	6e-34
Vitis vinifera	unnamed protein product	CAO44678.1	1e-32

Fungal sequences are in blue, animal sequences are in purple, plant sequences are in green.

Supplementary Data 25. Blastx hits to predicted ORF tagged in *path*-35

Organism	Annotation	Locus Accession	E-value
Neurospora crassa	carbamoyl-phosphate synthase	NCU02677	0.0
Gibberella zeae	hypothetical protein	FG01217.1	0.0
Chaetomium globosum	hypothetical protein	CHGG_02831	0.0
Podospora anserina	unnamed protein product	PODANSg2038	0.0
Aspergillus terreus	carbamoyl-phosphate synthase,	ATEG_04441	0.0
Aspergillus clavatus	carbamoyl-phosphate synthase	ACLA_069100	0.0
Neosartorya fischeri	carbamoyl-phosphate synthase	NFIA_085480	0.0
Aspergillus fumigatus	carbamoyl-phosphate synthase	AFUA_2G10070	0.0
Aspergillus oryzae	carbamoyl-phophate synthetase	AO090011000630	0.0
Coccidioides immitis	carbamoyl-phosphate synthase	CIMG_02226	0.0
Aspergillus nidulans	conserved hypothetical protein	AN5999.2	0.0
Ajellomyces capsulatus	carbamoyl-phosphate synthase	HCAG_02700	0.0
Pyrenophora tritici-repentis	carbamoyl-phosphate synthase	PTRG_07586	0.0
Coniothyrium minitans	carbamoyl-phosphate synthase	ABK58727.1	0.0
Magnaporthe grisea	hypothetical protein	MGG_04503	0.0
Pichia stipitis	Pyrimidine synthesis protein CAD	ABN68520.1	0.0
Phaeosphaeria nodorum	hypothetical protein	SNOG_04245	0.0
Candida albicans	likely carbamoyl-phosphate synthetase	EAK98963.1	0.0
Yarrowia lipolytica	hypothetical protein	YALI0C23969g	0.0
Schizosaccharomyces pombe	carbamoyl-phosphate synthase Arg4	CAA22122.1	0.0
Kluyveromyces lactis	unnamed protein product	KLLA0F03190g	0.0
Saccharomyces cerevisiae	carbamoyl phosphate synthetase Cpa2p	EDV12846.1	0.0
Ashbya gossypii	Carbamoyl-phosphate synthase	ABR157Wp	0.0
Candida glabrata	hypothetical protein	CAGL0C04917g	0.0
Cryptococcus neoformans	hypothetical protein	CNBM1030	0.0
Lodderomyces elongisporus	carbamoyl-phosphate synthase	LELG_00181	0.0
Malassezia globosa	hypothetical protein	MGL_1974	0.0
Coprinopsis cinerea	hypothetical protein	CC1G_11823	0.0
Laccaria bicolor	carbamoyl-phosphate synthase	EDR09112.1	0.0

Supplementary Data 26. Blastx hits to predicted ORF tagged in *path*-36 and *path*-38.

Organism	Annotation	Locus Accession	E-value
Chaetomium globosum	hypothetical protein	CHGG_07317	0.0
Gibberella zeae	hypothetical protein	FG01854.1	0.0
Neurospora crassa	hypothetical protein	NCU03690	0.0
Magnaporthe grisea	hypothetical protein	MGG_09208	0.0
Botryotinia fuckeliana	hypothetical protein	BC1G_11788	0.0
Aspergillus terreus	conserved hypothetical protein	ATEG_05200	0.0
Neosartorya fischeri	importin beta-2 subunit, putative	NFIA_009420	0.0
Aspergillus fumigatus	importin beta-2 subunit, putative	AFUA_1G15900	0.0
Emericella nidulans	KapC	ABC69299.1	0.0
Aspergillus clavatus	importin beta-2 subunit, putative	ACLA_019460	0.0
Ajellomyces capsulatus	conserved hypothetical protein	HCAG_02231	0.0
Aspergillus niger	hypothetical protein	An01g14330	0.0
Schizosaccharomyces pombe	karyopherin Kap104	NP_594385.1	2e-149
Coprinopsis cinerea	hypothetical protein	CC1G_04693	9e-135
Ustilago maydis	hypothetical protein	UM04397.1	8e-134
Danio rerio	similar to transportin 1	LOC562607	4e-129
Pan troglodytes	transportin 2 (karyopherin beta 2b)	XP_512411.2	8e-128
Homo sapiens	transportin 2, karyopherin beta 2b	BAE06093.1	8e-128
Anopheles gambiae	predicted protein	AGAP005892-PA	8e-128
Nematostella vectensis	predicted protein	EDO40587.1|	1e-127
Bos taurus	Transportin 1	AAI03375.1	2e-127
Macaca mulatta	similar to transportin 1	XP_001095625.	2e-127
Ornithorhynchus anatinus	similar to transportin 1	LOC100082217	2e-127
Mus musculus	Transportin-2 (Karyopherin beta-2b)	EDL10988.1|	4e-127
Canis lupus familiaris	transportin 1	XP_535270.2	7e-127
Culex quinquefasciatus	importin ß-2	EDS25719.1	7e-127
Bos taurus	importin 3, karyopherin ß 2b	XP_001790098.1	7e-127
Drosophila mojavensis	predicted protein	GI12093	7e-127
Rattus norvegicus	importin 3, karyopherin ß 2b	EDL92165.1	9e-127
Equus caballus	timportin 3, karyopherin ß 2b	XP_001504938.2	1e-126

Fungal sequences are in blue, animal sequences are in purple. Not all significant hits are shown.

References

Abuodeh, R. O., Porbach, M. J., Mandel, M. A., Das, A., Galgiani, J. N. 2000. Genetic transformation of *Coccidioides immitis* facilitated by *Agrobacterium tumefaciens*. J. Infect. Dis. 181:2106-2110.

Acosta-Rodriguez, I., Pinon-Escobedo, C., Zavala-Paramo, M. G., Lopez-Romero, E., Cano-Camacho, H. 2005. Degradation of cellulose by the bean-pathogenic fungus *Colletotrichum lindemuthianum*. Production of extracellular cellulolytic enzymes by cellulose induction. Antonie Van Leeuwenhoek. 87:301-10.

Adachi, K., Nelson, G. H., Peoples, K. A., Frank, S. A., Montenegro-Chamorro, M. V., DeZwaan, T. M., Ramamurthy, L., Shuster, J. R., Hamer, L., Tanzer, M. M. 2002. Efficient gene identification and targeted gene disruption in the wheat blotch fungus *Mycosphaerella graminicola* using TAGKO. Curr. Genet. 42:123-127.

Adams, D. J. 2004. Fungal cell wall chitinases and glucanases. Microbiology. 150:2029-35.

Aitchisinson, J. D., Blobel, G., Rout, M. P. 1996. Kap104p: a karyopherin involved in the nuclear transport of messenger RNA binding proteins. Science. 274:624-627.

Allen, E. A., Hazen, B. E., Hoch, H. C., Kwon, Y., Leinhos, G. M. E., Staples, R. C., Stumpf, M. A., Terhune, B. T. 1991. Appressorium formation in response to topographical signals by 27 rust species. Phytopathology. 81:323-331.

Almaguer, C., Cheng, W., Nolder, C., Patton-Vogt, J. 2004. Glycerophosphoinositol, a novel phosphate source whose transport is regulated by multiple factors in *Saccharomyces cerevisiae*. J. Biol. Chem. 279:31937-42.

Alonso, J. M., Stepanova, A. N., Leisse, T. J., Kim, C. J., Chen, H., Shinn, P., Stevenson, D. K., Zimmerman, J., Barajas, P., Cheuk, R., Gadrinab, C., Heller, C., Jeske, A., Koesema, E., Meyers, C. C., Parker, H., Prednis, L., Ansari, Y., Choy, N., Deen, H., Geralt, M., Hazari, N., Hom, E., Karnes, M., Mulholland, C., Ndubaku, R., Schmidt, I., Guzman, P., Aguilar-Henonin, L., Schmid, M., Weigel, D., Carter, D. E., Marchand, T., Risseeuw, E., Brogden, D., Zeko, A., Crosby, W. L., Berry, C. C., Ecker, J. R. 2003. Genome-wide insertional mutagenesis of *Arabidopsis thaliana.* Science. 301:653-7.

Amey, R. C., Athey-Pollard, A., Burns, C., Mills, P. R., Bailey, A., Foster, G. D. 2002. PEG-mediated and *Agrobacterium*-mediated transformation in the mycopathogen *Verticullium fungicola*. Mycol. Res. 106:4-11.

Amnuaykanjanasin, A., Epstein, L. 2003. A class V chitin synthase gene, *chsA* is essential for conidial and hyphal wall strength in the fungus *Colletotrichum graminicola* (*Glomerella graminicola*). Fungal Genet. Biol. 38:272-285.

Anderson, J. T., Wilson, S. M., Datar, K. V., Swanson, M. S. 1993. NAB2: a yeast nuclear polyadenylated RNA-binding protein essential for cell viability. Mol Cell Biol. 13:2730-41.

Asakura, M., Okuno, T., Takano, Y. 2006. Multiple contributions of peroxisomal metabolic function to fungal pathogenicity in *Colletotrichum lagenarium*. Appl. Environ. Microbiol. 72:6345-6354.

Atkinson, T. G., Shaw, M. 1955. Occurrence of acid phosphatase in association with the haustoria of powdery mildew on barley. Nature. 175:993-4.

Azpiroz-Leehan, R., Feldmann, K. A. 1997. T-DNA insertion mutagenesis in Arabidopsis: going back and forth. Trends Genet. 13:152-6.

Baca, O. G., Roman, M. J., Glew, R. H., Christner, R. F., Buhler, J. E., Aragon, A. S. 1993. Acid phosphatase activity in *Coxiella burnetii*: a possible virulence factor. Infect. Immun. 61:4232-9.

Bae, C. Y., Kim, S., Choi, W. B., Lee, Y. H. 2007. Involvement of extracellular matrix and integrin-like proteins on conidial adhesion and appressorium differentiation in *Magnaporthe oryzae*. J. Microbiol. Biotechnol. 17:1198-203.

Bailey, A., Mueller, E., Bowyer, P. 2000. Ornithine decarboxylase of *Stagonospora (Septoria) nodorum* is required for virulence toward wheat. J. Biol. Chem. 275:14242-14247.

Bailey, J. A., Jeger, M. J. 1992. *Colletotrichum*- Biology, Pathology and Control, CABI, Wallingford, UK.

Baladron, V., Ufano, S., Duenas, E., Martin-Cuadrado, A. B., del Rey, F., Vazquez de Alana, C. R. 2002. Eng1p, an endo-1,3-*ß*-glucancase localized at the daughter side of the septum, is involved in cell separation in *Saccharomyces cerevisae*. Eukaryot. Cell. 1 774-786.

Balhadére, P. V., Foster, A. J., Talbot, N. J. 1999. Identification of pathogenicity mutants of the rice blast fungus *Magnaporthe grisea* by insertional mutagenesis. Mol. Plant Microbe Interac. 12:129-142.

Ballance, D. J., Buxton, F. P., Turner, G. 1983. Transformation of *Aspergillus nidulans* by the ornithine-5'-phosphate decarboxylase gene of *Neurospora crassa*. Biochemical and Biophysical Research Communications. 112:284-289.

Barakat, A., Gallois, P., Raynal, M., Mestre-Ortega, D., Sallaud, C., Guiderdoni, E., Delseny, M., Bernardi, G. 2000. The distribution of T-DNA in the genomes of transgenic *Arabidopsis* and rice. FEBS Lett. 471:161-164.

Barhoom, S., Kupiec, M., Zhao, X., Xu, J. R., Sharon, A. 2008. Functional characterization of CgCTR2, a putative vacuole copper transporter that is involved in germination and pathogenicity in *Colletotrichum gloeosporioides*. Eukaryot. Cell. 7:1098-108.

Becker, B. F., Reinholz, N., Özcelik, T., Leipert, B., Gerlach, E. 1989. Uric acid as radical scavenger and antioxidant in the heart. Pflueg. Arch. Eur. J. Physiol. 415:127-135.

Betts, M. F., Tucker, S. L., Galadima, N., Meng, Y., Patel, G., Li, L., Donofrio, N., Floyd, A., Nolin, S., Brown, D., Mandel, M. A., Mitchell, T. K., Xu, J. R., Dean, R. A., Farman, M. L., Orbach, M. J. 2007. Development of a high throughput transformation system for insertional mutagenesis in *Magnaporthe oryzae*. Fungal Genet. Biol. 44:1035-49.

Bhambra, G. K., Wang, Z. Y., Soanes, D. M., Wakley, G. E., Talbot, N. J. 2006. Peroxisomal carnitine acetyl transferase is required for elaboration of penetration hyphae during plant infection by *Magnaporthe grisea*. Mol. Microbiol. 61:46-60.

Birnboim, H., Doly, J. 1979. Rapid alkaline extraction procedure for screening recombinant plasmid DNA. Nuc. Acids Res.7:1513-1523.

Blaise, F., Remy, E., Meyer, M., Zhou, L., Narcy, J. P., Roux, J., Balesdent, M. H., Rouxel, T. 2007. A critical assessment of *Agrobacterium tumefacien*s-mediated transformation as a tool for pathogenicity gene discovery in the phytopathogenic fungus *Leptosphaeria maculans*. Fungal Genet. Biol. 44:123-38.

Boddi, S., Comparini, C., Calamassi, R., Pazzagli, L., Cappugi, G., Scala, A. 2004. Cerato-platanin protein is located in the cell walls of ascospores, conidia and hyphae of Ceratocystis fimbriata f. sp. platani. FEMS Microbiol. Lett. 233:341-6.

Bolker, M., Bohnert, H. U., Braun, K. H., Gorl, J., Kahmann, R. 1995. Tagging pathogenicity genes in *Ustilago maydis* by restriction enzyme-mediated integration (REMI). Mol. Gen. Genet. 248:547-552.

Bolton, M. D., van Esse, H. P., Vossen, J. H., de Jonge, R., Stergiopoulos, I., Stulemeijer, I. J., van den Berg, G. C., Borrás-Hidalgo, O., Dekker, H. L., de Koster, C. G., de Wit, P. J., Joosten, M. H., Thomma, B. P. 2008. The novel *Cladosporium fulvum* lysin motif effector Ecp6 is a virulence factor with orthologues in other fungal species. Mol. Microbiol.

Bonifaci, N., Moroianu, J., Radu, A., Blobel, G. 1997. Karypherin ß2 mediates nuclear import of a mRNA binding protein. Proc. Natl. Acad. Sci. U.S.A. 94:5055-5060.

Bouizgarne, B., El-Maarouf-Bouteau, H., Frankart, C., Reboutier, D., Madiona, K., Pennarun, A. M., Monestiez, M., Trouverie, J., Amiar, Z., Briand, J., Brault, M., Rona, J. P., Ouhdouch, Y., El Hadrami, I., Bouteau, F. 2006. Early physiological responses of *Arabidopsis thaliana* cells to fusaric acid: toxic and signalling effects. New Phytol. 169:209-18.

Bowyer, P., Clarke, B. R., Lunness, P., Danels, M. J., Osbourn, A. E. 1995. Host range of a plant pathogenic fungus determined by a saponin detoxifying enzyme. Science. 267:371-374-.

Brakhage, A. A., Liebmann, B. 2005. *Aspergillus fumigatus* conidial pigment and cAMP signal transduction: significance for virulence. Med. Mycol. 43 Suppl 1:S75-82.

Bun-Ya, M., Nishimura, M., Harashima, S., Oshima, Y. 1991. The *PHO84* gene of *Saccharomyces cerevisiae* encodes an inorganic phosphate transporter. Mol. Cell Biol. 11:3229-38.

Bundock, P., den Dulk-Ras, A., Alice, B., Hooykaas, P. J. J. 1995. Trans-kingdom T-DNA transfer from *Agrobacterium tumefaciens* to *Saccharomyces cerevisiae*. The EMBO J. 14:3206-3214.

Bundock, P., Hooykaas, P. J. J. 1996. Integration of *Agrobacterium tumefaciens* T-DNA in the *Saccharomyces cerevisiae* Genome by Illegitimate Recombination. Proc. Natl. Acad. Sci. U.S.A. 93:15272-15275.

Bundock, P., Mroczek, K., Winkler, A. A., Steensma, H. Y., Hooykaas, P. J. 1999. T-DNA from *Agrobacterium tumefaciens* as an efficient tool for gene targeting in *Kluyveromyces lactis*. Mol. Gen. Genet. 261:115-121.

Cangelosi, G. A., Best, E. A., Martinetti, G., Nester, E. W. 1991. Genetic analysis of *Agrobacterium*. Methods in Enzymology. 204:384-397.

Carlile, M. J., Watkinson, S. C., Gooday, G. W. 2001. Spores, dormancy and dispersal. In: The fungi. Academic Press London:185-244.

Carzaniga, R., Fiocco, D., Bowyer, P., O'Connell, R. 2002. Localization of melanin in conidia of *Alternatia alternata* using phage display antibodies. Mol. Plant Microbe Interact. 3:216-224.

Castillo-Lluva, S., Alvarez-Tabares, I., Weber, I., Steinberg, G., Perez-Martin, J. 2007. Sustained cell polarity and virulence in the phytopathogenic fungus *Ustilago maydis* depends on an essential cyclin-dependent kinase from the Cdk5/Pho85 family. J. Cell Sci. 120:1584-95.

Centis, S., Dumas, B., Fournier, J., Marolda, M., EsquerreTugaye, M. T. 1996. Isolation and sequence analysis of *Clpg1*, a gene coding for an endopolygalacturonase of the phytopathogenic fungus *Colletotrichum lindemuthianum*. Gene. 170:125-129.

Centis, S., Guillas, I., Sejalon, N., EsquerreTugaye, M. T., Dumas, B. 1997. Endopolygalacturonase genes from *Colletotrichum lindemuthianum*: cloning of *CLPG2* and comparison of its expression to that of *CLPG1* during saprophytic and parasitic growth of the fungus. Mol. Plant Microbe Interact. 10:769-775.

Chang, P. K. 2008. A highly efficient gene-targeting system for *Aspergillus parasiticus*. Lett Appl Microbiol. 46:587-92.

Choi, J., Park, J., Jeon, J., Chi, M. H., Goh, J., Yoo, S. Y., Park, J., Jung, K., Kim, H., Park, S. Y., Rho, H. S., Kim, S., Kim, B. R., Han, S. S., Kang, S., Lee, Y. H. 2007. Genome-wide analysis of T-DNA integration into the chromosomes of *Magnaporthe oryzae*. Mol. Microbiol. 66:371-82.

Chook, Y. M. 2007. Traffic Rules for nuclear import pathways: Karyopherin beta2 and Kap104p FASEB J. 21:820.1.

Christopherson, M. R., Schmitz, G. E., Downs, D. M. 2008. YjgF is required for isoleucine biosynthesis when Salmonella enterica is grown on pyruvate medium. J. Bacteriol. 190:3057-62.

Clergeot, P. H., Gourgues, M., Cots, J., Laurans, F., Latorse, M. P., Pepin, R., Tharreau, D., Notteghem, J. L., Lebrun, M. H. 2001. PLS1, a gene encoding a tetraspanin-like protein, is required for penetration of rice leaf by the fungal pathogen *Magnaporthe grisea*. Proc Natl Acad Sci U S A. 98:6963-8.

Collemare, J., Pianfetti, M., Houlle, A. E., Morin, D., Camborde, L., Gagey, M. J., Barbisan, C., Fudal, I., Lebrun, M. H., Bohnert, H. U. 2008. *Magnaporthe grisea* avirulence gene ACE1 belongs to an infection-specific gene cluster involved in secondary metabolism. New Phytol. 179:196-208.

Collins, N. C., Thordal-Christensen, H., Lipka, V., Bau, S., Kombrink, E., Qiu, J. L., Huckelhoven, R., Stein, M., Freialdenhoven, A., Somerville, S. C., Schulze-Lefert, P. 2003. SNARE-protein-mediated disease resistance at the plant cell wall. Nature. 425:973-977.

Combier, J. P., Melayah, D., Raffier, C., Gay, G., Marmeisse, R. 2003. Agrobacterium tumefaciens-mediated transformation as a tool for insertional mutagenesis in the symbiotic ectomycorrhizal fungus *Hebeloma cylindrosporum*. FEMS Microbiol. Lett. 220:141-8.

Cvitanich, C., Judelson, H. S. 2003. Stable transformation of the oomycete, *Phytophtora infestans*, using microprojectile bombardment. Curr. Genet. 42:228-235.

da Silva Ferreira, M. E., Kress, M. R., Savoldi, M., Goldman, M. H., Hartl, A., Heinekamp, T., Brakhage, A. A., Goldman, G. H. 2006. The akuB(KU80) mutant deficient for nonhomologous end joining is a powerful tool for analyzing pathogenicity in *Aspergillus fumigatus*. Eukaryot Cell. 5:207-11.

Daboussi, M. J., Capy, P. 2003. Transposable elements in filamentous fungi. Annual Rev. Microbiol. 57:275-299.

Davidson, R. C., Cruz, M. C., Sia, R. A. L. 2000. Gene disruption by biolistic transformation in serotype D strains of *Cryptococcus neoformans*. Fungal Genet. Biol. 29:38-48.

Davis, R. H., Morris, D. R., Coffino, P. 1992. Sequestered end products and enzyme regulation: the case of ornithine decarboxylase. Microbiol. Rev. 56:280-90.

De Groot, M. J. A., Bundock, P., Hooykaas, P. J. J., Beijersbergen, A. G. M. 1998. *Agrobacterium tumefaciens*-mediated transformation of filamentous fungi. Nature Biotechnol. 16:839-842.

de Jong, J. C., McCormack, B. J., Smirnoff, N., Talbot, N. J. 1997. Glycerol generates turgor in rice blast. Nature. 389:244-245.

De Lorenzo, G., Ferrari, S. 2002. Polygalacturonase-inhibiting proteins in defense against phytopathogenic fungi. Curr. Opin. Plant Biol. 5:295-299.

De Queiroz, M. V., Daboussi, M. J. 2003. Impala, a transposon from *Fusarium oxysporum*, is active in the genome of *Penicillium griseoroseum*. FEMS Microbiol. Lett. 218:317-321.

Dean, R. A. 1997. Signal pathways and appressorium morphogenesis. Annu. Rev. Phytopathol. 35:211-34.

Degefu, Y., Hanif, M. 2003. *Agrobacterium tumefaciens*-mediated transformation of *Helminthosporium turcicum*, the maize leaf-blight fungus. Arch. Microbiol. 180:279-84.

Deighton, N., Muckenschnabel, I., Colmenares, A. J., Collado, I. G., Williamson, B. 2001. Botrydial is produced in plant tissues infected by *Botrytis cinerea*. Phytochemistry. 57:689-92.

Deising, H., Nicholson, R. L., Haug, M., Howard, R. J., Mendgen, K. 1992. Adhesion pad formation and the involvement of cutinase and esterases in the attachment of uredospores to the host cuticle. Plant Cell. 4:1101-1111.

Deising, H. B., Werner, S., Wernitz, M. 2000. The role of fungal appressoria in plant infection. Microbes Infect. 2:1631-41.

DeZwaan, T. M., Carroll, A. M., Valent, B., Sweigard, J. A. 1999. *Magnaporthe grisea* pth11p is a novel plasma membrane protein that mediates appressorium differentiation in response to inductive substrate cues. Plant Cell. 11:2013-30.

Dickman, M. B., Ha, Y. S., Yang, Z., Adams, B., Huang, C. 2003. A protein kinase from Colletotrichum trifolii is induced by plant cutin and is required for appressorium formation. Mol. Plant Microbe Interact. 16:411-21.

Divon, H. H., Fluhr, R. 2007. Nutrition acquisition strategies during fungal infection of plants. FEMS Microbiol. Lett. 266:65-74.

Divon, H. H., Rothan-Denoyes, B., Davydov, O., Di Pietro, A., Fluhr, R. 2005. Nitrogen responsive genes are differentially regulated *in planta* during *Fusarium oxysporum* f. sp. *lycopersici* infection. Mol. Plant Pathol. 6:459-470.

Dodds, P. N., Lawrence, G. J., Catanzariti, A. M., Ayliffe, M. A., Ellis, J. G. 2004. The *Melampsora lini* AvrL567 avirulence genes are expressed in haustoria and their products are recognized inside plant cells. Plant Cell. 16:755-768.

Doehlemann, G., Berndt, P., Hahn, M. 2006. Different signalling pathways involving a Galpha protein, cAMP and a MAP kinase control germination of Botrytis cinerea conidia. Mol. Microbiol. 59:821-35.

Doss, R. P., Deisenhofer, J., Krug von Nidda, H. A., Soeldner, A. H., McGuire, R. P. 2003. Melanin in the extracellular matrix of germlings of *Botrytis cinerea*. Phytochemistry. 63:687-91.

Dufresne, M., Bailey, J. A., Dron, M., Langin, T. 1998. *clk1*, a serine/threonine protein kinase-encoding gene, is involved in pathogeicity of *Colletotrichum lindemuthianum* on common bean. Mol. Plant Microbe Interact. 11:99-108.

Dufresne, M., Perfect, S., Pellier, A. L., Bailey, J. A., Langin, I. 2000. A GAL4-like protein is involved in the switch between biotrophic and necrotrophic phases of the infection process of *Colletotrichum lindemuthianum* on common bean. Plant Cell. 12:1579-1589.

Durrenberger, F., Wong, K., Kronstad, J. W. 1998. Identification of a cAMP-dependent protein kinase catalytic subunit required for virulence and morphogenesis in *Ustilago maydis*. Proc. Natl. Acad. Sci. U.S.A. 95:5684-9.

Egan, M. J., Wang, Z. Y., Jones, M. A., Smirnoff, N., Talbot, N. J. 2007. Generation of reactive oxygen species by fungal NADPH oxidases is required for rice blast disease. Proc. Natl. Acad. Sci. U.S.A. 104:11772-7.

El Gueddari, N. E., Rauchhaus, U., Raab, T. K., Deising, H. B. 2002. Developmentally regulated conversion of surface-exposed chitin to chitosan in cell walls of plant pathogenic fungi. New Phytol. 156:103-112.

Eriksson, S., Lucchini, S., Thompson, A., Rhen, M., Hinton, J. C. 2003. Unravelling the biology of macrophage infection by gene expression profiling of intracellular *Salmonella enterica*. Mol. Microbiol. 47:103-18.

Escobar, M. A., Dandekar, A. M. 2003. *Agrobacterium tumefaciens* as an agant of disease. Trends Plant Sci. 8:380-386.

Fan, X. C., Steitz, J. A. 1998. HNS, a nuclear-cytoplasmic shuttling sequence in HuR. Proc. Natl. Acad. Sci. U.S.A. 95:15293-8.

Felman, K. A., Marks, M. D. 1987. *Agrobacterium*-mediated transformation of germinating seeds of *Arabidopsis thaliana*: A non-tissue culture approach. Mol. Gen Genet. 208:1-9.

Finchman, J. R. S. 1989. Transformation in fungi. Microbiol. Rev. 53:148-170.

Firon, A., Villalba, F., Beffa, R., D' Enfert, C. 2003. Identification of essencial genes in human fungal pathogen *Aspergillus fumigatus* by transposon mutagenesis. Eukaryot. Cell. 2:247-255.

Fitzgerald, A. M., Mudge, A. M., Gleave, A. P., Plummer, K. M. 2003. *Agrobacterium* and PEG-mediated transformation of the phytopathogen *Venturia inaequalis*. Mycol Res. 107:

Flaishman, M. A., Kolattukudy, P. E. 1994. Timing of fungal invasion using host's ripening hormone as a signal. Proc. Natl Acad. Sci. U.S.A. 91:6579-83.

Flowers, J. L., Vaillancourt, L. J. 2005. Parameters affecting the efficiency of *Agrobacterium tumefaciens*-mediated transformation of *Colletotrichum graminicola*. Curr. Genet. 48:380-388.

Forbes, P. J., Milliam, S., Hooker, J. E., Harrier, L. A. 1998. Transformation of the arbuscular mycorrhiza *Gigaspora rosea* by particle bonbardment. Mycol. Res. 102:497-501.

Forsbach, A., Schubert, D., Lechtenberg, B., Gils, M., Schmidt, R. 2003. A comprehensive characterization of single-copy T-DNA insertions in the Arabidopsis thaliana genome. Plant Mol Biol. 52:161-76.

Fotopoulos, V., Gilbert, M. J., Pittman, J. K., Marvier, A. C., Buchanan, A. J., Sauer, N., Hall, J. L., Williams, L. E. 2003. The monosaccharide transporter gene, AtSTP4, and the cell-wall invertase, Atbetafruct1, are induced in *Arabidopsis* during infection with the fungal biotroph *Erysiphe cichoracearum*. Plant Physiol. 132:821-9.

Galan, J. E., Wolf-Watz, H. 2006. Protein delivery into Eukaryotic cells by type III secretion machines. Nature. 444:567-73.

Gilbert, M. J., Thornton, C. R., Wakley, G. E., Talbot, N. J. 2006. A P-type ATPase required for rice blast disease and induction of host resistance. Nature. 440:535-539.

Gilbert, R. D., Johnson, A. M., Dean, R. A. 1996. Chemical signals responsible for appressorium formation in the rice blast fungus. Physiol. Mol. Plant. Pathol. 48:335-346.

Giulia, M., Nicosia, L. D., Brocard-Masson, C., Demais, S., Hua Van, A., Daboussi, M. J., Scazzocchio, C. 2001. Heterologous transposition in *Aspergillus nidulans*. Mol. Microbiol. 39:1330-1344.

Goins, C. L., Gerik, K. J., Lodge, J. K. 2006. Improvements to gene deletion in the fungal pathogen *Cryptococcus neoformans*: absence of Ku proteins increases homologous recombination, and co-transformation of independent DNA molecules allows rapid complementation of deletion phenotypes. Fungal Genet.Biol. 43:531-44.

Gold, S., Duncan, G., Barrett, K., Kronstad, J. 1994. cAMP regulates morphogenesis in the fungal pathogen *Ustilago maydis*. Genes Dev. 8:2805-16.

Goodwin, P. H., Chen, G. Y. 2002. High expression of a sucrose non-fermenting (SNF1)-related protein kinase from *Colletotrichum gloeosporoides* f. sp. *malvae* is associated with penetration of *Malva pusilla.* FEMS Microbiol. Lett. 215:169-74.

Goodwin, P. H., Li, J. R., Jin, S. M. 2001. A catalase gene of *Colletotrichum gloeosporioides* f. sp *malvae* is highly expressed during the necrotrophic phase of infection of round-leaved mallow, *Malva pusilla*. FEMS Microbiol. Lett. 202:103-107.

Gourgues, M., Brunet-Simon, A., Lebrun, M. H., Levis, C. 2004. The tetraspanin BcPls1 is required for appressorium-mediated penetration of *Botrytis cinerea* into host plant leaves. Mol. Microbiol. 51:619-29.

Govrin, E. M., Levine, A. 2000. The hypersensitive response facilitates plant infection by the necrotrophic pathogen *Botrytis cinerea.* Curr. Biol. 10:751-7.

Gow, N. A., Netea, M. G., Munro, C. A., Ferwerda, G., Bates, S., Mora-Montes, H. M., Walker, L., Jansen, T., Jacobs, L., Tsoni, V., Brown, G. D., Odds, F. C., Van der Meer, J. W., Brown, A. J., Kullberg, B. J. 2007. Immune recognition of *Candida albicans* beta-glucan by dectin-1. J. Infect. Dis. 196:1565-71.

Green, J. R., Pain, N. A., Cannell, M. E., Jones, G. L., Leckie, C. P., McCready, S., Mendgen, K., Mitchell, A. J., Callow, J. A., O'Connell, R. J. 1995. Analysis of differentiation and development of the specialized infection structures formed by biotrophic fungal giant pathogens using monoclonal antibodies. Can. J. Bot. 73:408-417.

Guevara-Olvera, L., Xoconostle-Cazares, B., Ruiz-Herrera, J. 1997. Cloning and disruption of the ornithine decarboxylase gene of *Ustilago maydis*: evidence for a role of polyamines in its dimorphic transition. Microbiology. 143 (Pt 7):2237-45.

Gupta, A., Chattoo, B. B. 2007. A novel gene MGA1 is required for appressorium formation in *Magnaporthe grisea*. Fungal Genet. Biol. 44:1157-69.

Haarmann, T., Lorenz, N., Tudzynski, P. 2008. Use of a nonhomologous end joining deficient strain (Deltaku70) of the ergot fungus Claviceps purpurea for identification of a nonribosomal peptide synthetase gene involved in ergotamine biosynthesis. Fungal Genet Biol. 45:35-44.

Hahn, M., Mendgen, K. 2001. Signal and nutrient exchange at biotrophic plant-fungus interfaces. Curr. Opin. Plant Biol. 4:322-327.

Hamer, J. E., Howard, R. J., Chumley, F. G., Valent, B. 1988. A mechanism for surface attachment in spores of a plant pathogenic fungus. Science. 239:288-290.

Hamer, J. E., Talbot, N. J. 1998. Infection-related development in the rice blast fungus *Magnaporthe grisea*. Curr. Opin. Microbiol. 1:693-7.

Hamer, L., Adachi, K., Montenegro-Chamorro, M. V., Tanzer, M. M., Mahanty, S. K., Lo, C., Tarpey, R. W., Skalchunes, A. R., Heiniger, R., W., Frank, S. A., Darveaux, B. A., Lampe, D., J., Slater, T. M., Ramamurthy, L., DeZwaan, T. M., Nelson, G. H., Shuster, J. R., Woessner, J., Hamer, J. E. 2001. Gene discovery and gene function assignment in filamentous fungi. Proc. Natl. Acad. Sci. U.S.A. 98:5110-5115.

Hazell, B. W., RTeo, V. S. J., Bradner, J. R., Berquist, P. L., Nevalainen, K. M. H. 2000. Rapid transformation of high secreting mutant strains of *Trichoderma reesei* by microprojectile bombarment. Lett. Appl. Microbiol. 30:282-286.

Herbert, C., O'Connell, R., Gaulin, E., Salesses, V., Esquerre-Tugaye, M. T., Dumas, B. 2004. Production of a cell wall-associated endopolygalacturonase by *Colletotrichum lindemuthianum* and pectin degradation during bean infection. Fungal Genet Biol. 41:140-147.

Hogan, L. H., Klein, B. S. 1994. Altered expression of surface alpha-1,3-glucan in genetically related strains of *Blastomyces dermatitidis* that differ in virulence. Infect. Immun. 62:3543–3546.

Hoi, J. W. S., Herbert, C., Bacha, N., O'Connell, R., Lafitte, C., Borderies, G., Rossignol, M., Rougé, P., Dumas, B. 2007. Regulation and role of a STE12-like transcription factor from the plant pathogen *Colletotrichum lindemuthianum*. Mol. Microbiol. 64:68-82.

Hooykaas, P. J., Beijersbergen, A. G. 1994. The virulence system of *Agrobacterium tumefaciens*. Annu. Rev. Phytopathol. 32:157-179.

Hou, Z., Xue, C., Peng, Y., Katan, T., Kistler, H. C., Xu, J. R. 2002. A mitogen-activated protein kinase gene (MGV1) in Fusarium graminearum is required for female fertility, heterokaryon formation, and plant infection. Mol .Plant Microbe Interact. 15:1119-27.

Howard, R. J., Ferrari, M. A., Roach, D. H., Money, N. P. 1991. Penetration of hard substrates by a fungus employing enormous turgor pressures. Proc. Natl. Acad. Sci. U.S.A. 88:11281-11284.

Howard, R. J., Valent, B. 1996. Breaking and entering: host penetration by the fungal rice blast pathogen Magnaporthe grisea. Annu. Rev. Microbiol. 50:491-512.

Howlett, B. J., Idnurm, A., Pedras, M. S. 2001. Leptosphaeria maculans, the causal agent of blackleg disease of Brassicas. Fungal Genet. Biol. 33:1-14.

Hurst, L. D., Pal, C., Lercher, M. J. 2004. The evolutionary dynamics of eukaryotic gene order. Nat. Rev. Genet. 5:299-310.

Hwang, C.-S., Kolattukudy, P. E. 1995. Isolation and characterization of genes expressed uniquely during appressorium formation by *Colletotrichum gloeosporiodes* conidia induced by the host suraface wax. Mol. Gen. Genet. 247:282-294.

Idnurm, A., Howlett, B. J. 2002. Isocitrate lyase is essential for pathogenicity of the fungus *Leptosphaeria maculans* to canola (Brassica napus). Eukaryot. Cell. 1:719-24.

Ikeda, R., Sugita, T., Jacobson, E. S., Shinoda, T. 2003. Effects of melanin upon susceptibility of *Cryptococcus* to antifungals. Microbiol. Immunol. 47:271-7.

Inoue, S., Kato, T., Jordan, V. W. L., Brent, K. J. 1987. Inhibition of appressorial adhesion of *Pyricularia oryzae* to barley leaves by fungicides. Pestic. Science. 19:145-152.

Iwamoto, M., Takeuchi, Y., Takada, Y., Kohno, S., Matsumoto, I., Yamaoka, N. 2007. Coleoptile cuticle of barley is necessary for the increase in appressorial turgor pressure of *Blumeria graminis* for penetration J.Gen. Plant Pathol. 73:38-40.

Jelitto, T. C., Page, H. A., Read, N. D. 1994. Role of external signals in regulating the pre-penetrationphase of infectionby the rice blast fungus *Magnaporthe grisea*. Planta. 194:471-477.

Jenczmionka, N. J., Schafer, W. 2005. The Gpmk1 MAP kinase of *Fusarium graminearum* regulates the induction of specific secreted enzymes. Curr. Genet. 47:29-36.

Jensen, L. T., Ajua-Alemanji, M., Culotta, V. C. 2003. The *Saccharomyces cerevisiae* high affinity phosphate transporter encoded by *PHO84* also functions in manganese homeostasis. J. Biol. Chem. 278:42036-40.

Jeon, J., Park, S.-Y., Chi, M.-H., Choi, J., Park, J., Rho, H.-S., Kim, S., Goh, J., Yoo, S., Choi, J., Park, J.-Y., Yi, M., Yang, S., Kwon, M.-J., Han, S.-S.-, Kim, B. R., Khang, C. H., Park, B., Lim, S.-E., Jung, K., King, S., Karunakaran, M., Oh, H.-S., Kim, H., Kim, S., Park, J., Kang, S., Choi, W.-B., Kang, S., Lee, Y.-H. 2007. Genome-wide functional analysis of pathogenicity genes in the rice blast fungus. Nature Genet.

Jeong, J. S., Mitchell, T. K., Dean, R. A. 2007. The *Magnaporthe grisea* snodprot1 homolog, MSP1, is required for virulence. FEMS Microbiol. Lett. 273:157-65.

Jia, J., Wheals, A. 2000. Endopolygalacturonase genes and enzymes from *Saccharomyces cerevisiae* and *Kluyveromyces marxianus*. Curr. Genet. 38:264-70.

Jia, Y., McAdams, S. A., Bryan, G. T., Hershey, H. P., Valent, B. 2000. Direct interaction of resistance gene and avirulence gene products confers rice blast resistance. EMBO J. 19:4004-14.

Joosten M. H. A. J., de Wit, P. J. G. M. 1999. The tomato-*Cladosporium fulvum* interaction: A versatile experimental system to study plant-pathogen interactions. Annu. Rev. Phytopathol. 37: 335–367.

Jones, J. D. G., Dangl, J. L. 2006. The plant immune system. Nature. 444:323-329.

Jones, M. J., Epstein, L. 1989. Adhesion of *Nectria haematococca* macroconidia. Physiol. Plant. Pathol. 35:453-461.

Kahmann, R., Basse, C. 1999. REMI (Restriction Enzyme Mediated Integration) and its impact on the isolation of pathogenicity genes in fungi attacking plants. Eur. J. Plant Pathol. 105:221-229.

Kamakura, T., Yamaguchi, S., Saitoh, K., Teraoka, T., Yamaguchi, I. 2002. A novel gene, CBP1, encoding a putative extracellular chitin-binding protein, may play an important role in the hydrophobic surface sensing of *Magnaporthe grisea* during appressorium differentiation. Mol. Plant Microbe Interact. 15:437-44.

Kämper, J., Kahmann, R., Bölker, M., Ma, L.-J., Brefort, T., Saville, B. J., Banuett, F., Kronstad, J. W., Gold, S. E., Müller, O., Perlin, M. H., Wösten, H. A. B., de Vries, R., Ruiz-Herrera, J. R.-P., C. G., Snetselassr, K., McCann, M., Perez-Martin, J., Feldbrügge, M., Basse, C. W., Steinberg, G., Ibeas, J. I., Holloman, W., Guzman, P., Farman, M., Stajich, J. E., Sentandreu, R., Gonzalez-Pietro, J. M., Kennell, J. C., Molina, L., Schirawski, J., Mendoza-Mendoza, A., Greilinger, D., Münch, K., Rössel, N., Scherer, M., Vranes, M., Ladendorf, O., Vincon, V., Fuchs, U., Sandrock, B., Meng, S., Ho, E. C. H., Cahill, M. J., Boyce, K. J., Klose, J., Klosterman, S. J., Deelstra, H. J., Ortiz-Castellanos, L., Li, W., Sanchez-Alonso, P., Schreier, P. H., Häuser-Hahn, I., Vaupel, M., Koopman, E., Friedrich, G., Voss, H., Schülter, T., Margolis, J., OPlatt, D., Swimmer, C., Gnirke, U., Münsterkötter, M., Hase, D., Oesterheld, M., Mewes, H. W., Mauceli, E. W., DeCaprio, D., Wade, C. W., Butler, J., Young, S., Jaffe, D. B., Calvo, S., Nusbaum, C., Galagan, J., Birren, B. W. 2006. Insights from the genome of the biotrophic fungal plant pathogen *Ustilago maydis*. Nature. 444:97-101.

Kemen, E., Kemen, A. C., Rafiqi, M., Hempel, U., Mendgen, K., Hahn, M., Voegele, R. T. 2005. Identification of a protein from the rust fungi transferred from haustoria into infected plant cells. Mol. Plant Microbe Interact.. 18:1130-1139.

Kempken, F., Kuck, U. 2000. Tagging of a nitrogen pathway-specific regulator gene in *Tolypocladium inflatum* by the transposon Restless. Mol. Gen. Genet. 263:302-308.

Kim, H., Ahn, J. H., Gorlach, J. M., Caprari, C., Scott-Craig, J. S., Walton, J. D. 2001. Mutational analysis of beta-glucanase genes from the plant-pathogenic fungus *Cochliobolus carbonum*. Mol. Plant Microbe Interact. 14:1436-43.

Kim, Y. K., Kawano, T., Li, D. X., Kolattukudy, P. E. 2000. A mitogen-activated protein kinase kinase required for induction of cytokinesis and appressorium formation by host signals in the conidia of *Colletotrichum gloeosporioides*. Plant Cell. 12:1331-1343.

Kim, Y. K., Li, D., Kolattukudy, P. E. 1998. Induction of Ca^{2+}-calmodulin signaling by hard-surface contact primes *Colletotrichum gloeosporioides* conidia to germinate and form appressoria. J. Bacteriol. 180:5144-50.

Kim, Y. K., Wang, Y., Liu, Z. M., Kolattukudy, P. E. 2002. Identification of a hard surface contact-induced gene in *Colletotrichum gloeosporioides* conidia as a sterol glycosyl transferase, a novel fungal virulence factor. Plant J. 30:177-187.

Kimura, A., Takano, Y., Furusawa, I., Okuno, T. 2001. Peroxisomal metabolic function is required for appressorium-mediated plant infection by *Colletotrichum lagenarium*. Plant Cell. 13:1945-1957.

Kleemann, J., Takahara, H., Stuber, K., O'Connell, R. 2008. Identification of soluble secreted proteins from appressoria of *Colletotrichum higginsianum* by analysis of expressed sequence tags. Microbiology. 154:1204-17.

Klimpel, A., Schilze-Gronover, C., Williamson, B., Stewart, J. A., Tudzynski, B. 2002. The adenylate cyclase (BAC) in *Botrytis cinerea* is required for full pathogenicity. Mol. Plant Pathol. 3:439-450.

Klimpel, K. R., Goldman, W. E. 1988. Cell walls from avirulent variants of *Histoplasma capsulatum* lack alpha-(1,3)-glucan. Infect. Immun. 56:2997-3000.

Koelle, M. R. 2006. Heterotrimeric G protein signaling: Getting inside the cell. Cell. 126:25-7.

Kojima, K., Kikuchi, T., Takano, Y., Oshiro, E., Okuno, T. 2002. The mitogen-activated protein kinase gene *MAF1* is essential for the early differentiation phase of appressorium formation in *Colletotrichum lagenarium*. Mol. Plant Microbe Interact. 15:1268-1276.

Kooistra, R., Hooykaas, P. J., Steensma, H. Y. 2004. Efficient gene targeting in *Kluyveromyces lactis*. Yeast. 21:781-92.

Krappmann, S., Sasse, C., Braus, G. H. 2006. Gene targeting in *Aspergillus fumigatus* by homologous recombination is facilitated in a nonhomologous end- joining-deficient genetic background. Eukaryot. Cell. 5:212-5.

Kubo, Y., Takano, Y., Endo, N., Yasuda, N., Tajima, S., Furusawa, I. 1996. Cloning and structural analysis of the melanin biosynthesis gene *SCD1* encoding scytalone dehydratase in *Colletotrichum lagenarium*. Appl. Environ. Microbiol. 62:4340-4344.

Kulkarni, R. D., Thon, M. R., Pan, H., Dean, R. A. 2005. Novel G-protein-coupled receptor-like proteins in the plant pathogenic fungus *Magnaporthe grisea*. Genome Biol. 6:R24.

Kunoh, H., Yamakoa, N., Yoshioka, H., Nicholson, R. L. 1988. Preparation of the infection ocurt by *Erysiphe graminis* I. Contact-mediated changes in morphology of the conidium surface. Exp. Mycol. 12.

Kuo, C. Y., Chou, S. Y., Huang, C. T. 2004. Cloning of glyceraldehyde-3-phosphate dehydrogenase gene and use of the *gpd* promoter for transformation in *Flammulina velutipes*. Applied Microbiology and Biotechnology. 35:593-599.

Kuspa, A. 2006. Restriction enzyme-mediated integration (REMI) mutagenesis. Methods Mol. Biol. 346:201-209.

Ladendorf, O., Brachmann, A., Kamper, J. 2003. Heterologous transposition in *Ustilago maydis*. Mol. Genet. Genomics. 269:395–405.

Lagerstedt, J. O., Voss, J. C., Wieslander, A., Persson, B. L. 2004. Structural modeling of dual-affinity purified Pho84 phosphate transporter. FEBS Lett. 578:262-8.

Lange, A., Mills, R. E., Devine, S. E., Corbett, A. H. 2008. A PY-NLS nuclear targeting signal is required for nuclear localization and function of the *Saccharomyces cerevisiae* mRNA-binding protein Hrp1. J. Biol. Chem. 283:12926-34.

Lee, B. J., Cansizoglu, A. E., Suel, K. E., Louis, T. H., Zhang, Z., Chook, Y. M. 2006. Rules for nuclear localization sequence recognition by karyopherin beta 2. Cell. 126:543-58.

Lee, C. M. Y., Aitchisin, J. D. 1999. Kap104-mediated nuclear im: nuclear localization signals in mRNA-binding protiens and the role of RAN and RNAport. J. Biol. Chem. 274:29031-23037.

Lee, D. A., Chen, A., Schroeder, J. I. 2003. *ars1*, an *Arabidopsis* mutant exhibiting increased tolerance to arsenate and increased phosphate uptake. Plant J. 35:637-646.

Lee, M. H., Bostock, R. M. 2006. *Agrobacterium* T-DNA-mediated integration and gene replacement in the brown rot pathogen *Monilinia fructicola*. Curr. Genet. 49:309-322.

Lev, S., Sharon, A., Hadar, R., Ma, H., Horwitz, B. A. 1999. A mitogen-activated protein kinase of the corn leaf pathogen *Cochliobolus heterostrophus* is involved in conidiation, appressorium formation, and pathogenicity: diverse roles for mitogen-activated protein kinase homologs in foliar pathogens. Proc. Natl. Acad Sci U S A. 96:13542-7.

Li, G., Zhou, W., Liu, G., Zheng, F., C., H. 2007. Characterization of T-DNA insertion patterns in the genome of rice blast fungus *Magnaporthe oryzae*. Curr. Genet. 51:233-243.

Li, J. R., Jin, S. M., Hsiang, T., Goodwin, P. 2001. A novel actin-related protein gene of *Colletotrichum gloeosporioides* f. sp *malvae* shows altered expression corresponding with spore production. FEMS Microbiol. Lett. 197:209-214.

Li, Y., Rosso, M. G., Ulker, B., Weisshaar, B. 2006. Analysis of T-DNA insertion site distribution patterns in Arabidopsis thaliana reveals special features of genes without insertions. Genomics. 87:645-52.

Lipka, V., Dittgen, J., Bednarek, P., Bhat, R., Wiermer, M., Stein, M., Landtag, J., Brandt, W., Rosahl, S., Scheel, D., Llorente, F., Molina, A., Parker, J., Somerville, S., Schulze-Lefert, P. 2005. Pre- and postinvasion defenses both contribute to nonhost resistance in *Arabidopsis*. Science. 310:1180-1183.

Liu, X. H., Lu, J. P., Zhang, L., Dong, B., Min, H., Lin, F. C. 2007. Involvement of a *Magnaporthe grisea* serine/threonine kinase gene, MgATG1, in appressorium turgor and pathogenesis. Eukaryot. Cell. 6:997-1005.

Liu, Z.-M., Kolattukudy, P. E. 1998. Identification of a gene product induced by hard surface contact of *Colletotrichum gloeosporioides* conidia as a ubiquitin-conjugating enzyme by yeast complementation. J. Bacteriol. 180:3592-3597.

Liu, Z. M., Kolattukudy, P. E. 1999. Early expression of the calmodulin gene, which precedes appressorium formation in *Magnaporthe grisea*, is inhibited by self-inhibitors and requires surface attachment. J. Bacteriol. 181:3571-7.

Lopez-Millan, A. F., Morales, F., Abadıa, A., Abadıa, J. 2000. Effects of iron deficiency on the composition of the leaf apoplastic fluid and xylem sap in sugar beet. Implications for iron and carbon transport. Plant Physiol. 124:873-884.

Lorito, M., Hayes, C. K., Di Pietro, A., Harman, G. E. 1993. Biolistic transformation of *Trichoderma harzinum* and *Gliocladium virens* using plasmid and genomic DNA. Curr. Genet. 24:349-356.

Lu, S., Lyngholm, L., Yang, G., Bronson, C., Yoder, O. C., Turgeon, B. G. 1994. Tagged mutations at the *Tox1* locus of *Cochliobolus heterostrophus* by restriction enzyme-mediated integration. Proc. Natl. Acad. Sci. U.S.A. 91:12649-12653.

MacHardy, W. E., Gadoury, D. M., Gessler, C. 2001. Parasitic and biological fitness of Venturia inaequalis: relationship to disease management strategies. Plant. Dis. 85:1036-1051.

Madrid, M. P., Di Pietro, A., Roncero, M. I. 2003. Class V chitin synthase determines pathogenesis in the vascular wilt fungus *Fusarium oxysporum* and mediates resistance to plant defence compounds. Mol. Microbiol. 47:257-66.

Mahlert, M., Leveleki, L., Hlubek, A., Sandrock, B., Bolker, M. 2006. Rac1 and Cdc42 regulate hyphal growth and cytokinesis in the dimorphic fungus *Ustilago maydis*. Mol. Microbiol. 59:567-78.

Maier, F. J., Schafer, W. 1999. Mutagenesis via insertional- or restriction enzyme-mediated-integration (REMI) as a tool to tag pathogenicity related genes in plant pathogenic fungi. Biol. Chem. 7-8:855-864.

Malonek, S., Meinhardt, F. 2001. *Agrobacterium tumefaciens*-mediated genetic transformation of the phytopathogenic ascomycete *Calonectria morganii*. Curr. Genet. 40:152-5.

Mansfield, J.W. 1980. Mechanisms of resistance to *Botrytis*. In: Coley-Smith JR, Verhoeff K and Jarvis WR (eds) The Biology of *Botrytis*. Academic Press, London, UK. pp. 181-218

Manteau, S., Abouna, S., Lambert, B., Legendre, L. 2003. Differential regulation by ambient pH of putative virulence factor secretion by the phytopathogenic fungus *Botrytis cinerea*. FEMS Microbiol. Ecol.. 43:359-366.

Marchand, G., Fortier, E., Neveu, B., Bolduc, S., Belzile, F., Belanger, R. R. 2007. Alternative methods for genetic transformation of *Pseudozyma antarctica*, a basidiomycetous yeast-like fungus. J. Microbiol. Methods. 70:519-27.

Martin-Hernandez, A. M., Dufresne, M., Hugouvieux, V., Melton, R., Osbourn, A. 2000. Effects of targeted replacement of the tomatinase gene on the interaction of *Septoria lycopersici* with tomato plants. Mol. Plant Microbe Interact. 13:1301-11.

Martin, F., Aerts, A., Ahren, D., Brun, A., Danchin, E. G., Duchaussoy, F., Gibon, J., Kohler, A., Lindquist, E., Pereda, V., Salamov, A., Shapiro, H. J., Wuyts, J., Blaudez, D., Buee, M., Brokstein, P., Canback, B., Cohen, D., Courty, P. E., Coutinho, P. M., Delaruelle, C., Detter, J. C., Deveau, A., DiFazio, S., Duplessis, S., Fraissinet-Tachet, L., Lucic, E., Frey-Klett, P., Fourrey, C., Feussner, I., Gay, G., Grimwood, J., Hoegger, P. J., Jain, P., Kilaru, S., Labbe, J., Lin, Y. C., Legue, V., Le Tacon, F., Marmeisse, R., Melayah, D., Montanini, B., Muratet, M., Nehls, U., Niculita-Hirzel, H., Oudot-Le Secq, M. P., Peter, M., Quesneville, H., Rajashekar, B., Reich, M., Rouhier, N., Schmutz, J., Yin, T., Chalot, M., Henrissat, B., Kues, U., Lucas, S., Van de Peer, Y., Podila, G. K., Polle, A., Pukkila, P. J., Richardson, P. M., Rouze, P., Sanders, I. R., Stajich, J. E., Tunlid, A., Tuskan, G., Grigoriev, I. V. 2008. The genome of *Laccaria bicolor* provides insights into mycorrhizal symbiosis. Nature. 452:88-92.

Martinez-Pacheco, M., Rodriguez, G., Reyna, G., Calvo-Mendez, C., Ruiz-Herrera, J. 1989. Inhibition of the yeast-mycelial transition and the morphogenesis of Mucorales by diamino butanone. Arch. Microbiol. 151:10-4.

Martinez, P., Persson, B. L. 1998. Identification, cloning and characterization of a derepressible Na^+-coupled phosphate transporter in *Saccharomyces cerevisae*. Mol. Gen. Genet.. 258:628-638.

Martinez, P., Zvyagilskaya, R., Allard, P., Persson, B. L. 1998. Physiological regulation of the derepressible phosphate transporter in *Saccharomyces cerevisiae*. J Bacteriol. 180:2253-6.

Marton, L. J., Pegg, A. E., Morris, D. R. 1991. Directions for polyamine research. J Cell. Biochem. 45:7-8.

Maruthachalam, K., Nair, V., Rho, H. S., Choi, J., Kim, S., Lee, Y. H. 2008. *Agrobacterium tumefaciens*-mediated transformation in *Colletotrichum falcatum* and *C. acutatum*. J. Microbiol. Biotechnol. 18:234-41.

Mayer, A. M., Staples, R. C., Gil-ad, N. L. 2001. Mechanisms of survival of necrotrophic fungal plant pathogens in hosts expressing the hypersensitive response. Phytochemistry. 58:33-41.

Mayorga, M. E., Gold, S. E. 1999. A MAP kinase encoded by the ubc3 gene of *Ustilago maydis* is required for filamentous growth and full virulence. Mol. Microbiol. 34:485-97.

Mehrabi, R., Zwiers, L.-H., de Waard, M. A., Kema, G. H. J. 2006. *MgHog1* regulates dimorphism and pathogenicity in the fungal wheat pathogen *Mycosphaerella graminicola*. Mol. Plant Microbe Interact.. 19:1262-1269.

Mendgen, K., Hahn, M. 2002. Plant infection and the establishment of fungal biotrophy. Trends Plant Sci. 7:352-356.

Meng, Y., Patel, G., Heist, M., Betts, M. F., Tucker, S. L., Galadima, N., Donofrio, N. M., Brown, D., Mitchell, T. K., Li, L., Xu, J. R., Orbach, M., Thon, M., Dean, R. A., Farman, M. L. 2007. A systematic analysis of T-DNA insertion events in **Magnaporthe oryzae.** Fungal Genet. Biol. 44:1050-64.

Mercure, E. W., Kunoh, H., Nicholson, R. L. 1995. Visualisation of materials released from adhered, ungerminated conidia of *Colletotrichum graminicola*. Physiol. Mol. Plant. Pathol. 46:121-135.

Mercure, E. W., Leite, B., Nicholson, R. L. 1994. Adhesion of ungerminated conidia of *Colletotrichum graminicola* to artificial hydrophibic surfaces. Physiol. Mol. Plant. Pathol. 45:421.

Meyer, V., Mueller, D., Strowig, T., Stahl, U. 2003. Comparison of different transformation methods for Aspergillus giganteus. Curr. Genet. 43:371-7.

Michielse, C. B., Hooykaas, P. J. J., van den Hondel, C., Ram, A. F. J. 2005. *Agrobacterium*-mediated transformation as a tool for functional genomics in fungi. Curr.Genet. 48:1-17.

Mimura, T., Yin, Z.-H., Wirth, E., Dietz, K.-J. 1992. Phosphate transport and apoplastic phosphate homeostasis in barley leaves. Plant Cell Physiol. 33:563-568.

Minguet, E. G., Vera, F., Marina, A., Carbonell, J., Blazquez, M. A. 2008. Evolutionary diversification in polyamine biosynthesis. Mol. Biol. Evol.

Mishra, N. C., Tatum, E. L. 1973. Non-Mendelian inheritance of DNA-mediated inositol independence in *Neurospora*. Proc. Natl. Acad. Sci. U.S.A. 70:3875-3879.

Molina, L., Kahmann, R. 2007. An *Ustilago maydis* gene involved in H2O2 detoxification is required for virulence. Plant Cell. 19:2293-309.

Morgan, W., Kamoun, S. 2007. RXLR effectors of plant pathogenic oomycetes. Curr. Opin. Microbiol. 10:332-8.

Morishita, R., Kawagoshi, A., Sawasaki, T., Madin, K., Ogasawara, T., Oka, T., Endo, Y. 1999. Ribonuclease activity of rat liver perchloric acid-soluble protein, a potent inhibitor of protein synthesis. J. Biol. Chem. 274:20688-92.

Mosammaparast, N., Pemberton, L. F. 2004. Karyopherins: from nuclear-transport mediators to nuclear function regulator. Trends Cell Biol. 14:547-556.

Mouyna, I., Sarfati, J., Recco, P., Fontaine, T., Henrissatz, B., Latge, J. P. 2002. Molecular characterization of a cell wall-associated beta(1-3)endoglucanase of *Aspergillus fumigatus*. Med. Mycol. 40:455-64.

Mullins, E. D., Chen, X., Romaine, P., Raina, R., Geiser, D. M., Kang, S. 2001. *Agrobacterium*-mediated transformation of *Fusarium oxysporum*: An efficient tool for insertional mutagenesis and gene transfer. Phytopathology. 91:173-180.

Mullins, E. D., Kang, S. 2001. Transformation: a tool for studying fungal pathogens of plants. Cell. Mol. Life Sci. 58:2043-2052.

Nakielny, S., Dreyfuss, G. 1997. Nuclear export of proteins and RNAs. Curr. Opin. Cell Biol. 9:420-9.

Namiki, F., Matsunaga, M., Okuda, M., Inoue, I., Nishi, K., Fujita, Y., Tsuge, T. 2001. Mutation of an arginine biosynthesis gene causes reduced pathogenicity in *Fusarium oxysporum* f. sp. *melonis*. Mol. Plant Microbe Interact. 14:580-4.

Narusaka, Y., Narusaka, M., Park, P., Kubo, Y., Hirayama, T., Seki, M., Shiraishi, T., Ishida, J., Nakashima, M., Enju, A., Sakurai, T., Satou, M., Kobayashi, M., Shinozaki, K. 2004. RCH1, a locus in *Arabidopsis* that confers resistance to the hemibiotrophic fungal pathogen *Colletotrichum higginsianum*. Mol. Plant Microbe Interact.. 17:749-762.

Nayak, T., Szewczyk, E., Oakley, C. E., Osmani, A., Ukil, L., Murray, S. L., Hynes, M. J., Osmani, S. A., Oakley, B. R. 2006. A versatile and efficient gene-targeting system for *Aspergillus nidulans*. Genetics. 172:1557-66.

Ninomiya, Y., Suzuki, K., Ishii, C., Inoue, H. 2004. Highly efficient gene replacements in Neurospora strains deficient for nonhomologous end-joining. Proc. Natl. Acad. Sci. U.S.A. 101:12248-53.

Nishida, E., Gotoh, Y. 1993. The MAP kinase cascade is essential for diverse signal transduction pathways. Trends Biochem. Sci. 18:128-31.

Nishimura, M. T., Stein, M., Hou, B.-H., Vogel, J. P., Edwards, H., Somerville, S. C. 2003. Loss of a callose synthase results in salicylic acid-dependent disease resistance. Science. 301:969-972.

O'Connell, R. J. 1987. Absence of a specialised interface between infection hyphae of *Colletotrichum lindemuthianum* and *Phaseolus vulgaris*. New Phytol. 107:725-734.

O'Connell, R. J., Herbert, C., Sreenivasaprasad, S., Khatib, M., Esquerre-Tugaye, M. T., Dumas, B. 2004. A novel *Arabidopsis-Colletotrichum* pathosystem for the Mol. dissection of plant-fungal interactions. Mol. Plant Microbe Interact.. 17:272-282.

Oeser, B., Heidrich, P. M., Muller, U., Tudzynski, P., Tenberge, K. B. 2002. Polygalacturonase is a pathogenicity factor in the Claviceps purpurea/rye interaction. Fungal Genet Biol. 36:176-86.

Okuno, T., Ishita, Y., Sawai, K., Matsumoto, T. 1974. Characterization of alternariolide, a host-specific toxin produced by *Alternaria mali* Roberts. Chem. Lett. . 1974:635-638.

Ortega, J. 1996. Pectolytic activity produced by the phytopathogenic fungus *Colletotrichum gloeosporiodes*. Tex. J. Sci. 48:123-128.

Ozeki, K., Kyoya, F., Hizume, K., Hamachi, M., Nunokawa, Y. 1994. Transformation of intact *Aspergillus niger* by electroporation. Biosci. Biotech. Biochem. 58:2224-2227.

Pan, X., Li, Y., Stein, L. 2005. Site preferences of insertional mutagenesis agents in *Arabidopsis*. Plant Physiol. 137:168-75.

Parisot, D., Dufresne, M., Veneault, C., Lauge, R., Langin, T. 2002. *clap1*, a gene encoding a copper-transporting ATPase involved in the process of infection by the phytopathogenic fungus *Colletotrichum lindemuthianum*. Mol. Genet. Genomics. 268:139-151.

Parker, D. M., Hilber, U. W., Bodmer, M. 1995. Production and transformation of conidia of *Venturia inaequalis*. Phytopathology. 85:87-91.

Patton-Vogt, J. L., Henry, S. A. 1998. GIT1, a gene encoding a novel transporter for glycerophosphoinositol in *Saccharomyces cerevisiae*. Genetics. 149:1707-15.

Pellier, A. L., Lauge, R., Veneault-Fourrey, C., Langin, T. 2003. CLNR1, the AREA/NIT2-like global nitrogen regulator of the plant fungal pathogen *Colletotrichum lindemuthianum* is required for the infection cycle. Mol. Microbiol. 48:635-655.

Perfect, S. E., Connell, R. J., Green, E. F., Doering-Saad, C., Green, J. R. 1998. Expression cloning of a fungal proline rich glycoprotein specific to the biotrophic interface formed in the *Colletotrichum*-bean interaction. Plant J. 15:273-279.

Perfect, S. E., Green, J. R. 2001. Infection structures of biotrophic and hemibiotrophic fungal plant pathogens. Mol. Plant Pathol. 2:101-108.

Perfect, S. E., Hughes, H. B., O'Connell, R. J., Green, J. R. 1999. Colletotrichum: a model genus for studies on pathology and fungal-plant interactions. Fungal Genet. Biol. 27:186-198.

Perfect, S. E., Pixton, K. L., O'Connell, R. J., Green, J. R. 2000. The distribution and expression of a biotrophy-related gene, *CIH1*, within the genus *Colletotrichum*. Mol. Plant Pathol. 1:213-221.

Perpetua, N. S., Kubo, Y., Yasuda, N., Takano, Y., Furusawa, I. 1996. Cloning and characterization of a melanin biosynthetic *THR1* reductase gene essential for appressorial penetration of *Colletotrichum lagenarium*. Mol. Plant Microbe Interact.. 9:323-329.

Petersson, J., Pattison, J., Kruckeberg, A. L., Berden, J. A., Persson, B. L. 1999. Intracellular localization of an active green fluorescent protein-tagged Pho84 phosphate permease in *Saccharomyces cerevisiae*. FEBS Lett. 462:37-42.

Piers, K. L., Heath, J. D., Liang, X., Stephens, K. M., Nester, E. W. 1996. *Agrobacterium tumefaciens*-mediated transformation of yeast. Proc. Natl. Acad. Sci. U.S.A. 4:1613-1318.

Podila, G. K., Rogers, L. M., Kolattukudy, P. E. 1993. Chemical signals from avocado Surface wax trigger germination and appressorium formation in C*olletotrichum gloeosporioides*. Plant Physiol. 103:267-272.

Poggeler, S., Kuck, U. 2006. Highly efficient generation of signal transduction knockout mutants using a fungal strain deficient in the mammalian ku70 ortholog. Gene. 378:1-10.

Popolo, L., Vai, M. 1999. The Gas1 glycoprotein, a putative wall polymer cross-linker. Biochim. Biophys. Acta. 1426:385-400.

Prusky, D., McEvoy, J. L., Leverentz, B., Conway, W. S. 2001. Local modulation of host pH by *Colletotrichum* species as a mechanism to increase virulence. Mol. Plant Microbe Interact. 14:1105-1113.

Pryce-Jones, E., Carver, T. L. W., Gurr, S. J. 1999. The roles of cellulase enzymes and mechanical force in host penetration by *Erysiphe graminis* f. sp. *hordei*. Physiol. Mol. Plant. Pathol. 55:175-182.

Quadbeck-Seeger, C., Wanner, G., Huber, S., Kahmann, R., Kamper, J. 2000. A protein with similarity to the human retinoblastoma binding protein 2 acts specifically as a repressor for genes regulated by the b mating type locus in *Ustilago maydis*. Mol. Microbiol. 38:154-66.

Rajam, M. V., Weinstein, L. H., Galston, A. W. 1985. Prevention of a plant disease by specific inhibition of fungal polyamine biosynthesis. Proc. Natl. Acad. Sci. U.S.A. 82:6874-8.

Redman, R. S., Ranson, J. C., Rodriguez, R. J. 1999. Conversion of the pathogenic fungus *Colletotrichum magna* to a nonpathogenic, endophytic mutualist by gene disruption. Mol. Plant Microbe Interact.. 12:969-975.

Reichmann, M., Jamnischek, A., Weinzierl, G., Ladendorf, O., Huber, S., Kahmann, R., Kamper, J. 2002. The histone deacetylase Hda1 from *Ustilago maydis* is essential for teliospore development. Mol. Microbiol. 46:1169-82.

Reilly, T. J., Baron, G. S., Nano, F. E., Kuhlenschmidt, M. S. 1996. Characterization and sequencing of a respiratory burst-inhibiting acid phosphatase from *Francisella tularensis*. J. Biol. Chem. 271:10973-83.

Reitz, M., Waiters, D., Moerschbacher, B. 1995. Germination and appressorial formation by uredospores of *Uromyces viciae-fabae* exposed to inhibitors of polyamine biosynthesis. Eur. J. Plant Pathol 101:573-578.

Rengarajan, J., Bloom, B. R., Rubin, E. J. 2005. Genome-wide requirements for Mycobacterium tuberculosis adaptation and survival in macrophages. Proc. Natl. Acad. Sci. U.S.A. 102:8327-32.

Reyes, I., Bernier, L., Antoun, H. 2002. Rock phosphate solubilization and colonization of maize rhizosphere by wild and genetically modified strains of *Penincillium rugulosum*. Microb. Ecol. 44:39-48.

Reyna-Lopez, G. E., Ruiz-Herrera, J. 2004. Specificity of DNA methylation changes during fungal dimorphism and its relationship to polyamines. Curr. Microbiol. 48:118-23.

Rho, H. S., Kang, S., Lee, Y. H. 2001. *Agrobacterium tumefaciens*-mediated transformation of the plant pathogenic fungus, *Magnaporthe grisea*. Mol. Cells 12:407-411.

Riggle, P. J., Kumamoto, C. A. 1998. Genetic analysis in fungi using restriction-enzyme-mediated integration. Curr. Opin. Microbiol. 1:395-399.

Rivas, S., Thomas, C. M. 2005. Mol. interactions between tomato and the leaf mold pathogen *Cladosporium fulvum*. Annu. Rev. Phytopathol. 43:395-436.

Robson, G. D., Wiebe, M. G., Trinci, A. P. J. 1991. Involvement of Ca2+ in the regulation of hyphal extension and branching in *Fusarium graminearum* A 3/5. Exp. Mycol. 15:263-272.

Rogers, C. W., Challen, M. P., Green, J. R., Whipps, J. M. 2004. Use of REMI and *Agrobacterium*-mediated transformation to identify pathogenicity mutants of the biocontrol fungus, *Coniothyrium minitans*. FEMS Microbiol. Lett. 241:207-214.

Rolland, S., Jobic, C., Fevre, M., Bruel, C. 2003. *Agrobacterium*-mediated transformation of *Botrytis cinerea*, simple purification of monokaryotic transformants and rapid conidia-based identification of the transfer-DNA host genomic DNA flanking sequences. Curr. Genet. 44:164-71.

Roohparvar, R., De Waard, M. A., Kema, G. H., Zwiers, L. H. 2006. MgMfs1, a major facilitator superfamily transporter from the fungal wheat pathogen *Mycosphaerella graminicola*, is a strong protectant against natural toxic compounds and fungicides. Fungal Genet. Biol.

Rosas, A. L., Casadevall, A. 2001. Melanization decreases the susceptibility of *Cryptococcus neoformans* to enzymatic degradation. Mycopathologia. 151:53-6.

Saha, A. K., Dowling, J. N., LaMarco, K. L., Das, S., Remaley, A. T., Olomu, N., Pope, M. T., Glew, R. H. 1985. Properties of an acid phosphatase from *Legionella micdadei* which blocks superoxide anion production by human neutrophils. Arch. Biochem. Biophys. 243:150-60.

Sakaguchi, A., Miyaji, T., Tsuji, G., Kubo, Y. 2008. Kelch repeat protein Clakel2p and calcium signaling control appressorium development in *Colletotrichum lagenarium*. Eukaryot. Cell. 7:102-11.

Saleh, M. T., Belisle, J. T. 2000. Secretion of an acid phosphatase (SapM) by *Mycobacterium tuberculosis* that is similar to eukaryotic acid phosphatases. J. Bacteriol. 182:6850-3.

San-Blas, G., San-Blas, F., Serrano, L. E. 1977. Host-parasite relationships in the yeastlike form of *Paracoccidioides brasiliensis* strain IVIC Pb9. Infect. Immun. . 15:343–346.

Schmiedeknecht, G., Kerkhoff, C., Orso, E., Stohr, J., Aslanidis, C., Nagy, G. M., Knuechel, R., Schmitz, G. 1996. Isolation and characterization of a 14.5-kDa trichloroacetic-acid-soluble translational inhibitor protein from human monocytes that is upregulated upon cellular differentiation. Eur. J. Biochem. 242:339-51.

Schneeberger, R. G., Zhang, K., Tatarinova, T., Troukhan, M., Kwok, S. F., Drais, J., Klinger, K., Orejudos, F., Macy, K., Bhakta, A., Burns, J., Subramanian, G., Donson, J., Flavell, R., Feldmann, K. A. 2005. *Agrobacterium* T-DNA integration in *Arabidopsis* is correlated with DNA sequence compositions that occur frequently in gene promoter regions. Funct. Integr. Genomics. 5:240-53.

Schoonbeek, H., Del Sorbo, G., De Waard, M. A. 2001. The ABC transporter BcatrB affects the sensitivity of *Botrytis cinerea* to the phytoalexin resveratrol and the fungicide fenpiclonil. Mol. Plant Microbe Interact. 14:562-71.

Schouten, A., van Baarlen, P., van Kan, J. A. 2008. Phytotoxic Nep1-like proteins from the necrotrophic fungus *Botrytis cinerea* associate with membranes and the nucleus of plant cells. New Phytol. 177:493-505.

Seong, K., Hou, Z., Tracy, M., Kistler, H. C., Xu, J. R. 2005. Random insertional mutagenesis identies genes associated with virulence in the wheat scab fungus *Fusarium graminearum*. Phytopathology. 95:744-750.

Shih, J., Wei, Y. D., Goodwin, P. H. 2000. A comparison of the pectate lyase genes, *pel-1* and *pel-2*, of *Colletotrichum gloeosporiodes* f. sp. *malvae* and the relationship between their expression in culture and during necrotrophic infection. Gene. 243:139-150.

Shimada, C., Lipka, V., O'Connell, R., Okuno, T., Schulze-Lefert, P., Takano, Y. 2006. Nonhost resistance in *Arabidopsis-Colletotrichum* interactions acts at the cell periphery and requires actin filament function. Mol. Plant Microbe Interact.. 19:270-279.

Siriputthaiwan, P., Jauneau, A., Herbert, C., Garcin, D., Dumas, B. 2005. Functional analysis of CLPT1, a Rab/GTPase required for protein secretion and pathogenesis in the plant fungal pathogen *Colletotrichum lindemuthianum*. J. Cell Sci. 118:323-329.

Skamnioti, P., Gurr, S. J. 2007. *Magnaporthe grisea* cutinase2 mediates appressorium differentiation and host penetration and is required for full virulence. Plant Cell. 19:2674-89.

Skinner, W., Keon, J. P. R., Hargreaves, J. 2001. Gene information for fungal plant pathogens from expressed sequences. Curr. Opin. Microbiol. 4:381-386.

Solomon, P. S., Oliver, R. P. 2001. The nitrogen content of the tomato leaf apoplast increases during infection by *Cladosporium fulvum*. Planta. 213:241-9.

Solomon, P. S., Oliver, R. P. 2002. Evidence that gamma-aminobutyric acid is a major nitrogen source during *Cladosporium fulvum* infection of tomato. Planta. 214:414-20.

Soulie, M. C., Piffeteau, A., Choquer, M., Boccara, M., Vidal-Cros, A. 2003. Disruption of *Botrytis cinerea* class I chitin synthase gene Bcchs1 results in cell wall weakening and reduced virulence. Fungal Genet Biol. 40:38-46.

Stein, M., Dittgen, J., Sanchez-Rodriguez, C., Hou, B. H., Molina, A., Schulze-Lefert, P., Lipka, V., Somerville, S. 2006. Arabidopsis PEN3/PDR8, an ATP binding cassette transporter, contributes to nonhost resistance to inappropriate pathogens that enter by direct penetration. Plant Cell. 18:731-746.

Stephenson, S. A., Green, J. R., Manners, J. M., Maclean, D. J. 1997. Cloning and characterisation of glutamine synthetase from *Colletotrichum gloeosporioide*s and demonstration of elevated expression during pathogenesis on Stylosanthes guianensis. Curr. Genet. 31:447-54.

Stephenson, S. A., Hatfield, J., Rusu, A. G., Maclean, D. J., Manners, J. M. 2000. *CgDN3*: An essential pathogenicity gene of *Colletotrichum gloeosporioides* necessary to avert a hypersensitive-like response in the host *Stylosanthes guianensis*. Mol. Plant Microbe Interact.. 13:929-941.

Sugai, J. A., Leite, B., Nicholson, R. L. 1998. Partial characterization of the extracellular matrix released onto hydrophobic surfaces by conidia and conidial germlings of *Colletotrichum graminicola*. Physiol. Mol. Plant Pathol. 52:411-425.

Sunawaga, M., Magae, Y. 2002. Transformation of the edible mushroom *Pleurotus ostreatus* by particle bombardment. FEMS Microbiol. Lett. 211:143-146.

Sweigard, J. A., Carroll, A. M., Farrall, L., Chumley, F. G., Valent, B. 1998. *Magnaporthe grisea* pathogenicity mutants obtained through insertional mutagenesis. Mol. Plant Microbe Interact. 11:404-412.

Tabor, C. W., Tabor, H. 1985. Polyamines in microorganisms. Microbiol. Rev. 49:81-99.

Takahara, H., Tsuji, G., Kubo, Y., Yamamoto, M., Toyoda, K., Inagaki, Y., Ichinose, Y., Shiraishi, T. 2004. *Agrobacterium tumefaciens* mediated transformation as a tool for random mutagenesis of *Colletotrichum trifolii*. J. Gen. Plant Pathol. 70:93-96.

Takahashi, T., Masuda, T., Koyama, Y. 2006. Enhanced gene targeting frequency in ku70 and ku80 disruption mutants of *Aspergillus sojae* and *Aspergillus oryzae*. Mol. Genet.Genomics. 275:460-70.

Takano, Y., Kikuchi, H., Kubo, Y., Hamer, J. E., Mise, K., Furusawa, I. 2000. The *Colletotrichum lagenarium* MAP kinase gene *CMK1* regulates diverse aspects of fungal pathogenesis. Mol. Plant Microbe Interact. 13:374-383.

Takano, Y., Komeda, K., Kojima, K., Okuno, T. 2001. Proper regulation of cyclic AMP-dependent protein kinase is required for growth, conidiation, and appressorium function in the anthractnose fungus *Colletotrichum lagenarium*. Mol. Plant Microbe Interact. 14:1149-1157.

Takano, Y., Kubo, Y., Kawamura, C., Tsuge, T., Furusawa, I. I. 1997. The *Alternaria alternata* melanin biosynthesis gene restores appressorial melanization and penetration of cellulose membranes in the melanin-deficient albino mutant of *Colletotrichum lagenarium*. Fungal Genet. Biol. 21:131-40.

Takano, Y., Kubo, Y., Shimizu, K., Mise, K., Okuno, T., Furusawa, I. 1995. Structural analysis of *pks1*, a polyketide synthase gene involved in melanin biosynthesis in *Colletotrichum lagenarium*. Mol. Gen. Genet. 249:162-167.

Takano, Y., Takayanagi, N., Hori, H., Ikeuchu, Y., Suzuki, T., Kimura, A., Okuno, T. 2006. A gene involved in modifying transfer RNA is required for fungal pathogenicity and stress tolerance of *Colletotrichum lagenarium*. Mol. Microbiol. 60:81-92.

Talbot, N. J., Ebbole, D. J., Hamer, J. E. 1993. Identification and characterization of MPG1, a gene involved in pathogenicity from the rice blast fungus *Magnaporthe grisea*. Plant Cell. 5:1575-90.

Talbot, N. J., Kershaw, M. J., Wakley, G. E., De Vries, O., Wessels, J., Hamer, J. E. 1996. MPG1 encodes a fungal hydrophobin involved in surface interactions during infection-related development of *Magnaporthe grisea*. Plant Cell. 8:985-999.

Talhinhas, P., Muthumeenakshi, S., Neves-Martins, J., Oliveira, H., Sreenivasaprasad, S. 2008. *Agrobacterium*-mediated transformation and insertional mutagenesis in *Colletotrichum acutatum* for investigating varied pathogenicity lifestyles. Mol. Biotechnol. 39:57-67.

Tanaka, S., Yamada, K., Yabumoto, K., Fuki, S., Huser, A., Tsuji, G., Koga, H., Dohi, K., Mori, M., Shiraishi, O'Connell, R.,T., Kubo, Y. 2007. *Saccharomyces cerevisiae SSD1* orthologues are essential for host infection by the ascomycete plant pathogens *Colletotrichum lagenarium* and *Magnaporthe grisea*. Mol. Microbiol. 64:1332-1349.

Tang, W., Coughlan, S., Crane, E., Beattly, M., Duvick, J. 2006. The application of laser microdissection to in planta gene expression profiling of the maize anthracnose stalk rot fungus *Colletotrichum graminicola*. Mol. Plant Microbe Interact. 19:1240-1250.

Tanguay, P., Breuil, C. 2003. Transforming the sapstaining fungus *Ophiostoma piceae* with *Agrobacterium*-mediated transformation. Can. J. Microbiol. 49:301-304.

Tekaia, F., Latge, J. P. 2005. *Aspergillus fumigatus*: saprophyte or pathogen? Curr. Opin. Microbiol. 8:385-92.

Thines, E., Weber, R. W., Talbot, N. J. 2000. MAP kinase and protein kinase A-dependent mobilization of triacylglycerol and glycogen during appressorium turgor generation by *Magnaporthe grisea*. Plant Cell. 12:1703-18.

Thomas, S. W., Rasmussen, S. W., Glaring, M. A., Rouster, J. A., Christiansen, S. K., Oliver, R. P. 2001. Gene identification in the obligate fungal pathogen *Blumeria graminis* by expressed sequence tag analysis. Fungal Genet. Biol. 33:195-211.

Thon, M. R., Nuckles, E. M., Takach, J. E., Vaillancourt, L. J. 2002. *CPR1*: A gene encoding a putative signal peptidase that functions in pathogenicity of *Colletotrichum graminicola* to maize. Mol. Plant Microbe Interact. 15:120-128.

Thon, M. R., Nuckles, E. M., Vaillancourt, L. J. 2000. Restriction enzyme-mediated integration used to produce pathogenicity mutants of *Colletotrichum graminicola*. Mol. Plant Microbe Interact. 13:1356-1365.

Thordal-Christensen, H., Zhang, Z., Wei, Y. D., Collinge, D. B. 1997. Subcellular localization of H_2O_2 in plants. H_2O_2 accumulation in papillae and hypersensitive response during the barley-powdery mildew interaction. Plant J. 11 1187-1194.

Tonukari, N. J., Scott-Craig, J. S., Walton, J. D. 2000. The *Cochliobolus carbonum* SNF1 gene is required for cell wall-degrading enzyme expression and virulence on maize. Plant Cell. 12:237-48.

Truant, R., Kang, Y., Cullen, B. R. 1999. The human tap nuclear RNA export factor contains a novel transportin-dependent nuclear localization signal that lacks nuclear export signal function. J. Biol. Chem. 274:32167-71.

Tsuji, G., Fujii, S., Fujihara, N., Hirose, C., Tsuge, S., Shiraishi, T., Kubo, Y. 2003. *Agrobacterium tumefaciens*-mediated transformation for random insertional mutagenesis in *Colletotrichum lagenarium*. J. Gen. Plant Pathol. 69:230-239.

Tsuji, G., Fujii, S., Tsuge, S., Shiraishi, T., Kubo, Y. 2003. The *Colletotrichum lagenarium* Ste12-like gene *CST1* is essential for appressorium penetration. Mol. Plant Microbe Interact. 16:315-325.

Tsuji, G., Kenmochi, Y., Takano, Y., Sweigard, J., Farrall, L., Furusawa, I., Horino, O., Kubo, Y. 2000. Novel fungal transcriptional activators, *Cmr1p* of *Colletotrichum lagenarium* and *pig1p* of *Magnaporthe grisea*, contain Cys2His2 zinc finger and Zn(II)2Cys6 binuclear cluster DNA-binding motifs and regulate transcription of melanin biosynthesis genes in a developmentally specific manner. Mol. Microbiol. 38:940-954.

Tsurushima, T., Dinh Don, L., Kawashima, K., Murakami, J., Nakayashiki, H., Tosa, Y., Mayama, S. 2005. Pyrichalasin H production and pathogenicity of *Digitaria*-specific isolates of *Pyricularia grisea*. Mol. Plant Pathol. 6:605–613.

Tucker, S. L., Talbot, N. J. 2001. Surface attachment and pre-penetration stage development by plant pathogenic fungi. Annu. Rev. Phytopathol. 39:385.

Tudzynski, P. and Scheffer, J. 2004. *Claviceps purpurea*: molecular aspects of a unique pathogenic lifestyle. Mol. Plant Pathol. 5, 377–388.

Uhm, K. H., Ahn, L. P., Kim, S., Lee, Y. H. 2003. Calcium/calmodulin-dependent signaling for prepenetration development in *Colletotrichum gloeosporioides*. Phytopathology 93:82-87.

Urban, M., Bhargava, T., Hamer, J. E. 1999. An ATP-driven efflux pump is a novel pathogenicity factor in rice blast disease. EMBO J. 18:512-521.

van Esse, H. P., Bolton, M. D., Stergiopoulos, I., de Wit, P. J., Thomma, B. P. 2007. The chitin-binding *Cladosporium fulvum* effector protein Avr4 is a virulence factor. Mol. Plant Microbe Interact. 20:1092-101.

van Kan, J. A. 2006. Licensed to kill: the lifestyle of a necrotrophic plant pathogen. Trends Plant Sci. 11:247-53.

Veneault-Fourrey, C., Barooah, M., Egan, M., Wakley, G., Talbot, N. J. 2006. Autophagic fungal cell death is necessary for infection by the rice blast fungus. Science. 312:580-583.

Veneault-Fourrey, C., Lambou, K., Lebrun, M. H. 2006. Fungal Pls1 tetraspanins as key factors of penetration into host plants: a role in re-establishing polarized growth in the appressorium? FEMS Microbiol. Lett. 256:179-184.

Veneault-Fourrey, C., Parisot, D., Gourgues, M., Lauge, R., Lebrun, M. H., Langin, T. 2005. The tetraspanin gene *ClPLS1* is essential for appressorium-mediated penetration of the fungal pathogen *Colletotrichum lindemuthianum*. Fungal Genet. Biol. 42:306-318.

Viaud, M. C., Balhadere, P. V., Talbot, N. J. 2002. A *Magnaporthe grisea* cyclophilin acts as a virulence determinant during plant infection. Plant Cell. 14:917-30.

Vijayaraghavan, Y., Kapoor, M. 1996. Disruption of the NAD(+)-specific glutamate dehydrogenase of *Neurospora crassa* by means of the RIP (repeat-induced point mutations) process. Biochem. Cell Biol. 74:29-40.

Vijn, I., Govers, F. 2003. *Agrobacterium tumefaciens* mediated transformation of the oomycete plant pathogen *Phytophtora infestans*. Mol. Plant Pathol. 4:459-467.

Villalba, F., Collemare, J., Landraud, P., Lambou, K., Brozek, V., Cirer, B., Morin, D., Bruel, C., Beffa, R., Lebrun, M. H. 2008. Improved gene targeting in *Magnaporthe grisea* by inactivation of MgKU80 required for non-homologous end joining. Fungal Genet. Biol. 45:68-75.

Villalba, F., Lebrun, M.-H., Hua-Van, A., Daboussi, M. J., Grosjean-Cournoyer, M.-C. 2001. Transposon *impala*, a novel tool for gene tagging in the rice blast fungus *Magnaporthe grisea*. Mol. Plant Microbe Interact. 14:308-315.

Voegele, R. T., Hahn, M., Lohaus, G., Link, T., Heiser, I., Mendgen, K. 2005. Possible roles for mannitol and mannitol dehydrogenase in the biotrophic plant pathogen *Uromyces fabae*. Plant Physiol. 137:190-198.

Voegele, R. T., Struck, C., Hahn, M., Mendgen, K. 2001. The role of haustoria in sugar supply during infection of broad bean by the rust fungus *Uromyces fabae*. Proc. Natl. Acad. Sci. U.S.A. 98:8133-8138.

Voegele, R. T., Wirsel, S., Möll, U., Lechner, M., Mendgen, K. 2006. Cloning and characterisation of a novel invertase from the obligate biotroph *Uromyces fabae* and analysis of expression patterns of host and pathogen invertases in the course of infection. Mol. Plant Microbe Interact. 19:625-634.

Walters, D. R. 1995. Inhibition of polyamine biosynthesis in fungi. Mycol. Res. 99:129-139.

Walton, F. J., Idnurm, A., Heitman, J. 2005. Novel functions required for melanization of the human pathogen *Cryptococcus neoformans*. Mol. Microbiol. 57:1381-1386.

Wang, Z. Y., Soanes, D. M., Kershaw, M. J., Talbot, N. J. 2007. Functional analysis of lipid metabolism in *Magnaporthe grisea* reveals a requirement for peroxisomal fatty acid ß-oxidation during appressorium-mediated plant infection. Mol. Plant Microbe Interact. 20:475-491.

Wang, Z. Y., Thornton, C. R., Kershaw, M. J., Debao, L., Talbot, N. J. 2003. The glyoxylate cycle is required for temporal regulation of virulence by the plant pathogenic fungus *Magnaporthe grisea*. Mol. Microbiol. 47:1601-1612.

Ward, M., Kodama, K. H., Wilson, L. J. 1989. Transformation of *Aspergillus awamori* and *A. niger* by electroporation. Exp. Mycol. 13:289-293.

Warwar, V., Dickman, M. B. 1996. Effects of calcium and calmodulin on spore germination and appressorium development in *Colletotrichum trifolii*. Appl. Environ. Microbiol. 62:74-79.

Warwar, V., Oved, S., Dickman, M. B. 2000. Antisense expression of the calmodulin gene from *Colletotrichum trifolii* impairs prepenetration development(1). FEMS Microbiol. Lett. 191:213-9.

Wasmann, C., VanEtten, H. D. 1996. Transformation-mediated chromosome loss and disruption of a gene for pisatin demethylase decrease the virulence of *Nectria haematococca* on pea. Mol. Plant Microbe Interact. 9:793-803.

Wei, Y., Shih, J., Li, J., Goodwin, P. H. 2002. Two pectin lyase genes, pnl-1 and pnl-2, from *Colletotrichum gloeosporioides* f. sp. *malvae* differ in a cellulose-binding domain and in their expression during infection of *Malva pusilla*. Microbiology. 148:2149-57.

Weiergang, I. I., Dunkle, L. D., Wood, K. V., Nicholson, R. L. 1996. Morphogenic rRegulation of pathotoxin synthesis in *Cochliobolus carbonum*. Fungal Genet. Biol. 20:74-8.

Weld, R. J., Eady, C. C., Ridgway, H. J. 2006. *Agrobacterium*-mediated transformation of *Sclerotinia sclerotiorum*. J. Microbiol. Methods. 65:202-7.

Weld, R. J., Plummer, K. M., Carpenter, M. A., Ridgway, H. J. 2006. Approaches to functional genomics in filamentous fungi. Cell Research. 16:31-44.

Werner, S., Sugui, J. A., Steinberg, G., Deising, H. B. 2007. A chitin synthase with a myosin-like motor domain is essential for hyphal growth, appressorium differentiation, and pathogenicity of the maize anthracnose fungus *Colletotrichum graminicola*. Mol Plant Microbe Interact. 20:1555-67.

Whisson, S. C., Boevink, P. C., Moleleki, L., Avrova, A. O., Morales, J. G., Gilroy, E. M., Armstrong, M. R., Grouffaud, S., van West, P., Chapman, S., Hein, I., Toth, I. K., Pritchard, L., Birch, P. R. 2007. A translocation signal for delivery of oomycete effector proteins into host plant cells. Nature. 450:115-8.

White, D., Chen, W. 2006. Genetic transformation of *Ascochyta rabiei* using *Agrobacterium*-mediated transformation. Curr. Genet. 49:272-280.

Williams, R. J. P. 1992. Calcium and calmodulin. Cell Calcium. 13:355–362.

Wright, A. J., Carver, T. L. W., Thomas, B. J., Fenwick, N. I. D., Kunoh, H., Nicholson, R. L. 2000. The rapid and accurate determination of germ tube emergence site by *Blumeria graminis* conidia. Physiol. Mol. Plant. Pathol. 57:281-301.

Wykoff, D. D., O'Shea, E. K. 2001. Phosphate transport and sensing in *Saccharomyces cerevisae*. Genetics. 159:1491-1499.

Wynn, W. K. 1976. Appressorium formation over stomates by the bean rust fungus: response to the surface contact stimulus. Phytopathology. 66:136-146.

Xiao, J. Z., Ohshima, A., Kamakura, T., Ishiyama, T., Yamaguchi, I. 1994. Extracellular glycoprotein(s) associated with cellular-differentiation in *Magnaporthe grisea*. Mol. Plant Microbe Interact. 7:639-644.

Xu, J.-R. 2000. MAP kinases in fungal pathogens. Fungal Genet. Biol. 31:137-152.

Xu, J. R., Hamer, J. E. 1996. MAP kinase and cAMP signaling regulate infection structure formation and pathogenic growth in the rice blast fungus *Magnaporthe grisea*. Genes Dev. 10:2696-706.

Xu, J. R., Peng, Y. L., Dickman, M. B., Sharon, A. 2006. The dawn of fungal pathogen genomics. Annu Rev Phytopathol. 44:337-66.

Xu, J. R., Staiger, C. J., Hamer, J. E. 1998. Inactivation of the mitogen-activated protein kinase Mps1 from the rice blast fungus prevents penetration of host cells but allows activation of plant defense responses. Proc. Natl. Acad. Sci. U.S.A. 95:12713-8.

Xu, J. R., Urban, M., Sweigard, J. A., Hamer, J. E. 1997. The *CPKA* gene of *Magnaporthe grisea* is essential for appressorial penetration. Mol. Plant Microbe Interact.. 10:187-194.

Yamauchi, J., Takayanagi, N., Komeda, K., Takano, Y., Okuno, T. 2004. cAMP-pKA signaling regulates multiple steps of fungal infection cooperatively with Cmk1 MAP kinase in *Colletotrichum lagenarium*. Mol. Plant Microbe Interact.. 17:1355-1365.

Yang, Z., Dickman, M. B. 1999. *Colletotrichum trifolii* mutants disrupted in the catalytic subunit of cAMP-dependent protein kinase are nonpathogenic. Mol. Plant Microbe Interact.. 12:430-439.

Yi, M., Park, J. H., Ahn, J. H., Lee, Y. H. 2008. MoSNF1 regulates sporulation and pathogenicity in the rice blast fungus *Magnaporthe oryzae*. Fungal Genet. Biol.

You, B. J., Chung, K. R. 2007. Phenotypic characterization of mutants of the citrus pathogen *Colletotrichum acutatum* defective in a PacC-mediated pH regulatory pathway. FEMS Microbiol. Lett. 277:107-14.

Yun, S. H., Turgeon, B. G., Yoder, O. C. 1998. REMI-induced mutants of *Mycosphaerella zea-maydis* lacking the PM-toxin are deficient in pathogenesis to corn. Physiological and Mol. Plant Pathol. 52:53-66.

Zhang, J., Guo, D., Chang, Y., You, C., Li, X., Dai, X., Weng, Q., Zhang, J., Chen, G., Li, X., Liu, H., Han, B., Zhang, Q., Wu, C. 2007. Non-random distribution of T-DNA insertions at various levels of the genome hierarchy as revealed by analyzing 13 804 T-DNA flanking sequences from an enhancer-trap mutant library. Plant J. 49:947-59.

Zheng, L., Campbell, M., Murphy, J., Lam, S., Xu, J. R. 2000. The BMP1 gene is essential for pathogenicity in the gray mold fungus *Botrytis cinerea*. Mol Plant Microbe Interact. 13:724-32.

Zupan, J., Muth, T. R., Draper, O., Zambryski, P. 2000. The transfer of DNA from *Agrobacterium tumefaciens* into plants: A feast of fundamental insights. Plant J. 23:11-28.

Zwiers, L. H., De Waard, M. A. 2001. Efficient *Agrobacterium tumefaciens*-mediated gene disruption in the phytopathogen *Mycosphaerella graminicola*. Curr. Genet. 39:388-393.

Acknowledgements

First of all, I would like to thank Prof. Dr. Paul Schulze-Lefert for the opportunity to do my PhD in the plant-microbe interactions department, but also for inspiring and stimulating dicussions after my departemental seminars and journal club. Thank you.

I am very grateful to my supervisor Dr. Richard O'Connell, for all the support, motivation and advice he gave me during my PhD, for encouraging me to attend conferences, for his help at the microscope, for thoroughtly reading my thesis and working with me on my very first first author manuscript… the list goes on. Thank you very very much!!

A special thank to my PhD examination comittee: the examiners Prof. Dr. Paul Schulze-Lefert and Prof. Dr. Marcel Bucher, the "Vorsitzender" Prof. Dr. Ulf-Ingo Flügge and the the "Beisitzer", Dr. Jane Parker.

I am also grateful to Dr. Renier van der Hoorn, my second supervisor, for very good advice.

Für kostbare Hilfe im Labor, ich danke Wolfgang Schmalenbach, du kannst *Colletotrichum* transformieren wie ein Zauberer!

For scientific advice, I am very grateful to Dr. Hiroyuki Takahara, a master of molecular biology and to Dr. Cristina Micali who introduced me to Gateway cloning and showed me one can do more with yeast then just dough or bread.

A big thank to all the members of the O'Connell lab: Doris, Jochem, Hiroyuki, Wolfgang and Saurabh. You all helped me a lot, in the lab and in lab meetings – it was always pleasant with you! A special thank to Jochem for having taken so many PCR reactions out for me!

Special thanks to Doris and Dorit, for being good friends and for passing on to me their expert knowledge on how to write up a thesis and how to have fun with Photoshop. More special thank yous to the lunch crew: Doris, Dorit, Ana, Katharina, Enrico, Corinna and Jaqueline for precious mid-day distractions, to Nana for friendship, lunch am pool, advice and for listening to my complaints and of course to Moritz for more good advice, a lot of patience and for the meticulous reading of this looooooonng piece of work, chacun son tour! Merci!!

And for the great atmosphere in the department, I am very grateful to every single past and present member of the department!

Last but not least… un très grand merci à mes parents et mes soeurs, pour avoir été une inspiration et pour m'avoir aidé, motivé (et supporté) pendant ces 25 dernières années! Merci beaucoup!

Erklärung

Ich versichere, dass ich die von mir vorgelegte Dissertation selbständig angefertigt, die benutzten Quellen und Hilfsmittel vollständig angegeben und die Stellen der Arbeit - einschließlich Tabellen, Karten und Abbildungen -, die anderen Werken im Wortlaut oder dem Sinn nach entnommen sind, in jedem Einzelfall als Entlehnung kenntlich gemacht habe; dass diese Dissertation noch keiner anderen Fakultät oder Universität zur Prüfung vorgelegen hat; dass sie - abgesehen von den auf Seite III angegebenen Teilpublikationen - noch nicht veröffentlicht worden ist sowie, dass ich eine solche Veröffentlichung vor Abschluss des Promotionsverfahrens nicht vornehmen werde. Die Bestimmungen dieser Promotionsordnung sind mir bekannt. Die von mir vorgelegte Dissertation ist von Prof. Dr. Paul Schulze-Lefert betreut worden.

Köln, der _____

Lebenslauf

Angaben zur Person:

Name:	Aurelie Huser
Geburtsdatum:	02. April 1983
Geburtsort:	Epernay (Frankreich)
Nationalität:	französisch
Familienstand:	ledig

Ausbildung:

04. 2000	**International Baccalaureate** an der Frankfurt International School, Oberursel
10. 2000 – 06. 2003	**Bachelor-Studium** an der Imperial College of Science, Technology and Medecine, London, England Abschluss: Bachelor of Microbiology with First Class Honors
02. 2003 – 04. 2003	Bachelor Arbeit an der Imperial College of Science, Technology and Medecine. Leitung Dr. Spanu. Thema: Characterisation of catalase B overexpression mutant in *Magnapothe grisea*
08. 2003 – 07. 2005	**Master-Studium** an der Wageningen Universiteit, Wageningen, Niederlande Fachbereich Pflanzenbiotechnologie, Hauptfach: Pflanzenpathologie Abschluss: Master of Plant Biotechnology *cum laude*
05. 2004 – 11. 2004	Diplom Arbeit an der Wageningen Universiteit. Leitung Dr. de Waard. Thema: Modulator of ABC transporters as synergists of fungicides and plant defence compounds against *Mycosphaerella graminicola* and *Botrytis cinerea*.
02.2005 – 07. 2005	**Studiums-Auslandaufenthalt** am Eidgenössische Technische Hochschule Zürich Leitung: Dr. Maurhofer. Thema: The influence of plant phenolic compounds on the biosynthesis of the antimicrobial metabolites 2,4-diacetylphloroglucinol and pyoluteorin by the biocontrol *Pseudomonas fluorescens* strain CHA0
Seit August 2005	**Promotionarbeit** am Max Planck Institut für Zuchtungforschung, Köln AG. Dr. R. O'Connell. Leitung Prof. Dr. Paul Schulze-Lefert Thema: Identification of pathogenicity genes in the crucifer anthracnose *Colletotrichum higginsianum*

Publications:

Roohparvar R., **Huser A. C.** , Zwiers L. H., De Waard M. A. (2007). Control of *Mycosphaerella graminicola* on wheat seedlings by medical drugs known to modulate the activity of ATP-binding cassette transporters. Applied and Environmental Microbiology. 73(15):5011-5019

Tanaka S., Yamada K., Yabumoto K., Fujii S., **Huser A.**, Tsuji G., Koga H., Dohi K., Mori M., Shiraishi T., O'Connell R., Kubo Y. (2007). *Saccharomyces cerevisiae* SSD1 orthologues are essential for host infection by the ascomycete plant pathogens *Colletotrichum lagenarium* and *Magnaporthe grisea.* Molecular Microbiology. 64(5):1332-49.

Werra P., Baehler E., **Huser A.**, Keel C., Maurhofer M. (2008). Detection of plant-modulated alterations in antifungal gene expression in *Pseudomonas fluorescens* CHA0 on roots by flow cytometry. Applied and Environmental Microbiology. 74(5):1339-1349.

Huser. A. C., Takahara, H., Schmalenbach, W., O'Connell, R. Identification of pathogenicity genes in the crucifer anthracnose *Colletotrichum higginsianum*, using random insertional mutagenesis. (submitted)

Köln, der _____